



Norwegian University of  
Science and Technology

# Weight Estimation of Steam Cycle for CO<sub>2</sub> Capture System on Offshore Oil and Gas Installation

**Kjartan Christian Haug**

Master of Energy and Environmental Engineering

Submission date: June 2016

Supervisor: Lars Olof Nord, EPT

Co-supervisor: Rahul Anantharaman, SINTEF

Norwegian University of Science and Technology  
Department of Energy and Process Engineering



EPT-M-2016-52

**MASTER THESIS**

for

student Kjartan Christian Haug

Spring 2016

**Weight estimation of steam cycle for CO<sub>2</sub> capture system  
on offshore oil and gas installation****Background and objective**

One of the largest sources of CO<sub>2</sub> emissions from the Norwegian industry are offshore gas turbines that power the oil and gas installations. One option to decrease the emissions is to capture the CO<sub>2</sub> emitted from the gas turbines, followed by compression and storage of the CO<sub>2</sub> offshore. If CO<sub>2</sub> capture and storage (CCS) is to be implemented on the Norwegian continental shelf on oil and gas installations, the design needs to be compact and with low weight. The reboiler in the desorber section of the CO<sub>2</sub> capture plant requires steam. This project would relate to the design and analysis of a low weight steam cycle that could supply the steam for the reboiler in the CCS system.

The Master's thesis work should build on the specialization project completed in December, 2015, where the main objective of the work was to arrive at a simplified steam cycle weight model. The chosen steam cycle was based on a back-pressure steam turbine system which can be further developed in the Master's thesis. Expansion of the system boundary to include also flue gas cooler and sea water desalination should be considered. The possibility to also supply the necessary power to the CCS system should be investigated. Two approaches for weight estimation are sought for, one based on a polynomial representation and one based on a more analytical approach using scaling laws. The models should be verified against several case studies.

The main objective for the Master's thesis is to arrive at a reliable weight estimation method for steam bottoming cycles on offshore oil and gas installations.

**The following tasks are to be considered:**

1. Literature study on analytical approaches to weight estimation including scaling laws of turbomachinery and heat exchangers. Literature on polynomial representation and simplification of process models should also be sought after.
2. Further development of steam cycle design based on back-pressure steam turbine.
3. Test of validity of polynomial representation for weight estimation on case studies.
4. Build-up of weight estimation method based on scaling laws (similarity approach).
5. Comparison of methods based on polynomials and scaling laws for estimation of weight.

Within 14 days of receiving the written text on the master thesis, the candidate shall submit a research plan for his project to the department.

When the thesis is evaluated, emphasis is put on processing of the results, and that they are presented in tabular and/or graphic form in a clear manner, and that they are analyzed carefully.

The thesis should be formulated as a research report in English with summary, conclusion, literature references, table of contents etc. During the preparation of the text, the candidate should make an effort to produce a well-structured and easily readable report. In order to ease the evaluation of the thesis, it is important that the cross-references are correct. In the making of the report, strong emphasis should be placed on both a thorough discussion of the results and an orderly presentation.

The candidate is requested to initiate and keep close contact with his/her academic supervisor(s) throughout the working period. The candidate must follow the rules and regulations of NTNU as well as passive directions given by the Department of Energy and Process Engineering.

Risk assessment of the candidate's work shall be carried out according to the department's procedures. The risk assessment must be documented and included as part of the final report. Events related to the candidate's work adversely affecting the health, safety or security, must be documented and included as part of the final report. If the documentation on risk assessment represents a large number of pages, the full version is to be submitted electronically to the supervisor and an excerpt is included in the report.

Pursuant to "Regulations concerning the supplementary provisions to the technology study program/Master of Science" at NTNU §20, the Department reserves the permission to utilize all the results and data for teaching and research purposes as well as in future publications.

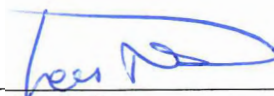
The final report is to be submitted digitally in DAIM. Based on an agreement with the supervisor, the final report and other material and documents may be given to the supervisor in digital format.

- Work to be done in lab (Water power lab, Fluids engineering lab, Thermal engineering lab)  
 Field work

Department of Energy and Process Engineering, 13. January 2016



Olav Bolland  
Department Head



Lars Nord  
Academic Supervisor

Co-supervisor: Rahul Anantharaman, SINTEF Energy

## Preface

This master's thesis is part of my MSc in Energy and Environmental Engineering at the Norwegian University of Science and Technology. It is composed at the Department of Energy and Process Engineering, Faculty of Engineering Science and Technology, during the spring semester of 2016. I would like to give a thanks to my supervisor Lars O. Nord for technical inputs and guidance. Rahul Anantharaman from SINTEF Energy has provided the background material for the CCS system.

I'd like to give special thanks to Monica Helle for final proofreading. Karoline S. Lindstad, Tor E. S. Lindstad and Haakon Lindstad have contributed with helpful comments and suggestions. I would also give a thanks to my superior officer in the Norwegian Home Guard for facilitating reduced service during "Cold Response 2016".

Basic technical knowledge in thermodynamics and applied mathematics are expected of the reader.

Trondheim, June 22, 2016.

A handwritten signature in black ink that reads "Kjartan Haug". The signature is written in a cursive style and is positioned above a horizontal line.

Kjartan Christian Haug



## Abstract

Climate change due to increasing anthropogenic CO<sub>2</sub> emissions is a major concern both in Norway, and globally. Greater environmental focus and increased taxes on emitted CO<sub>2</sub> have led to corporate efforts on reducing CO<sub>2</sub> emissions. Offshore gas turbines are one of the largest sources of CO<sub>2</sub> emissions from the Norwegian industry. One option to reduce the emissions is to capture CO<sub>2</sub> from the gas turbine exhaust gas, followed by compression and offshore storage. This process is known as carbon capture and storage (CCS). Due to strict sizing limitations on offshore oil and gas installations, implementation of CCS is totally dependent on a compact and low weight design. To run this process, the reboiler in the desorber section of the CO<sub>2</sub> capture plant requires steam. This steam is produced in a low weight steam bottoming cycle that is designed as a part of this study. The aim of this study is to answer the research question: "What is the preferred weight estimating method for steam bottoming cycles on offshore oil and gas installations, polynomial representation or scaling laws?"

To arrive at a reliable weight estimate, the steam cycle design is further developed from the specialization project, completed in December 2015. In the simulation software GT PRO, the steam cycle is integrated with CO<sub>2</sub> capture and desalination. Because of its importance, the major focus in the design phase was on weight reduction. The total weight is calculated for the fundamental steam cycle components; steam turbine, generator and heat recovery steam generator, and is found to be 437.8 tons. The proposed design produces  $37.7 \frac{kg}{s}$  of saturated steam at 5 bar and has a net positive power output of 5 MW with both CCS and desalination implemented, and is therefore self-sufficient with both steam and power.

Some promising results for weight estimation have been found. Two different methods were implemented; polynomial representation from weighted least squares method and scaling laws from robust fitting. The polynomial offers more flexibility, because more than one variable can be considered. If one desires a more detailed analysis, or if several design parameters are not yet determined, the polynomial approach is suited. The considered variables are steam and exhaust mass flow, and exhaust temperature. If the boundary conditions are fixed, as in this study, the scaling laws are spot on. Scaling laws form a very elegant linear solution when steam mass flow is considered in the weight estimation. The analyzed real weight data support a linear scaling relationship between weight and mass flow. The base case polynomial estimate made an error of 1.4%, while the scaling law estimate deviated by 0.5%. During validation tests, also outside the calculated range, the maximum errors were 2.2% and 3.1% respectively. The linear scaling law results were almost unrealistically consistent within its calculated range (<1%). This is most likely related to software limitations in GT PRO.





## Sammendrag

Menneskeskapte klimaendringer fra økte CO<sub>2</sub>-utslipp har skapt bekymring i Norge, og internasjonalt. Et tydeligere miljøfokus, og økte skatter på utslipp har ført til reduserende tiltak hos flere oljerelaterte bedrifter. Eksosgassen fra gassturbiner som opererer på den norske sokkelen bidrar til noen av de største totalutslippene fra norsk industri. Et aktuelt reduksjonstiltak er å fange, komprimere og lagre CO<sub>2</sub> fra eksosgassen offshore. Denne prosessen er kjent som karbonfangst og –lagring (CCS). Da dette systemet skal monteres offshore, stilles det høye krav til lav vekt og kompakt utførelse. Denne prosessen er avhengig av vanndamp for å utskille CO<sub>2</sub> i en desopsjonsprosess. Dampproduksjonen foregår i en lavvekts dampsyklus som er utviklet som en del av denne studien. Hovedmålet med studien er å svare på forskningsspørsmålet: "Hva er den foretrukne vektestimertingsmetoden for en offshore dampsyklus på olje- og gassinstallasjoner, polynomrepresentasjon eller skaleringslover?".

Et pålitelig vektestimert er avhengig av en realistisk prosessmodell. Dampsyklusen som ble designet i prosjektoppgaven (Desember 2015) har blitt videreutviklet, og er nå integrert med CO<sub>2</sub>-fangst og et avsaltingsanlegg i simuleringsprogrammet GT PRO. Siden lav vekt er kritisk for offshoreinstallasjoner, var hovedfokuset i designfasen på vektreduksjon. Totalvekten for dampsyklusen er 437,8 tonn, og er beregnet ut ifra hovedkomponentene: dampturbin, generator og dampgenerator. Dampsyklusen produserer  $37,7 \frac{kg}{s}$  med mettet damp ved 5 bar, og har et netto elektrisitetsoverskudd på 5 MW. Da er både CCS og avsaltingsanlegg implementert, som betyr at systemet er selvforsynt med både damp og elektrisitet.

Analyse av simuleringsdata viser lovende resultater for vektestimerting. To metoder ble utviklet, polynomrepresentasjon gjennom vektet minste kvadraters metode, og skaleringslover fra robust kurvetilpasning. Polynomrepresentasjonen er mer fleksibel siden flere variabler kan vurderes samtidig. Dette muliggjør en mer detaljert analyse, som er nødvendig dersom flere parametere er ubestemte. De analyserte variablene er massestrøm av damp og eksos, og temperaturen til eksosgassen. Hvis grensebetingelsene er låst, som i denne studien, er skaleringslover velegnet. Skaleringsresultatene danner en elegant løsning som er tilnærmet lineær når vekten analyseres med tanke på massestrøm. Den lineære sammenhengen støttes av analysert vektdata for reelle komponenter. Det kalkulerede polynomet hadde et avvik på 1,4%, mens skaleringsloven estimerte en vekt på 0,5% fra simuleringsverdien på designpunktet. Omfattende valideringstester, også utenfor definisjonsområdet til de aktuelle variablene, viste maksimale avvik på henholdsvis 2,2% og 3,1%. Resultatene for skaleringslovene var nærmest urealistisk entydig innenfor definisjonsområdet (<1%). Dette er mest sannsynlig relatert til begrensninger i simuleringsprogramvaren GT PRO.



# Contents

Preface . . . . .	I
Abstract . . . . .	II
Sammendrag . . . . .	III
<b>Contents</b>	<b>VII</b>
<b>List of Figures</b>	<b>VIII</b>
<b>List of Tables</b>	<b>XII</b>
<b>Nomenclature</b>	<b>XV</b>
<b>1 Introduction</b>	<b>1</b>
1.1 Background . . . . .	2
1.2 Objectives and Scope of Work . . . . .	5
1.3 Risk Assessment . . . . .	8
1.4 Limitations . . . . .	8
1.5 Software . . . . .	8
<b>2 Offshore Heat and Power Generation</b>	<b>10</b>
2.1 Power Generation . . . . .	11
2.1.1 Gas Turbines . . . . .	11
2.2 Heat Generation . . . . .	13
2.3 Emissions . . . . .	14
2.4 Offshore Combined Cycles . . . . .	15
2.4.1 Snorre B . . . . .	15
2.4.2 Oseberg D . . . . .	15
2.4.3 Eldfisk E . . . . .	15
2.5 Chapter Discussion . . . . .	18
<b>3 Combined Cycle Technology</b>	<b>20</b>
3.1 Steam Turbine . . . . .	21
3.2 Heat Recovery Steam Generator . . . . .	23
3.3 Generator . . . . .	29
3.4 Water Treatment . . . . .	30
3.5 Chapter Discussion . . . . .	34
<b>4 Power Cycles</b>	<b>36</b>
4.1 Gas Power Cycles . . . . .	37
4.2 Vapor Power Cycles . . . . .	38
4.3 Combined Power Cycles . . . . .	40
4.4 Chapter Discussion . . . . .	41

<b>5</b>	<b>CO<sub>2</sub> Capture, Transport and Storage</b>	<b>42</b>
5.1	MEA-System . . . . .	43
5.1.1	Absorption . . . . .	44
5.1.2	Regeneration . . . . .	46
5.2	Transport . . . . .	46
5.3	Storage . . . . .	46
5.4	Offshore Based Plant, Sleipner Vest . . . . .	48
5.5	Chapter Discussion . . . . .	51
<b>6</b>	<b>Mathematical Representation</b>	<b>52</b>
6.1	Interpolation . . . . .	53
6.2	Regression and Least Squares Fitting . . . . .	59
6.3	Scaling . . . . .	67
6.4	Chapter Discussion . . . . .	76
<b>7</b>	<b>Methodology</b>	<b>78</b>
7.1	Basic Equations . . . . .	79
7.2	Boundary Conditions . . . . .	81
7.3	Equations of State . . . . .	82
7.4	Steam Turbine Control . . . . .	84
7.5	Low Weight Steam Cycle . . . . .	86
7.6	Process Models and Simplification . . . . .	87
7.7	GT PRO Process Models . . . . .	89
7.8	GT PRO – Desalination Plant . . . . .	90
7.9	GT PRO – CO <sub>2</sub> Plant . . . . .	90
7.10	Polynomial Representation . . . . .	92
7.11	Scaling Laws . . . . .	94
<b>8</b>	<b>Results and Discussion</b>	<b>96</b>
8.1	Scaling Results from Literature Study . . . . .	97
8.1.1	Turbines . . . . .	97
8.1.2	Heat Exchangers . . . . .	102
8.2	GT PRO Process Models . . . . .	104
8.2.1	Model 1 – Steam Cycle . . . . .	105
8.2.2	Model 2 – CO <sub>2</sub> Capture . . . . .	107
8.2.3	Model 3 – CO <sub>2</sub> Capture and Desalination . . . . .	109
8.3	Polynomial Representation . . . . .	111
8.3.1	Model 1 – Polynomial 1 . . . . .	111
8.3.2	Model 1 – Polynomial 2 . . . . .	111
8.3.3	Model 2 – Polynomial 3 . . . . .	112
8.3.4	Testing and Validation . . . . .	113
8.4	Scaling Laws . . . . .	114

8.5	Discussion . . . . .	123
<b>9</b>	<b>Conclusions and Further Work</b>	<b>128</b>
9.1	Conclusion . . . . .	129
9.2	Further Work . . . . .	131
	<b>Bibliography</b>	<b>132</b>
	<b>Appendix</b>	<b>139</b>
<b>A</b>	<b>Supporting Literature</b>	<b>140</b>
A.1	Offshore Heat and Power Generation . . . . .	141
A.1.1	Onshore Power Supply . . . . .	141
A.2	Combined Cycle Technology . . . . .	143
A.2.1	Gas Turbine . . . . .	143
A.2.2	Condenser . . . . .	145
A.2.3	Pumps . . . . .	146
A.2.4	Deaeration . . . . .	147
A.2.5	Onshore Combined Cycle . . . . .	148
A.3	Power Cycles . . . . .	150
A.3.1	Alternative Bottoming Cycles . . . . .	150
A.4	CO <sub>2</sub> Capture, Transport and Storage . . . . .	151
A.4.1	Shore Based Simulations . . . . .	151
A.5	Mathematical Representation . . . . .	153
A.5.1	Scaling and Similitude . . . . .	153
A.5.2	Performance Parameters . . . . .	155
<b>B</b>	<b>Analytical Calculations</b>	<b>158</b>
B.1	Simplified Calculations for HRSG . . . . .	159
B.2	Heat Exchanger Design, Basis for Scaling . . . . .	162
B.2.1	Thermal Design of Shell and Tube Heat Exchanger . . . . .	163
<b>C</b>	<b>Additional Analysis, Figures and Tables</b>	<b>170</b>
C.1	Real Gas Turbine Weight Data – Scaling . . . . .	171
C.2	Airplane Engines Weight . . . . .	175
C.3	GT PRO – Model 1 . . . . .	179
C.4	GT PRO – Model 2 . . . . .	183
C.5	GT PRO – Model 3 . . . . .	188
C.6	GT PRO – Additional Figures for Scaling Laws . . . . .	195
C.6.1	Model 1 . . . . .	195
C.6.2	Model 2 . . . . .	196
C.7	Multivariate Polynomial Approach – Project Work Weight Estimation . . . . .	197
C.8	Large Tables . . . . .	204

<b>D</b>	<b>Computer Code</b>	<b>210</b>
D.1	Excel Code . . . . .	211
D.1.1	Heat Exchanger Scaling Model . . . . .	211
D.2	MATLAB Code . . . . .	214
D.2.1	km32.m . . . . .	214
D.2.2	combo_3_4.m . . . . .	216
D.2.3	poly_3_4.m . . . . .	217
D.2.4	poly_eval.m . . . . .	218

# List of Figures

Figure 1.1: Combined gas turbine and steam turbine cycle with CO <sub>2</sub> capture [1]. . . . .	1
Figure 2.1: Main gas turbine sections [20]. . . . .	10
Figure 2.2: Temperature and pressure through aeroderivative gas turbine [29]. . . . .	12
Figure 2.3: General Electric LM2500 [30]. . . . .	12
Figure 2.4: CO <sub>2</sub> emissions from the Norwegian petroleum sector in 2012 [2]. . . . .	14
Figure 2.5: Schematics of an offshore combined heat and power cycle. [36]. . . . .	16
Figure 2.6: Original design of the Oseberg D facility [36]. . . . .	17
Figure 2.7: Original design of the Eldfisk E facility [36]. . . . .	17
Figure 3.1: Back-pressure steam turbine [37]. . . . .	20
Figure 3.2: Heat recovery steam generator with steam drum and duct burner [40]. . . . .	23
Figure 3.3: Finned tube with main design parameters [28]. . . . .	24
Figure 3.4: Tube row arrangement [28]. . . . .	24
Figure 3.5: Tube spacing [28]. . . . .	24
Figure 3.6: Solid and serrated fins attached on tube [28]. . . . .	24
Figure 3.7: HRSG steam drum [28]. . . . .	27
Figure 3.8: Generator principle, producing electricity from rotation energy [47]. . . . .	29
Figure 3.9: Simplified multi stage flash (MSF) process diagram [49]. . . . .	31
Figure 3.10: Simplified multi effect distillation with thermal vapor compression (MED-TVC) process [50]. . . . .	32
Figure 3.11: Steam jet ejector for thermal vapor compression (TVC) [51]. . . . .	32
Figure 3.12: Condensate polisher with resin bed [52]. . . . .	33
Figure 4.1: Combined cycle [53]. . . . .	36
Figure 4.2: Brayton cycle [53]. . . . .	37
Figure 4.3: Thermodynamic Rankine cycle [53]. . . . .	38
Figure 4.4: Simple and combined cycles TS-diagram [55]. . . . .	39
Figure 5.1: Offshore transport and storage of CO <sub>2</sub> [56]. . . . .	42
Figure 5.2: Contributors to global warming in 2007 [61]. . . . .	43
Figure 5.3: Example of a MEA based CO <sub>2</sub> capture system [71]. . . . .	45
Figure 5.4: The stripper section of the MEA plant. Steam is entering the reboiler section [72]. . . . .	45

Figure 5.5:	CO <sub>2</sub> can be stored in e.g. unmineable coal seams, deep saline aquifers, and depleted oil and gas reservoirs [77]. . . . .	47
Figure 5.6:	Cap rock and possible modes for CO <sub>2</sub> storage in a reservoir [78]. . . . .	47
Figure 5.7:	Flow diagram for the Sleipner CO <sub>2</sub> removal system [79]. . . . .	49
Figure 5.8:	An illustration of the Sleipner CO <sub>2</sub> compression system [79]. . . . .	49
Figure 5.9:	Injection of CO <sub>2</sub> into the Utsira formation. The seismic monitoring is showing the evolving CO <sub>2</sub> plume. 10.1 million tons of CO <sub>2</sub> have been injected in the period 1996–2008 [81]. . . . .	50
Figure 6.1:	Fourth order representation of data points with two variables. . . . .	52
Figure 6.2:	Piecewise linear interpolation. . . . .	54
Figure 6.3:	Full degree polynomial interpolation. . . . .	54
Figure 6.4:	Shape preserving Hermite interpolation. . . . .	55
Figure 6.5:	Spline interpolation. . . . .	55
Figure 6.6:	Surface plot for two variable polynomial interpolation. . . . .	58
Figure 6.7:	Surface plot for two variable polynomial interpolation with extrapolation. . . . .	58
Figure 6.8:	Linear function, weighted and robust fit. . . . .	62
Figure 6.9:	Squared function, weighted and robust fit. . . . .	62
Figure 6.10:	Trigonometric function sin(x) with disturbance, weighted and robust fit. . . . .	63
Figure 6.11:	This is a zoomed in version of the previous figure, with the original sin(x) curve plotted. . . . .	63
Figure 6.12:	Different order polynomial regression on five data points. . . . .	64
Figure 6.13:	Residuals from different order polynomial regression on five data points. . . . .	64
Figure 6.14:	First order plane, with two variables. . . . .	65
Figure 6.15:	Second order plane, with two variables. . . . .	66
Figure 6.16:	Third order plane, with two variables. . . . .	66
Figure 6.17:	Steam turbine rotor, where the blades form two conical frustum geometries. . . . .	68
Figure 6.18:	Conical Frustum. . . . .	69
Figure 6.19:	Similarity for conical frustum. . . . .	69
Figure 7.1:	Shell and tube heat exchanger with fixed tubesheet [95]. . . . .	78
Figure 7.6:	Constant and sliding pressure in steam turbine [103]. . . . .	84
Figure 7.2:	HRSG performance at sliding pressure operation [102]. . . . .	85
Figure 7.3:	Expansion line for steam turbine with sliding pressure control [102]. . . . .	85
Figure 7.4:	Expansion line for steam turbine with nozzle control [102]. . . . .	85
Figure 7.5:	Expansion line for steam turbine with throttle control [102]. . . . .	85
Figure 7.7:	MED plant section from GT PRO. . . . .	90
Figure 7.8:	CO <sub>2</sub> plant model from GT PRO. . . . .	91
Figure 7.9:	km32.m, $W = a \cdot x^n + b$ , $n = 1.0$ . . . . .	95
Figure 7.10:	km32.m, $W = a \cdot x^n + b$ , $n = 1.5$ . . . . .	95
Figure 8.1:	Centaur 40, Centaur 50 and Taurus 60. . . . .	96
Figure 8.2:	Turbine assembly weight, Solar SoLoNOx turbines. . . . .	99
Figure 8.3:	Turbine assembly weight, Solar turbines. . . . .	99



Figure 8.4:	Total turbomachinery package weight, Solar turbines. . . . .	100
Figure 8.5:	Generator drive weight, Solar turbines. . . . .	100
Figure 8.6:	Elliot MYR steam turbines weight, varying with power. . . . .	101
Figure 8.7:	Shell and tube heat exchanger simulations from GT PRO, HX weight varying with surface area. . . . .	102
Figure 8.8:	Shell and tube heat exchanger simulations from GT PRO, HX weight varying with duty. . . . .	103
Figure 8.9:	Shell and tube heat exchanger simulations from GT PRO, HX weight varying with steam mass flow. . . . .	103
Figure 8.10:	GT PRO model 1, combined cycle with back-pressure turbine. . . . .	106
Figure 8.11:	GT PRO model 2, combined cycle with back-pressure turbine and CO <sub>2</sub> capture. . . . .	108
Figure 8.12:	GT PRO model 3, combined cycle with back-pressure turbine, CO <sub>2</sub> capture and desalination. . . . .	110
Figure 8.13:	Model 1, steam turbine weight as a function of steam mass flow. . . . .	116
Figure 8.14:	Model 1, steam turbine generator weight as a function of steam mass flow. . . . .	116
Figure 8.15:	Model 1, HRSG (dry) weight as a function of steam mass flow. . . . .	117
Figure 8.16:	Model 1, total weight as a function of steam mass flow power. . . . .	117
Figure 8.17:	Model 2, steam turbine weight as a function of steam mass flow. . . . .	120
Figure 8.18:	Model 2, steam turbine generator weight as a function of steam mass flow. . . . .	120
Figure 8.19:	Model 2, HRSG (dry) weight as a function of steam mass flow. . . . .	121
Figure 8.20:	Model 2, total weight as a function of steam mass flow power. . . . .	121
Figure 8.21:	Model 1, total weight for optimal "n"-value, $n = 0.77$ . . . . .	122
Figure 8.22:	Model 2, total weight for optimal "n"-value, $n = 0.84$ . . . . .	122
Figure 9.1:	What is the preferred method for weight estimation? . . . . .	128
Figure A.1:	Offshore installation can be connected to both offshore wind farms and onshore power grid [127]. . . . .	142
Figure A.2:	Possible electrification of the Utsira High on the Norwegian continental shelf [128] . . . . .	143
Figure A.3:	Direct water cooling condenser [130] . . . . .	146
Figure A.4:	Multistage centrifugal pump, where the flow pattern is indicated [131]. . . . .	147
Figure A.5:	Deaerator for removal of dissolved gases in the feedwater [132]. . . . .	148
Figure A.6:	Combined cycle with three pressure levels and reheat [28]. . . . .	149
Figure A.7:	TQ diagram for a HRSG with three pressure levels and reheat [28]. . . . .	149
Figure A.8:	Combined cycle without CO <sub>2</sub> capture [71] . . . . .	152
Figure A.9:	Combined cycle with MEA based CO <sub>2</sub> capture [71]. . . . .	152
Figure A.10:	h-s diagram for the stagnation states [136] . . . . .	154
Figure A.11:	Change in stagnation conditions across a turbine [136] . . . . .	156
Figure A.12:	Overall characteristic for turbines [136] . . . . .	157
Figure B.1:	TQ-diagram for HRSG [28] . . . . .	159
Figure B.2:	Correction factor, $F=F(P,R)$ [138]. . . . .	164
Figure B.3:	Common tube layouts for shell and tube heat exchangers [139] . . . . .	166
Figure B.4:	Baffle cut. . . . .	167
Figure B.5:	Effective tube length from heat transfer area [138]. . . . .	169
Figure B.6:	Values of $F_1$ [138] . . . . .	169
Figure B.7:	Values of $F_2$ [138] . . . . .	169

Figure B.8: Values of $F_3$ [138]	169
Figure C.1: Skid weight, Solar turbines.	171
Figure C.2: Solar turbines: Saturn 20, Centaur 50, Taurus 60 and Titan 130 varying with power.	173
Figure C.3: Mitsubishi heavy duty turbines: M501F3 – M701F4 – M701F5 varying with power.	173
Figure C.4: GE turbines: 106FA – 107FA – 109FA varying with power.	174
Figure C.5: GE turbines: 106FA – 107FA – 109FA varying with mass flow.	174
Figure C.6: International Aero Engines – V2530-A5 [143].	176
Figure C.7: Pratt & Whitney – PW4090 [144].	176
Figure C.8: General Electric – GE90-85B [145].	176
Figure C.9: CFM International – CFM56-7B27 [146].	176
Figure C.10: Airplane gas turbine engine weight, varying with $D^2$ .	176
Figure C.11: Airplane gas turbine engine weight, varying with mass flow.	177
Figure C.12: Airplane engine, high pressure turbine (HPT) weight.	177
Figure C.13: Airplane engine, low pressure turbine (LPT) weight.	178
Figure C.14: Airplane engine, burner section weight.	178
Figure C.15: GT PRO model 1, cycle flow schematic.	179
Figure C.16: GT PRO model 1, HRSG layout with Incoloy tubes.	180
Figure C.17: GT PRO model 1, feedwater tank and low temperature economizer (LTE).	181
Figure C.18: GT PRO model 1, HRSG TQ diagram.	181
Figure C.19: GT PRO model 1, steam turbine expansion path.	182
Figure C.20: GT PRO model 1, plant exergy chart.	182
Figure C.21: GT PRO model 2, cycle flow schematic.	183
Figure C.22: GT PRO model 2, HRSG layout with Incoloy tubes.	184
Figure C.23: GT PRO model 2, feedwater tank.	185
Figure C.24: GT PRO model 2, HRSG TQ diagram.	185
Figure C.25: GT PRO model 2, CO <sub>2</sub> capture plant.	186
Figure C.26: GT PRO model 2, steam turbine expansion path.	187
Figure C.27: GT PRO model 2, plant exergy chart.	187
Figure C.28: GT PRO model 3, cycle flow schematic.	188
Figure C.29: GT PRO model 3, HRSG layout with Incoloy tubes.	189
Figure C.30: GT PRO model 3, feedwater tank.	190
Figure C.31: GT PRO model 3, HRSG TQ diagram.	190
Figure C.32: GT PRO model 3, CO <sub>2</sub> capture plant.	191
Figure C.33: GT PRO model 3, steam turbine expansion path.	192
Figure C.34: GT PRO model 3, plant exergy chart.	192
Figure C.35: GT PRO model 3, desalination plant. Multi-Effect Distillation (MED) circuit.	193
Figure C.36: GT PRO model 3, MED circuit TQ diagram.	194
Figure C.37: Model 1, HRSG (dry) weight as a function of heat surface area.	195

Figure C.38: Model 1, steam turbine weight as a function of steam turbine power. . . . .	195
Figure C.39: Model 2, HRSG (dry) weight as a function of heat surface area. . . . .	196
Figure C.40: Model 2, steam turbine weight as a function of steam turbine power. . . . .	196
Figure C.41: Second order curve fitting from varying parameter $x_1$ . . . . .	200
Figure C.42: Second order curve fitting from varying parameter $x_2$ . . . . .	200
Figure C.43: Second order curve fitting from varying parameter $x_{34}$ . . . . .	200
Figure C.44: Second order curve fitting from varying parameter $x_5$ . . . . .	200
Figure C.45: Weight estimating polynomial implemented in Excel . . . . .	203
Figure D.1: Heat exchanger model built in Excel. . . . .	211
Figure D.2: Heat exchanger model built in Excel, formulas. . . . .	212
Figure D.3: Heat exchanger scaling model in Excel, weight varying with heat transfer surface area. . . . .	213
Figure D.4: Heat exchanger scaling model in Excel, weight varying with total steam flow area. . . . .	213



# List of Tables

Table 2.1:	Existing offshore combined cycles on the Norwegian continental shelf [36]. . . . .	16
Table 6.1:	Nomenclature for turbine scaling. . . . .	71
Table 6.2:	Scaling ratios from GE gas turbines and compressors. . . . .	74
Table 7.1:	Exhaust gas mass flow [ $\frac{kg}{s}$ ] from the "FPSO" case. . . . .	81
Table 7.2:	Exhaust gas composition from the "FPSO" case. . . . .	81
Table 7.3:	Plant criteria and assumptions from the "FPSO" case. . . . .	81
Table 7.4:	Steam property specifications for the reboiler section in the CO <sub>2</sub> capture plant. . . . .	81
Table 7.5:	Properties in the GT PRO CO <sub>2</sub> plant model. . . . .	90
Table 7.6:	Variables used in polynomial weight representation. . . . .	92
Table 8.1:	The gas turbine assembly weight for Solar SoLoNOx turbines. . . . .	97
Table 8.2:	The gas turbine assembly and total weight for Solar turbines. . . . .	98
Table 8.3:	Solar gas turbine weight for generator drive. . . . .	98
Table 8.4:	Elliot MYR steam turbine weight. . . . .	98
Table 8.5:	GT PRO results from shell and tube type condenser – Shell (Heat Exchanger). . . . .	102
Table 8.6:	GT PRO results from shell and tube type condenser – Tubes (Heat Exchanger). . . . .	102
Table 8.7:	GT PRO model 1, weight estimates. . . . .	105
Table 8.8:	GT PRO model 1, overall plant results. . . . .	105
Table 8.9:	GT PRO model 2, weight estimates. . . . .	107
Table 8.10:	GT PRO model 2, overall plant results. . . . .	107
Table 8.11:	GT PRO model 2, CO <sub>2</sub> plant. . . . .	107
Table 8.12:	GT PRO model 3, weight estimates. . . . .	109
Table 8.13:	GT PRO model 3, overall plant results. . . . .	109
Table 8.14:	The model 1 polynomial variables and their given range. . . . .	112
Table 8.15:	The model 2 polynomial variables and their given range. . . . .	112
Table 8.16:	Coefficients for polynomial 1, 64 nodes. . . . .	112
Table 8.17:	Coefficients for polynomial 2, 128 nodes. . . . .	112
Table 8.18:	Coefficients for polynomial 3, 64 nodes. . . . .	112
Table 8.19:	Validation test for all polynomials. . . . .	113
Table 8.20:	Testing base case values for the scaling laws from model 1. . . . .	115

Table 8.21: Testing total weight for model 1 scaling law, $n = 1.0$ .	115
Table 8.22: Testing total weight for model 1 scaling law, $n = 0.77$ .	115
Table 8.23: Testing base case values for the scaling laws from model 2.	119
Table 8.24: Testing total weight for model 2 scaling law, $n = 1.0$ .	119
Table 8.25: Testing total weight for model 2 scaling law, $n = 0.84$ .	119
Table 8.26: Positive and negative factors for weight estimating methods.	125
Table A.1: Important gas turbine aspects for onshore and offshore operations.	143
Table A.2: Most significant auxiliary loads for both cases	151
Table A.3: Performance summary for both cases	151
Table C.1: Solar skid weight for generator set.	171
Table C.2: Airplane gas turbine engine weight, fan mass flow and diameter.	175
Table C.3: Weight of high pressure turbine, low pressure turbine and burner section in airplane engines.	175
Table C.4: Variables in weight estimating polynomial	197
Table C.5: Saturation temperatures	198
Table C.6: Parameters used in weight estimating polynomial	202
Table C.7: Compared weight from polynomial calculations and GT PRO simulations.	202
Table C.8: Sizing data for Solar skids with generator set [140]	204
Table C.9: GT PRO model 1, size estimates.	204
Table C.10: GT PRO model 2, size estimates.	204
Table C.11: GT PRO model 3, size estimates.	204
Table C.12: GT PRO model 3, CO <sub>2</sub> plant.	205
Table C.13: GT PRO model 3, desalination plant.	205
Table C.14: Validation of polynomial 1, 64 nodes.	205
Table C.15: Validation of polynomial 2, 128 nodes.	206
Table C.16: Validation of polynomial 3, 64 nodes.	206
Table C.17: GT PRO simulation on model 1 for scaling analysis.	207
Table C.18: GT PRO simulation on model 2 for scaling analysis.	208

# Nomenclature

## Abbreviations

**BC** Base Case

**BP** Back-Pressure

**CC** Combined Cycle

**CCS** Carbon Capture and Storage

**CHP** Combined Heat and Power

**DCC** Direct Contact Cooler

**ECO** Economizer

**EVA** Evaporator

**FPSO** Floating Production, Storage  
and Offloading Unit

**GE** General Electric

**GT** Gas Turbine

**HP** High Pressure

**HPT** High Pressure Turbine

**HRSG** Heat Recovery Steam Generator

**HX** Heat Exchanger

**IP** Intermediate Pressure

**LHV** Lower Heating Value

**LP** Low Pressure

**LPT** Low Pressure Turbine

**LTE** Low Temperature Economizer

**MEA** Monoethanolamine

**MED** Multi Effect Distillation

**MSF** Multi Stage Flash

**NCS** Norwegian Continental Shelf

**NG** Natural Gas

**OTSG** Once Through Heat Recovery  
Steam Generator

**SCR** Selective Catalytic Reduction

**SG** Steam Generator

**ST** Steam Turbine

**SUP** Superheater

**TVC** Thermal Vapor Compression

**WHRU** Waste Heat Recovery Unit

## Latin Symbols

$E$	Energy	[J]
$E$	Exergy	[J]
$Q$	Specific Heat	[J]
$\dot{W}$	Power	[W]
$\dot{Q}$	Heat Transfer	[W]
$T$	Temperature	[K] or [°C]
$P$	Pressure	[bar]
$V$	Volume	[m <sup>3</sup> ]
$u$	Internal Energy	[ $\frac{kJ}{kg}$ ]
$h$	Enthalpy	[ $\frac{kJ}{kg}$ ]
$s$	Entropy	[ $\frac{kJ}{kg \cdot K}$ ]
$n$	Mole	[mol]
$v$	Velocity	[ $\frac{m}{s}$ ]
$\dot{m}$	Mass Flow	[ $\frac{kg}{s}$ ]
$\dot{V}$	Volume Flow	[ $\frac{m^3}{s}$ ]
$c_p$	Heat Capacity	[ $\frac{kJ}{kg \cdot K}$ ]
$g$	Gravitational Force	[ $\frac{m}{s^2}$ ]
$z$	Height	[m]
$A$	Area	[m <sup>2</sup> ]
$x$	Steam Quality	[-]
$R$	Universal Gas Constant	[ $\frac{J}{mol \cdot K}$ ]
$Z$	Compressibility Factor	[-]
$W$	Weight	[kg]



## Greek Symbols

$\rho$	Density	$[\frac{kg}{m^3}]$
$\eta$	Efficiency	$[\frac{kJ}{kg \cdot K}]$
$\sigma$	Entropy Production	[-]

## Subscripts

$i$	Inlet
$e$	Exit
$l$	Cold
$h$	Hot
$BP$	Back-Pressure
$th$	Thermal
$p$	Constant Pressure
$exh$	Exhaust
$ECO$	Economizer
$EVA$	Evaporator
$SUP$	Superheater
$CV$	Control Volume
$amb$	Ambient
$sat$	Saturated
$ST$	Steam turbine
$Gen$	Generator
$Tot$	Total
$HRSG$	Heat Recovery Steam Generator



# Chapter 1

## Introduction

### Contents

1.1	Background	2
1.2	Objectives and Scope of Work	5
1.3	Risk Assessment	8
1.4	Limitations	8
1.5	Software	8

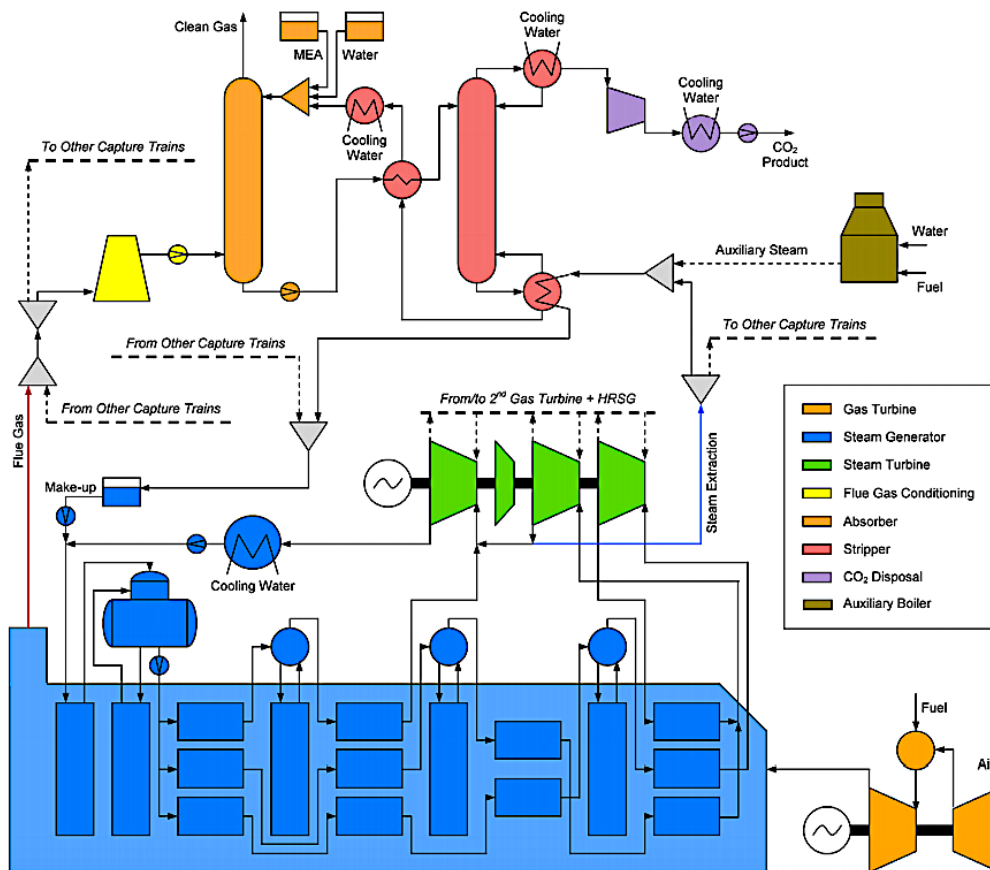


Figure 1.1: Combined gas turbine and steam turbine cycle with CO<sub>2</sub> capture [1].

## 1.1 Background

On the Norwegian continental shelf (NCS), 14.7 million<sup>1</sup> CO<sub>2</sub> equivalents are released to the atmosphere annually. CO<sub>2</sub> emissions from the offshore industry is primarily due to combustion of natural gas in gas turbines (GT), flaring of natural gas and diesel engines. In 2012, the exhaust from gas turbines was accountable for about 79.4% of the total offshore CO<sub>2</sub> emissions in Norway [2]. The gas turbines provide power and process heat in addition to mechanical shaft work on offshore oil and gas installations. Since petroleum activities accounted for about 27.3% of the total Norwegian CO<sub>2</sub> emissions in 2014 [3], the offshore gas turbines represent about 21.7% of the Norwegian carbon footprint. This master's thesis aim to contribute in the limiting measures of these anthropogenic CO<sub>2</sub> emissions.

Carbon capture and storage (CCS) is one of the available technologies that can reduce CO<sub>2</sub> emissions from the use of fossil fuels [4]. According to the International Energy Agency (IEA), carbon intensive fossil fuels will continue to be a huge part of the future energy mix, if no major policy changes are made. The big advantage with CCS, is the opportunity to continue with power production in existing plants. Together with renewable energy, energy efficiency measures, and fuel switching, CCS can be one of the major contributors to a more sustainable future. CCS is today the only commercial technology that can reduce CO<sub>2</sub> emissions from large-scale fossil fuel power plants and industrial facilities [4].

The Intergovernmental Panel on Climate Change (IPCC) estimates that inclusion of CCS in a mitigation portfolio reduces the costs of stabilizing atmospheric CO<sub>2</sub> concentrations by 30% [5]. IEA have stated the BLUE Map Scenario, which implies a 50% reduction in CO<sub>2</sub> emissions (2005 levels) from the energy sector by 2050. This includes a 19% contribution from CCS, that corresponds to 9.1 Gton of CO<sub>2</sub> [6]. In their analysis, IEA predicts that CCS will be the single share with the largest impact on CO<sub>2</sub> reduction. To reach this ambitious goal, more than 3000 CCS facilities with an average capturing capacity of 3 Mton CO<sub>2</sub> need to be built globally by 2050 [6].

The limited number of CCS projects in operation today [7], reflects a very difficult environment for large scale CCS. Political incentives and regulations/taxes on emission are varying around the world, which lead to financial uncertainty for investors. The United Nations agreement in Paris, December 2015, could potentially increase the chances for a large-scale commitment to carbon capture and storage [8]. With the Sleipner Vest Field, Norway was the first country in the world with large scale CO<sub>2</sub> storage in a shallow underground aquifer in 1996 [9]. Up to 1.7 Mton of CO<sub>2</sub> are stored here annually [2].

---

<sup>1</sup>This number is only specified for oil and gas production, can therefore also include onshore activities.

The Norwegian government has worked to reduce CO<sub>2</sub> emission from the petroleum sector for decades. The first petroleum related CO<sub>2</sub> tax was introduced in 1991 [2]. One of the modern measures discussed is introducing electric cables from shore. These cables and the accompanying infrastructure are very expensive, and radical measures were therefore necessary to introduce this as a realistic alternative. It was suggested in 2012, in what is known as "Klimameldingen", to significantly increase the CO<sub>2</sub> tax for the oil and gas industry. In 2013 the government increased the CO<sub>2</sub> tax with NOK 200 per ton CO<sub>2</sub> for all petroleum companies operating on the Norwegian continental shelf [10]. In 2015 the total CO<sub>2</sub> tax is about NOK 450 per ton CO<sub>2</sub> [11]. This increased the incentives for the operating companies to choose energy efficient solutions. The financial reality is simple; the cost of emissions needs to be higher than the implementation and use of cleaner solutions. With the trend of increasing CO<sub>2</sub> taxes, this could be the case for many offshore installations. Today, all new offshore projects need to be designed for possible connection with the onshore power grid.

For reduced emission of CO<sub>2</sub> an alternative to onshore power supply is a more efficient offshore power production. Extensive research has been started, e.g. the Research Council of Norway have funded the project "EFFORT" by SINTEF [12]. The goal for this project is to contribute with a 30% reduction in CO<sub>2</sub> emissions from the Norwegian continental shelf. SINTEF's main concept is based in implementing a bottoming cycle with the existing topping cycle from the gas turbines. This will increase the overall efficiency and reduce the CO<sub>2</sub> emissions by getting the same power output with reduced amount of fuel. When these cycles are joined together, they form what is known as a combined cycle (CC). This master's thesis is continuing SINTEF's work, with focus on a low weight steam bottoming cycle.

The technology for both CO<sub>2</sub> capture and storage already exists, but is expensive and challenging to implement on offshore installations. This is also true for steam cycles, mainly because of space and weight limitations and a harsh offshore environment. It is therefore necessary to develop a customized design that deals with these challenges. L. Nord, O. Bolland and E. Martelli have already started the design work with papers like: "Weight and Power Optimization of Steam Bottoming Cycle for Offshore Oil and Gas Installations" [13], "Design and Off-Design Simulations of Combined Cycles for Offshore Oil and Gas Installations" [14], and "Steam Bottoming Cycles Offshore - Challenges and Possibilities" [15]. These designs are not integrated with CCS and do not include a methodology for weight estimation. This thesis will continue the development of the steam cycle, for it to allow integration with CO<sub>2</sub> capture and desalination. The most important part will be to find a design that meets the CCS requirements and enables consistent and reliable weight estimation.

## 1.2 Objectives and Scope of Work

The main objectives of this master's thesis are to design and look into weight estimation methods for low weight steam cycles for offshore implementation. This work is a continuation of the specialization project completed in December 2015 [16]. The research question for this thesis is defined as:

“What is the preferred weight estimating method for steam bottoming cycles on offshore oil and gas installations, polynomial representation or scaling laws?”

To find the best method for weight estimation, it is necessary to have an accurate, realistic and well-planned steam cycle design. In this study, the final steam cycle design will be implemented as a process model in the GT PRO software for simulations. The design will be assessed on the following criterion:

- Weight.
- Reliable steam production to the CO<sub>2</sub> capture plant.
- Power generation. The necessary electricity for the CCS system should ideally be provided from the steam cycle, which will give a self-sufficient system.
- Possibility for offshore desalination.

The proposed design is based on a given case with six gas turbines on a floating production, storage and offloading unit (FPSO). For this "FPSO" case, detailed weight calculations will be presented. To generalize these findings, weight estimating polynomials and scaling laws are developed from simulation data in GT PRO. Validation is very important for this work. It is therefore essential to analyze real weight data as well.

To finalize the given objectives and answer the research question, the following tasks were performed:

- Literature study on relevant aspects:
  - Steam bottoming cycles, with emphasis on offshore installations.
  - Carbon capture and storage (CCS).
  - Mathematical representation, with emphasis on polynomials and scaling.
  - Available weight data for similar turbomachinery and heat exchangers.

- Developing of a low weight steam cycle design, including integration with CO<sub>2</sub> capture and desalination.
- Implementation and simplification of process models in Thermoflow software GT PRO.
- Analytical work on weight data from literature study, and simulations in Excel and GT PRO.
- Developing methodology for steam cycle weight estimation based on polynomial representation and scaling laws.
- Calculation, testing and validation of the weight estimating methods.
- Evaluating all results to form a conclusion, with emphasis on comparing the methods for weight estimation.
- Suggestions on further work.

## Thesis Disposition

This thesis is organized into 9 chapters. Chapters 2-6 are theoretical and are based on the literature study. Supporting literature for these chapters are found in the first appendix. The relevant components that were excluded from the weight calculations (mainly because of software limitations), and additional analysis for a deeper understanding are collected here. To simplify the reading, the most relevant information and the authors own analysis are collected in a chapter discussion in the end of each theoretical chapter.

The theoretical part is followed by the methodology Chapter, which is supported by analytical methodology in the second appendix. Based on the overall analysis, results are presented and discussed in Chapter 8. Complementary analysis and results, additional figures and tables are found in the third appendix. Conclusions and further work are located in the last chapter. The last appendix contains the computer code used in this study. If this thesis is read digitally, all references and citations are implemented as hyperlinks for easy navigation.

- Chapter 2 – Offshore Heat and Power Generation
  - this chapter concerns offshore heat and power generation, and contains some background information on offshore operations. A brief introduction to offshore related CO<sub>2</sub> emissions is also given. Combined cycles and cogeneration are a big part of this thesis. The existing offshore combined cycles on the Norwegian continental shelf are therefore presented.

- Chapter 3 – Combined Cycle Technology
  - Offshore designs do not include all systems that are common in an onshore combined cycle. In this chapter, only the most relevant systems for this study are presented; steam turbine, generator, heat recovery steam generator, and water treatment. Other relevant systems are available as supporting literature in Appendix A.2.
- Chapter 4 – Power Cycles
  - Power cycles are important to understand from a thermodynamic point of view. In this thesis, two power cycles are combined: the gas turbine Brayton cycle and the steam turbine Rankine cycle.
- Chapter 5 – CO<sub>2</sub> Capture, Transport and Storage
  - Carbon capture and storage (CCS) is essential for this thesis, even though no technical work is done on the capturing plant itself. The most important aspects for CO<sub>2</sub> capture are introduced in this chapter.
- Chapter 6 – Mathematical Representation
  - A major part of this thesis is analytical approaches to weight estimation. In this chapter, scaling, regression and interpolation are introduced. Some mathematical relations that are directly relevant for the steam cycle are also discussed.
- Chapter 7 – Methodology
  - The methodology chapter is very important, and describes among other the thermodynamic relations, low weight steam cycle design, process model simplification, and how the weight estimating methods were developed.
- Chapter 8 – Results and Discussion
  - In this chapter, the results are presented and analyzed. The results are divided into four sections: scaling results from the literature study, process models from GT PRO, polynomial representation and scaling laws. Sources of error are also presented.
- Chapter 9 – Conclusions and Further Work
  - The last chapter focuses on conclusions, limitations and suggestions on further work.



### 1.3 Risk Assessment

This thesis was completed without any excursions or laboratory work. No extensive risk assessment was therefore necessary.

### 1.4 Limitations

The most important limitations in this thesis are:

- All simulations are performed at design conditions for steady state operations. No off-design operations or transient analysis are considered.
- The six gas turbines are considered as one mass flow in GT PRO.
- The heat recovery steam generator and steam turbine designed from scratch, may not be economically or technically feasible.
- Accuracy limitations in the simulation software GT PRO.
- Calculated weights are not representing the total weight for an offshore steam cycle. Only the major components, namely steam turbine, generator and heat recovery steam generator are considered. GT PRO is not estimating the weight of the CO<sub>2</sub> plant.
- Only main components are considered in simulations, based on simplification of process models.

### 1.5 Software

- Mathematical analysis and plotting are done in MATLAB R2014b by MathWorks [17].
- Calculations, modeling and data analysis are done in Excel 15.16 by Microsoft Office [18].
- All process simulations in this project work are performed in GT PRO 25.0 by Thermoflow Inc. [19]. GT PRO module ELINK is used in combination with Excel.



# Chapter 2

## Offshore Heat and Power Generation

### Contents

- 2.1 Power Generation . . . . . 11
  - 2.1.1 Gas Turbines . . . . . 11
- 2.2 Heat Generation . . . . . 13
- 2.3 Emissions . . . . . 14
- 2.4 Offshore Combined Cycles . . . . . 15
  - 2.4.1 Snorre B . . . . . 15
  - 2.4.2 Oseberg D . . . . . 15
  - 2.4.3 Eldfisk E . . . . . 15
- 2.5 Chapter Discussion . . . . . 18

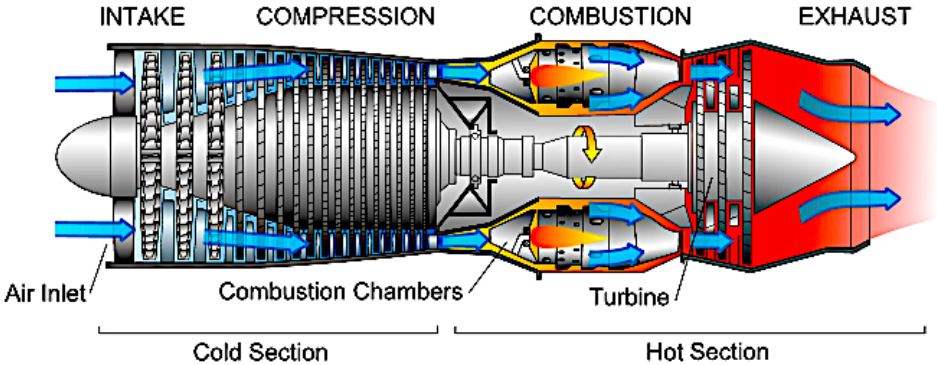


Figure 2.1: Main gas turbine sections [20].

Oil and gas production is very energy intensive because of operations like well drilling, natural gas compression and stripping of components like CO<sub>2</sub>. Shaft work, electricity, and process heat are some examples of what are needed for these operations. On offshore installations, none of these are available and needs to be produced on site. Broadly speaking, the necessary supply is a combination of heat and power. Systems that provide both are called cogeneration or combined heat and power (CHP). On the Norwegian continental shelf, both heat and power are normally provided from running gas turbines [21].

In this chapter, the most common processes for combined heat and power will be introduced with emphasis on offshore applications. Before reviewing the existing offshore cogeneration facilities on the NCS, the CO<sub>2</sub> emissions from oil and gas activities will be introduced. Onshore power supply is discussed in Appendix A.1.1 and a more detailed description of offshore gas turbines are found in Appendix A.2.1.

## 2.1 Power Generation

### 2.1.1 Gas Turbines

On the Norwegian continental shelf, gas turbines are the leading power supply [22]. In 2008, 167 gas turbines were running with an approximate total capacity of 3000 MW [23]. That is about 10% of the total capacity in the Norwegian hydropower portfolio in 2015 [24] and gives an average installed effect of 18 MW per gas turbine. That corresponds to about 9 full size 2 MW windmills [25]. Most of the running gas turbines are in the range of 20–30 MW, smaller turbines are installed for backup power [23] and peak load supply. Processed gas from the reservoirs is normally used as fuel in the gas turbines. Lower heating value (LHV) for natural gas is about  $37 \frac{MJ}{Sm^3}$ <sup>1</sup> [26] and the efficiency for gas turbines can be more than 40%, but the average is 31.4% on the NCS [23]. Many offshore turbines are dual-fuel types [27], which give the opportunity to run on other fuels like diesel.

The internal parts of both the compressor and turbine are divided into what are known as stages. One stage is designed with two rows of blades, one row is attached to the shaft (rotating, rotors) and the other row is connected to the casing (fixed, stators). Through these stages, pressure, velocity, and temperature are changed to produce power, see Figure 2.2. In the compressor, rotors are receiving rotation energy from the shaft. In the turbine, expanding gases exert a force on the rotors that contribute to rotation of the shaft. Typically, the turbine generates twice the power consumed by the compressor [28].

---

<sup>1</sup>Standard cubic meter (Sm<sup>3</sup>) is defined at 15°C and 1.01325 bar.

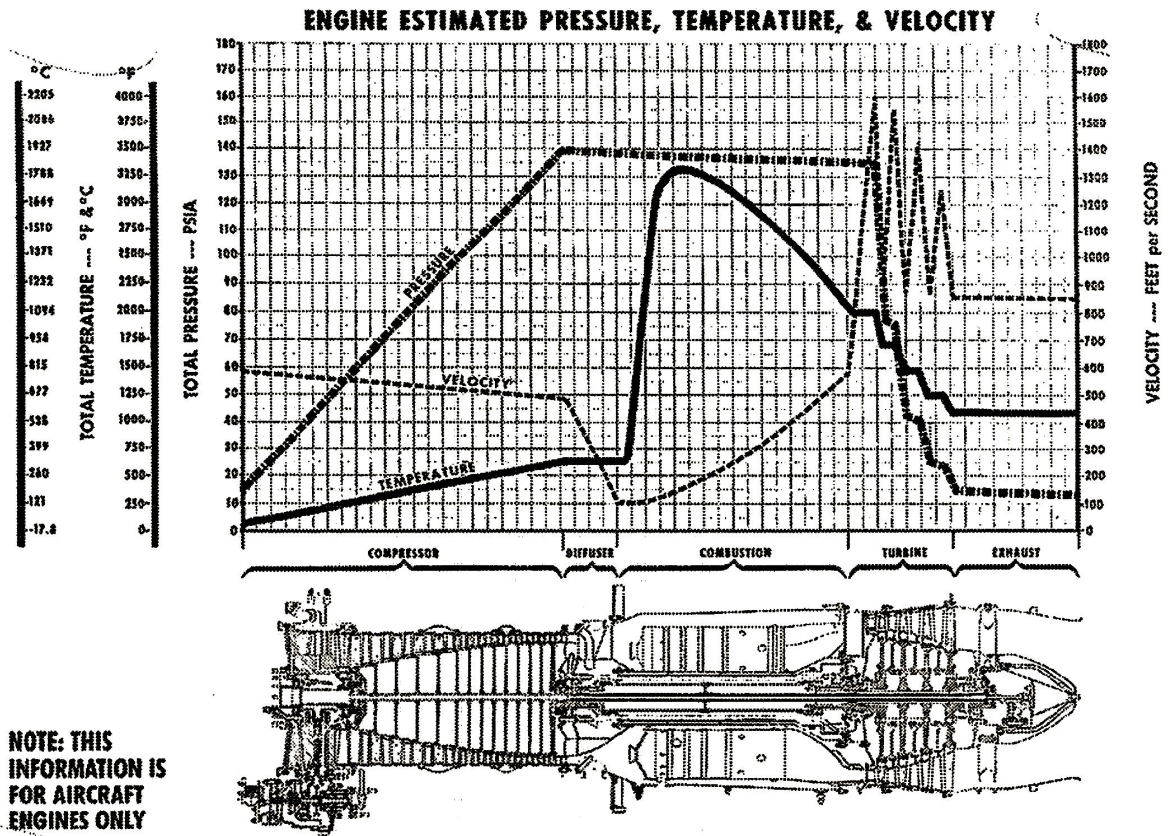


Figure 2.2: Temperature and pressure through aeroderivative gas turbine [29].

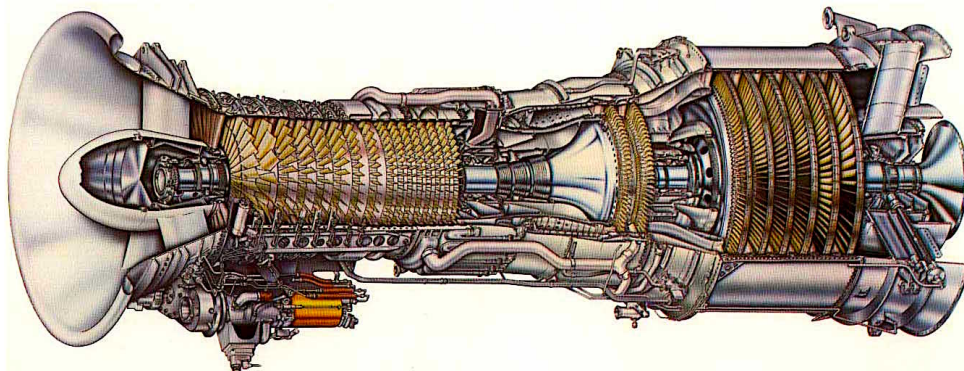


Figure 2.3: General Electric LM2500 [30].

The main components in a gas turbine are (see Figure 2.1):

- Air inlet.
- Combustion chamber.
- Compressor.
- Turbine.

This net power output on the shaft, is normally used to produce electricity in an electric generator or drive huge natural gas compressors or pumps directly. To achieve high efficiencies, it is not possible to just connect an arbitrary compressor and turbine with a combustion chamber [28]. They have to be matched carefully, and is one of the reasons why the gas turbine manufacturers are very conservative on design changes. This is supporting the possibility for scaling relationships.

The weight is critical for offshore gas turbines, luckily, the aviation industry has developed light weight turbines for decades. These turbines can be modified to produce shaft work or electricity in a generator, rather than thrust for an airplane. The most used offshore gas turbine on the NCS is the GE LM2500, see Figure 2.3, which is a derivative from the CF6 aircraft engine. Such turbines are classified as aeroderivative, and are very common on oil and gas installations, and marine applications like warships.

## 2.2 Heat Generation

Because of the increased incentives for energy efficient solution, new technology can be economically feasible on offshore installations. Process heat is necessary, and this heat is normally collected from some sort of heat exchange with the exhaust gas from the gas turbines. A common way to do this, is by installing a waste heat recovery unit (WHRU). Today, 59 gas turbines are integrated with WHRUs on the Norwegian continental shelf [31]. Many of the most promising solutions for CO<sub>2</sub> reductions are exploiting the heat from the gas turbine exhaust gas.

The heat recovery steam generator that will be described more in Chapter 3.2, is necessary for the implementation of a steam cycle. This unit produces steam, which can be utilized for power production and various heat loads. In this work, steam is needed in the CO<sub>2</sub> capture plant reboiler. Ideally, a steam turbine will expand the steam, and produce enough electricity to operate the CO<sub>2</sub> plant. Combined cycles can be a very efficient way to fulfill both the heat and power requirements on offshore installations. Heat recovery steam generators are fitted on all the installations introduced in Section 2.4. The big advantage with this system is that more power can be produced with the same amount of fuel in the gas turbines. Normally, large amounts of energy leaves with the high temperature exhaust. On the other hand, price and offshore weight limitations are great challenges.

## 2.3 Emissions

Some of the greatest challenges with operating simple gas turbine cycles are the huge amount of unwanted emissions like CO<sub>2</sub>. Public attention, increasing CO<sub>2</sub> taxes, and global warming are some of the reasons why new solutions are needed for offshore power generation. CO<sub>2</sub> emission from the offshore industry is mentioned in Section 1.1, and the source distribution can be seen in Figure 2.4. Gas turbines (79.4%), flaring (9.6%) and engines (8.0%), normally diesel types, are the major contributors.

Flaring is controlled combustion of natural gas, and is allowed because of its feature as a safety mechanism. On the NCS, flaring is due to high emissions regulated by the government. In an environmental perspective it is better to burn the natural gas and release CO<sub>2</sub> instead of methane, the major component in natural gas. Methane has a much higher potential for global warming than CO<sub>2</sub> [32]. The amount of flaring, consequently also CO<sub>2</sub> emissions, is significantly reduced with technological development. Carbon capture and storage could be the next step for reducing emitted CO<sub>2</sub>, and this work will contribute to weight reduction on the necessary steam cycle. The technology is already available, but has to be designed according to offshore specifications.

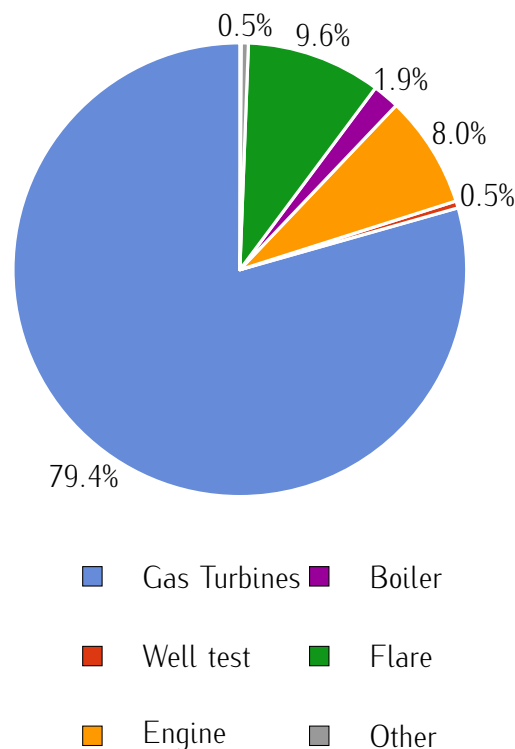


Figure 2.4: CO<sub>2</sub> emissions from the Norwegian petroleum sector in 2012 [2].

## 2.4 Offshore Combined Cycles

### 2.4.1 Snorre B

In terms of reduced CO<sub>2</sub> emissions compared to running a standard gas turbine cycle, Snorre B is the largest operating combined cycle on the NCS, see Table 2.1. The plant is also designed to deliver steam for process heat at 6 bar. At maximum steam extraction, the process heat delivered is about 8 MW, without any extraction, the steam turbine delivers 17.3 MW. The surplus power from the steam turbine can be sent to Snorre A, which is not self-sufficient with power, through a 22 MW electric cable [33]. Under special circumstances it is also possible for Snorre B to receive power from the three gas turbines installed on Snorre A, that can deliver  $3 \times 18.5 = 55.5$  MW. Snorre B has two GE LM2500+ turbines installed, which deliver 29 MW each. The HRSG or synonymously WHRU-SG on Snorre B is vertical with a double inlet, one for each gas turbine.

### 2.4.2 Oseberg D

The Oseberg D combined cycle is producing both heat and power from two GE LM2500+ turbines. Originally the HRSG was designed with a single pressure drum, see Figure 2.6. Today it has been replaced by a once through heat recovery steam generator (OTSG) [34]. The plant is also designed to deliver steam for process heat at 1 bar. At maximum steam extraction the process heat delivered is about 11.7 MW, without any extraction the steam turbine delivers 15.8 MW. The most special feature with the Oseberg design, is that steam from the OTSG is transported in a 400-meter pipe. This pipe ends up at the interconnected platform, Oseberg Field Center, where the steam turbine is placed. Schematics of a quite generalized offshore combined heat and power cycle with the most important components can be seen in Figure 2.5.

### 2.4.3 Eldfisk E

This combined cycle is mainly designed for electricity production, so no steam extraction is possible. Some steam is produced in a separate system to evaporate seawater for desalination. The original design can be seen in Figure 2.7, but has later been modified. A total of three gas turbines are feeding two once through heat recovery steam generators [35], that produces steam for the 10.3 MW steam turbine. One of the major tasks for Eldfisk is seawater injection into the reservoir. To save work, this seawater is first used for cooling in the steam turbine condenser.



Table 2.1: Existing offshore combined cycles on the Norwegian continental shelf [36].

	Snorre B	Oseberg D	Eldfisk E
Steam turbine power [MW] (No heat extraction)	17.3	15.8	10.3
Steam turbine power [MW] (Full heat extraction)	15.2	14.3	
Process heat [MW]	8.0	11.7	
CO <sub>2</sub> reduction [ $\frac{kton}{year}$ ] (vs. simple cycle)	92	80	50
Fuel savings [ $\frac{MSm^3}{year}$ ] (vs. simple cycle)	39	36	23

### Technical Data and Schematics for Offshore Cycles

The most important values for heat and power generation on the existing offshore cogeneration plants on the Norwegian continental shelf are gathered in Table 2.1. It is sensible to take notice of these cycles when the new steam cycle design is developed. Especially the modifications, like retrofit with once through heat recovery steam generators are interesting. Indirectly, this is telling something about the experiences from operating offshore steam cycles.

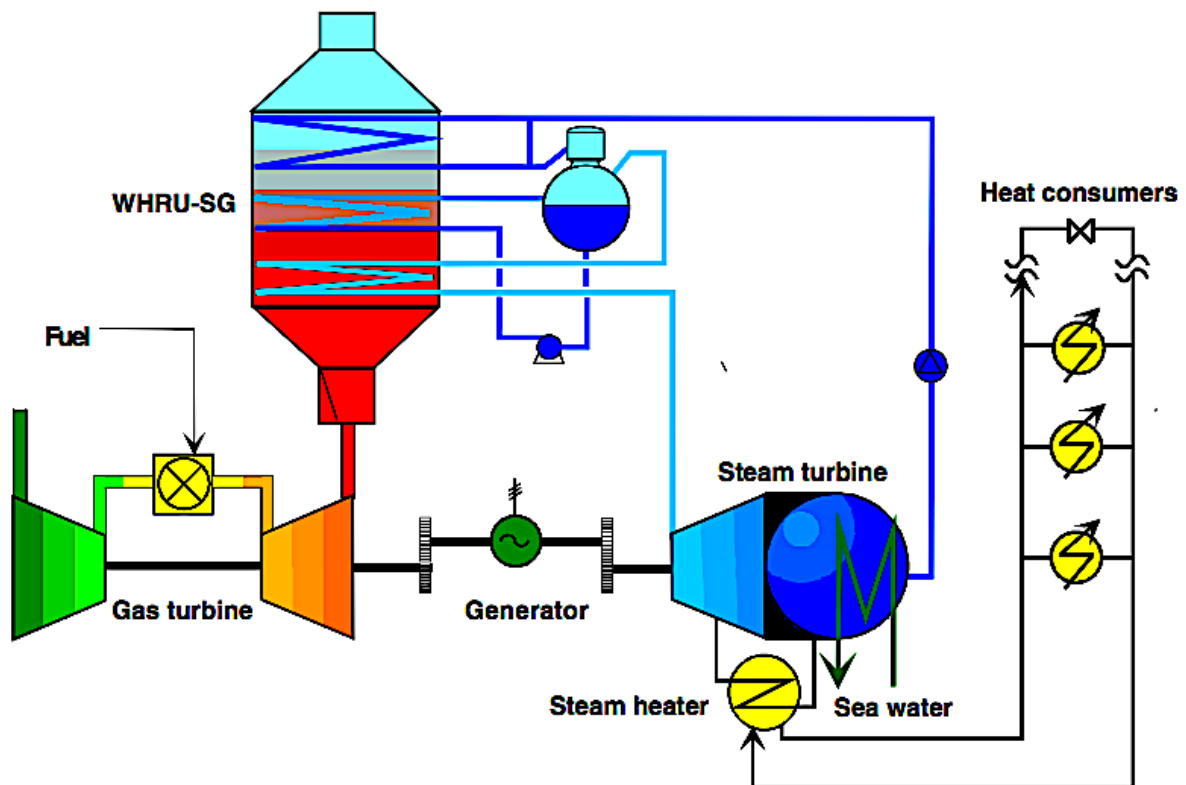


Figure 2.5: Schematics of an offshore combined heat and power cycle. [36].

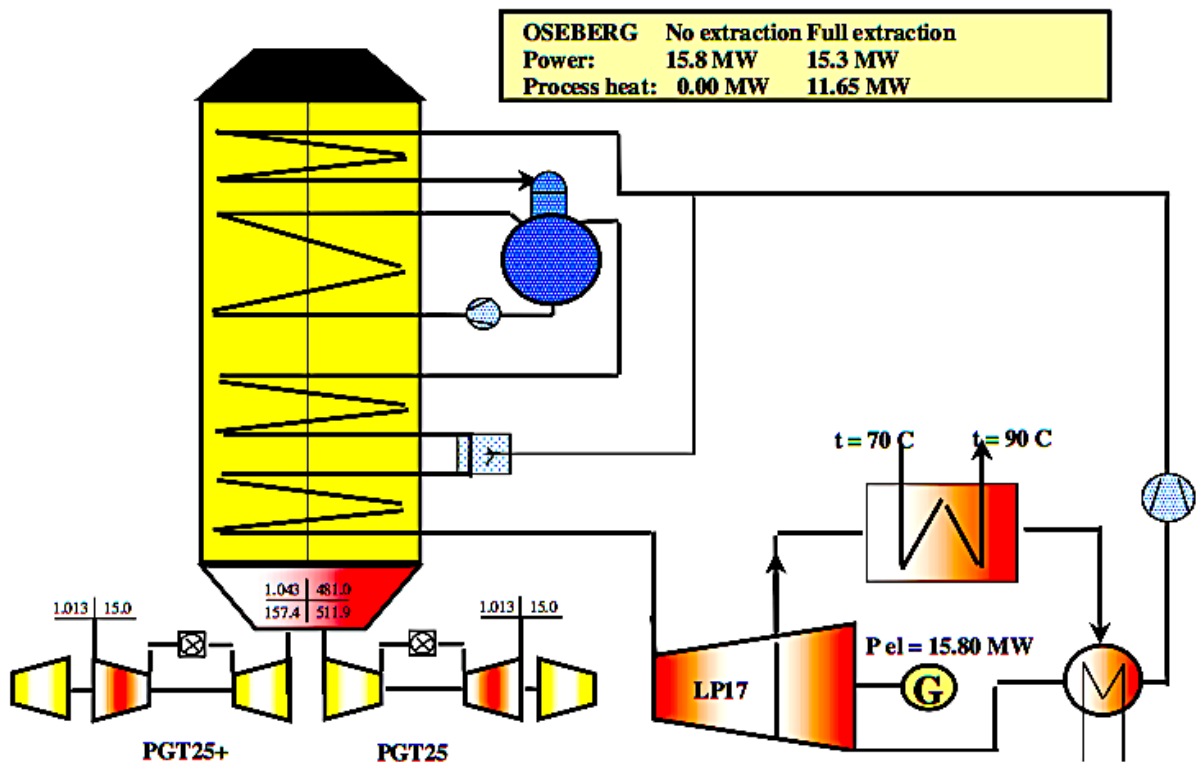


Figure 2.6: Original design of the Oseberg D facility [36].

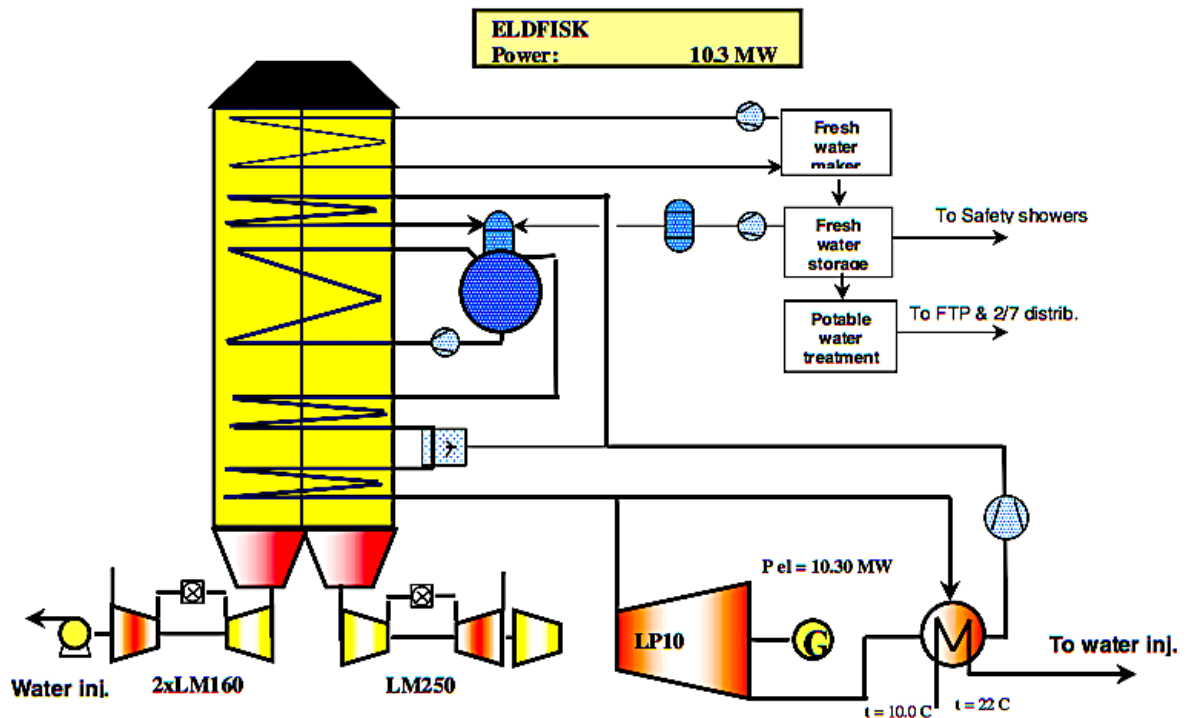


Figure 2.7: Original design of the Eldfisk E facility [36].

## 2.5 Chapter Discussion

The gas turbine design and setup are fixed for all the cases considered in this thesis. On most installations, including the cases in this work, the gas turbines provide the major electrical power production. Some back-up capacity is normally available for peak loads, but it is most likely not enough to cover the added power load from a CO<sub>2</sub> plant. Because onshore power supply is not discussed here, this power needs to be produced on site. This is also true for the process heat, here in terms of steam that goes into the CO<sub>2</sub> plant. Snorre B, Oseberg D and Eldfisk E have demonstrated the possibility of operating combined cycles on offshore installations. The Oseberg D plant is able to deliver 15.8 MW of electrical power and 11.7 MW of process heat simultaneously. That seems like an attractive basis for a steam cycle design that is to be integrated with CO<sub>2</sub> capture.

The main motivation for installing a CO<sub>2</sub> capture plant, is obviously to reduce the amount of released CO<sub>2</sub> to the atmosphere. After reviewing the available technology for offshore heat and power generation, it should be possible to develop a first class steam cycle design for offshore integration with CCS. Once through heat recovery steam generators and extraction based steam turbines are most common on the existing offshore installations. Back-pressure turbine was chosen as the most promising technology in the specialization project, mainly because of its weight reducing potential. This will be investigated further in the next chapter.



# Chapter 3

## Combined Cycle Technology

### Contents

- 3.1 Steam Turbine . . . . . 21
- 3.2 Heat Recovery Steam Generator . . . . . 23
- 3.3 Generator . . . . . 29
- 3.4 Water Treatment . . . . . 30
- 3.5 Chapter Discussion . . . . . 34

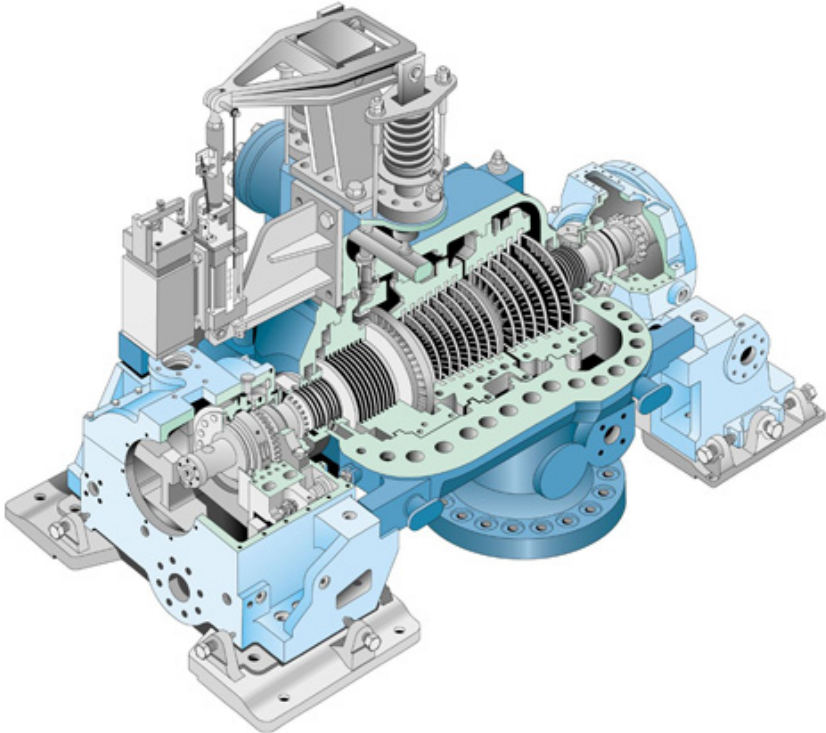


Figure 3.1: Back-pressure steam turbine [37].

This chapter will introduce the major components in a cogeneration power plant. The technology behind every component is very extensive, so in depth analysis is not possible. Therefore, most of the evaluations will be based on the relevant aspects for this thesis. Gas turbine, condenser, pump, deaerator and a generalized combined cycle are found in Appendix A.2.

### 3.1 Steam Turbine

A steam turbine (ST) is a much used construction for power production. There are mainly two types of steam turbines, the condensing and back-pressure (non-condensing) turbine. In this work, the steam turbine will provide both power and steam at a certain pressure level. For condensing turbines, steam can be extracted through the casing. Special governors and valves are necessary for constant pressure extraction for varying loads. The remaining steam is completely expanded and exhausted to a condenser, this is implemented on the existing offshore steam cycles. In a back-pressure turbine, see Figure 3.1, the steam leaves at the pressure required by the process [28]. In this case determined from the CO<sub>2</sub> capture plant specification. Because the steam is not expanded to a sub atmospheric pressure, the condenser is superfluous and the sizing requirements are reduced. From a weight perspective, this is very promising, especially when the condenser weight is included.

The main parts in the steam turbine are:

- Rotors.
- Stators.
- Nozzles/Flow passages.
- Casing.

Advanced turbines operate at multiple stages, normally divided into low pressure (LP), intermediate pressure (IP) and high pressure (HP). Reheat is also common, and can in short terms be described as additional heating of the steam between turbine stages. The existing plants mentioned in Section 2.4 contains single pressure steam turbines, mainly because of size and weight limitations. The requirements for a modern steam turbine are [28] [38]:

- Offshore: Low weight and compact design.
- Reheat for increased efficiency.
- Multistage for increased efficiency.
- Wide range of operations for varying loads.

- Efficient over the whole operational range.
- Fast startups for both hot and cold system.
- Modular for fast installations.

Weight and size limitation are fundamental for offshore steam turbines. That is the main reason why reheat and multistage systems will not be examined further in this thesis. In the same way as for gas turbines, the offshore steam turbines should be designed as a skid module. Operational load is often fluctuating frequently during offshore operations, therefore is good performance over a wide range of operations important.

### **Offshore Steam Turbine Skid**

It is assumed that the size of a 15–20 MW steam turbine skid has approximately the same size as a typical gas turbine skid [36]. This estimate is based on the existing steam turbines installed offshore. The weight should then be in the range of 150–175 tons, and contain these parts:

- Steam turbine.
- Intake (admission) system.
- Turbine bypass system.
- Speed reduction gear.
- (Steam extraction valves).
- Lubrication system.
  - Pumps, filters and tanks.
- Hydraulic system.
  - Pumps.
- Control system.
- (Condenser).
  - Evacuation system.
- Enclosures and internal piping.
- Generator.

### 3.2 Heat Recovery Steam Generator

Heat recovery steam generators utilize the heat from the gas turbine exhaust to produce steam. This important component is essential for cogeneration or combined heat and power (CHP) plants. In this thesis, the HRSG will be designed for fulfilling steam requirements on flow rate, temperature and pressure. This steam will be used in the reboiler of a CO<sub>2</sub> capturing plant. It is also possible to utilize this steam in a steam turbine to produce power. For additional steam production, it is possible to implement a duct burner for fresh air firing in the HRSG. When sufficient steam production is critical, this could be used as a backup system. Because the CO<sub>2</sub> capture plant is handling the gas turbine exhaust, it may be unnecessary with additional heating. If one or more gas turbines stops, the necessary amount of steam is also reduced.

The main designs for heat recovery steam generators can be divided into vertical and horizontal, which refers to the exhaust gas flow direction relative to the ground. Water/steam is flowing in tubes normal to the direction of exhaust gas. This implies that in a horizontal HRSG the water/steam flow will have natural circulations due to gravity, see tube direction in Figure 3.2. For vertical design, the gravity component will be approximately zero, and circulating pumps may be required [39]. The footprint is in general smaller for vertical HRSGs, and can potentially be placed on top of the gas turbines. Therefore is vertical designs promising for offshore installation.

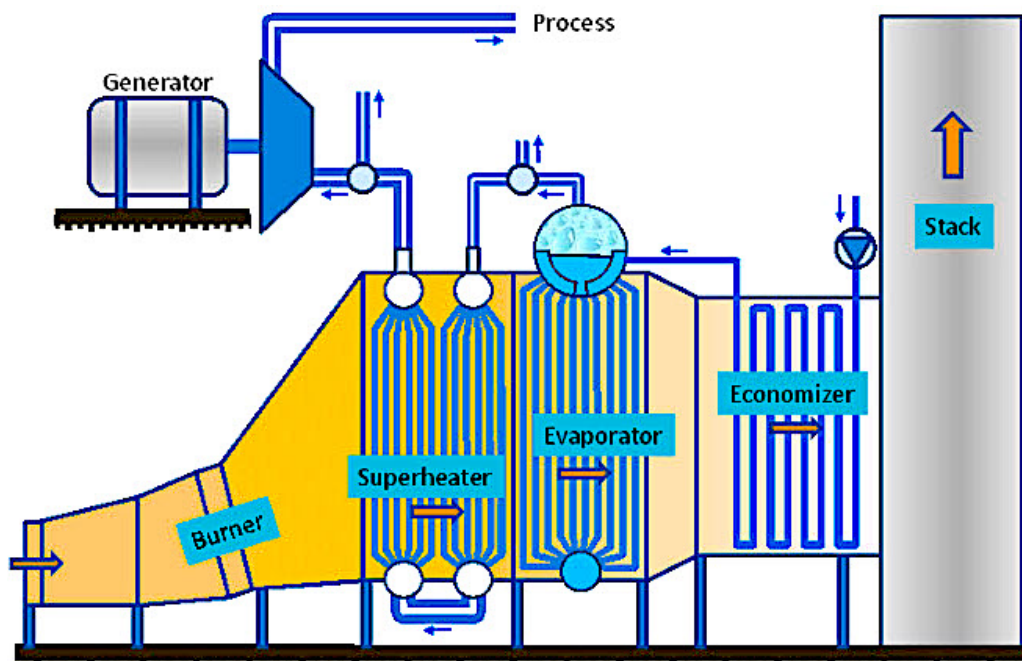


Figure 3.2: Heat recovery steam generator with steam drum and duct burner [40].



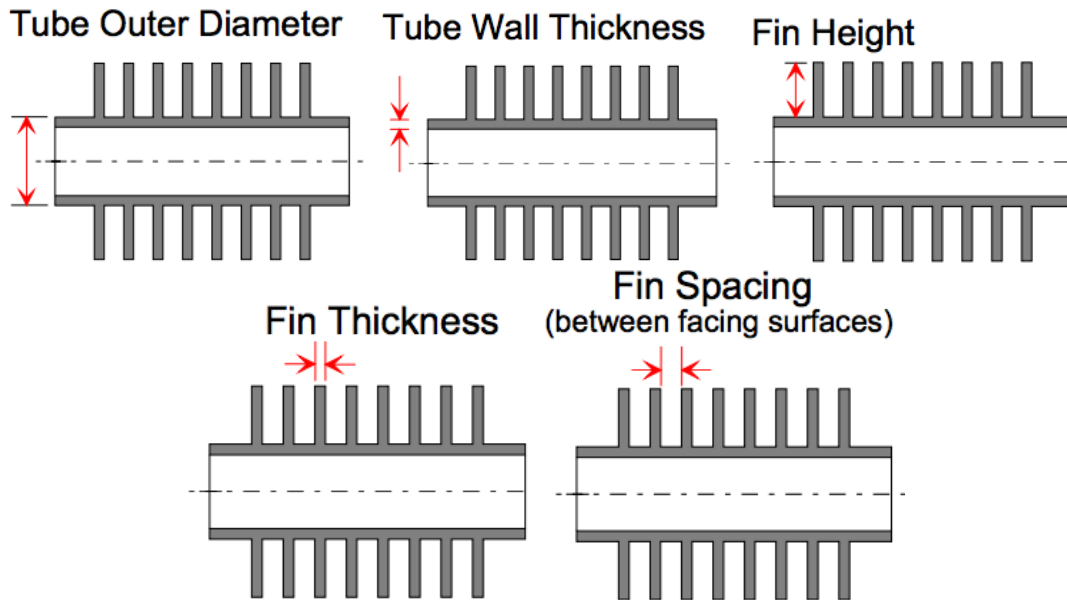


Figure 3.3: Fined tube with main design parameters [28].

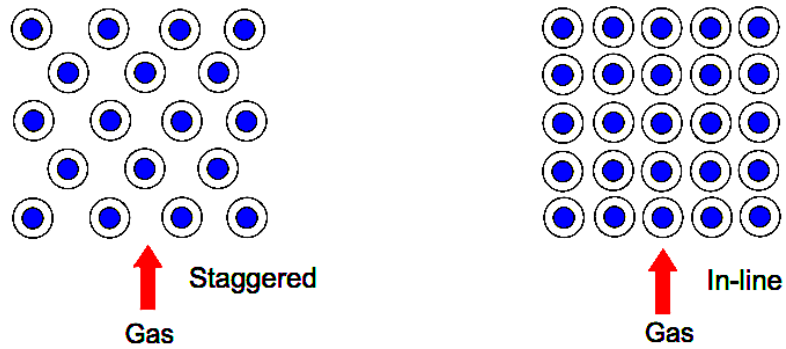


Figure 3.4: Tube row arrangement [28].

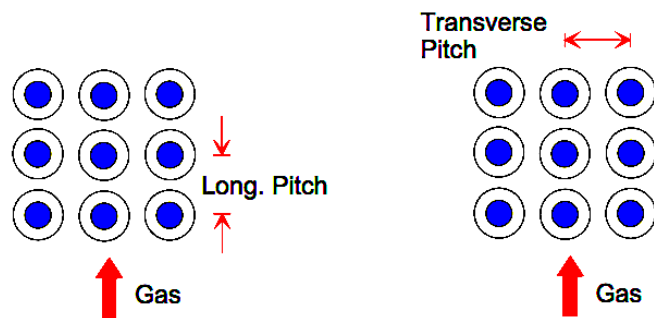


Figure 3.5: Tube spacing [28].

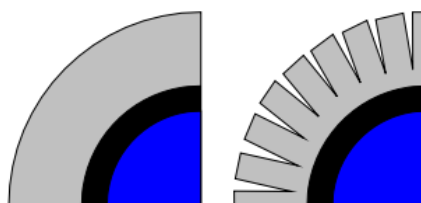


Figure 3.6: Solid and serrated fins attached on tube [28].

The standard heat recovery steam generator design contains three sections:

- Economizer (ECO). Heating of water to saturation.
- Evaporator (EVA). Turns the liquid water into water vapor. Also called boiler.
- Superheater (SUP). Heating of steam to high temperatures.

Auxiliary equipment for heat recovery steam generator can include [28]:

- Duct burners.
- Pumps.
- Fans.
- Deaerators.
- CO and selective catalytic reduction (SCR) catalyst.

### **Pinch Point Temperature Difference**

The pinch point temperature difference (Pinch/Pinch temperature) is an essential design parameter for heat recovery steam generators. It is the smallest temperature difference between the water/steam and exhaust gas, and is strongly affecting the weight. In general, a high pinch allow lighter equipment, and values over 30K is not unrealistic for offshore plants. For gas turbine exhaust, the pinch point is normally located in the transition between economizer and evaporator, see Fig. B.1.

### **Tubes**

Tube bundles with specified arrangements and spacing, see Figures 3.4 and 3.5 , are covering the cross sectional area at multiple stages through the HRSG, see Figure 3.2. This design will affect the exhaust gas pressure drop, which is proportional to the gas velocity squared. The allowed pressure drop is normally defined and impacts the HRSG sizing.

- Small  $\Delta P$  allowed = Large cross sectional area and short HRSG in longitudinal direction.
- Large  $\Delta P$  allowed = Small cross sectional area an long HRSG in longitudinal direction.

The heat transfer is determined by the number and configuration of tubes, because heat transfer area is proportional to the number of tubes. Design parameters for tubes are normally outer diameter and wall thickness, see Figure 3.3. A vertical HRSG allow for smaller tube diameters if circulation pumps are installed. This increases power consumptions, but could potentially reduce weight.

## Fins

The heat transfer coefficient is much higher for the water/steam inside the tubes than for the exhaust gas on the outside. To compensate for this difference, the heat transfer area needs to be increased on the outside. One solution is to attach fins around the pipe, which increases the contact surface between exhaust gas and tube. This leads to a more efficient heat transfer between exhaust gas and the flowing medium in the tubes. Three different design parameters for fins are showed in Figure 3.3. Fins could either be continuous/solid or split/serrated, see Figure 3.6. Serrated fins are most common; their advantage is increased fin height and enhanced heat transfer due to turbulence at the tip [41]. The boundary layer is therefore reduced, consequently is the heat transfer coefficient increased. Typical heat transfer coefficient in the HRSG are:

- Economizer  $\approx 3000\text{--}5000 \frac{W}{m^2K}$
- Evaporator  $\approx 4000\text{--}8000 \frac{W}{m^2K}$
- Superheater  $\approx 500\text{--}2000 \frac{W}{m^2K}$
- Exhaust gas @ 1atm  $\approx 30\text{--}50 \frac{W}{m^2K}$

## Exhaust Gas Dew Point

When the exhaust gas temperature is reduced through the HRSG, sulfur and water dew point could potentially lead to corrosion. For natural gas (NG) the sulfur content is normally very low, so this is not a big concern when gas turbine exhaust gas is considered. Liquid water can form nitric or sulfur acid in contact with flue gas and is therefore undesirable on the gas side. Water dew point is typically around 40°C for gas turbine exhaust [28]. Bulk temperatures are normally much higher, but close to cold surfaces liquid dropout could occur. To eliminate this risk completely, the industrial standard is to heat the feedwater to minimum 60°C [28].

## Drums

Steam drums connects the different sections in the heat recovery steam generator; economizer, evaporator and superheater. The main tasks are to separate liquid water from saturated steam, and remove impurities in the feedwater. Because of continuous condensation and evaporation inside the drum, impurities will accumulate in the liquid. They can be removed by draining some of the liquid, this is called blowdown (Typically 0.1–1.0% [28]). The drum is filled with about 50% liquid water, where the surface is boiling. For plants with multiple pressure levels, it is one drum for each level.

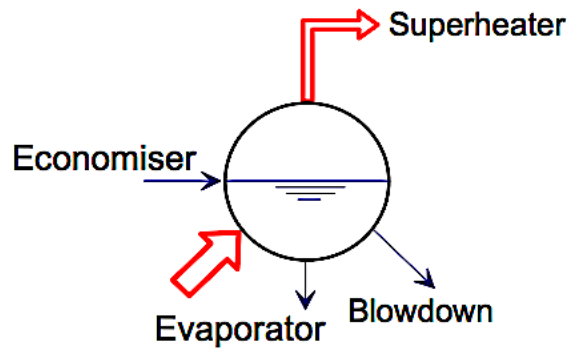


Figure 3.7: HRSG steam drum [28].

Hot water from ECO enters through perforated pipes in the drums liquid section. Liquid water is then flowing to the EVA, and two phase mixture is returned. This mixture goes through hydro cyclones to separate steam and liquid. At the top, steam is flowing through scrubber elements before it enters the SUP, see Figure 3.7. Steam drums were originally installed on all offshore steam cycles, but some have later been modified.

### Materials

The most common materials used in heat recovery steam generators are [42]:

- Tubing.
  - ASTM A335<sup>1</sup> [44]
    - \* Grade T22: ECO and EVA.
    - \* Grade T91: SUP.
- Downstream.
  - Carbon steel.
- Fins.
  - Stainless steel, ASTM A176 TP409.
  - or Carbon steel.

The Incoloy alloy has some very promising specifications for offshore applications like once through steam generators. This alloy is produced by the Special Metals Corporation:

<sup>1</sup>ASTM A335 Pipe is a seamless ferritic Alloy-Steel Pipe for high temperature service. Pipe ordered to this specification shall be suitable for bending, flanging and similar forming operations, and for fusion welding. [43]

"INCOLOY alloy, first developed as an aerospace superalloy and now used in a range of industrial applications, combines excellent strength and fabricability with outstanding resistance to prolonged exposure up to 1300°C. Its exceptional properties result from the mechanical alloying process by which it is made; a process which allows a fine distribution of yttrium oxide particles to be incorporated into a highly corrosion-resistant Fe-Cr-Al alloy [45]."

Special materials like this could eliminate the need of a separate bypass stack, which is both heavy and bulky. This reduction in material usage will offset some of the extra cost for these materials. An integrated stack is also favorable for the flexibility regarding the power demand. If a sudden drop in the power load occurs, it may be necessary to run the gas turbine as a simple cycle. Then it is very favorable to have the possibility to just close the feedwater and run the OTSG dry. It is common to run the gas turbine cycles on part load during normal operation offshore [46]. Another important aspect with Incoloy, as mentioned by the producer, is corrosion resistance. That applies both for the internals with water contaminants and externals with harsh ambient conditions offshore [15].

#### **Once Through Heat Recovery Steam Generator**

An once through heat recovery steam generator (OTSG) is quite different from a more standardized HRSG. They are very relevant for offshore installations, and have replaced drum based systems on two out of three combined cycles on the Norwegian continental shelf. The main motivation is reduced size and weight, while the biggest concern is increased purity requirements on the feedwater.

Once through heat recovery steam generators are more flexible and opens the possibility for weight reduction from removing the steam drums and the bypass stack. With proper material selection, exhaust gas can flow through the system when no steam is produced. The defined sections from standard heat recovery steam generators; economizer, evaporator and superheater are not present in this design. Varying with load, the sections where preheating of water, evaporation and superheating occurs will be displaced. In an OTSG, the feedwater enters at the cold end and flows through continuous piping to the hot side. The hot side is where exhaust gas enters from the gas turbine's outlet.

Superheated steam is produced, and can be utilized in either a steam turbine or in various heat demanding processes. The major disadvantage with OTSGs compared to more standardized HRSGs, is no possibility for blowdown [28]. This leads to extreme requirements for the purity of the feed and makeup water. Accumulated impurities are not easily dealt with in these systems. Simulations

done on OTSGs designed for offshore applications resulted in an approximate weight reduction of 67% compared to an onshore HRSG [15]. The net plant efficiency was reduced by about 3% with this steam generator design.

### Offshore HRSG Skid

These components should be part of the HRSG skid [36]. Some design modifications are necessary if an OTSG is chosen instead of drums based HRSG:

- Economizer, Boiler bank and Superheater (or OTSG).
- Main and bypass stack (OTSG can operate without a bypass stack).
- Steam drum and blow down tank (Not for OTSG).
- Makeup water pumps.
- Chemical dosing station.
- Control systems.
- Internal piping.

## 3.3 Generator

The offshore power is produced in a generator. Necessary mechanical energy is supplied from the rotating shaft of a gas turbine or steam turbine. Electrical energy is generated from electromagnetic induction that leads to electric current in wires out of the generator, see Figure 3.8. Rotational speed of the turbine shaft into the generator determines electric frequency, normally either 50 or 60 Hz (rotations per second). Higher frequencies usually lead to more compact equipment. In Norway 50 Hz is normal onshore, hence both 50 and 60 Hz is used offshore on the Norwegian continental shelf.

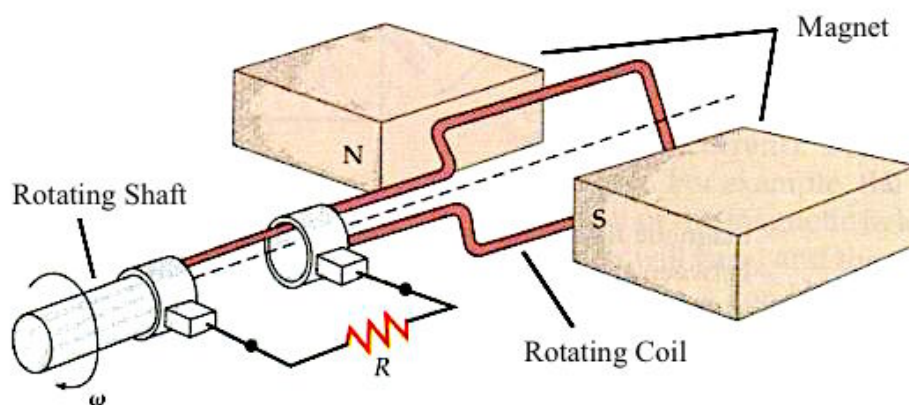


Figure 3.8: Generator principle, producing electricity from rotation energy [47].

### 3.4 Water Treatment

Easy access to fresh water is a significantly challenge offshore. The necessary amount of water needed for running the steam demanding systems and operating the platform (drinking water, cleaning etc.) needs to either be transported by tankers or produced offshore in a desalination plant. Seawater can be processed and made into fresh water by either distillation or membrane technology. Other technologies are also available, but these two are the most common.

It is essential with very purified water in an OTSG system, because no natural outlets for salts and other contaminants exists. As mentioned in Section 2.4, a desalination plant exists at Eldfisk. In addition to desalination, these systems are necessary for satisfactory water quality if a once through heat recovery design is preferred [15]:

- Deaeration.
  - Removal of components.
    - \* Oxygen.
    - \* CO<sub>2</sub>.
    - \* Argon.
    - \* Nitrogen.
- Mixed-Bed demineralization.
  - Removal of minerals from seawater.
- Chemical additives/Condensate polishing.
  - Hydrazine for oxygen removal.
  - Ammonia for pH control.

#### Desalination

The technologies for desalination can be divided in two groups. For this work, only distillation processes are considered. Distillation utilizes the excess heat from other processes to produce fresh water with a minimum of electrical power consumption.

- Membrane processes.
  - Reverse Osmosis (RO).
  - Electrodialysis (ED).

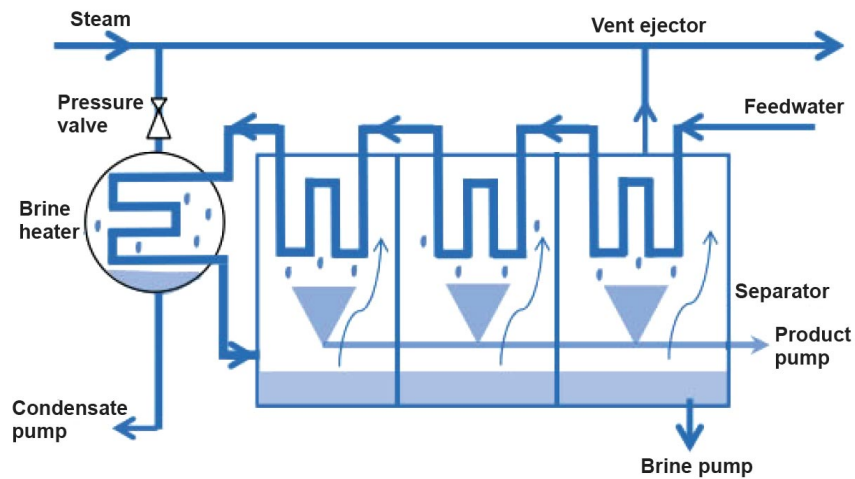


Figure 3.9: Simplified multi stage flash (MSF) process diagram [49].

- Distillation processes.
  - Multi Stage Flash (MSF).
  - Multi Effect Distillation (MED).
  - Vapor Compression (VC).

According to the GT PRO help files [48], MSF technology dominated the desalination industry before the 1990s. However, due to its intensive energy demand, it is not widely used in new construction. Multi-effect distillation (MED) plants can operate with a top brine temperature (Highest water temperature in the system) of lower than 70°C. Brine is a solution of salt dissolved in water. The MED process can be combined with a thermal vapor compression (TVC) process, to form the hybrid desalination process MED-TVC. The thermal efficiency of this hybrid system is significantly improved. In the past decade, MED has become the major thermal desalination technology in new constructions.

### Multi Stage Flash (MSF)

In the multi stage flash system, the external steam goes to a brine heater. From here, the heated brine flows into an evaporator which consist of a heat recovery section and a heat recovery section. The rejection section is cooled by sea water, which also is used for makeup to the system. In the recovery section, brine is preheated before entering the heater. This section is a series if flash chambers operating at different pressures [48]. In the first chamber, the high temperature brine is entering in the bottom. Because the chamber pressure is lower than the saturation temperature for the brine, vapor is formed. This flashed vapor is passing through a demister, before it condenses on the cool brine carrying tube walls in the top of the chamber. The condensate is collected and brought to the next, lower pressure chamber, to repeat the process and produce fresh water, see Fig 3.9.



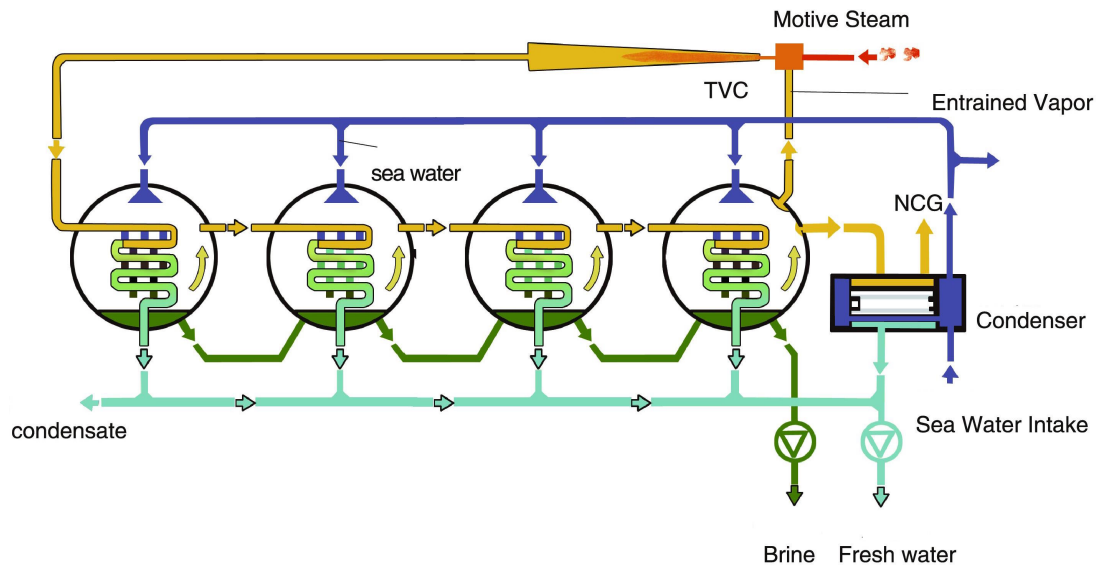


Figure 3.10: Simplified multi effect distillation with thermal vapor compression (MED-TVC) process [50].

### Multi Effect Distillation (MED)

To distill the brine, the MED technology evaporates brine in multiple stages. Each evaporation stage is called an effect. The evaporated water is in theory forming a salt free vapor, even though some containments will be brought along. Multiple stages increase the thermal efficiency, see TQ diagram in Fig. C.36, and help to increase the purity of the fresh water. The fresh water is produced from vapor condensation, which releases heat that is utilized to evaporate additional brine at a lower pressure. This design causes the external steam to be necessary for the first effect only, where the highest pressure in the system is found. All the other effects are using the heat recovered from condensation in the neighboring higher pressure effect.

The efficiency of the MED process can be increased by adding a thermal vapor compression (TVC) system [48]. With TVC, a fraction of the vapor from the final low pressure effect is sucked (LP Suction) and compressed by a steam jet ejector. The jet ejector is driven by the motive steam from the steam turbine (HP Motive), see Fig. 3.11. This mixture (Discharge) enters the first effect, acting as an additional heating source for MED process. This combined system forms a MED-TVC desalination plant.

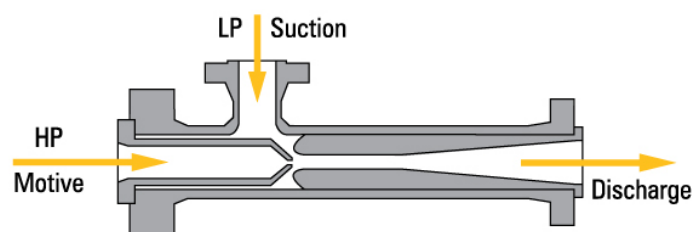


Figure 3.11: Steam jet ejector for thermal vapor compression (TVC) [51].

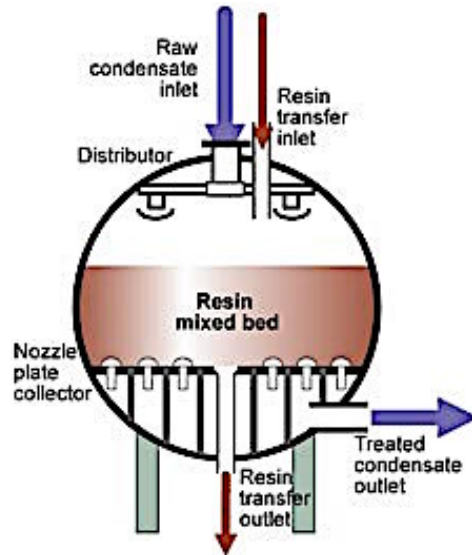


Figure 3.12: Condensate polisher with resin bed [52].

### Water from Shore

The other alternative for offshore fresh water is supply by tankers. Purified water from shore can then be transported in stainless steel tanks to site. The system can then be filled with the necessary amount. Makeup water can be stored in feedwater tanks on the installation. Regardless of chosen alternative, a feedwater tank needs to be installed. The best alternative must be assessed from the balance between cost and weight/size.

### Condensate Polishing

Condensate polishing is a method for removing particles like minerals or other contaminations. The condensed water is normally relatively pure, but some deposits will accumulate over time. Therefore, they need to be removed so that the high water quality is maintained. Raw condensate is flowing through a bed of resin that collects the contaminants. Treated condensate leaves at the polisher bottom, see Figure 3.12. It may also be necessary to add chemicals like hydrazine and ammonia to ensure no dissolved oxygen and the optimal pH level.

### 3.5 Chapter Discussion

When combined cycles are considered, there are many sub-systems to take into account. It was not necessary to evaluate all these systems in detail for this work, but all the major ones are briefly described here or in Appendix A.2. In terms of electric generators, higher frequencies are normally correlating with lower weight and more compact systems. Airplanes can typically operate on 400 Hz frequencies, but the consequence is reduced efficiency. To save weight and space, 60 Hz is chosen as the best alternative for the offshore steam turbine design. On land based combined cycles, it is possible to operate both the gas turbine and the steam turbine on the same generator. If this is possible to implement offshore, it could potentially make a more compact system.

The steam turbine is a big part of the work done in this thesis. From the specialization project [16] on the same subject, a back-pressure turbine was chosen as the best alternative for offshore implementation. Off-design and part load simulations are not performed in this study, but should be investigated in further work. It would be interesting to look at how sensitive the steam cycle power production is to changes in e.g. gas turbine mass flow and temperature. These type of changes would also affect the CO<sub>2</sub> system. Based on previous findings and the ongoing literature study, the back-pressure steam turbine technology is continued for the steam cycle design.

To reduce the footprint of the heat recovery steam generator, a vertical design is attractive. There exist examples of HRSGs that are placed on the top of the gas turbine(s). This would reduce the total footprint, even though height restrictions are relevant for offshore installations. A compact and efficient integration of the different systems in the steam cycle should be investigated further. Such detailed design considerations for the plant are not possible to perform in GT PRO. The once through heat recovery steam generator was in the previous work selected as the best design for an offshore steam cycle. This is also supported from the modifications on the existing offshore steam cycles. With Incoloy tubes and stainless steel fins, a lot of weight is saved by avoiding the necessity of a bypass stack. These materials can handle the gas turbine exhaust gas temperature, even though no water is circulating in the HRSG. Compared to other common HRSG materials, reduced corrosion from harsh offshore conditions is expected for Incoloy. A high pinch temperature is beneficial for further weight reduction, primarily because less heat transfer surface area is necessary in the HRSG.

Water treatment is important for combined cycles and adds complexity to the offshore system. If OTSGs are used, the extreme requirements on water purity are possibly best fulfilled with water from shore. Even with drum based steam generators including blowdown, Statoil have experienced

problems accompanying the water quality on some of the existing offshore cogeneration plants. This information emerged during discussions with professor Olav Bolland. Regardless of this, it would be interesting to test the modern desalination technology. Based on available literature and GT PRO simulations, multi effect distillation stand out as the best alternative. According to GT PRO simulations, the thermal vapor compression system had a negligible effect on the total weight, and is therefore included. Significantly higher weight and older technology is working against the multi stage flash technology, even though a smaller footprint is beneficial. MED-TVC technology is therefore chosen as the best alternative if desalination is to be integrated with the steam cycle design. To reach the necessary level of water purity, condensate polishing should be implemented.

It is very expensive to install equipment offshore, and everything are limited on size and weight. Therefore, compact and light weight equipment that can still deliver adequate efficiencies are necessary. In other words, offshore cycles should deliver a low weight-to-power ratio. Steam cycles are not frequently used offshore today, mainly because of weight and size limitations, harsh conditions and technical requirements on treated water. From the ongoing discussion, the chosen basis for a steam bottoming cycle design is listed below:

- Back-pressure steam turbine without condenser.
- One pressure level.
  - Reduced weight because of less tubes/equipment.
- OTSG technology.
  - Reduced weight without bypass stack and drums.
  - Flexibility with dry operations in the OTSG.
  - Tubes in Incoloy with serrated fins in stainless steel, TP409.
- Exhaust gas pressure drop:  $\approx 25$  mbar.
- High pinch point temperature difference.

Based on a related design, simulations on simple vs. combined cycles for offshore installations were performed by Lars O. Nord and Olav Bolland [14]. The following results were obtained:

- Net plant efficiency was improved with 26–33%.
- CO<sub>2</sub> reduction of 20–25%.
- Weight-to-power ratio was increased with 60–70%.

# Chapter 4

# Power Cycles

### Contents

- 4.1 Gas Power Cycles . . . . . 37
- 4.2 Vapor Power Cycles . . . . . 38
- 4.3 Combined Power Cycles . . . . . 40
- 4.4 Chapter Discussion . . . . . 41

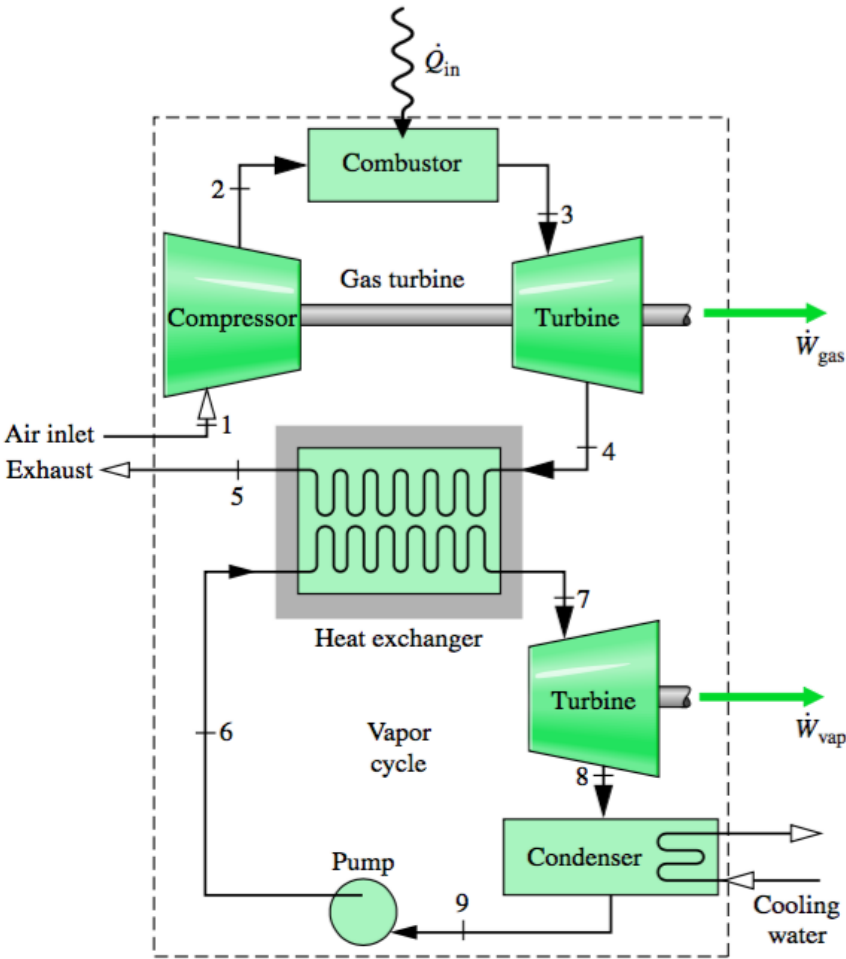


Figure 4.1: Combined cycle [53].

## 4.1 Gas Power Cycles

### Brayton Cycle

For simplicity and the purpose of basic understanding some assumptions are done. Stray heat transfer, potential and kinetic energy changes are set to zero in addition to steady state operations. In Figure 4.2, the process flow diagram and the TS-diagram are shown. The states 2s and 4s are assumed states for isentropic, ref. Eq. 7.6, compressor and turbine.

The main components in the Brayton cycle [53]:

- Compressor.
- Combustion chamber (for simplicity modeled as: Heat Exchanger (HX)).
- Gas turbine.

### Compressor

The cycle starts when ambient air is sucked into the compressor to increase the pressure at state 1. Typically, pressure out of the compressor section is in the range of 10–35 bar [28], depending on what type of gas turbine is considered. The temperature is also increased to about 300°C when state 2 is reached.

### Combustion Chamber/HX

After the air has passed through the compressor it is going into the combustion chamber. Here the combustion air is normally mixed with natural gas (about 80% of all gas turbines [28] runs on natural gas), but other fuels are also possible. The combustion in the Brayton Cycle is continuous, and leaves the combustion products (exhaust/flue gas) at temperatures up to 1500°C in state 3.

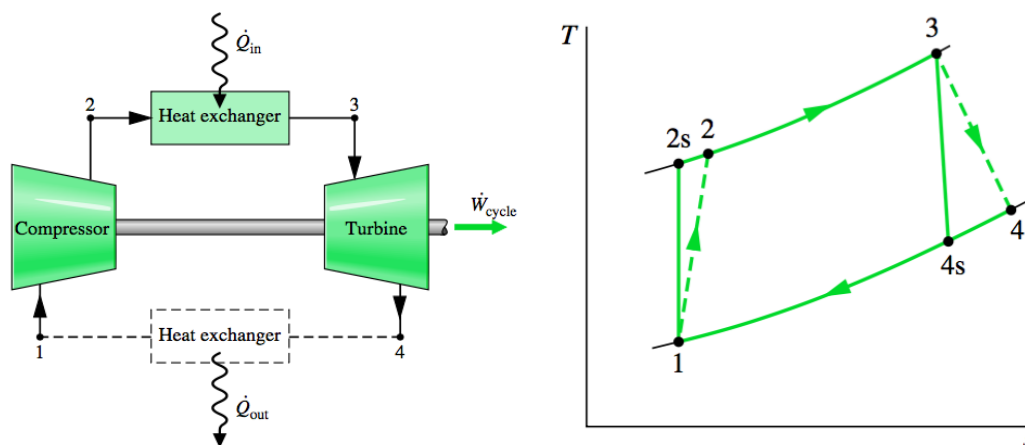


Figure 4.2: Brayton cycle [53].

## Gas Turbine

The hot gases are then expanded through a turbine that is designed to match the compressor and combustion chamber [54]. The exhaust temperature out of the turbine is in the range of 450–650°C.

The Brayton cycle is often called the topping cycle, because it is on the top of the Rankine cycle in a TS-diagram, see Figure 4.4.

## 4.2 Vapor Power Cycles

### Rankine Cycle

For simplicity and the purpose of basic understanding some assumptions are done. Stray heat transfer, potential and kinetic energy changes are set to zero in addition to steady state operations. In Figure 4.3 the process flow diagram and the TS-diagram are shown. The states 2s and 4s are assumed states for isentropic, ref. Eq. 7.6, turbine and pump. The main components in the Rankine cycle are [53]:

- Steam turbine.
- Condenser.
- Pump.
- Boiler.

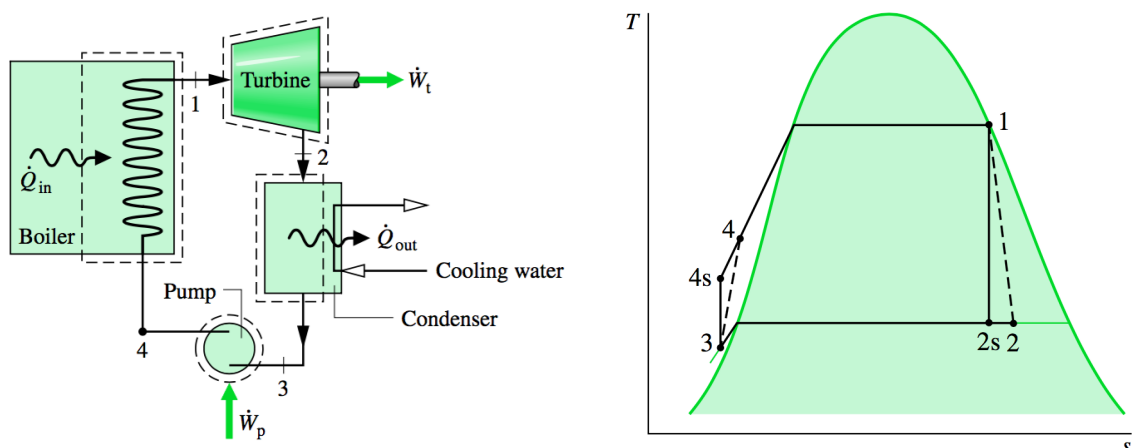


Figure 4.3: Thermodynamic Rankine cycle [53].

### Steam Turbine

From state 1, vapor with high temperature and pressure is expanded through the turbine to produce work ( $\dot{W}_t$ ). At state 2, the pressure is lowered and the vapor has started to condense. From here it is sent to the condenser.

### Condenser

To continue the condensation of vapor, heat is transferred away from the vapor ( $\dot{Q}_{out}$ ) in the condenser. Normally this heat is absorbed by circulating cooling water, that transfer the heat away and turns the vapor into liquid water at state 3.

### Pump

To increase the pressure and circulate the liquid water from the condenser it is sent through a pump to reach state 4 at compressed liquid water. From here it is sent to the boiler as feedwater for the steam production.

### Boiler

In the boiler heat is added ( $\dot{Q}_{in}$ ) and the liquid is heated to saturation and evaporated. It is also possible to superheat the vapor, but that is not shown here in Figure 4.3. This vapor is then feed to the turbine, and the cycle is completed.

The Rankine cycle is often called bottoming cycle, because it is underneath the Brayton cycle in a TS-diagram, see Figure 4.4. Alternatives to the steam bottoming cycle are found in Appendix A.3.1.

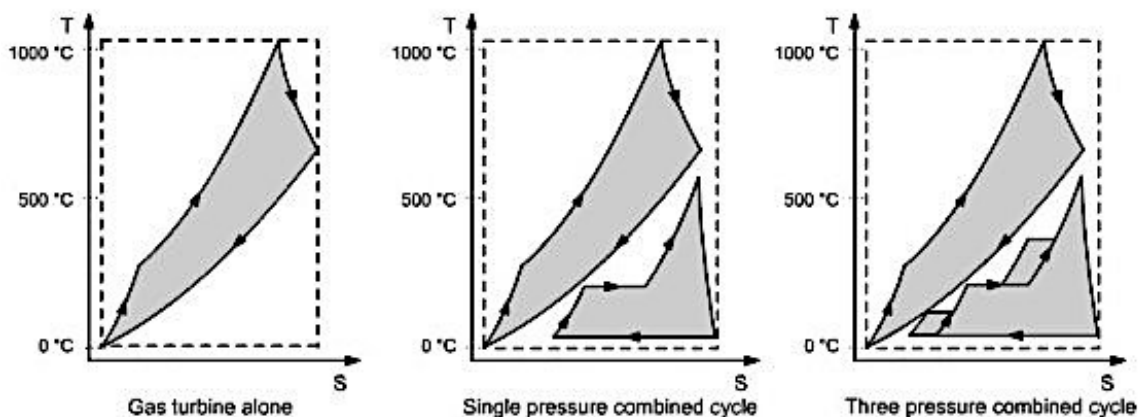


Figure 4.4: Simple and combined cycles TS-diagram [55].



### 4.3 Combined Power Cycles

A combined cycle takes advantage of properties for different working mediums, where one of the cycles (bottoming) utilizes the heat discharged from the other cycle (topping) [39]. In this case, the exhaust gas leaving the gas turbine is at a high temperature. This heat is used as the boiler (HRSG) in the Rankine cycle, which increases the overall efficiency (up to approximately 60%) and reduces the fuel consumption [53]. The heat recovery steam generator connects the two cycles and leaves the exhaust gas in the range of 80–200°C for onshore plants [28]. Steam is produced with temperature and pressure in the range of 450–560°C and 30–170 bar. It is common to have the two turbines on the same shaft, producing power in the same generator. For the possibility to run the gas turbine separately in case of insufficient steam production, a clutch is installed between the generator and steam turbine.

On its own, the Brayton cycle has a high temperature of heat rejection,  $T_L$ , and the Rankine cycle has a low temperature of heat addition,  $T_H$ . If they are combined, the new cycle has a lower  $T_L$  from the Rankine cycle and a higher  $T_H$  from the Brayton cycle, which is positive for the efficiency.

From Figure 4.1 some important parameters can be calculated. The Brayton cycle heat rejection temperature;

$$T_L = \frac{h_8 - h_9}{s_8 - s_9} \quad (4.1)$$

and the Rankine cycle heat addition temperature:

$$T_H = \frac{h_3 - h_2}{s_3 - s_2} \quad (4.2)$$

The thermal efficiency is given as:

$$\eta_{th} = \frac{\dot{W}_{gas} + \dot{W}_{steam}}{\dot{Q}_{in}} \leq 1 - \frac{T_L}{T_H} \quad (4.3)$$

It is observed that a high  $T_H$  and low  $T_L$  are favorable for high thermal efficiency, which is achieved by combining these power cycles.

## 4.4 Chapter Discussion

To find the best design for the offshore steam cycle, it is necessary to understand the underlying thermodynamic cycles. The steam Rankine cycle forms the basis for the steam turbine, which is a major component in this study. Rankine cycles are normally operated at multiple pressure levels. To reduce the weight and complexity, one pressure level is attractive for an offshore cycle. No alternatives to the steam bottoming cycle will be investigated in this thesis. Since some cycles have interesting characteristics for offshore implementation, they are described in Appendix A.3.1. The back-pressure turbine has no need for a condenser, because the steam leaves at the pressure determined by the process. In this case, the pressure is controlled by the CCS system and the steam will be condensed inside the reboiler in the desorber section.

The gas turbine Brayton cycle is fixed, but it is still important to pay attention to how it will affect the performance of the combined cycle. This is important to reach high efficiencies, even though this is not the only concern for offshore implementation. As discussed earlier, weight reduction is highly emphasized. The exhaust temperature and mass flow are determined from the gas turbine model and quantity, and are very important parameters for the finished steam cycle design. These parameters are not only affecting the steam production, but also the requirements for the CO<sub>2</sub> capture plant and the power production in the steam turbine. The exhaust needs to be cooled down to about 30°C before it enters the CO<sub>2</sub> plant, which is much lower than normal exhaust temperatures for combined power cycles. This heat should ideally be utilized for some kind of preheating; this will be discussed further.

From a thermodynamic point of view, the combined cycle is very attractive. This becomes evident from the thermal efficiency, see Eq. 4.3. Especially if all the heat from the exhaust gas down to 30°C can be utilized, a high thermal efficiency is expected. The middle frame in Fig. 4.4 is indicating the proposed combined cycle for offshore implementation. The advancement is clearly displayed compared to the single gas turbine cycle in the first frame.

# Chapter 5

## CO<sub>2</sub> Capture, Transport and Storage

### Contents

- 5.1 MEA-System . . . . . 43
  - 5.1.1 Absorption . . . . . 44
  - 5.1.2 Regeneration . . . . . 46
- 5.2 Transport . . . . . 46
- 5.3 Storage . . . . . 46
- 5.4 Offshore Based Plant, Sleipner Vest . . . . . 48
- 5.5 Chapter Discussion . . . . . 51

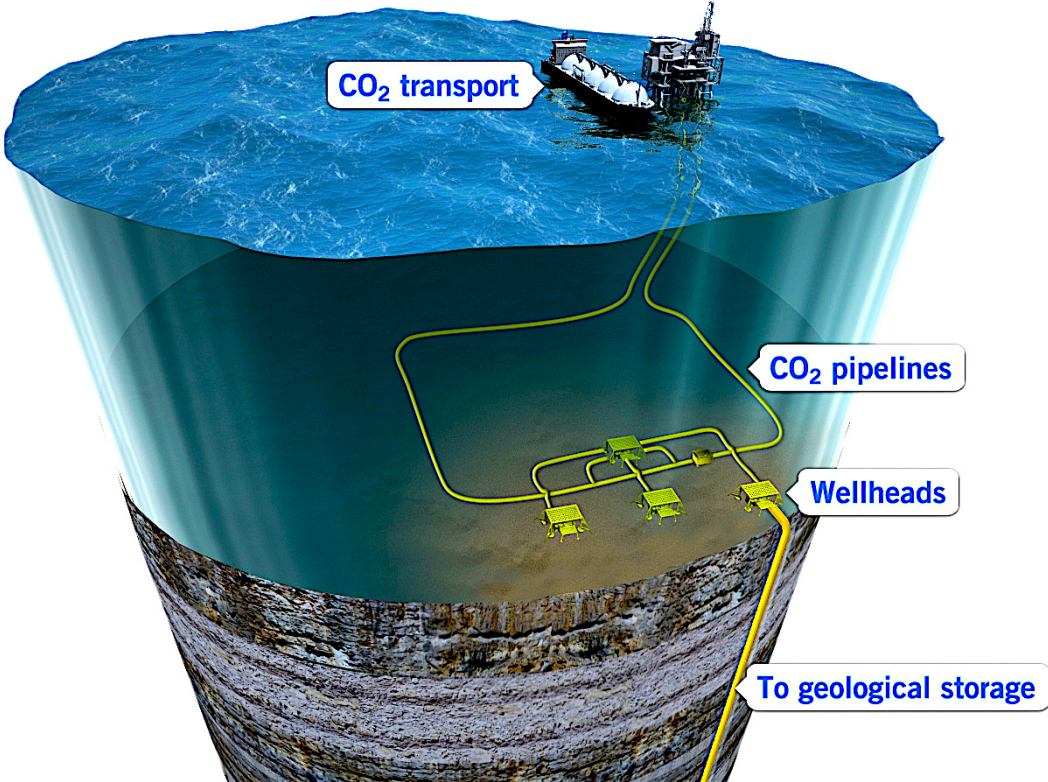


Figure 5.1: Offshore transport and storage of CO<sub>2</sub> [56].

In a global perspective, CO<sub>2</sub> emissions from fossil fuels are the biggest contributor to global warming with approximately 57% [32] of the total impact in 2007, see Fig. 5.2. It is a global mission to reduce and control these emissions. Some of the most famous attempts on joint measures are the Kyoto Protocol [57] and the Doha amendment [58]. Carbon capture and storage with Monoethanolamine (MEA) is one of the promising solutions. It is mature technology [59] that are ready to be implemented in large scale on multiple plants around the world [60].

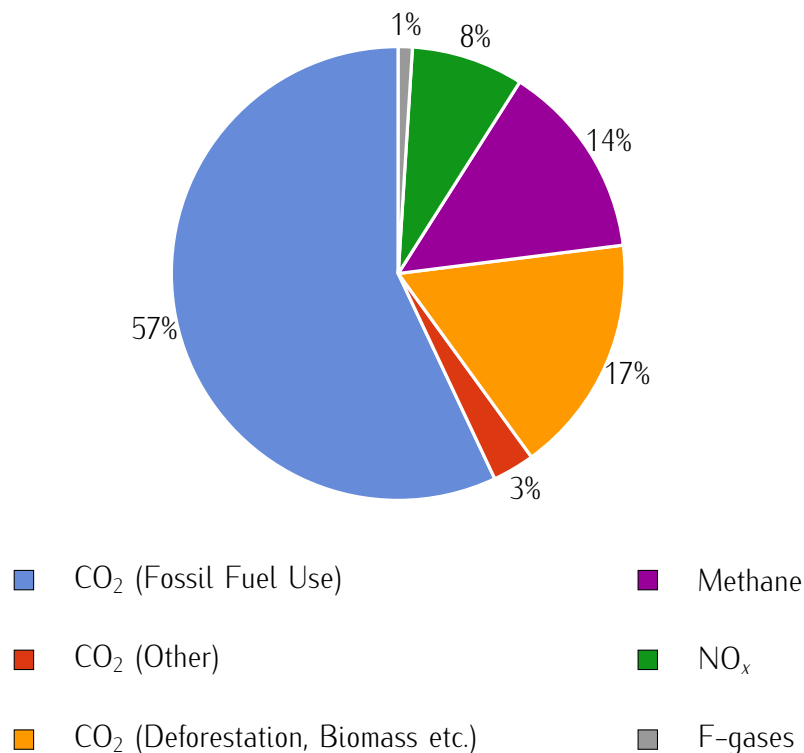


Figure 5.2: Contributors to global warming in 2007 [61].

## 5.1 MEA-System

To regenerate rich MEA, it is necessary with steam or other types of thermal energy. The MEA based CO<sub>2</sub> capturing systems are therefore exerting a considerable energy penalty on the plant. For offshore installations, this steam needs to be produced on site. In terms of operating challenges, degradation of the amines is one of the most severe. Thermal degradation is most prominent, and is a function of initial amine concentration, CO<sub>2</sub> loading<sup>1</sup>, and temperature in the absorber/stripper unit [63]. This lowers the potential for CO<sub>2</sub> capture, and increases the risk for corrosion in the system [64]. Some of the measures to avoid this is distillation of the amine, refill of fresh amine and lower amine concentrations. Lower concentrations is not beneficial for an offshore plant, because bulkier components are necessary.

<sup>1</sup> Loading = The maximum concentration of solute(s) that a solution/solvent can contain under specified conditions [62].

The main components in the MEA system are listed below, and can be seen in Figure 5.3.

- Absorber.
- Stripper/Desorber.
- Pump.
- Fan.
- Heat Exchanger (HX).

This is the most basic type of a MEA based CO<sub>2</sub> capture system. Many interesting modifications and innovative solutions are investigated [65] [66] [67], but they are not in the scope of this thesis. The parameters with the most significant impact on the capturing performance and energy saving potential for the MEA system are [68] [69]:

- Feed gas CO<sub>2</sub> mole fraction.
- Amine solvent concentration.
- Lean solvent loading.
- Absorber pressure.
- Stripper pressure.

### 5.1.1 Absorption

Flue/Exhaust gas is entering the absorber after it is cooled down in a direct contact cooler (DCC) to the optimal temperature of about 30–40°C [70]. Then the gas is blown into the absorber to overcome the pressure drop through the column. Normally these absorbers contain packed beds for maximum contact area between solvent and exhaust gas. The gas is flowing upwards from the entry in the lower part of the absorber. Liquid lean MEA solvent is flowing downwards from above the gas inlet. Through the packing, solvent is contacting the gas and the active components binds to the CO<sub>2</sub> molecules and form rich solvent in liquid form. The CO<sub>2</sub> reduced exhaust gas is going through a water washer, to regenerate the MEA droplets that follows the gas stream. From gravity, the rich solvent leaves the absorber in the bottom. Then it is pumped through a HX for heating in cross-flow with the lean solvent coming to the absorber. The last stop for the rich solvent is the stripper, where it is regenerated to lean solvent and the CO<sub>2</sub> is released. A reboiler is connected to the stripper, and it is here the steam cycle is connected to the CO<sub>2</sub> plant.

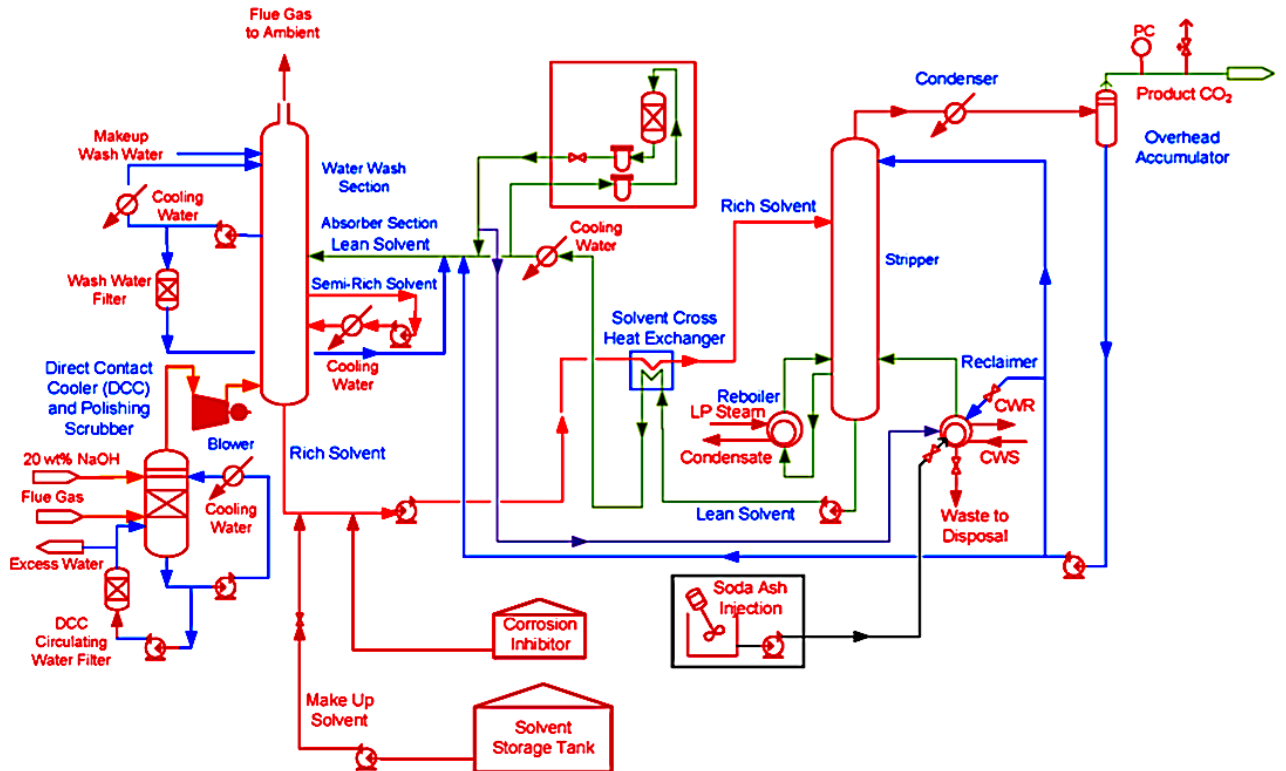


Figure 5.3: Example of a MEA based CO<sub>2</sub> capture system [71].

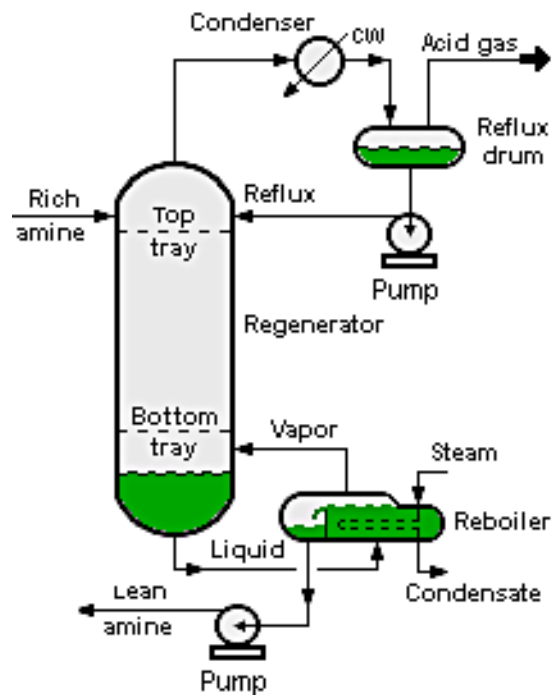


Figure 5.4: The stripper section of the MEA plant. Steam is entering the reboiler section [72].

### 5.1.2 Regeneration

Rich solvent enters at the top of the stripper where it receives heat from lean solvent vapor. This heat comes from the reboiler, where LP steam is entering, see Fig. 5.4. The stripper operates at around atmospheric pressures, and the temperature is normally in the range of 110–120°C [73]. As mentioned earlier, the energy penalty for CO<sub>2</sub> capture is huge, and the stripper section consumes the most with potentially 15–30% of the total power plant output [65]. The liquid lean solvent is collected at the bottom of the stripper. From here it is pumped through the earlier mentioned HX for cooling. At the stripper top, CO<sub>2</sub> and some amine droplets are sent to a condenser. The liquid MEA solvent is pumped back to the stripper, while the pure CO<sub>2</sub> is compressed and transported.

## 5.2 Transport

The most common way to transport CO<sub>2</sub> is in a pipeline, but it is also possible with ship, train or trailer [74]. If CO<sub>2</sub> is in a dense phase, it behaves like a liquid, and is therefore more efficient to transfer. The pipeline diameter can then be reduced in comparison with transportation in the gas phase. In the US, it already exist about 6000 km of CO<sub>2</sub> pipeline [75].

## 5.3 Storage

CO<sub>2</sub> is normally stored underground in geological formations, see Figure 5.5. Suitable formations can be located both onshore and offshore, normally they consist of porous but dense materials [76]. Above this, an impermeable layer of rock stops further dispersion of CO<sub>2</sub>, and is therefore a secure trap for the gas. This is the same mechanism as for oil and gas reservoirs, that potentially have held on the hydrocarbons in thousands of years. The impermeable layer is called cap rock or seal, see Fig. 5.6. Developing over time, CO<sub>2</sub> that is injected into such reservoirs will be trapped in different ways. The most common types of storage, in chronological order are [76]:

- Residual storage.
  - CO<sub>2</sub> trapped in microscopic pores (Trapping of separated droplets).
- Dissolution storage.
  - CO<sub>2</sub> dissolved in salty water. Will increase the density and sink to the bottom.
- Mineral storage.
  - CO<sub>2</sub> will chemically and irreversibly to surrounding rock (Mineral formation).

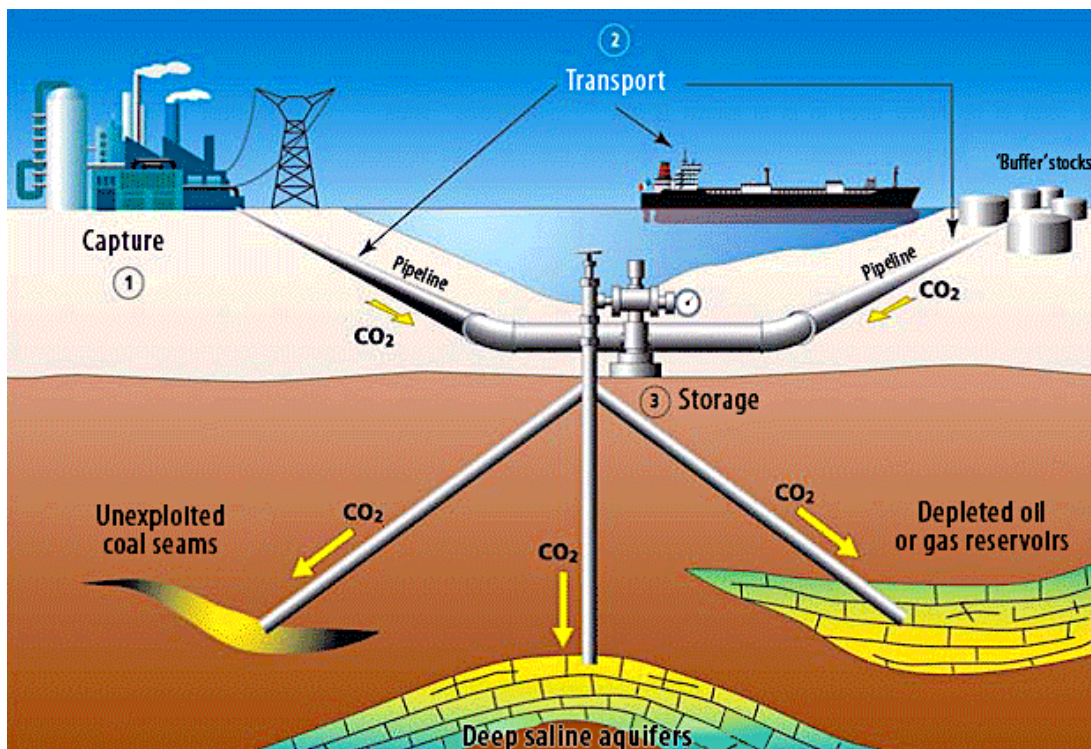


Figure 5.5: CO<sub>2</sub> can be stored in e.g. unmineable coal seams, deep saline aquifers, and depleted oil and gas reservoirs [77].

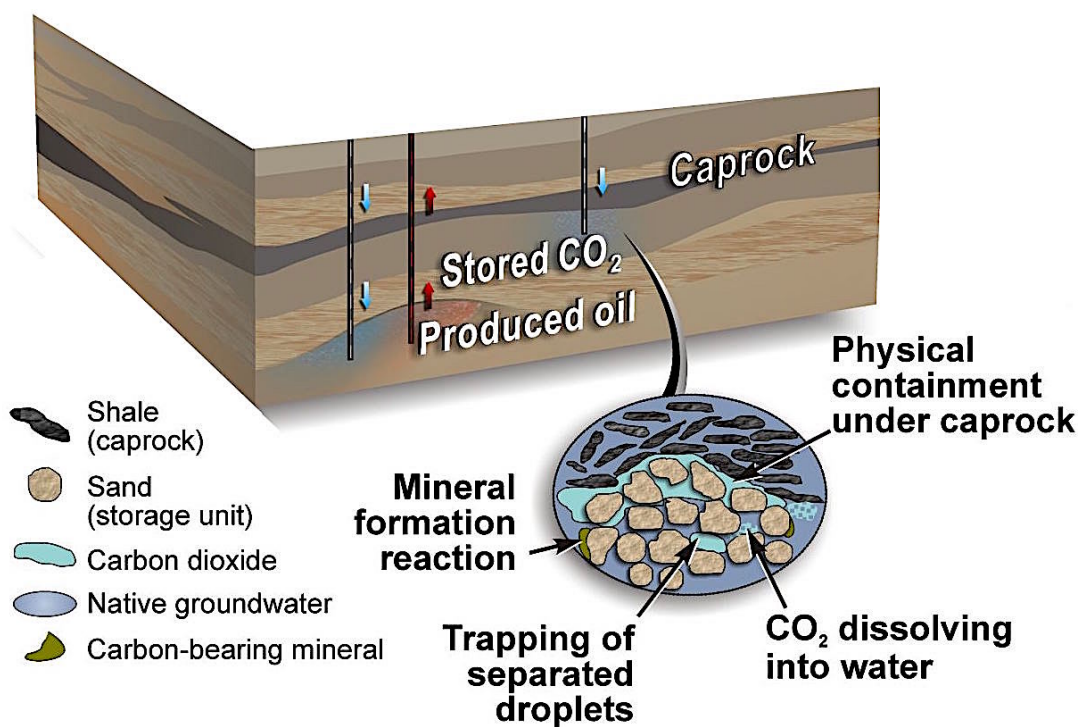


Figure 5.6: Cap rock and possible modes for CO<sub>2</sub> storage in a reservoir [78].



## 5.4 Offshore Based Plant, Sleipner Vest

Simulations on an onshore plant can be seen in Appendix A.4.1. These results are still relevant for the work done in this study.

The Sleipner carbon capture plant is removing the CO<sub>2</sub> from a natural gas (NG) stream, and not an exhaust gas stream. Nevertheless, many of the same principles apply, and are relevant for this thesis. The natural gas from the respective reservoir contains about 9 mole% of CO<sub>2</sub>, while the export quality specification is 2.5 mole% [79]. Methyldiethanolamine (MDEA) is used to capture the CO<sub>2</sub> before it is injected for permanent storage about 800–1000 m below sea level [80]. When the module was installed, the total weight was 8200 tons and the footprint 1000 m<sup>2</sup> [79]. Approximately one million tons of CO<sub>2</sub> is stored annually.

Natural gas is entering two absorbers named A & B in Fig. 5.7, at this stage the pressure and temperature are about 100 bara and 70°C. Rich amine is then sent through Pelton turbines to produce power from a pressure reduction; they generate around 5 MW of electricity. In the first flash drum co-absorbed hydrocarbons and some CO<sub>2</sub> are stripped off at about 15 bara and 70°C [79]. Most of the CO<sub>2</sub> (>95%) [81] is released in the second flash drum, that operates at around 1.2 bara. About 10% of the amine solution goes through a stripper column to get fully regenerated with a similar process to the one described in Section 5.1. Steam is generated in the amine reboiler, and nearly all the CO<sub>2</sub> is stripped off [9]. The reason for this process is to regenerate some very lean amine, compared to the amine solution from the flash drum. This results in increased CO<sub>2</sub> capture, and makes it possible to control the overall solvent loading. The main difference between this plant and the previous considered plants are the use of pressure change instead of heat/temperature change to separate the CO<sub>2</sub> from the amine solution. This is known as pressure vs. temperature swing adsorption. Because the natural gas enters with a high pressure compared to gas turbine exhaust gas, pressure swing is the natural choice for this plant.

The CO<sub>2</sub> gas from the last flash drum and the stripper column are undergoing a four step compression, see Fig. 5.8. Between each stage, the stream is cooled and liquid dropout is removed. Compressed CO<sub>2</sub> at around 65 bara is then injected into the Utsira formation, a water filled aquifer on the NCS [79], see Fig. 5.9. At this depth, CO<sub>2</sub> behaves as a supercritical fluid, with temperature and pressure above critical values (31.1°C and 73.9 bar). The reservoir temperature and pressure are about 41°C and 80 bar at the top and 110 bar at the bottom [82]. CO<sub>2</sub> will expand like a gas, but have the density similar to that of a liquid.

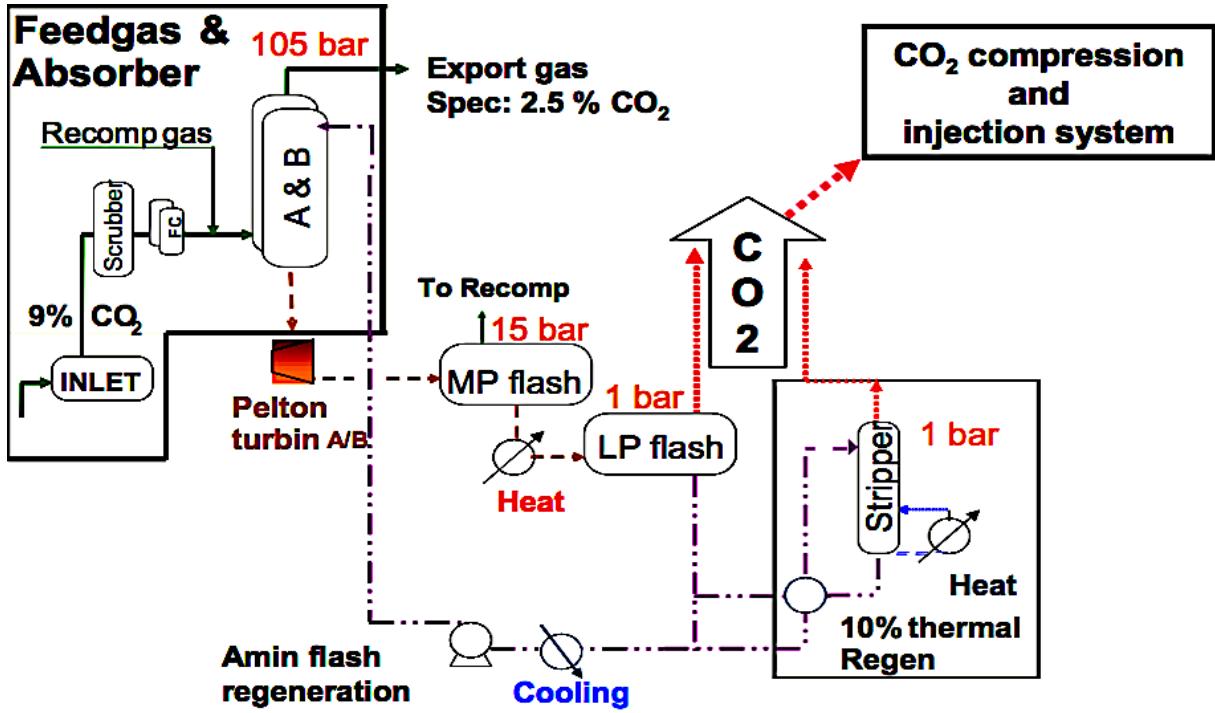


Figure 5.7: Flow diagram for the Sleipner CO<sub>2</sub> removal system [79].

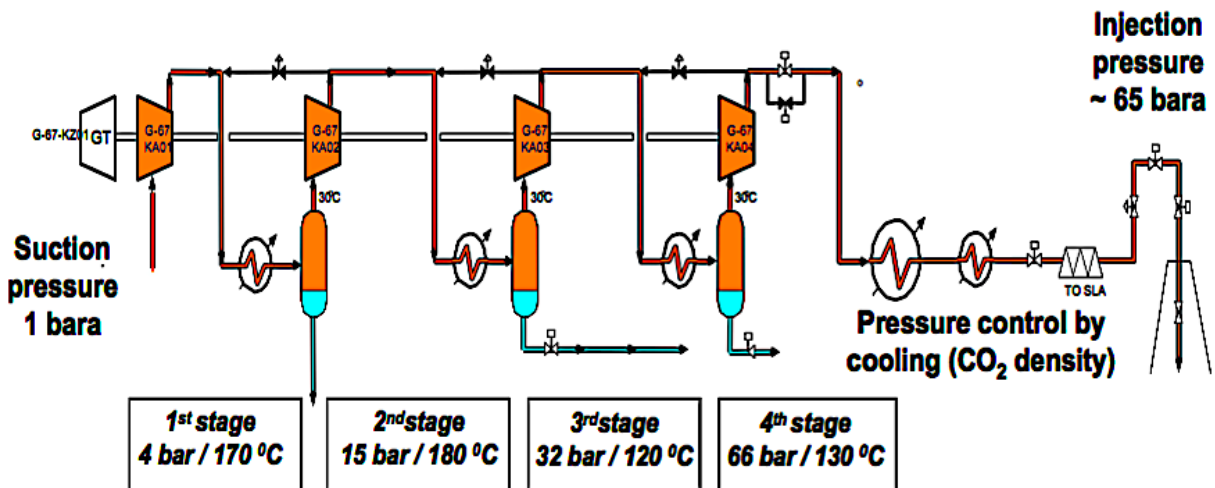


Figure 5.8: An illustration of the Sleipner CO<sub>2</sub> compression system [79].

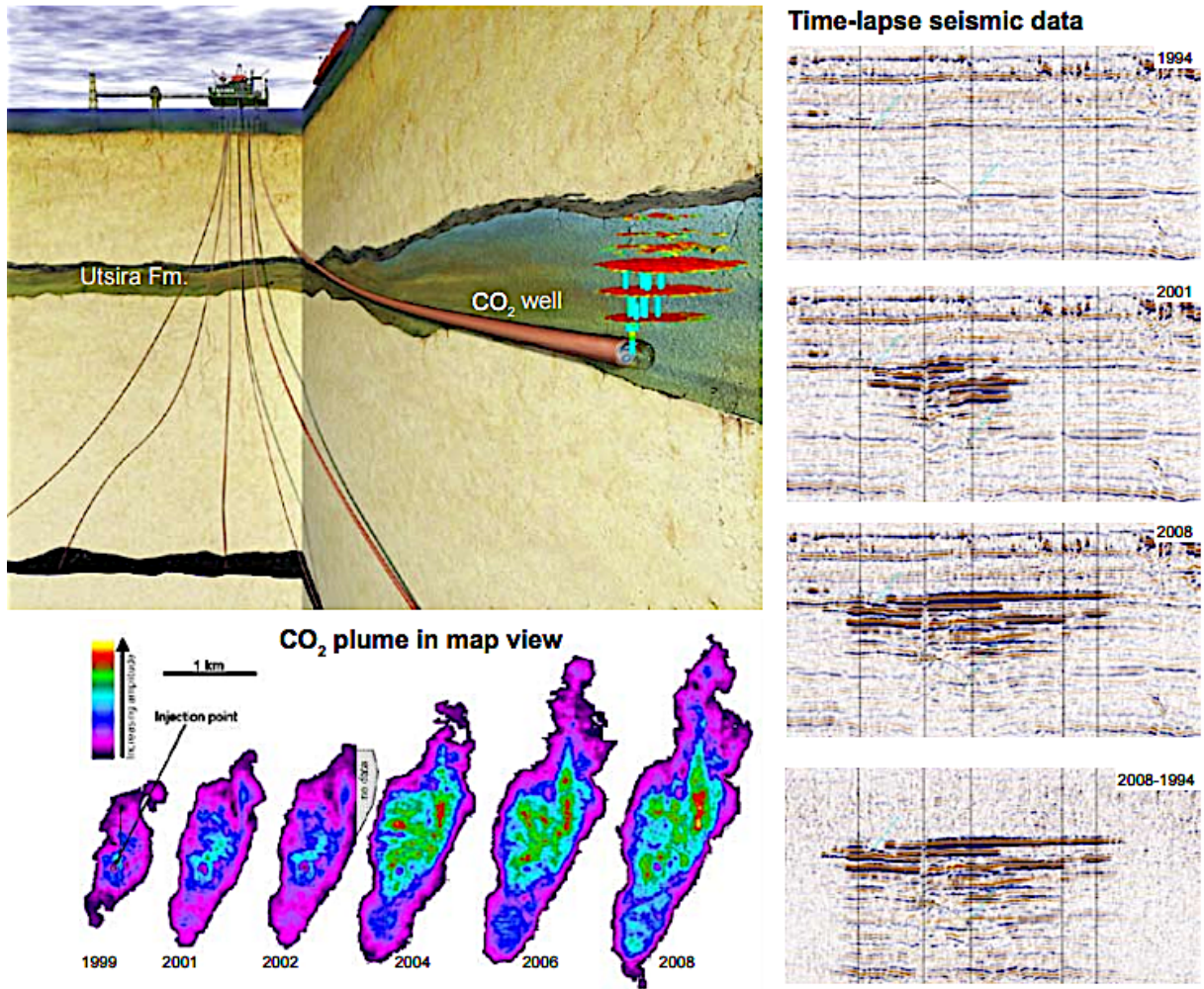


Figure 5.9: Injection of CO<sub>2</sub> into the Utsira formation. The seismic monitoring is showing the evolving CO<sub>2</sub> plume. 10.1 million tons of CO<sub>2</sub> have been injected in the period 1996–2008 [81].

## 5.5 Chapter Discussion

No technical considerations are done on the MEA system itself in this study. This work is already performed by SINTEF, even though the capture technology undergoes continuous research driven improvements. In addition to the steam delivered to the reboiler, the steam cycle design can influence the inlet conditions of the exhaust. This is done in GT PRO by changing the HRSG pressure drop and pinch point temperature difference. The steam mass flow will influence the exhaust temperature, before it enters the CO<sub>2</sub> plant exhaust gas cooler. In the simulations performed in this study, the steam mass flow is determined from the pinch point temperature difference.

The exhaust gas cooler, see direct contact cooler in Fig. 5.3, should ideally be integrated with some other system. The exhaust temperature leaving the heat recovery steam generator, is typically in the range of 200–250°C for offshore operations. If the CO<sub>2</sub> plant requires an exhaust temperature of 30°C, a lot of heat is available. If a desalination plant is considered, it would be great to integrate the direct contact cooler as preheating for the distillation process. A simple design for integration would be continuous piping from a seawater pump through the direct contact cooler, before ending in the desalination plant. It could also be possible to integrate this cooler with the feedwater tank to raise the feedwater temperature. This can potentially reduce the weight of the heat recovery steam generator, if the low temperature section can be scaled down. Since the feedwater can not lower the exhaust temperature to 30°C, a two stage cooling is therefore necessary. This would most likely increase the weight, hence desalination is the preferred alternative for integration with the exhaust gas cooler.

As mentioned in Chapter 3, the water dew point is normally about 40°C for gas turbine exhaust gas. Corrosion related issues are therefore highly relevant, and precautions should be taken to avoid any problems near the exhaust gas cooler. This is outside the scope of this work, but should be addressed in further work.

CO<sub>2</sub> storage should ideally be initialized directly from the offshore installation. The Sleipner field has proven the technology for offshore CO<sub>2</sub> compression and storage, even though technical improvements and local adaption should be considered. The CO<sub>2</sub> injection in the Utsira formation is operated at about 65 bar. This pressure level will be used further in this study to analyze the power consumption for CO<sub>2</sub> compression in GT PRO. The finished steam cycle should ideally be able to fulfill the power demand from both the capturing plant itself, and the compression system. This will be investigated in the simulation work.

# Chapter 6

## Mathematical Representation

### Contents

6.1	Interpolation . . . . .	53
6.2	Regression and Least Squares Fitting . . . . .	59
6.3	Scaling . . . . .	67
6.4	Chapter Discussion . . . . .	76

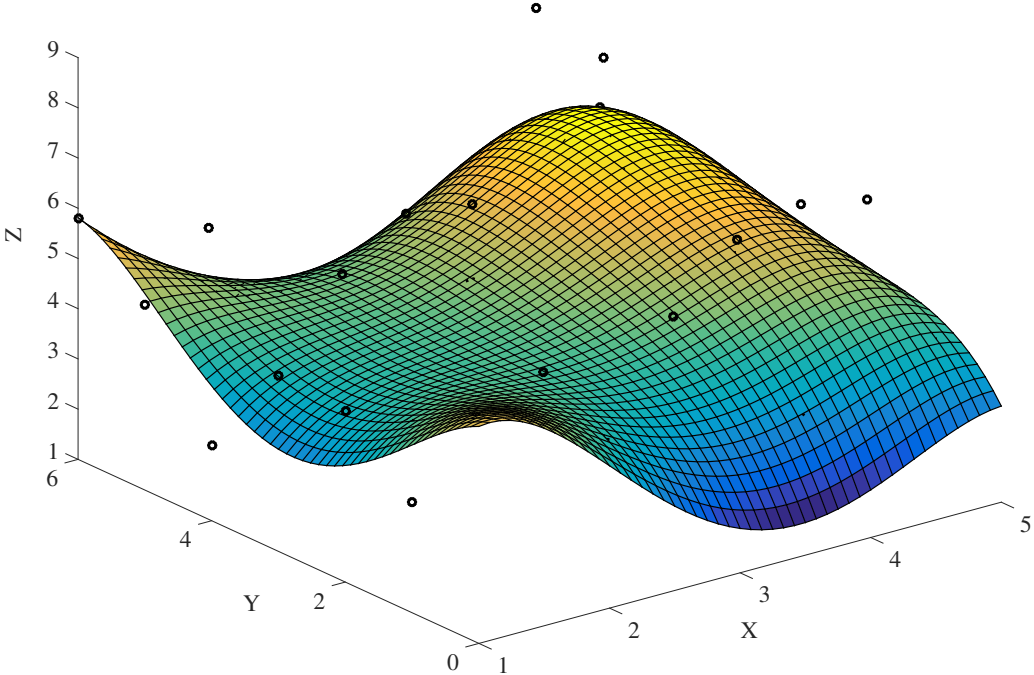


Figure 6.1: Fourth order representation of data points with two variables.

## 6.1 Interpolation

In the mathematical field of numerical analysis, interpolation is a method of constructing new data points within the range of a discrete set of known data points. In engineering and science, one often has a number of data points, obtained by simulation or experimentation, which represent the values of a function (weight) for a limited number of values of the independent variable (e.g. steam mass flow). It is often required to interpolate (i.e. estimate) the value of that function for an intermediate value of the independent variable. This may be achieved by curve fitting or regression analysis. [83]. Interpolation is a common approach to finding a polynomial representation, in this section, four different interpolation methods are investigated.

### Piecewise Linear Interpolation

$$L(x) = y_k + s \cdot \delta_k \quad (6.1)$$

The interval index  $k$  need to be determined so that [84]:

$$x_k \leq x < x_{k+1}$$

The local variable,  $s$ , is given by:

$$s = (x - x_k)$$

and the first divided difference,  $\delta_k$ , is:

$$\delta_k = \frac{y_{k+1} - y_k}{x_{k+1} - x_k}$$

which equals:

$$L(x) = y_k + (x - x_k) \frac{y_{k+1} - y_k}{x_{k+1} - x_k} \quad (6.2)$$

MATLAB function: `piecelin`. See Fig. 6.2.

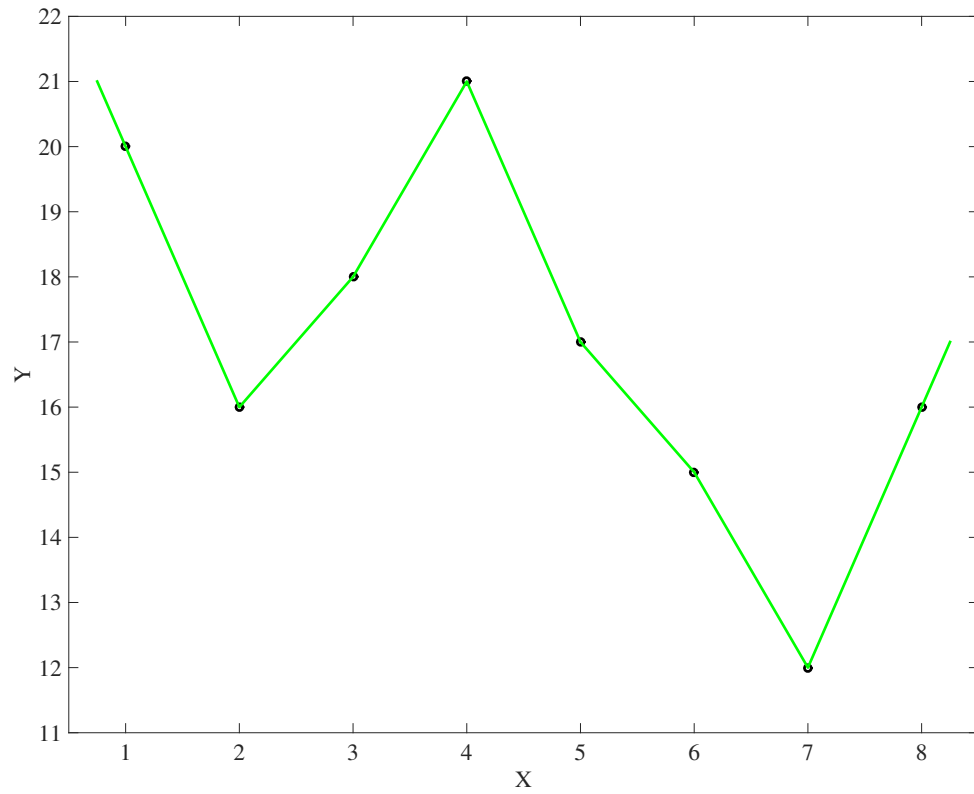


Figure 6.2: Piecewise linear interpolation.

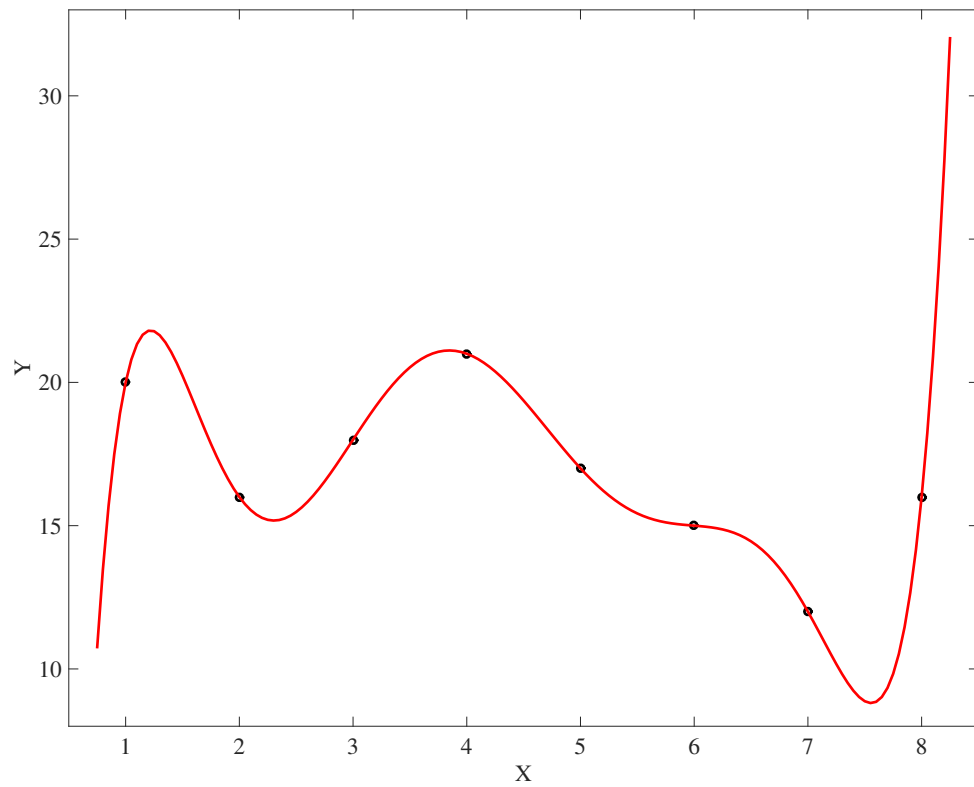


Figure 6.3: Full degree polynomial interpolation.

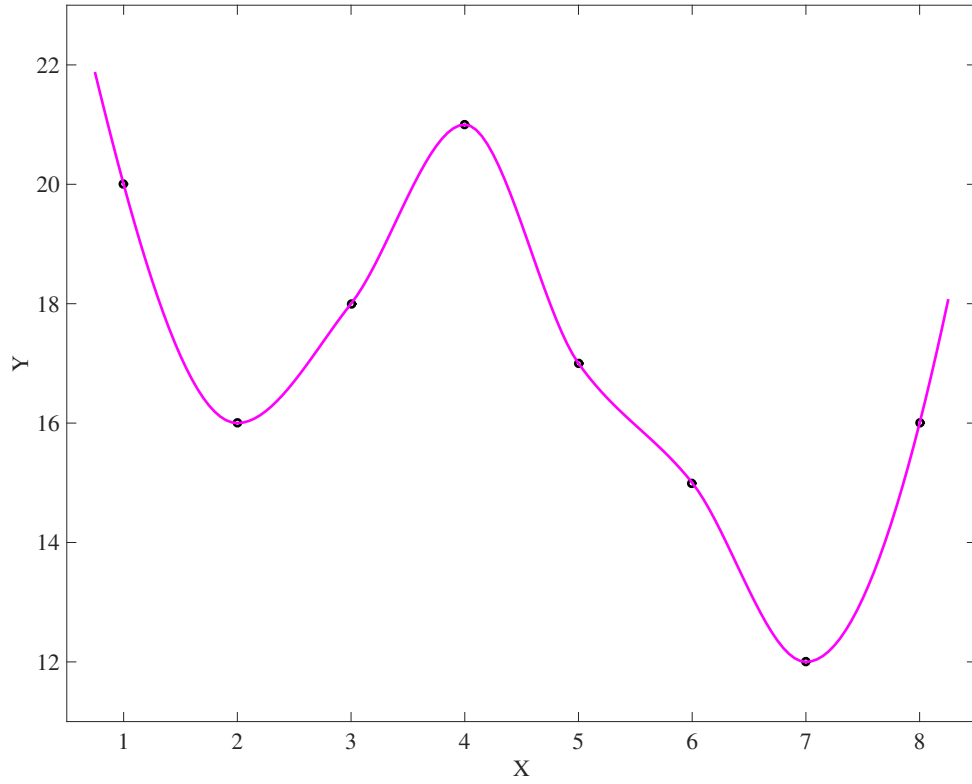


Figure 6.4: Shape preserving Hermite interpolation.

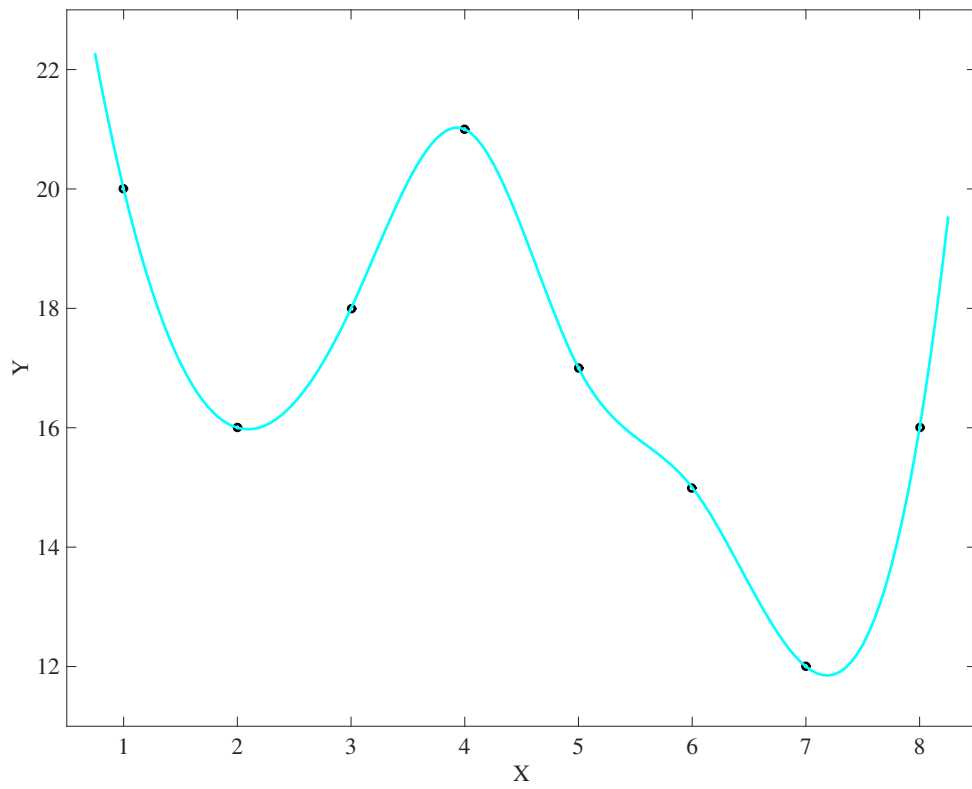


Figure 6.5: Spline interpolation.



**Full Degree Polynomial Interpolation**

The full degree polynomial interpolation is exactly reproducing the given data,

$$P(x_k) = y_k, \quad k = 1, \dots, n. \quad (6.3)$$

and the most compact representation is the Lagrange form:

$$P(x) = \sum_k \left( \prod_{j \neq k} \frac{x - x_j}{x_k - x_j} \right) y_k \quad (6.4)$$

The polynomial's degree will always be less than or equal to  $n - 1$ .

MATLAB function: `polyinterp`. See Fig. 6.3.

**Piecewise Cubic Hermite Interpolation**

"Functions that satisfy interpolation conditions on derivatives are known as Hermite or osculatory interpolants, because of the higher order contact at the interpolation sites. (*Osculari* means "to kiss" in Latin.)" [85]

In this types of interpolation some varying order of derivatives will match in each data point. It is many possible ways to do this, where the different approaches are based on how the slopes are defined. All of these methods are based on a cubic function. A method that satisfy continuous first order derivatives, is the shape preserving Hermite interpolation (`pchip`). For continuity on the second order derivative, the spline interpolation is used.

The world of splines extends far beyond the basic cubic interpolatory spline described here. There are multidimensional, high-order, and approximating splines. A good reference for the mathematical background and software for splines is: "A Practical Guide to Splines", by Carl de Boor [86]. In a general matter, the basic interpolatory spline can be expressed as:

$$S_i(x) = a_i(x - x_i)^3 + b_i(x - x_i)^2 + c_i(x - x_i) + d_i, \quad x \in [x_i, x_{i+1}] \quad (6.5)$$

where,

$$S_i(x_i) = y_i$$

$$S_i(x_{i+1}) = y_{i+1}$$

and both these criteria are fulfilled for the first and second order derivatives:

$$S'_{i-1}(x_i) = S'_i(x_i)$$

$$S''_{i-1}(x_i) = S''_i(x_i)$$

These apply for:  $i = 1, 2, \dots, n - 1$ . To solve the system, some criteria for the second derivative is necessary, the most common approach is [87]:

$$S''_0(x_0) = 0$$

$$S''_{n-1}(x_n) = 0$$

MATLAB functions: `pchip` and `spline`.

### Comparing Interpolation Methods

It is observed that extrapolation is a delicate matter, and is very dependent on the chosen method. The estimated value for  $x = 0$  is totally different when e.g. full degree polynomial ( $<10$ ) and spline ( $>22$ ) are considered. Within the considered range, shape preserving Hermite interpolation and spline are quite similar. From the data point in  $x = 1$ , it is observed that these methods estimate a smoother fit than the full degree polynomial interpolation. The local maxima between  $x = 1$  and  $x = 2$  is not present for any of the other methods. It is important to make careful assessments, to choose the best method for the specific application.

### Two Variable Interpolation

Interpolation is also possible to use for multivariate data points. The accuracy is sensitive to the chosen mesh grid, this can be observed in Fig. 6.6. Because the grid is defined to wide, the interpolation scheme is not able to enclose all data points. This is as for all mathematical computation methods a trade-off between accuracy and running time. Interpolation results can also be extrapolation for multivariate analysis, see Fig. 6.7. Multidimensional higher order approximating splines is the most promising interpolation method for the weight estimating polynomial.

MATLAB function: `scatteredInterpolant`.

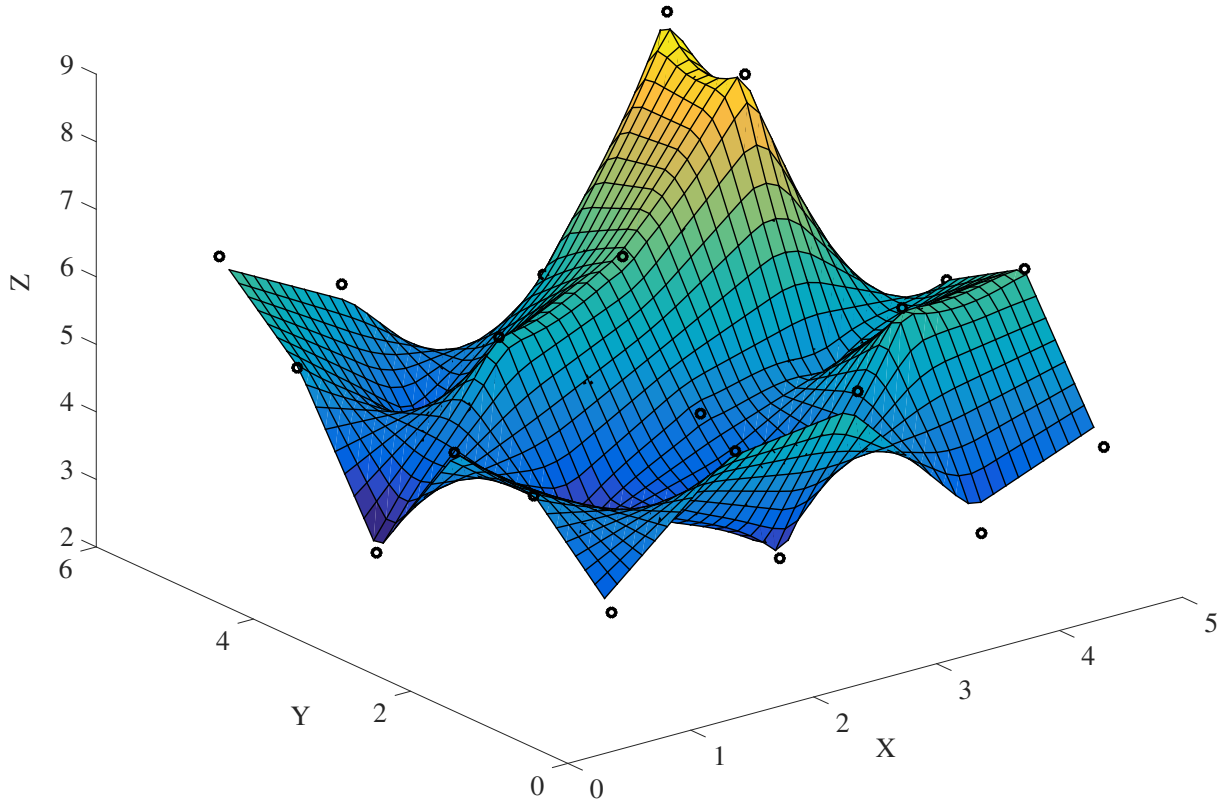


Figure 6.6: Surface plot for two variable polynomial interpolation.

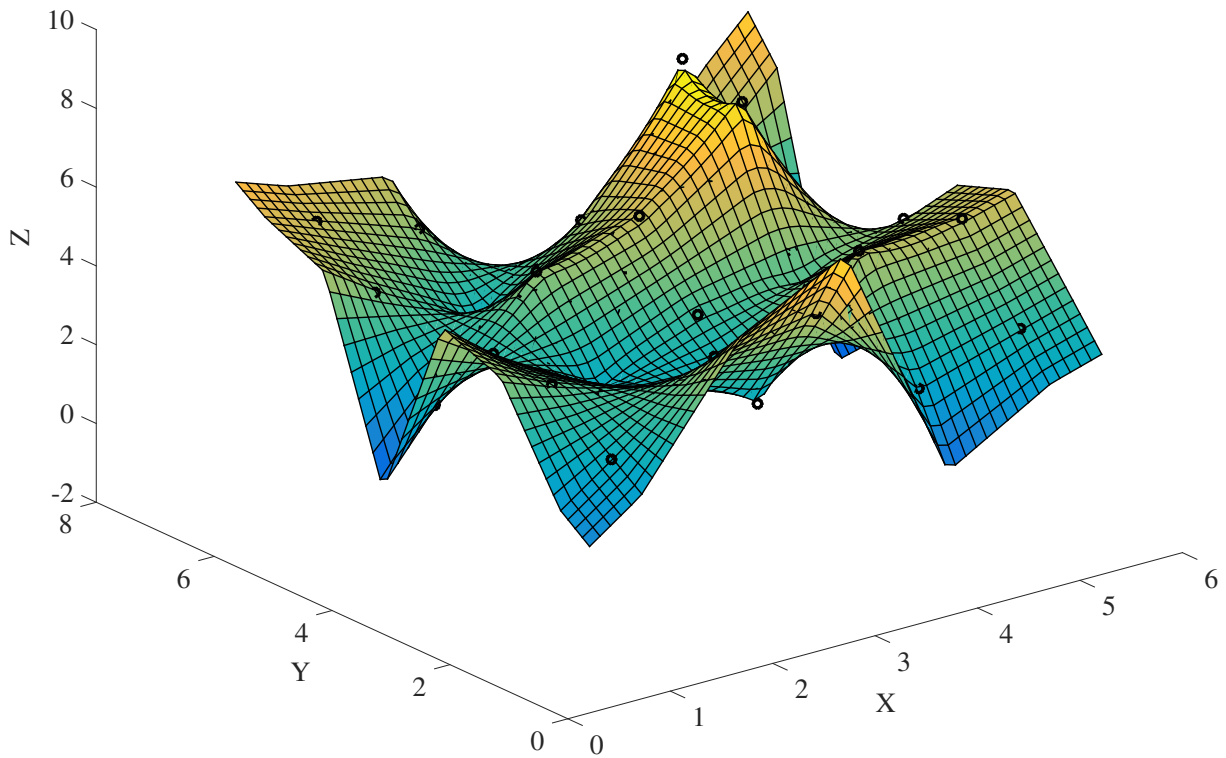


Figure 6.7: Surface plot for two variable polynomial interpolation with extrapolation.

## 6.2 Regression and Least Squares Fitting

Regression analysis is used for estimating the relationships among variables. The focus is on the relationship between a dependent variable (weight) and one or more independent variables (mass flow, diameter, power etc.). More specifically, regression analysis helps one understand how the typical value of the dependent variable changes when any one of the independent variables is varied, while the other independent variables are held fixed. It is also used to understand which among the independent variables are related to the dependent variable, and to explore the forms of these relationships (could be used to find scaling relationships). Regression analysis is widely used for estimation and forecasting. Many techniques for carrying out regression analysis have been developed, e.g. ordinary least squares regression, where a finite number of unknown parameters are estimated from the data [88]. Least squares fitting is chosen as the preferred regression technique for this work.

### Residuals

A residual is the difference between a data point ( $y_i$ ) and the associated value ( $\hat{y}_i$ ) from the chosen regression model:

$$r_i = y_i - \hat{y}_i \quad (6.6)$$

### Coefficient of Determination

This parameter, also known as  $R^2$  ("R squared") is used to determine how good a regression fits the actual data points. It is defined as:

$$R^2 = 1 - \frac{\sum_i^n (y_i - \hat{y}_i)^2}{\sum_i^n (y_i - \bar{y})^2} \quad (6.7)$$

Where the mean is defined as,

$$\bar{y} = \frac{1}{n} \sum_{i=1}^n y_i \quad (6.8)$$

### Least Squares Fitting

The least squares fitting is based on minimizing  $S$ :

$$S = \sum_{i=1}^n r_i^2 = \sum_{i=1}^n (y_i - \hat{y}_i)^2 \quad (6.9)$$

Where the error is given by:

$$\text{Error} \sim N(0, \sigma^2)$$

There exist four basic types of least squares fitting:

1) Linear least squares.

$$\hat{y}_i = a \cdot x + b$$

$$S = \sum_{i=1}^n r_i^2 = \sum_{i=1}^n (y_i - (a \cdot x_i + b))^2 \quad (6.10)$$

2) Weighted linear least squares.

$$S = \sum_{i=1}^n w_i \cdot r_i^2 = \sum_{i=1}^n w_i (y_i - (a \cdot x_i + b))^2 \quad (6.11)$$

It is possible to set weights manually based on e.g. importance of different data points, or if some points are single values, while others are average value from multiple measurements.

3) Robust least squares.

- LAR
  - Finds a curve that minimizes the absolute difference,  $\text{abs}(y_i - \hat{y}_i)$ , of the residuals instead of the squared difference. This method is used if a limited amount of disturbance is expected. All data points is considered with this method.
- Bi square weights
  - Finds a curve by minimizing a weighted sum. The weights are determined by each point's distance from the fitted line. Points near the line get high weights, and extreme values get low or zero weight. The basis for this method is the normal least squares approach, and is therefore normally the preferred setting for robust fitting.

## 4) Nonlinear least squares.

This type of fitting allow all kinds of non linear functions,  $g(x)$ :

$$S = \sum_{i=1}^n w_i (y_i - g(x_i))^2 \quad (6.12)$$

**Robust and Weighted Least Squares**

In this section, some analytical work in MATLAB will be presented. Three different functions were implemented with some added disturbance; the functions are listed below.

- $f(x) = x$  in Fig. 6.8.
- $f(x) = x^2$  in Fig. 6.9.
- $f(x) = \sin(x)$  in Fig. 6.10.

For reference, a fit with all the data points was made for all functions. To reduce the influence of extreme values, some points were excluded. The criteria for exclusion was based on the standard deviation (std) of residuals from the first fit. For every point, it was tested if 1.5 times the standard deviation was larger than the absolute value of the residual. The number 1.5 can of course be changed for a more conservative or radical adjustment. It is also possible to give different weights based on this approach, e.g.  $w_{1.3} = 0.8$  for all points more than 1.3 times std away from the residual, and  $w_{1.5} = 0.2$  when exceeding 1.5 times standard deviation. In this work, the second fit was made with these points totally excluded. The last two fits are performed with the MATLAB functions for robust fitting with both Bi square and LAR settings.

For the linear function, the robust fitting using LAR gives the best fit. In this case, it makes an almost perfect fit with the original line. The second order function is best estimated by the robust fitting using Bi square settings. Because most of the disturbance is high values, all fittings overestimates the original function.

When analyzing the trigonometric fit, it is not an obvious method that estimates the original function best. The noise is computed randomly, and the best fit varies from each run. The Bi square approach seems to have the closest estimates in terms of amplitude in most of the tests. The LAR calculations is often very accurate in fitting zero at  $x = 2\pi$ . For all functions in this section, it is obvious that robust fitting is much more accurate than standard fitting on all data points.

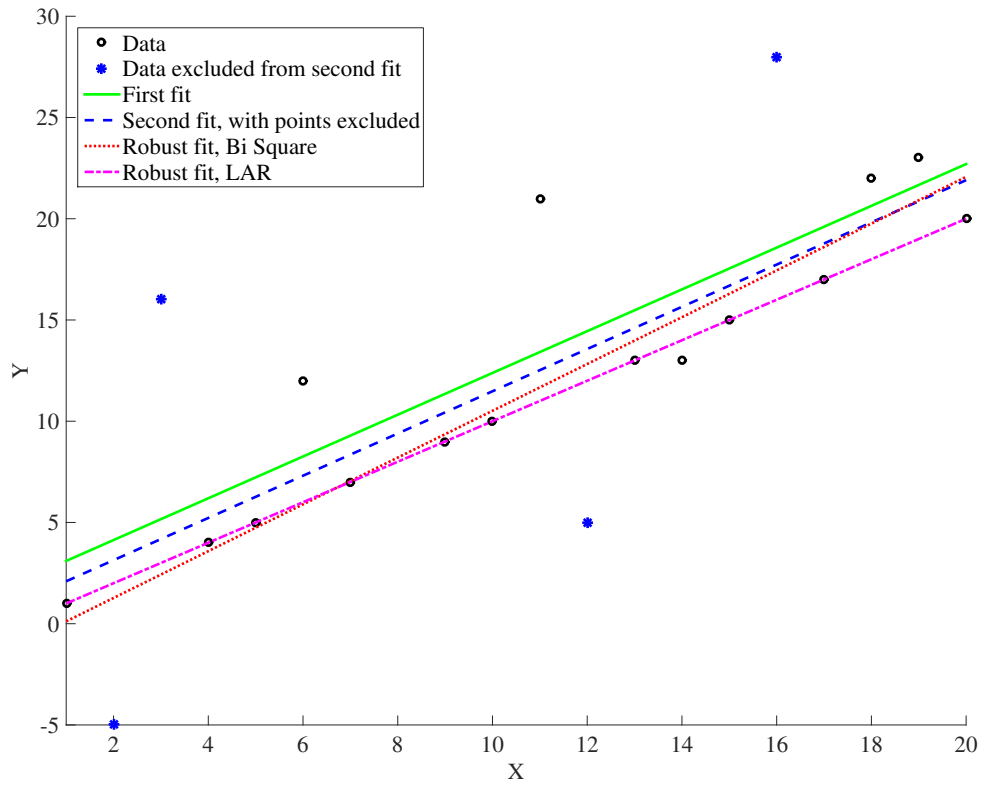


Figure 6.8: Linear function, weighted and robust fit.

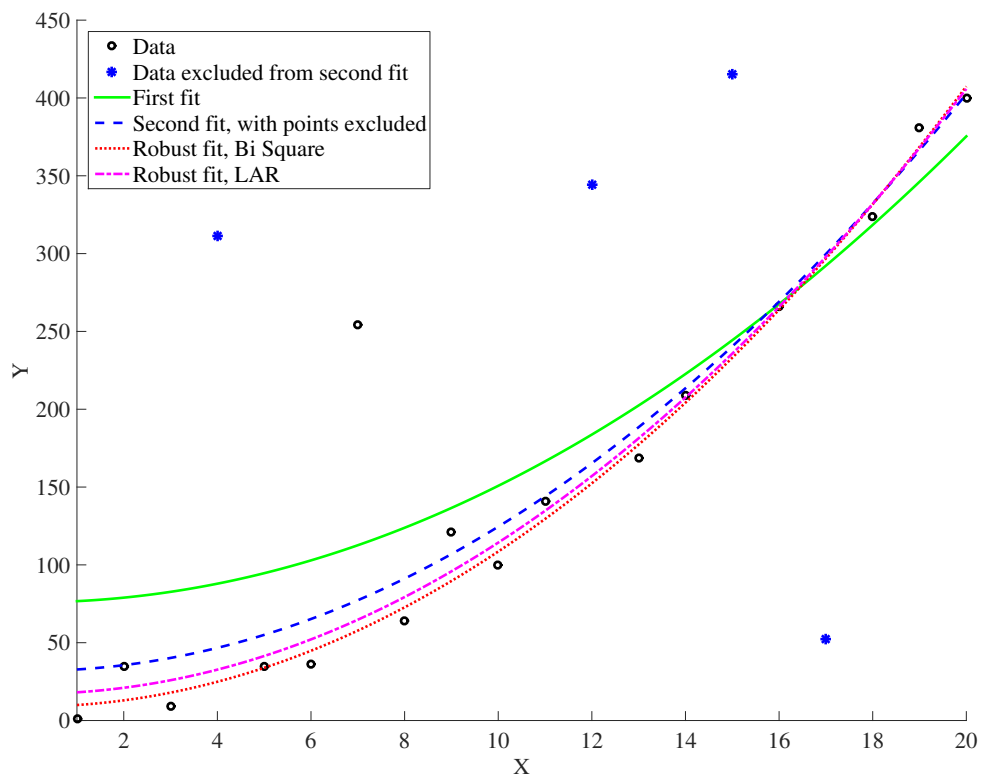
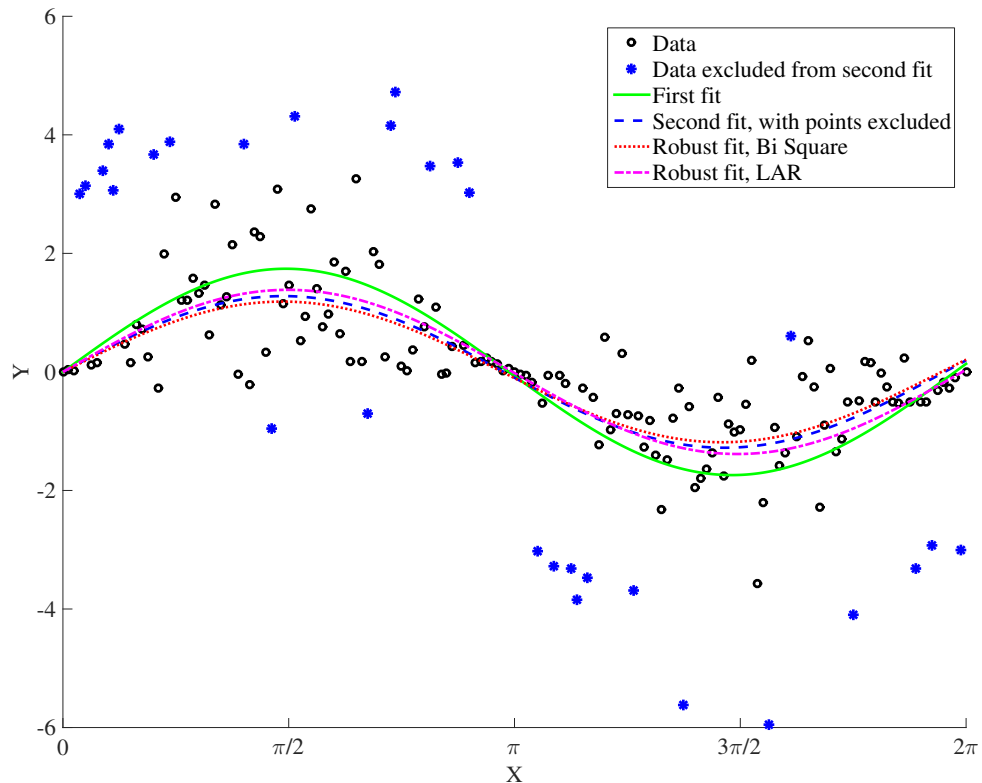
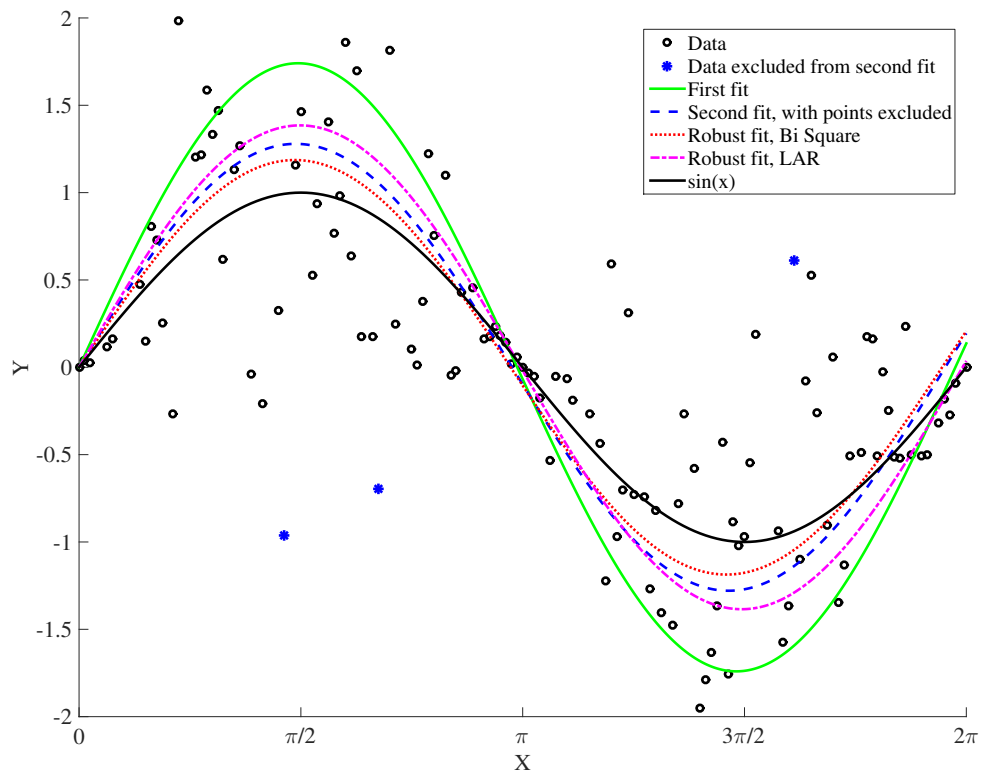


Figure 6.9: Squared function, weighted and robust fit.

Figure 6.10: Trigonometric function  $\sin(x)$  with disturbance, weighted and robust fit.Figure 6.11: This is a zoomed in version of the previous figure, with the original  $\sin(x)$  curve plotted.



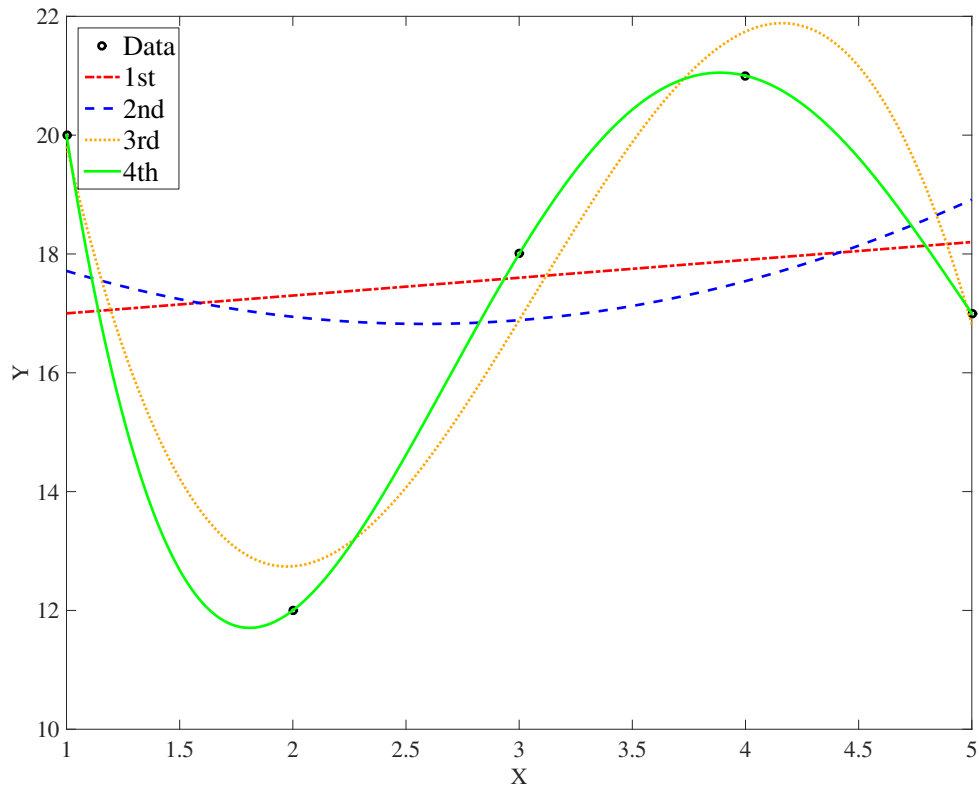


Figure 6.12: Different order polynomial regression on five data points.

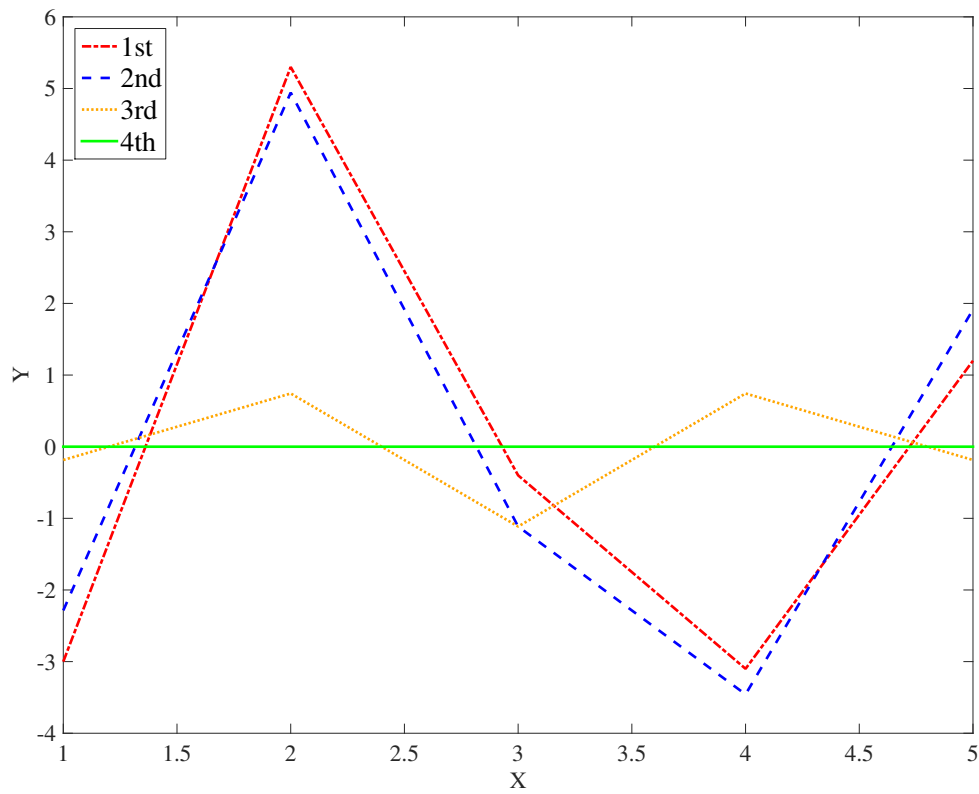


Figure 6.13: Residuals from different order polynomial regression on five data points.

## Polynomial Regression

This section shows the performance of different order polynomial regression. When five data points are considered, the fourth order polynomial is able to contain all the data points, see Fig 6.12, hence the residual is zero, see Fig 6.13. All the lower order regressions can not handle all the information from the data set, so they approximate the data as good as they can. The first and second order polynomial are both performing a poor estimate, this is also observed from large residuals.

MATLAB functions: `polyfit` and `polyval`.

## Two Variable Polynomial Regression

Regression is obviously also possible to perform on multivariate data sets. It is possible to fit the data to all kinds of mathematical functions, but only different order polynomials are presented here. For a given data set, the first order plane is observed in Fig. 6.14. The second order polynomial fit is presented in Fig. 6.15. This means that the fitted polynomial has second order terms like  $x^2$ ,  $y^2$  and  $x \cdot y$ . A third order plane is seen in Fig. 6.16. It is easy to observe that the higher order fittings is more accurate for these data points, which are the same as in the two variable interpolation part.

MATLAB functions: `fit`, `polyfitn` and `polyvaln`.

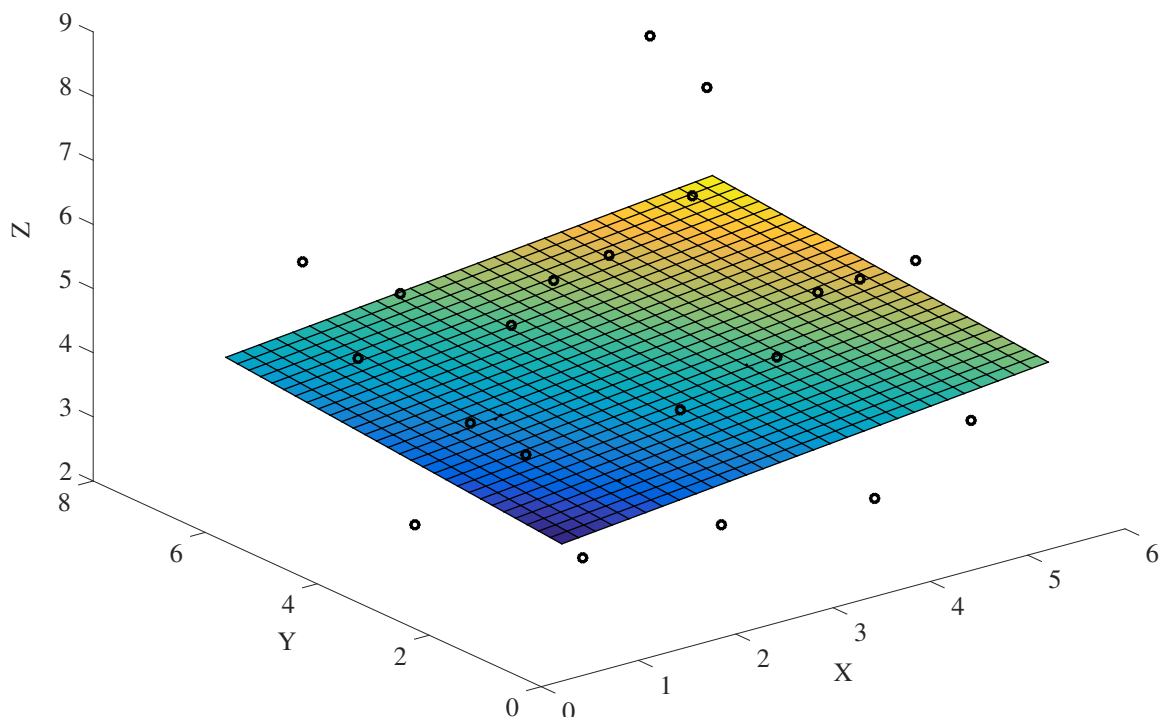


Figure 6.14: First order plane, with two variables.

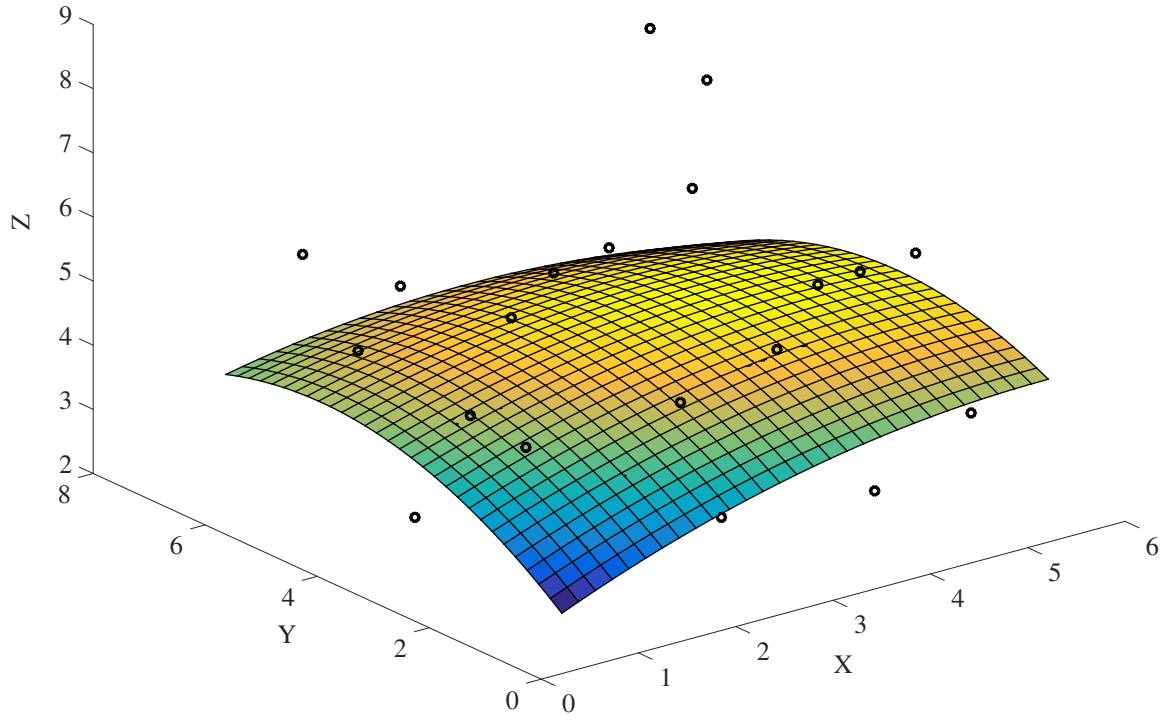


Figure 6.15: Second order plane, with two variables.

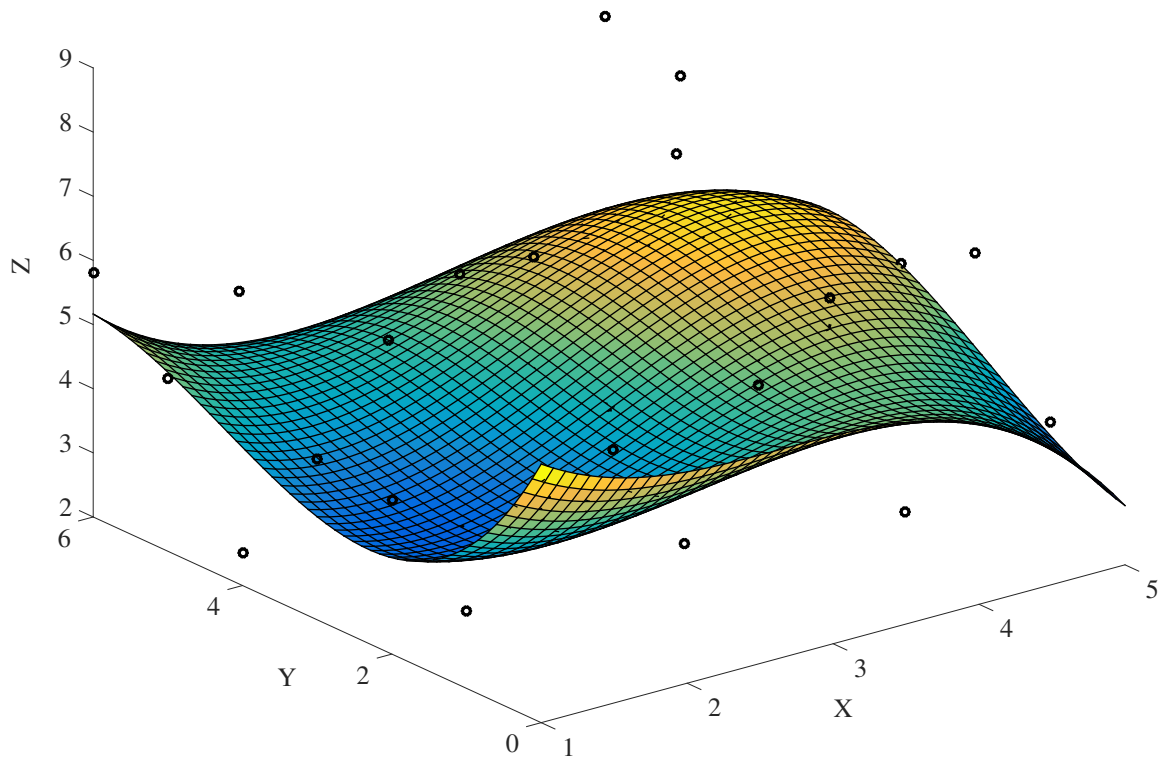


Figure 6.16: Third order plane, with two variables.

### 6.3 Scaling

Uniform scaling is a linear transformation that diminishes or enlarges objects by the same scale factor in all directions [89]. Non-uniform scaling is also possible, like directional scaling and stretching. These types of scaling have a separate scale factor for each direction or segment. This will normally also change the shape of the object, e.g. from square to rectangle. The basic understanding for turbine and heat exchanger scaling can be obtained from two basic aspects, proportionality and geometry. The analysis of these aspects will be followed by scaling of turbomachinery, and analytical work on turbine and heat exchanger weight.

#### Proportionality

Proportionality is an important aspect when scaling is considered. Variables are said to be proportional if a constant multiplier defines the change between them. This constant is called the proportionality constant.

The equation,

$$y = k \cdot x$$

gives that  $y$  is directly proportional to  $x$ :

$$y \propto x$$

with the proportionality constant:

$$k = \frac{y}{x}$$

On more example, where weight ( $W$ ) is a function of diameter ( $D$ ),  $a$  and  $b$  are constants.

$$W = a \cdot D^2 + b \implies W \propto D^2$$

The weight is proportional to the square of the diameter.

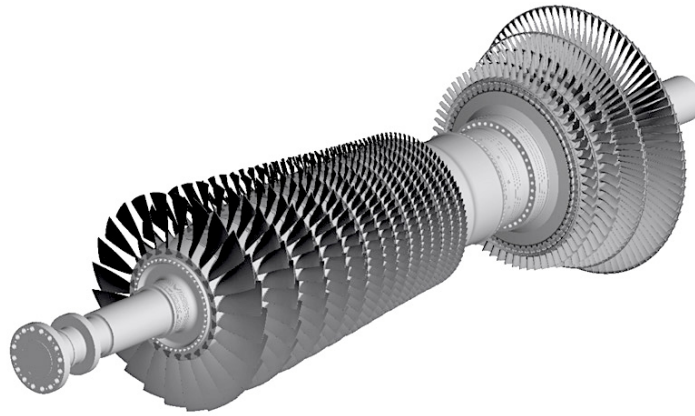


Figure 6.17: Steam turbine rotor, where the blades form two conical frustum geometries.

## Geometry

To look into the fundamental understanding of weight, a good starting point is the geometry. In a turbine, the major components in terms of weight, are forming a certain geometry that can be identified. If we consider e.g. a steam turbine, the rotor blades forms something similar to a conical frustum, see Figure 6.17 and 6.18. The weight is a function of the material density and its volume, which is given by the geometry.

### Conical Frustum - Turbine

In this analysis, a turbine is modeled as a conical frustum with a given and constant average overall density,  $\bar{\rho}$ . This density is given by the fraction of material vs. empty air inside the considered geometry.

Volume for conical frustum:

$$V = \frac{\pi}{12} h (D_1^2 + D_1 D_2 + D_2^2) \quad (6.13)$$

Assume similarity/uniform scaling for an enlarged turbine, see Figure 6.19:

$$V = \frac{\pi}{12} (kh) (k^2 D_1^2 + k D_1 k D_2 + k^2 D_2^2) = k^3 \left[ \frac{\pi}{12} h (D_1^2 + D_1 D_2 + D_2^2) \right] \quad (6.14)$$

Because uniform scaling is assumed, the relationship between  $h$  and  $D$  is given by:

$$h \propto D \quad (6.15)$$

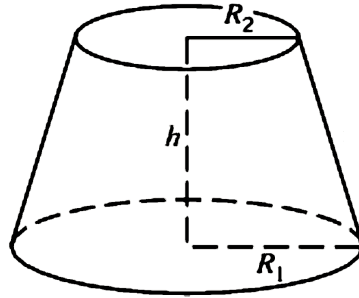


Figure 6.18: Conical Frustum.

Since  $D_1$  and  $D_2$  is linked in the same way, the relationship between volume and diameter is:

$$V \propto D^3 \tag{6.16}$$

Then it is assumed that a flow with the same thermodynamic properties is going through the turbines. The mass flow is proportional to the square of the diameter:

$$\dot{m} = \rho Av = \rho \frac{\pi D^2}{4} v \propto D^2 \tag{6.17}$$

Weight of a conical frustum/turbine is given by product of volume and the average density:

$$W = \bar{\rho} V \tag{6.18}$$

That gives the following relationship:

$$W \propto D^3 \propto \dot{m}^{\frac{3}{2}} \tag{6.19}$$

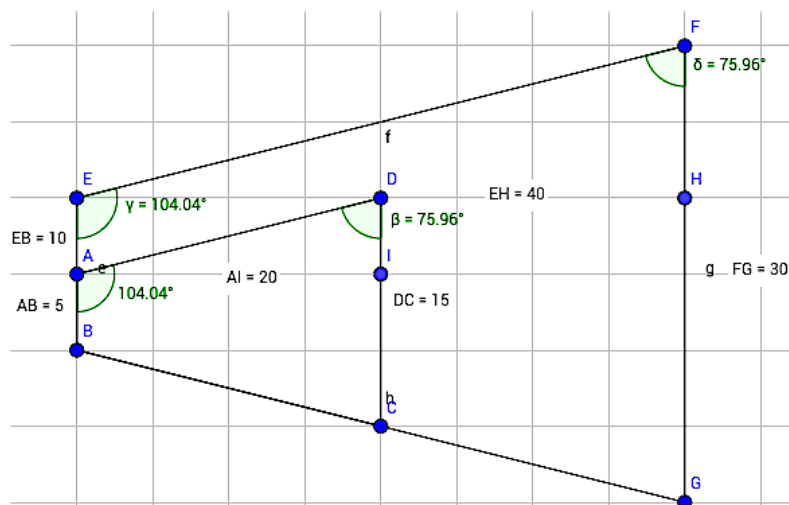


Figure 6.19: Similarity for conical frustum.

### Composed Geometry – Heat Exchanger

The fundamental understanding of heat exchanger scaling is not straightforward, because the geometry has to change in some extent. Variables like tube and shell thickness could stay constant, while e.g. number of tubes and shell diameter would change. The underlying design criteria for shell and tube heat exchangers can be found in Appendix B.2. Based on this criteria and GT PRO simulations, some basic non-uniform scaling relations for shell and tube heat exchangers were developed and implemented in Excel. These are found in Appendix D.1.1, where Figures D.1 and D.2 shows the Excel model.

The Excel model is based on an analytical approach, where the volume of the major components are calculated. In terms of volume, they are casing/shell, baffles and tubes. The shell is modeled as a cylinder with two disks, the baffles are disk segments and the tubes as cylinders. Based on the design criteria and other available data, the model was tuned in terms of non-uniform scaling for length, diameter, number of tubes etc. The tube thickness and diameter are assumed constant. Because the weight is proportional to the total volume, the weight estimate is derived directly from the fundamental geometry. This model is indicating a linear relationship between weight and both heat transfer surface area and the total tube flow area,

$$\boxed{W \propto A} \quad (6.20)$$

Eq. 6.17 gives this relationship with the steam mass flow:

$$\boxed{W \propto \dot{m}} \quad (6.21)$$

The simulation results from GT PRO is found in Section 8.1.2, and the Excel model analysis is found in the Appendix, Figures D.3 and D.4.

Table 6.1: Nomenclature for turbine scaling.

Parameter	Property
D	Rotor diameter, $m$
A	Area, $m^2$
c	Absolute velocity, $\frac{m}{s}$
H	Head, $m$
k	Coefficient
N	Rotative speed, rpm
u	Peripheral speed, $\frac{m}{s}$
Q	Volume flow, $\frac{m^3}{s}$
W	Weight, kg
Subscript	
s	Standard turbine
ad	Adiabatic
1	Inlet of machine
2	Before turbine rotor
3	Outlet of machine

### Scaling of Turbomachinery

The aim of scaling analysis is to compare the performance of two turbomachines of similar design. Non dimensional variables are used to express the relevant relations. Similitude broadly refers to similarity in geometry and flow in two turbomachines. [90].

### Similarity Relations for Turbine Designs

This part is based on O. E. Balje's work on similarity relations and design criteria of turbines [91]. The purpose of similarity parameters is to define the operating and design conditions where turbines with the same geometry experience similar fluid dynamic conditions.

The volumetric flow,  $Q_3$  passing through the turbine exhaust is proportional to the characteristic velocity,  $c$ , and the through flow area,  $A$ . It is then showed, because:  $c \propto u \propto ND$ , that the flow is proportional to the product of rotational speed,  $N$ , and the cube of the rotor diameter,  $D$ .

$$Q_3 \propto cA \propto cD^2 \propto ND^3 \quad (6.22)$$

From Eq. 6.22, comparing a new turbine with the standard one, denoted with the subscript 's'. The standard turbine is assumed to have characteristic values at unity, which implies  $Q_{3s} = H_{ad,s} = 1$ .

$$\frac{Q_3}{Q_{3s}} = \frac{ND^3}{N_s D_s^3} \quad (6.23)$$

The adiabatic head,  $H_{ad}$ , expanded in the turbine is proportional to the characteristic velocity,  $c$ , squared, and consequently proportional to the product of the square of  $N$  and  $D$ .



$$H_{ad} \propto c^2 \propto N^2 D^2 \quad (6.24)$$

From Eq. 6.24, comparing with the standard turbine.

$$\frac{H_{ad}}{H_{ad,s}} = \frac{N^2 D^2}{N_s^2 D_s^2} \quad (6.25)$$

When solving Eq. 6.23 and Eq. 6.25 in terms of  $D$ , the following relationships are found.

$$D = \frac{Q_3^{1/3} N_s^{1/3} D_s}{N^{1/3}} = \frac{H_{ad}^{1/2} N_s D_s}{N} \quad (6.26)$$

Rearranging the terms,  $N_s$  is found, which usually is referred to as the specific speed.

$$N_s = \frac{N Q_3^{1/2}}{H_{ad}^{3/4}} \quad (6.27)$$

When solving Eq. 6.23 and Eq. 6.25 in terms of  $N$ , it is possible to rearrange to find an expression for the specific diameter,  $D_s$ .

$$N = \frac{Q_3 N_s D_s^3}{D^3} = \frac{H_{ad}^{1/2} N_s D_s}{D} \quad (6.28)$$

$$D_s = \frac{D H_{ad}^{3/4}}{Q_3^{1/2}} \quad (6.29)$$

From  $N_s$  and  $D_s$ , it follows that as long as Reynolds-number and Mach-number effects are neglected, turbines of similar design geometry which have the same specific speed and diameter have the same efficiency. This forms the basis for how turbines are scaled, and consequently how the weight will vary according to this. More theory on turbine scaling is available in Appendix A.5.1.

### Turbine Weight

For turbine weight estimation, there exist some previous analysis. They are not very generous in terms of how the results are developed, but should give some good indications on what to expect when further analysis is performed. The first weight estimate for turbines is given by O. E. Balje [91], and gives the unit weight as:

$$\boxed{W = k_g D^2} \quad (6.30)$$

It is said to be valid for rotor diameters in the range 0.9–3.0 m. From Eq. 6.17,

$$D^2 \propto \dot{m} \quad (6.31)$$

and the weight is proportional to the mass flow:

$$\boxed{W = k_m \dot{m} \propto \dot{m}} \quad (6.32)$$

Where:

$$k_m = \frac{4k_g}{\pi\rho v} \quad (6.33)$$

The second relationship is given by F. Whittle. He has written a textbook on gas turbines in aviation, and writes the following: "It will be obvious that, for geometrically similar engines with the same thermal cycles, the power will be proportional to the square of the diameter while the weight would be proportional to the cube of the diameter. It would seem to pay to use 4 small engines instead of one engine with twice the size, but unfortunately, though the aerodynamic scale down is feasible, the apparent potential 50% weight saving would not be achieved at reasonable cost because mechanical and manufacturing problems are greatly increased by size reduction." [92].

This can be summarized in mathematical terms as:

$$\boxed{W \propto D^3 \propto \dot{m}^{\frac{3}{2}}} \quad (6.34)$$

The weight is proportional to mass flow raised to the power of 1.5.

D.E. Brandt and R.R. Wesorick have written a very interesting paper named "GE Gas Turbine Design Philosophy" [93]. In this paper, they inform about the General Electric product line: "A highly successful principle of GE's product line has been geometric scaling of both compressors and turbines. Scaling is based on the principle that one can reduce or increase the physical size of a machine while simultaneously increasing or decreasing rotational speed to produce an aerodynamically and mechanically similar line of compressors and turbines."

The scale factor is defined as the diameter ratio, and they developed a table that displays how different turbine properties vary with this factor. The most important properties for this thesis are listed in Table 6.2.

Table 6.2: Scaling ratios from GE gas turbines and compressors.

Scale factor	0.5	1	2
Flow	0.25	1	4
Power	0.25	1	4
Weight	0.125	1	8

From the scale factor and mass flow, the following relationships are found:

$$\dot{m} \propto D^2 \quad (6.35)$$

$$D \propto \dot{m}^{\frac{1}{2}} \quad (6.36)$$

The power ( $P$ ) can then be expressed as:

$$P \propto D^2 \propto \dot{m} \quad (6.37)$$

If turbine weight is considered, the following relationships is easily derived:

$$W \propto D^3 \propto \dot{m}^{\frac{3}{2}} \quad (6.38)$$

This is the same result as F. Whittle presented in his work.

A. Rivera-Alvarez has written an article about ship weight reduction through combined power cycles [94].

In this paper, the weight for a similar set of turbines are given by:

$$W = k_{Turbine} \cdot \dot{m}_{Turbine}^{\frac{3}{2}} \quad (6.39)$$

To include non-size dependent components of the system, the article uses this representation of the weight:

$$W = k_{Turbine} \cdot \dot{m}_{Turbine}^{\frac{3}{2}} + W_{Turbine,0} \quad (6.40)$$

This is the same weight estimate that has previously presented, but he clearly defines that only the mechanical parts of the system is included in this weight:

"It is important to clarify that the considered weights for the gas and steam turbines just include

the mechanical parts for the equipment itself, disregarding any required gearbox, electric generator, or powered system. All these additional equipment, in fact, could add a very significant amount of weight (for a typical industrial gas turbine-generator package, the gas turbine itself could have a weight as low as 15% of the total)." [94].

### HRSG and Heat Exchanger Weight

A. Rivera-Alvarez is also considering the heat recovery steam generator in his article [94], the weight is given as a linear function of the heat transfer area:

$$W = k_{HRSG} \cdot A_{HRSG} + W_{HRSG,0} \quad (6.41)$$

This weight estimate should be a pretty radical simplification, because the HRSG geometry and design are quite complex. The most important assumptions for a linear relationship between surface area and weight are listed below. Eq. 6.41 is also applicable for heat exchanger weight estimation. The dry weight of a HRSG can in general terms be decomposed in: Heat transfer arrangement, external structure, and non-size dependent components.

Assumptions for a linear relationship:

- Constant heat transfer coefficient. When the scaling is performed, it is assumed that the flow configuration and the magnitude of heat transfer coefficients are maintained.
  - When a HRSG is considered, this applies for the heat transfer coefficient in both economizer, evaporator and superheater.
  - For heat exchangers, it is the overall heat transfer coefficient that is considered.
- The heat exchange surface has constant tube and fin thickness.
- For external components like shell, insulation and structural parts, the thickness is fixed.
  - This assumption represent the greatest simplification, and is the biggest source for uncertainties related to the weight estimation.

## 6.4 Chapter Discussion

Mathematical representation is important when the behavior of a physical system is described. The main application in this thesis is to arrive at a reliable weight estimating method for steam bottoming cycles on offshore oil and gas installations. Two different methods are considered; a weight estimating polynomial, and scaling laws from similarity approach. The interpolation techniques are not found to be the best approach for this study. The weight estimates should seek to find a trend in the data, not necessarily end up at already known data points. Hence, multidimensional higher order approximating splines could potentially have been used with good accuracy. This method was proposed by some mathematicians, when the steam cycle weight estimation was discussed on mathematical Internet forums. After discussing with mathematicians like Dag Wessel-Berg, and analyzing available literature, regression in terms of least squares method is preferred for polynomial representation.

Least squares fitting is a frequently used method, when polynomials are developed. In many applications, this polynomial, which represents some behavior from the physical system, is used for optimization. This is not directly relevant for this work, because most of the variables are already fixed. This includes e.g. gas turbine exhaust temperature and mass flow, that in large extent determines the necessary sizing parameters for the steam cycle. From the analysis in this chapter, a weighted least squares method should be implemented. From the analytical work discussed, it seems possible to find some correlation between the weight and thermodynamic variables. In terms of a weight estimating polynomial, it should be sufficient to fit a second order multivariate polynomial.

Regression in terms of curve fitting will be used to analyze potential similarities in turbomachinery or heat exchanger data. Both data from manufacturers and simulation results will be tested. From the analytical approaches to weight estimation, very simple relations are proposed:

$$W = a \cdot x + b, \quad W = a \cdot x^{\frac{3}{2}} + b, \quad x = \dot{m}, P, A, D^2$$

These equations will be the starting point for further analysis on scaling relationships. The linear relationship between weight and mass flow stands out as the most promising. The standalone weight of e.g. mechanical parts for a turbine will never be considered separately for studies like the "FPSO" case, because it is the total weight that matters. The major steam cycle variables, when weight impact is considered, are gas turbine exhaust temperature and the mass flow of exhaust and steam. When scaling is considered, a constant exhaust temperature will be assumed. The similarity approach will primarily be tested for similar components that are analyzed in terms of mass flow at the design point.



# Chapter 7

# Methodology

## Contents

- 7.1 Basic Equations . . . . . 79
- 7.2 Boundary Conditions . . . . . 81
- 7.3 Equations of State . . . . . 82
- 7.4 Steam Turbine Control . . . . . 84
- 7.5 Low Weight Steam Cycle . . . . . 86
- 7.6 Process Models and Simplification . . . . . 87
- 7.7 GT PRO Process Models . . . . . 89
- 7.8 GT PRO - Desalination Plant . . . . . 90
- 7.9 GT PRO - CO<sub>2</sub> Plant . . . . . 90
- 7.10 Polynomial Representation . . . . . 92
- 7.11 Scaling Laws . . . . . 94

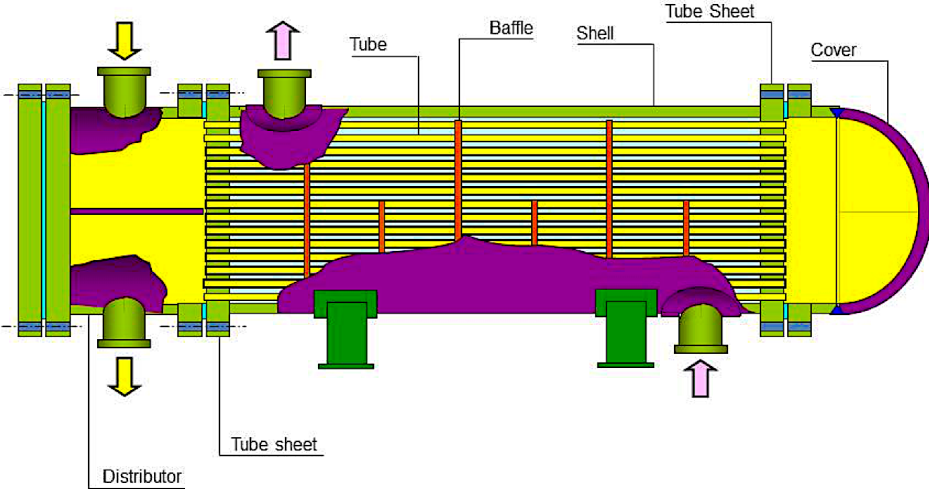


Figure 7.1: Shell and tube heat exchanger with fixed tubesheet [95].

## 7.1 Basic Equations

In this section, some basic thermodynamic equations that are forming the fundamental understanding of the work done in this thesis are collected. All thermodynamic calculations will be based on these, and should be fully understood by the reader. For a more comprehensive review of the thermodynamic principles, a textbook like Moran and Shapiro's "Fundamentals of Engineering thermodynamics" [53] is recommended.

### Mass Balance

$$\frac{dm_{CV}}{dt} = \sum_i \dot{m}_i - \sum_e \dot{m}_e \quad (7.1)$$

### Energy Balance

$$\frac{dE_{CV}}{dt} = \dot{Q}_{CV} - \dot{W}_{CV} + \sum_i \dot{m}_i \left( h + \frac{1}{2}v^2 + gz \right)_i - \sum_e \dot{m}_e \left( h + \frac{1}{2}v^2 + gz \right)_e \quad (7.2)$$

### Entropy Balance

$$\frac{dS_{CV}}{dt} = \sum_j \frac{\dot{Q}_j}{T_j} + \sum_i \dot{m}_i s_i - \sum_e \dot{m}_e s_e + \dot{\sigma}_{CV} \quad (7.3)$$

### Exergy Balance

$$\frac{dE_{CV}}{dt} = \sum_j \left( 1 - \frac{T_0}{T_j} \right) \dot{Q}_j - \left( \dot{W}_{CV} - p_0 \frac{dV_{CV}}{dt} \right) + \sum_i \dot{m}_i e_{fi} - \sum_e \dot{m}_e e_{fe} - \dot{E}_d \quad (7.4)$$

### Steady State

$$\frac{d}{dt} = 0 \quad (7.5)$$

### Isentropic Process

$$\Delta S = 0 \quad (7.6)$$

### Carnot-Efficiency

$$\eta_C = 1 - \frac{T_l}{T_h} \quad (7.7)$$

### Heat Capacity

$$c_p = \left( \frac{dh}{dt} \right)_p \quad (7.8)$$



**Change in Enthalpy**

$$dh = c_p(T)dt \implies \int_1^2 dh = \int_1^2 c_p(T)dt$$

$$\Delta h = \int_1^2 c_p(T)dt \quad (7.9)$$

$$\xrightarrow{c_p=const.} \Delta h = c_p \Delta T \quad (7.10)$$

**Volume Flow**

$$\dot{V} = \frac{\dot{m}}{\rho} = A \cdot v \quad (7.11)$$

## 7.2 Boundary Conditions

The boundary conditions are given in SINTEF documents. They describe different simulation cases where carbon capture and storage could be applicable [96] [97] [98]. For this thesis work, the "FPSO" case is analyzed.

The exhaust from the gas turbines are fixed in terms of temperature, pressure and mass flow. The total mass is given in Table 7.1. The exhaust gas composition is very important, especially for the capture plant, which is adjusted for optimal efficiency on different compositions. For the considered case, the composition is given in Table 7.2. The criteria for the designed cycle, and the assumptions for the ambient conditions are given in Table 7.3. The steam properties for the reboiler section are fixed, and listed in Table 7.4.

Table 7.1: Exhaust gas mass flow [ $\frac{kg}{s}$ ] from the "FPSO" case.

Name	One turbine	Six turbines
CO <sub>2</sub>	3.1	18.6
H <sub>2</sub> O	2.9	17.1
N <sub>2</sub>	49.7	298.3
O <sub>2</sub>	10.9	65.1
Argon	0.8	5.1
Sum	67.4	404.2

Table 7.2: Exhaust gas composition from the "FPSO" case.

Name	Mass%	M [ $\frac{kg}{kmol}$ ]	Mole%
CO <sub>2</sub>	4.59	44.01	2.98
H <sub>2</sub> O	4.23	18.02	6.67
N <sub>2</sub>	73.80	28.01	75.1
O <sub>2</sub>	16.12	32.00	14.36
Argon	1.26	39.98	0.90

Table 7.3: Plant criteria and assumptions from the "FPSO" case.

Ambient temperature $T_{amb}$	15	[°C]
Exhaust temperature $T_{exh}$	466	[°C]
Ambient pressure $P_{amb}$	1.013	[bar]
Ambient relative humidity	60	[%]
Frequency	60	[Hz]
Cooling water inlet temperature	9	[°C]
Cooling water outlet temperature	23	[°C]

Table 7.4: Steam property specifications for the reboiler section in the CO<sub>2</sub> capture plant.

Steam mass flow	28.89	$[\frac{kg}{s}]$
Steam temperature	152	[°C]
Steam pressure	4.0	[barg]

### 7.3 Equations of State

From Moran and Shapiro's "Fundamentals of Engineering thermodynamics" [53]: "An essential ingredient for the calculation of properties such as the specific internal energy, enthalpy, and entropy of a substance is an accurate representation of the relationship among pressure, specific volume, and temperature. Analytical formulations, called equations of state, constitute a way of expressing the  $p$ - $v$ - $T$  relationship". In this thesis work, the preferred equations of state are specified in GT PRO. Some common representations are:

#### Ideal Gas Law

$p$  = pressure (absolute).

$V$  = volume.

$n$  = number of moles.

$R$  = ideal gas constant,  $8.3145 \frac{J}{molK}$ .

$T$  = temperature (absolute).

$Z$  = compressibility factor.

$$pV = nRT \quad (7.12)$$

#### Real Gas Approximation

Ideal gas law corrected for non-ideality ( $Z \neq 1$ ):

$$pV = nZRT \quad (7.13)$$

#### Redlich-Kwong Equation

$V_m = \frac{V}{n}$  = molar volume.

$T_c$  = critical temperature (absolute).

$p_c$  = critical pressure (absolute).

$$p = \frac{RT}{V_m - b} - \frac{a}{\sqrt{T} V_m (V_m + b)} \quad (7.14)$$

$$a = \frac{0.42748 R^2 T_c^{5/2}}{p_c} \quad b = \frac{0.08664 R T_c}{p_c} \quad (7.15)$$

**Peng–Robinson**

Peng–Robinson is much used in oil and gas simulations in e.g. HYSYS, Pro II and UNISIM.

$\omega$  = acentric factor of the species.

$T_r = \frac{T}{T_c}$  = reduced temperature.

$$p = \frac{RT}{V_m - b} - \frac{a\alpha}{V_m^2 + 2bV_m - b^2} \quad (7.16)$$

$$a = \frac{0.457235 R^2 T_c^2}{p_c} \quad b = \frac{0.077796 R T_c}{p_c} \quad (7.17)$$

$$\alpha = (1 + \kappa (1 - T_r^{0.5}))^2 \quad (7.18)$$

$$\kappa = 0.37464 + 1.54226 \omega - 0.26692 \omega^2 \quad (7.19)$$

**IAPWS**

Boiler and steam turbine calculations can not be based on ideal gas equations. Therefore, real gas properties and correct behavior for liquid water are needed. The most updated equations are collected by the International Association for the Properties of Water and Steam (IAPWS). These properties are given in steam/liquid tables and computer codes [28].

**Pruß and Wagner**

“In 1995, after careful consideration, IAPWS at its meeting in Paris adopted the equation of state developed by Pruß and Wagner as the new scientific standard under the name: The IAPWS Formula-tion 1995 for the Thermodynamic Properties of Ordinary Water Substance for General and Scientific Use” [99]. For further detail and updated equations/tables/codes, see: <http://www.iapws.org/relguide/IF97-Rev.html>.

All simulations in this thesis are based on IAPWS-IF97 water and steam properties [100] [101].

## 7.4 Steam Turbine Control

Because the heat and power demand are varying, the steam turbine will not operate under constant conditions. Some of the possible ways to regulate the steam turbine for partial load are:

- Constant pressure, same pressure for all loads (No regulation), see Figure 7.6.
  - Leads to high thermal stress in the turbine [103].
- Sliding pressure operations, see Figures 7.2 and 7.4.
  - Most used, will be discussed further [39].
- Throttle control, see Figure 7.5.
  - Reduce amount of steam through the turbine by installation of a throttle valve in front of the steam turbine. Constant inlet pressure.
- Nozzle control, see Figure 7.3.
  - Partly opened or closed control valves.

The most used and chosen technology is sliding pressure operation. This mode allows the live steam pressure to decrease with reduced load, see Figure 7.6. For very small loads, the mode is switched to a low but constant pressure operation. According to different sources, this switch is normally set around 50% for combined cycles [39]. The effectiveness of sliding pressure operation, compared to the other options, increases with reduced gas turbine load [102].

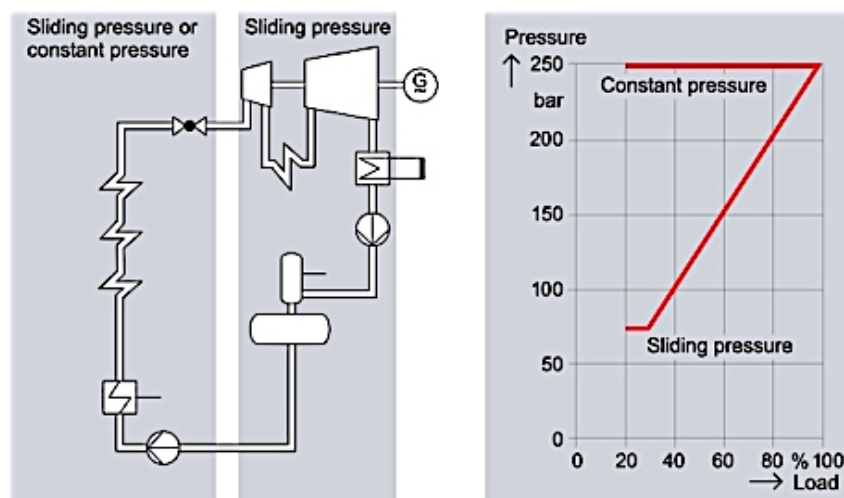


Figure 7.6: Constant and sliding pressure in steam turbine [103].

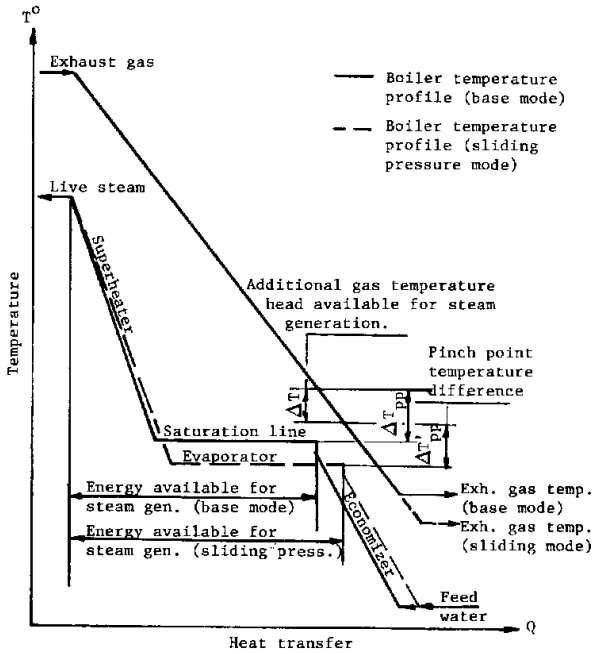


Figure 7.2: HRSG performance at sliding pressure operation [102].

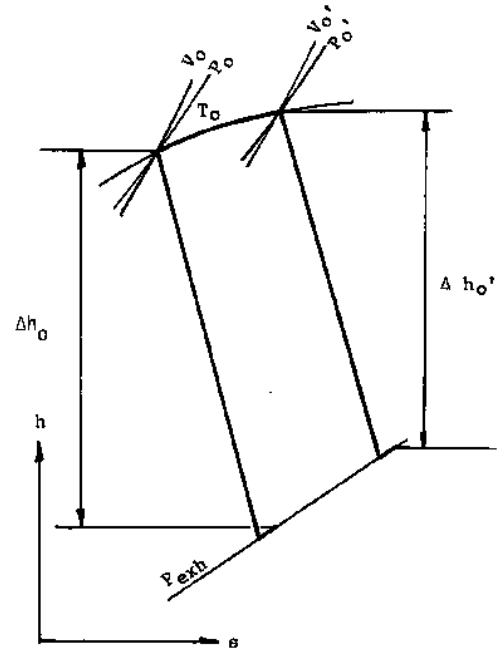


Figure 7.3: Expansion line for steam turbine with sliding pressure control [102].

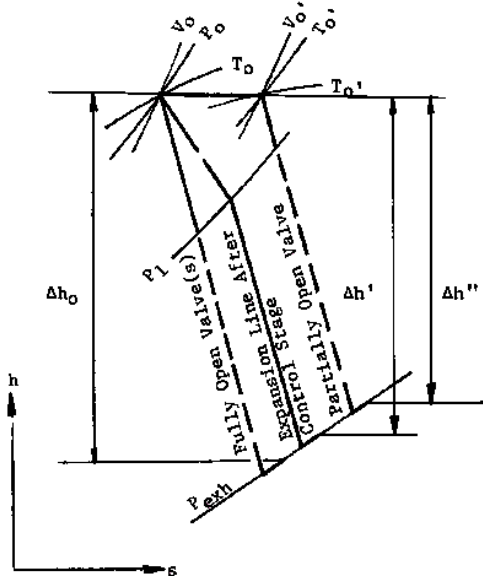


Figure 7.4: Expansion line for steam turbine with nozzle control [102].

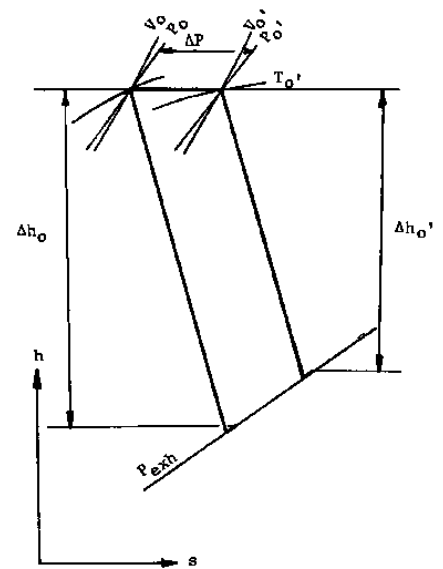


Figure 7.5: Expansion line for steam turbine with throttle control [102].

## 7.5 Low Weight Steam Cycle

From previous work in the specialization project, the most important measures for arriving at low weight steam cycle were identified. The boundary conditions for the designed cycles are given in Tables 7.1–7.4. This case is named "FPSO", and these table values are defining the base case (BC). Maximizing plant efficiency is rarely the best approach for offshore cycles, because the weight and sizing limitations would be exceeded. In this work, all cycles were built and analyzed in GT PRO [104], with emphasis on low weight within acceptable efficiencies. The thermodynamic laws allow lighter equipment for less efficient processes, this should be quite intuitive.

Several design parameters are fixed from the boundary conditions. In the designed cycles, the type of heat recovery steam generator, pinch point temperature difference ( $\Delta T_{pinch}$ ), steam turbine design and chosen materials were the most important. The chosen design parameters are:

- Once through heat recovery steam generator, without drums and bypass stack.
- $\Delta T_{pinch} = 33\text{K}$ .
- Back-pressure turbine.
- Incoloy as HRSG tube material, stainless steel fins.

Once through heat recovery steam generator was chosen as the best alternative for offshore implementation. This choice is based on previous work, findings in the literature study and GT PRO simulations. This approach is also used for the pinch point temperature difference. Several values were tested to find the optimal balance between heat output, efficiency and weight. From this analysis, a  $\Delta T_{pinch} = 33\text{K}$  was chosen. Compared to available data, this pinch is high, but not unrealistic for offshore installations [28]. The general effects of higher pinch temperature are reduced weight and lower efficiency from decreased steam production and higher exhaust temperature. This  $\Delta T_{pinch}$ -value should be considered if the designed plant is within the respective space and weight limitations for the considered installation. A high efficiency is always desired, so it should be no reason to choose a higher pinch point temperature than necessary.

The specialization project found a back-pressure turbine to be the best steam turbine design for this steam cycle. Based on previous results and an extensive literature study, Incoloy alloy was found to be the best alternative for the tube material. Without a buy pass stack, the weight is reduced even further. This material, together with the stainless steel fins, should manage to withstand the harsh offshore conditions.

## 7.6 Process Models and Simplification

### Process Models

"In the past, sophisticated modeling tools were a luxury that only large companies could afford, where savings in large production runs justified the costs in computer software and specialized engineers. Today, modeling has become an indispensable element of research and process development, and realistic models of advanced systems are feasible on a personal computer" [105].

In programs like GT PRO it is possible to build a quite realistic model of a physical system. In more advanced programs, one single simulation can take numerous days on a super computer for a given model. Therefore, is simplification a precious commodity for all types of process models. Mathematical equations form the fundamental for all models, although most of the modern software for process modeling has a visual and interactive user interface.

### Sensitivity Analysis

Sensitivity analysis finds the uncertainty in output for a given model, in this work related to the weight of a chosen component in the designed cycle. To decide which parameters to consider, the change in output is examined for different input values. If the change in output is relatively large for a small change in the input parameter, the model is sensitive to this parameter. Normally models are more sensitive to some parameters than others. Therefore, is it important to identify those with the greatest impact. If the weight is almost independent of changes in one actual parameter, it is no reason to spend time on implementing it into the model. This analysis was performed to find which parameters to implement in both the polynomial representation and the scaling laws.

### Simplification

When a process model should be developed, it is very important to determine the necessary level of detail. Even the smallest component can add a great deal of complexity to the model. Removing components, create black boxes and disregard e.g. auxiliary systems are some of the simplifications that always should be considered when a process model is developed.

R. L. Eberlein [106] has done extensive research on process models and simplification. He says that tools for model understanding are still rare and generally inaccessible. One powerful approach to understanding a model, is through simplification. He clearly points out that the simplification of a model is, itself, a complete model.



According to A. K. Saysel and Y. Barlas [107], model simplification is an approach to identify essential structures of a large scale model. In large simulation models, it may be impossible to detect and avoid structures not contributing to the analysis objectives and to its understanding. Simplification increases the quality, usefulness and understanding for all dynamic systems, and helps with problem identification, boundary selection, model formulation and testing. They propose to perform the simplification as a late step, after model building and validation of the original large scale model is finished. At this stage, you have the knowledge to decide the best simplification measures, increasing the quality of the simplified model. Another use of simplification could be to help obtain general models from case specific models, this is very relevant for the work done in this thesis.

Y. Barlas [108] suggests that final step in all dynamic modeling should be model simplification. The goal is to end up with a much simpler, fundamental version of the working model. He is fundamentally against the common “this model is unrealistically simple” type of criticism. Many modelers are tempted to build large and too detailed models, which makes the situation worse, since the final product often is very complex, but still unrealistic.

It should be mentioned, that the GT PRO models that are built in this thesis, is very simplified. Advanced process models for combined cycles, includes detailed description and dynamic behavior for every component, even small ones like valves and pumps. For this work, only the major components are considered in the process models. All GT PRO models in this work, have emphasis on the steam turbine and heat recovery steam generator. Motivated by Saysel and Barlas, all simplifications in this work are performed in a late step. One example of this, is that the gas turbines are replaced with a custom exhaust mass flow.

## 7.7 GT PRO Process Models

The GT PRO models are used to understand, analyze and illustrate the thermodynamic processes and get weight estimation for components like steam turbine, generator, heat recovery steam generator and desalination plant. To build a model, all relevant conditions and settings are put into predefined tabs for the different systems like steam turbine, gas turbine, HRSG, etc. If more information about the software is desired, see [http://www.thermoflow.com/combinedcycle\\_GTP.html](http://www.thermoflow.com/combinedcycle_GTP.html). Three separate models were built, all of them are based on the low weight steam cycle described in Section 7.5.

- Model 1: OTSG and back-pressure turbine.
- Model 2: OTSG, back-pressure turbine and CO<sub>2</sub> capture.
- Model 3: OTSG, back-pressure turbine, CO<sub>2</sub> capture and desalination.

In the development of these final cycles, multiple designs were tested and analyzed in GT PRO. Validation is always important, to ensure that the given simulation results were thermodynamically valid, additional calculations were performed. These were based on the method found in Appendices A.4.1 and B.1, and equations in Section 7.1.

To get the correct composition, temperature, pressure, and mass flow rate according to the defined base case, a user-defined exhaust flow was implemented in GT PRO. The total weight ( $W_{Tot}$ ) is calculated for all GT PRO models, and is defined as the weight of steam turbine, generator and steam generator, where dry conditions are considered. For model 1 and 2, this total weight is also estimated by a polynomial approach and calculated scaling laws.

The final models are found in Section 8.2.1, 8.2.2 and 8.2.3.

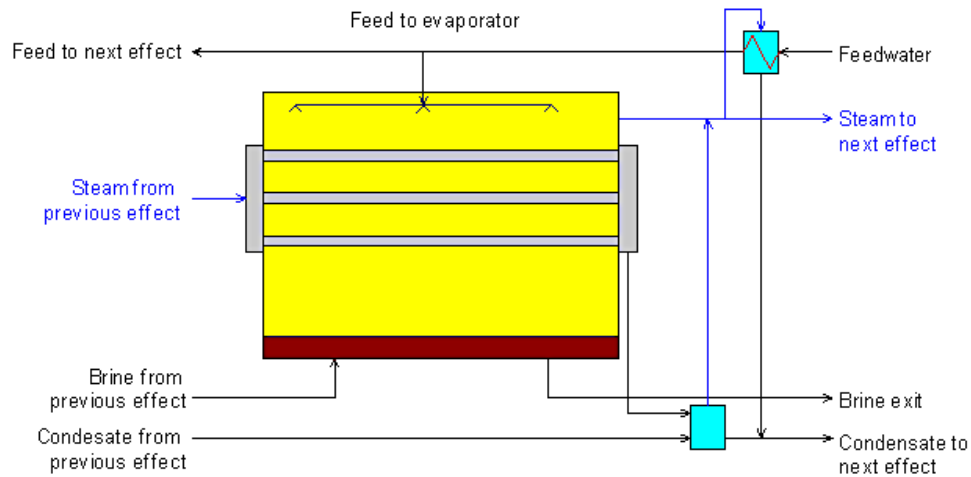


Figure 7.7: MED plant section from GT PRO.

## 7.8 GT PRO - Desalination Plant

The chosen desalination technology is MED-TVC, see Section 3.5. This system was implemented and tested in GT PRO. The finished design is found in Fig C.35. The salt concentration on the sea water is assumed to be 3.4% at 9°C.

## 7.9 GT PRO - CO<sub>2</sub> Plant

To complete the GT PRO model, an amine based post combustion CO<sub>2</sub> plant was added. Based on the documentations from SINTEF [98], the model was tuned and tested. Different simulation software is used, so a perfect reproduction was not possible. Some important values that were implemented is collected in Table 7.5. With the tuned model, the steam temperature, pressure and mass flow were perfect in terms of the specifications, see Fig. 7.8.

The plant was also tested with CO<sub>2</sub> compression, respectively up to 65, 150 and 200 bar. When considering the power demand, it would be very desired if the steam turbine could supply this amount. The total electrical power consumption with compression was 8.2 MW for 65 bar, 9.0 MW for 150 bar, and 9.2 MW for 200 bar. 65 bar is the CO<sub>2</sub> injection pressure at Sleipner, see Section 5.4.

Table 7.5: Properties in the GT PRO CO<sub>2</sub> plant model.

Property	Unit	SINTEF	GT PRO
$T_{cooler}$	[°C]	33.7	33.7
Heat input/CO <sub>2</sub>	[ $\frac{kJ}{kg}$ ]	3685	3639
Electricity consumption	[kW]	3294	3492

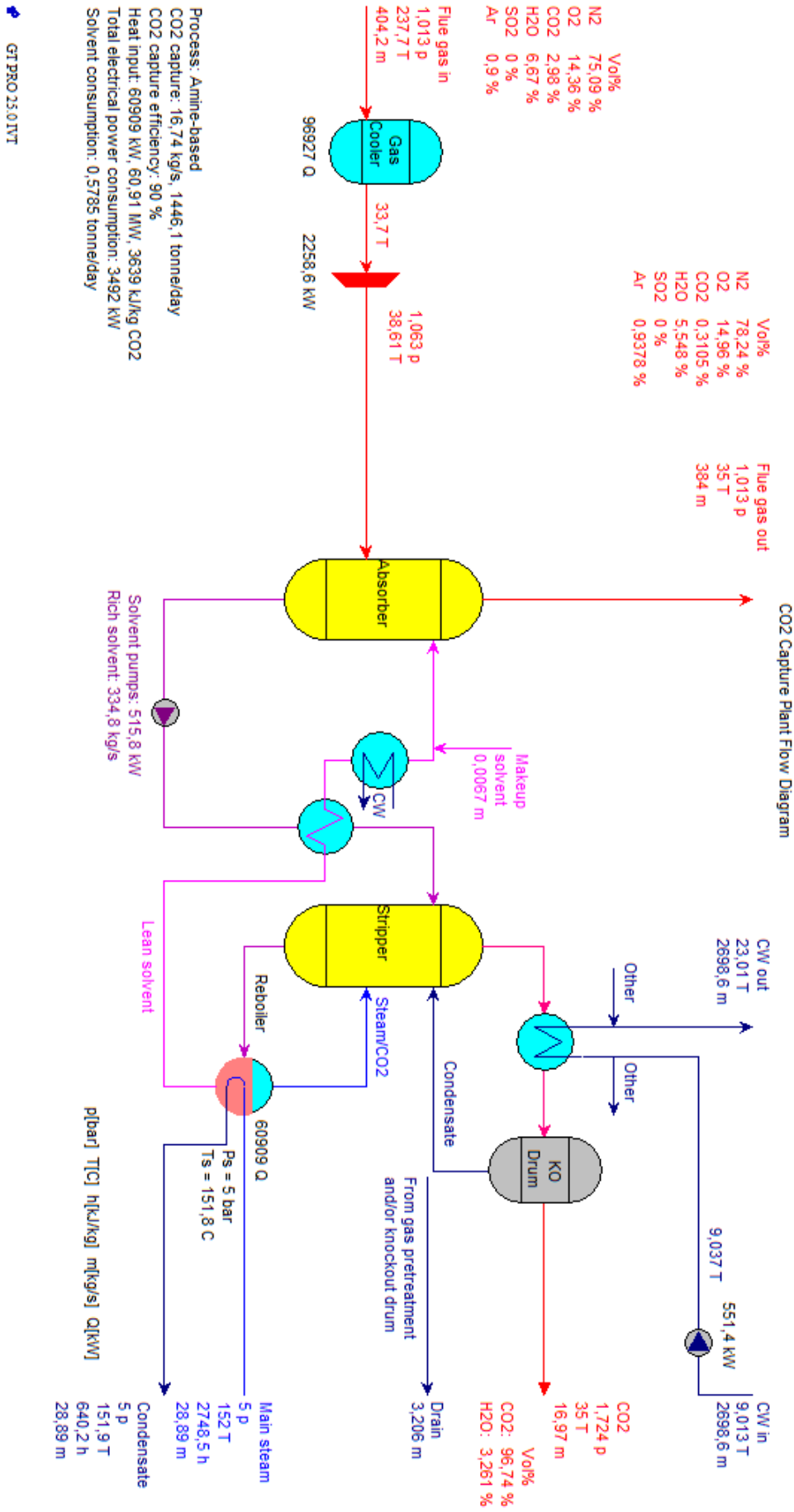


Figure 7.8: CO<sub>2</sub> plant model from GT PRO.

Table 7.6: Variables used in polynomial weight representation.

Name	Parameter	Property
Exhaust mass flow	$x_1$	$\dot{m}_{exh}$
Exhaust temperature	$x_2$	$T_{exh}$
Steam mass flow	$x_3$	$\dot{m}_{steam}$

## 7.10 Polynomial Representation

After discussions with the academic supervisor Lars Nord, associate professor Kjell Kolsaker and senior scientist Dag Wessel-Berg, a new approach to the polynomial representation was made. The previous approach can be seen in Appendix C.7. The new approach is based on weighted non-linear least squares method, and is performed in MATLAB.

Because GT PRO only allow interaction with Excel, some intermediate calculations had to be exported and imported. Fictitious cases were made to test different methods for the least squares method. Weights based on the Bi square method was chosen as the best alternative. This method is recommended by several mathematicians, and is the default setting for multivariate weighted least squares fitting in MATLAB.

From sensitivity analysis in GT PRO, experiences from the specialization project, physical limitations and gas turbine data, each variable were given a reasonable range of variation. To limit the complexity and simplify the validation process, it was decided to restrict the polynomial to three variables.

The chosen variables are collected in Table 7.6. Based on academic discussion and sensitivity analysis, they are selected as the most relevant variables for weight estimation. The exhaust mass flow and temperature represent the gas turbine, where the outlet pressure is assumed to be constant for all turbines (Given by the ambient conditions). The steam mass flow is going through the heat recovery steam generator and the steam turbine, and is highly influencing the weight of these components. This variable is also ensuring sufficient steam mass flow to the CO<sub>2</sub> plant, which is partly determined from  $x_1$  and  $x_2$ . The steam temperature and pressure out of the turbine is assumed constant, because they are determined from the CO<sub>2</sub> plant's specifications. Other weight affecting parameters like pinch point temperature difference is treated as a design parameter, and therefore not included in the weight estimation.

Even with only three variables ( $m = 3$ ), the number of necessary simulations, from here referred to as nodes, grows cubic with the chosen grid. The grid is given by how many subintervals each variable's total range is divided into. In this approach, the range was divided into four ( $n = 4$ ). To make even distributed nodes within the range for all variables, a script was made in MATLAB (combo\_3\_4.m, D.2.2). This script calculated all the 64 ( $n^m$ ) values for  $x_1$ ,  $x_2$  and  $x_3$  that went into the GT PRO simulations in the Excel module ELINK. To simplify the simulation work, this script organizes and saves all values into a .xlsx file. These values can then be copy-pasted directly into ELINK.

The most time consuming part is to extract the simulation results from Excel. From each round of simulation, the values for  $x_1$ ,  $x_2$ ,  $x_3$  and  $W_{total}$  were exported to a spreadsheet. This sheet was then imported in MATLAB by a different script (poly\_3\_4.m, D.2.3). To ensure complete control of the process, and the possibility to adjust the polynomial later, each term in the polynomial were defined in a MATLAB function handle. For this work, a second order polynomial was implemented, see Eq. 8.1.

To ensure a well-balanced regression, all variables are scaled by the maximum value for the respective variable. This step compensates for the variables difference in magnitude, which is very important for the accuracy on the final result. To ensure that the polynomial ends up with the correct magnitude in the end, a correction vector was made. Based on the scaling factors, a correction term was calculated for all the terms in the polynomial.

With some additional settings, all data were passed over to the MATLAB function "fitnlm.m". This function performs the weighted least squares method on all the nodes, and calculates important parameters like coefficient of performance and polynomial coefficients. Based on these coefficients, a simple function (poly\_eval.m, D.2.4) was made to calculate the new polynomial for all  $x_1$ ,  $x_2$  and  $x_3$ . This function simplified the testing and verification of the polynomial.

The least squares method works best with independent variables, but discussions with Dag Wessel-Berg confirmed that enough nodes, with reasonable variable combinations should capture each variable's dependence within the polynomial. In some sense, the polynomial "learn" how the variables influences each other.

## 7.11 Scaling Laws

The similarity approach seeks to find scaling relationships among a group of similar objects, in this study the different components in a steam cycle. For example; is there a mathematical relationship that describes how the weight of a similar series of steam turbines develop as a function of mass flow?

It would be very insightful to look at GT PRO's algorithms for weight estimation. That would tell if their estimates are based on some sort of scaling relationship, or a totally different method. After emailing the developers, it was not possible get access to this information. For the steam turbine, the following answer was given: "I cannot share with you the proprietary algorithm Thermoflow uses to estimate steam turbine weight, but I can advise you of the parameters upon which it depends. The primary dependence is steam turbine output power. Adjustments are made for inlet pressure, inlet temperature, the number of casings, and for the number and size of exhaust ends. Additions are made for auto-extraction valvegear." Mass flow is not mentioned as one of the dependent variables, which implies that their weight estimates for steam turbines may not be based on a scaling relationships related to steam mass flow.

From the earlier discussion on mathematical scaling relations, the weight is suggested to follow Eq. 7.20, with  $n = 1$  or  $n = 1.5$  as the most promising exponents. From the same variable analysis as in the polynomial approach, steam mass flow is the desired variable to test. Additionally, to compare it with the analytical results, other variables like power, diameter and heat transfer surface area are also analyzed. To be able to test for different data sets, a MATLAB function (km32.m, D.2.1) was made. This function takes several arguments, but the most important ones are two "n"-values. Both this values are computed and compared with each other. The comparison is based on the best coefficient of performance ( $R^2$ ) from robust least squares fitting.

$$W = a \cdot x^n + b \quad (7.20)$$

To display the result, the function with the best fit is plotted. To be able to use the result for further analysis, the polynomial coefficients and the  $R^2$  value is printed in the figure. Fig. 7.9 and 7.10 shows two fictive examples with "n"-values of 1.0 and 1.5. This function provides a very helpful tool for analyzing different data sets. If a high  $R^2$  value is found for a similar set of equipment, it is most likely possible to define a scaling law.

The MATLAB code for km32.m can be seen in Appendix D.2.1.

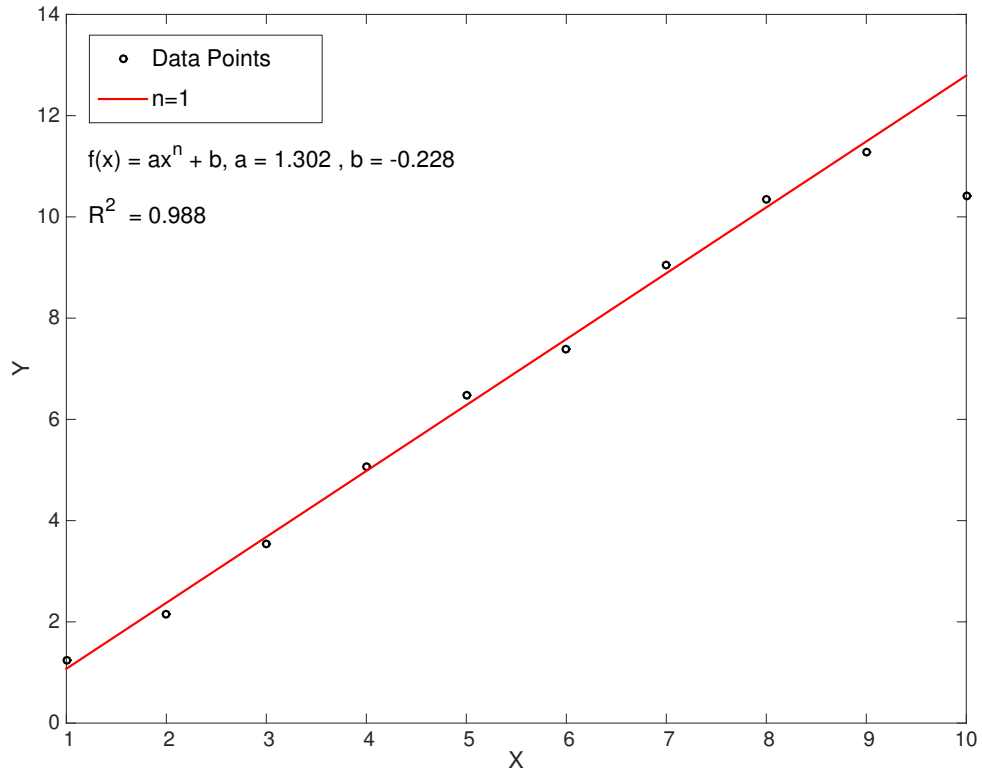


Figure 7.9: km32.m,  $W = a \cdot x^n + b$ ,  $n = 1.0$ .

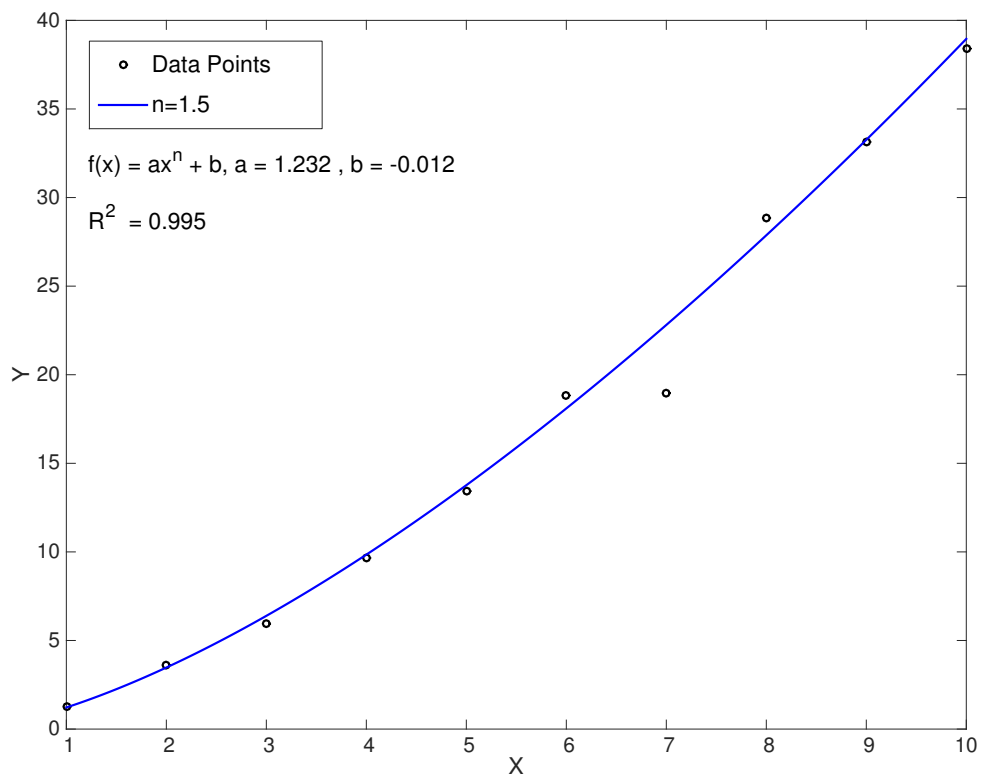


Figure 7.10: km32.m,  $W = a \cdot x^n + b$ ,  $n = 1.5$ .



# Chapter 8

## Results and Discussion

### Contents

- 8.1 Scaling Results from Literature Study . . . . . 97
  - 8.1.1 Turbines . . . . . 97
  - 8.1.2 Heat Exchangers . . . . . 102
- 8.2 GT PRO Process Models . . . . . 104
  - 8.2.1 Model 1 – Steam Cycle . . . . . 105
  - 8.2.2 Model 2 – CO<sub>2</sub> Capture . . . . . 107
  - 8.2.3 Model 3 – CO<sub>2</sub> Capture and Desalination . . . . . 109
- 8.3 Polynomial Representation . . . . . 111
  - 8.3.1 Model 1 – Polynomial 1 . . . . . 111
  - 8.3.2 Model 1 – Polynomial 2 . . . . . 111
  - 8.3.3 Model 2 – Polynomial 3 . . . . . 112
  - 8.3.4 Testing and Validation . . . . . 113
- 8.4 Scaling Laws . . . . . 114
- 8.5 Discussion . . . . . 123

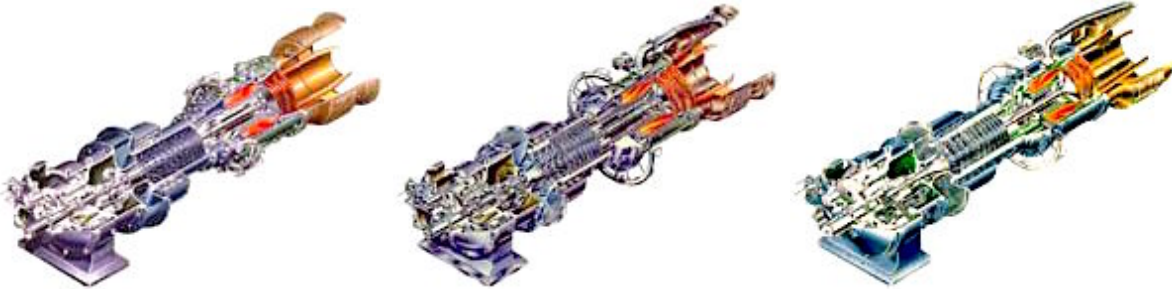


Figure 8.1: Centaur 40, Centaur 50 and Taurus 60.

This chapter will present and discuss the results found from the literature study, GT PRO simulations and analytic work done on weight estimation. The methodology is found in Chapter 7. The results are divided into four sections.

- 8.1: The scaling results from the literature study, with focus on turbine data. Heat exchanger results are also presented.
- 8.2: Three GT PRO process models.
- 8.3: Polynomial representation of the first two models.
- 8.4: Scaling laws for the first two models.

## 8.1 Scaling Results from Literature Study

In this section, the results from analyzing available documents, e-mails with the industry and academic discussions are collected. A huge amount documents are presenting weight data for different manufacturers, therefore is a limited selection analyzed based on the likelihood of similarity.

### 8.1.1 Turbines

For this turbine part, the existing theory has not reached an agreement in terms of scaling laws. Some literature suggest the relationship  $W \propto \dot{m}^{\frac{3}{2}}$ , while others support the relationship  $W \propto \dot{m}$ . When data are collected from the manufactures; it is not always clearly defined which turbine parts that are included in the weight estimate. Because of detailed documentation and similar design across models, Solar gas turbines are selected as the basis for this analysis. For comparison and validation, other manufacturers are also considered, this is found in Appendix C.1. Airplane engine weight is also relevant in terms of aeroderivative gas turbines for offshore implementation, the results from this analysis are found in Appendix C.2.

#### Solar - SoLoNOx Weight

The Solar SoLoNOx weight data set is given by several internal Solar documents [109] [110] [111], see Table 8.1.

Table 8.1: The gas turbine assembly weight for Solar SoLoNOx turbines.

Turbine	Weight [kg]	Flow [ $\frac{kg}{s}$ ]
Centaur 40	3493	19.0
Centaur 50	3538	19.1
Taurus 60	4173	21.8
Taurus 70	5630	26.9

### Solar – Turbomachinery Package Specification

Even internal documents from the manufacturer have some discrepancy in the given weight data. Here is data from the available Solar turbomachinery package specifications analyzed [110] [112] [113] [114] [115]. Both gas turbine assembly and total turbine weight are considered, see Table 8.2.

Table 8.2: The gas turbine assembly and total weight for Solar turbines.

Turbine	Weight [ton]	Total weight [ton]	Flow [ $\frac{kg}{s}$ ]
Saturn 20	0.54	6.80	6.46
Centaur 40	2.74	15.0	18.9
Taurus 60	3.29	15.4	21.6
Taurus 70	5.63	24.5	26.6
Mars 90	9.85	33.6	40.2

### Solar – Generator Drive

Solar generator drive packages are designed for power production [111]. The documentation is not clearly identifying which parts that are included in the weight data, see Table 8.3, but turbine assembly, casing and generator are certainly included.

Table 8.3: Solar gas turbine weight for generator drive.

Turbine	Weight [ton]	Flow [ $\frac{kg}{s}$ ]
Saturn 20	10.2	6.5
Centaur 40	30.5	19.0
Centaur 50	37.8	19.1
Taurus 60	37.9	21.8
Mars 100	82.1	42.6
Titan 130	94.4	49.8
Titan 250	141.2	68.2

### Elliot MYR Steam Turbines

Weight data for steam turbines are not as accessible as for gas turbines, mainly because steam turbines are more of a customized product. Some data are still available, e.g. Elliot MYR steam turbines [116] [117]. The steam mass flow at design condition is not given for these turbines, therefore is this analysis based on power, see Table 8.4.

Table 8.4: Elliot MYR steam turbine weight.

Turbine	Weight [ton]	Power [MW]
2DYZ3	4.31	3.73
2DYZ5	4.54	5.22
2DYZ7	7.71	7.50
2SQV6	11.5	11.0

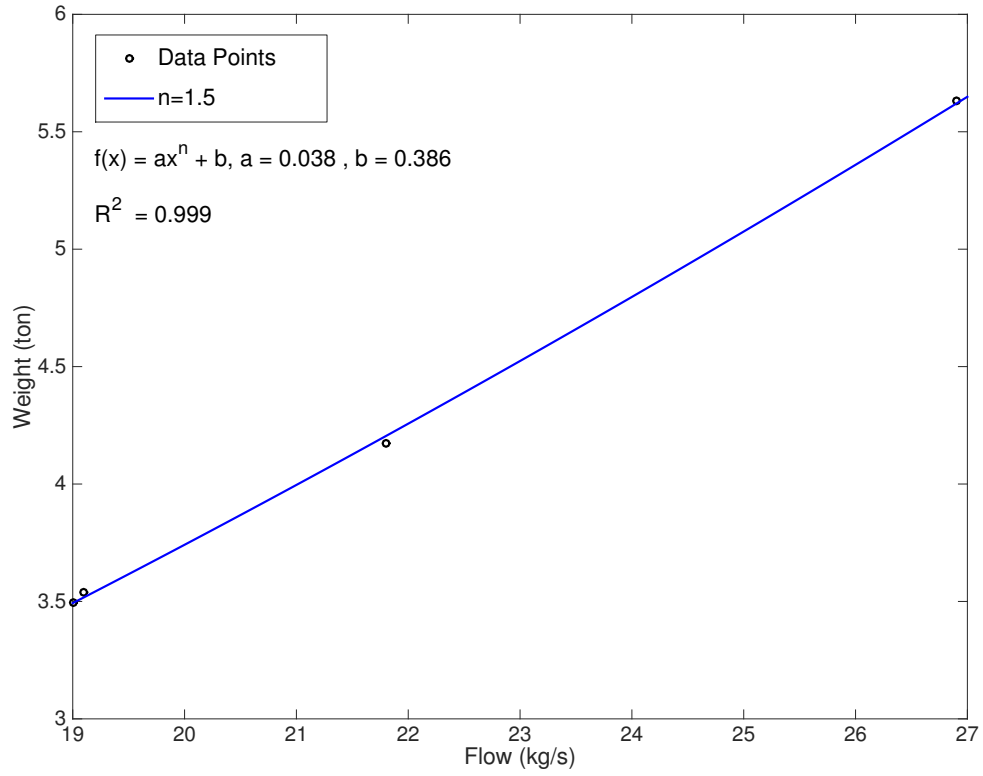


Figure 8.2: Turbine assembly weight, Solar SoLoNOx turbines.

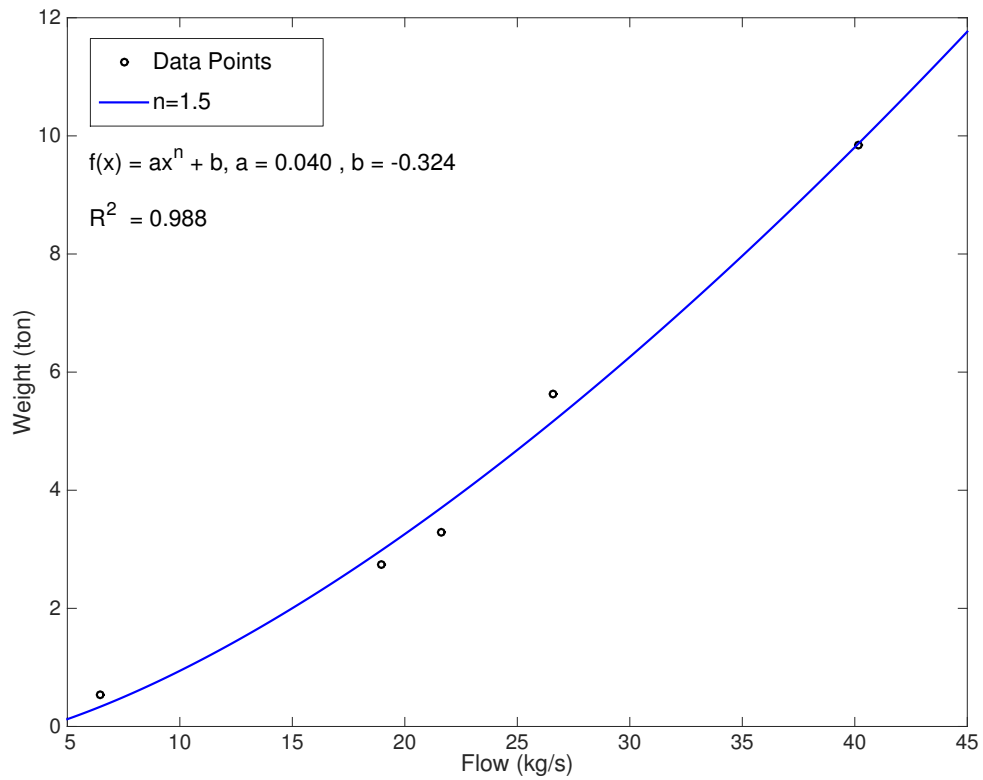


Figure 8.3: Turbine assembly weight, Solar turbines.

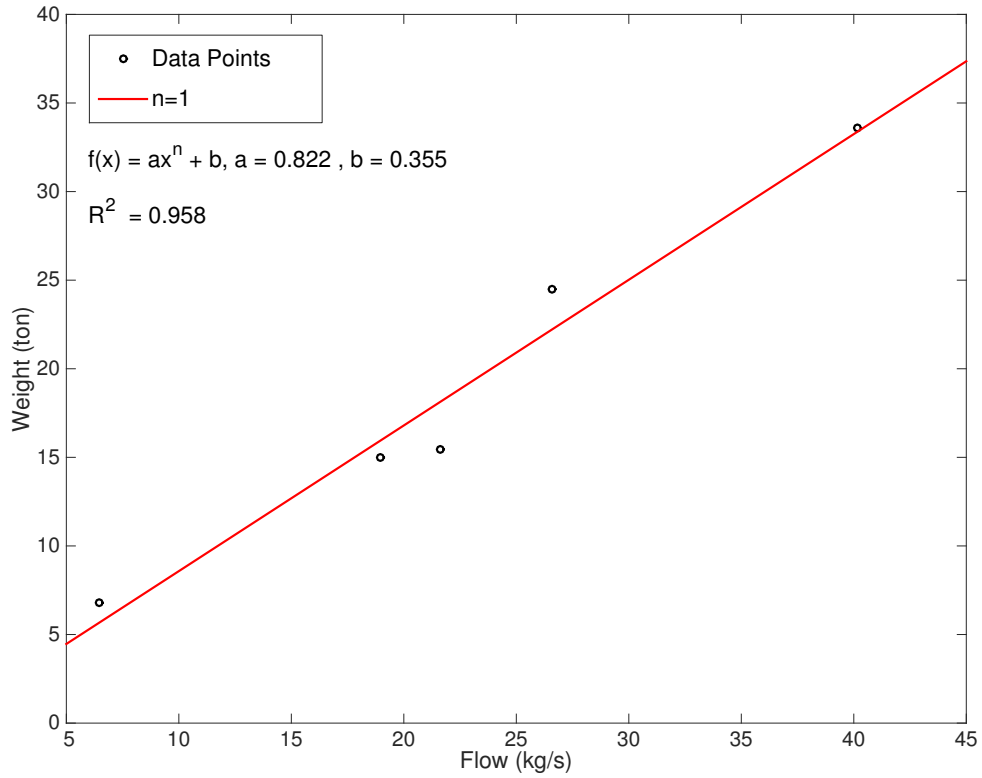


Figure 8.4: Total turbomachinery package weight, Solar turbines.

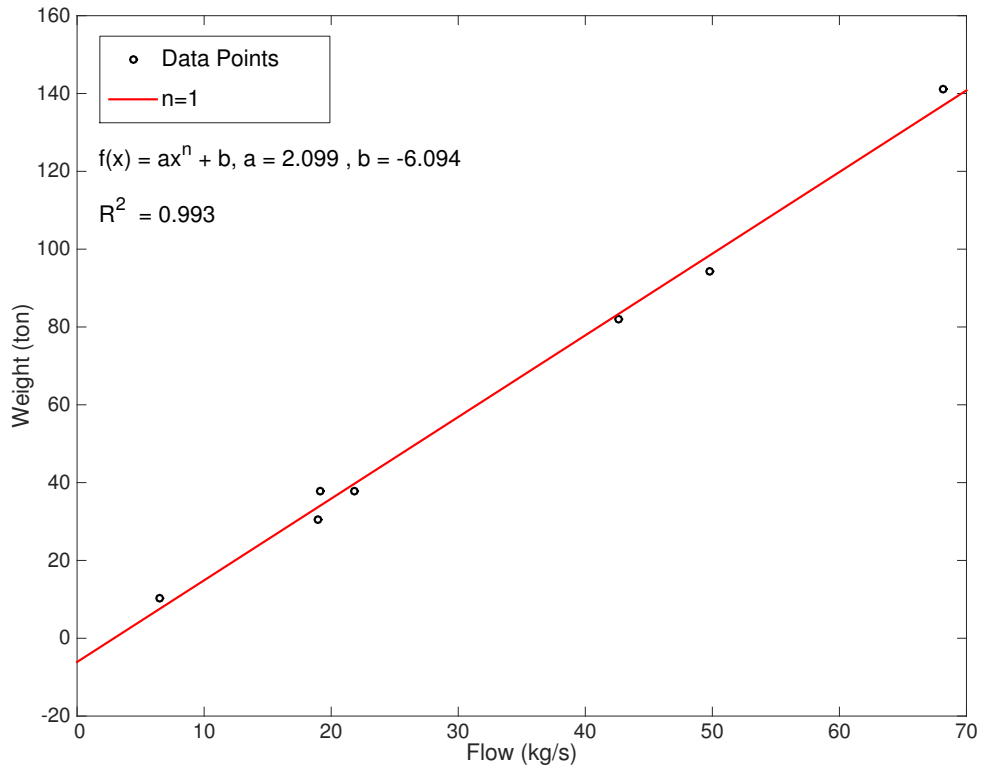


Figure 8.5: Generator drive weight, Solar turbines.

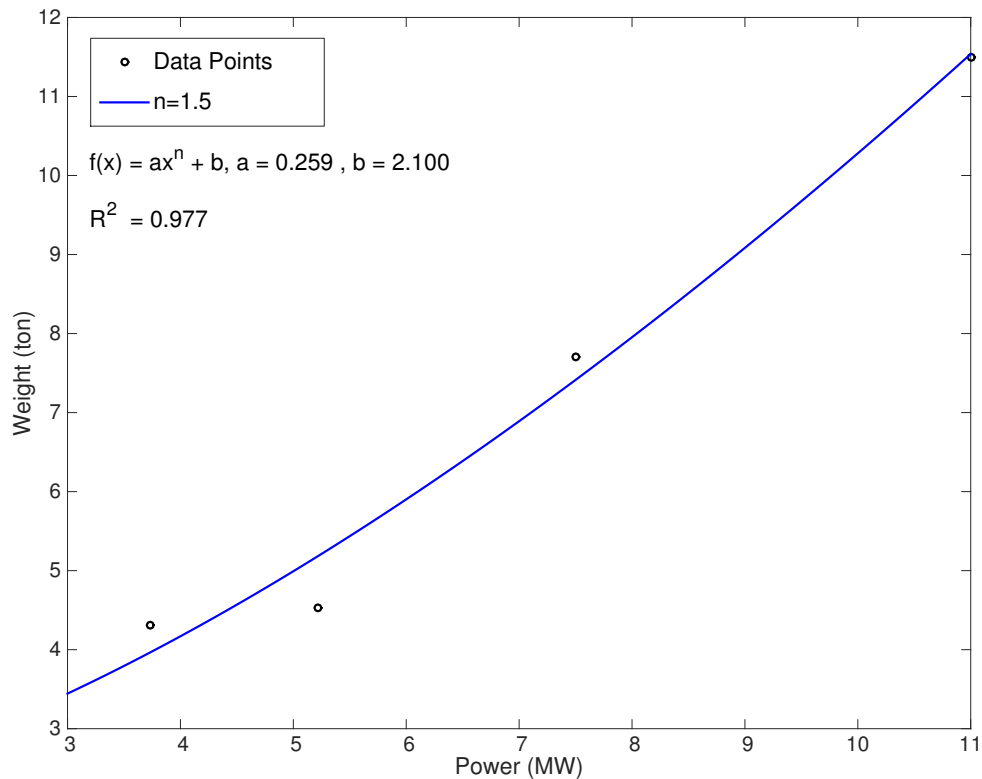


Figure 8.6: Elliot MYR steam turbines weight, varying with power.

The Solar SoLoNOx turbine assembly data set is supporting the scaling relationship,  $W = \dot{m}^{\frac{3}{2}}$ , see Fig. 8.2. Because only the turbine assembly is considered, it is comparable with A. Rivera-Alvarez's work in Section 6.3. The same trend is found for the gas turbine assembly in the Solar turbomachinery package specifications, see Fig. 8.3. These turbines are also analyzed in terms of total weight, see Fig. 8.4. According to the coefficient of performance, this fit is not very accurate for neither  $n = 1.0$  or  $n = 1.5$ , but is indicating a weak linear relationship ( $R^2=0.958$ ),  $W \propto \dot{m}$ . When the Solar generator data are plotted, see Fig. 8.5, a linear relationship between mass flow and weight is indicated. This fit is better ( $R^2=0.993$ ), and supports O. E. Balje's relationship, although he did not include the generator weight in his work.

In the Appendix, Table C.8 is presenting the sizing parameters for Solar skids. The volume of an imaginary box enclosing the skid is calculated for all turbines. It is interesting to observe that the average density of this box is quite consistent for all turbines. This supports the existence of a scaling relationship for these turbines.

For the steam turbines, the best fit is  $W \propto P^{\frac{3}{2}}$ , see Fig. 8.6. This fit is not very accurate ( $R^2=0.977$ ), but is indicating a trend which coincides with A. Rivera-Alvarez's work. Because of confidentiality issues, Elliot Group was not able to provide their turbine design philosophy. Based on the available documentation, these steam turbines are probably based on some sort of similarity.

### 8.1.2 Heat Exchangers

This scaling analyzes for shell and tube heat exchangers, are based on GT PRO simulations on a shell and tube condenser. The results are collected in Tables 8.5 and 8.6, and plotted in Figures 8.7–8.9. In terms of scaling laws, these results are promising. The most important result, is a good fit for the scaling relationship ( $R^2=0.998$ ),  $W \propto m$ . It is assumed that all thermodynamic properties but steam mass flow is kept constant.

Table 8.5: GT PRO results from shell and tube type condenser – Shell (Heat Exchanger).

Length [m]	7.6	7.7	7.7	7.9
Width [m]	25.4	25.4	25.4	25.4
Number of support plates	8	8	8	8
Thickness [mm]	9.525	9.525	9.525	9.525
Weight [kg]	16100	17970	19780	23160

Table 8.6: GT PRO results from shell and tube type condenser – Tubes (Heat Exchanger).

Passes	2	2	2	2
Surface area [m <sup>2</sup> ]	778	889	998	1210
Number of tubes	1691	1909	2119	2497
Length [m]	5.8	5.8	5.9	6.1
D <sub>o</sub> [mm]	25.4	25.4	25.4	25.4
D <sub>i</sub> [mm]	23.98	23.98	23.98	23.98
Thickness [mm]	0.711	0.711	0.711	0.711
Weight [kg]	4310	4930	5540	6710

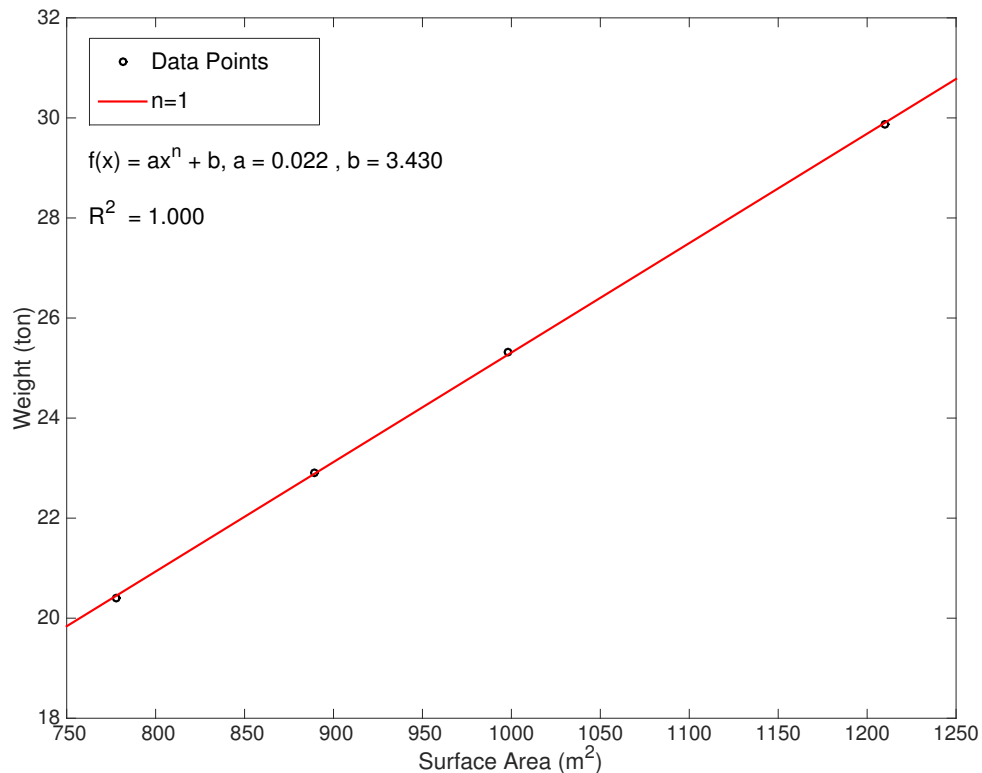


Figure 8.7: Shell and tube heat exchanger simulations from GT PRO, HX weight varying with surface area.

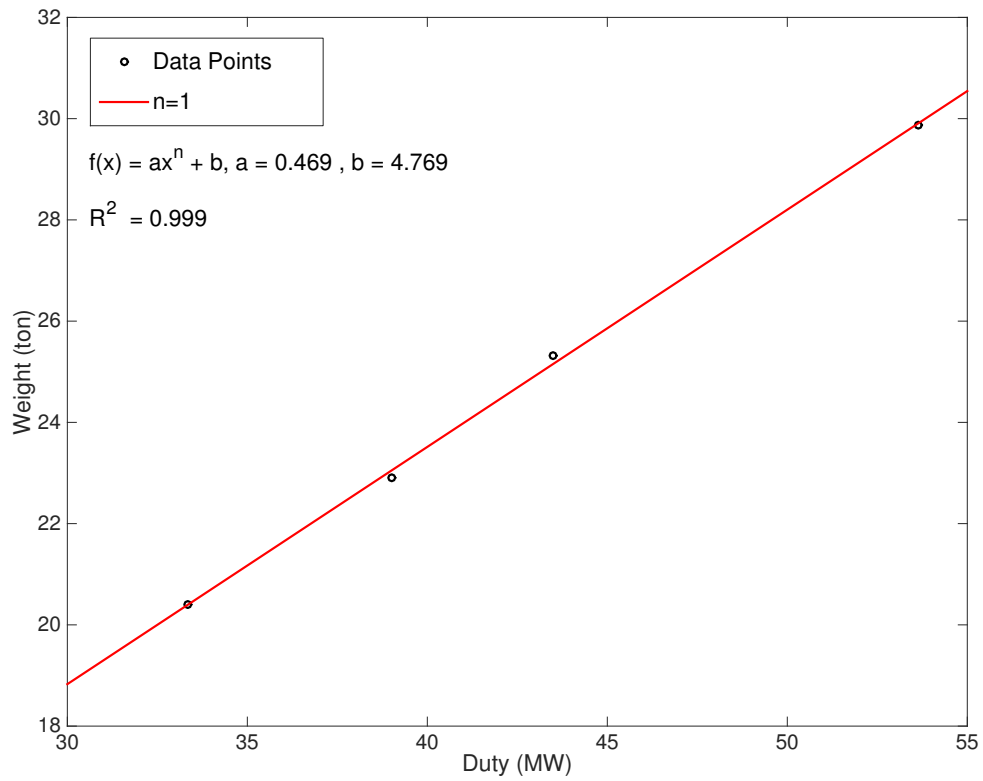


Figure 8.8: Shell and tube heat exchanger simulations from GT PRO, HX weight varying with duty.

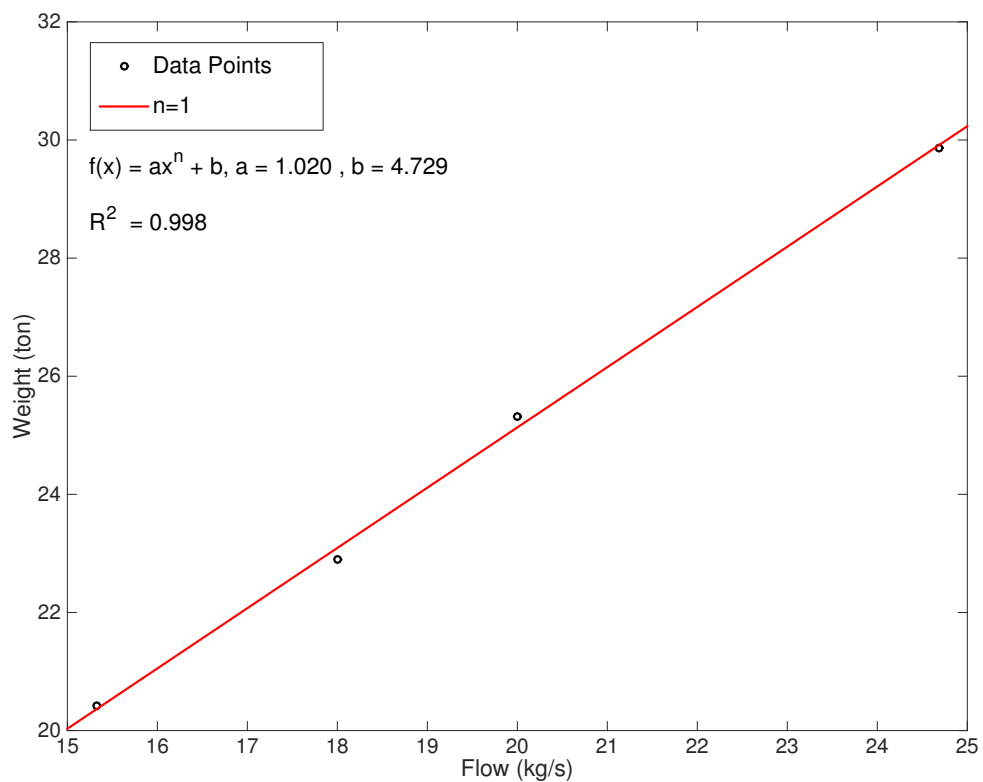


Figure 8.9: Shell and tube heat exchanger simulations from GT PRO, HX weight varying with steam mass flow.



## 8.2 GT PRO Process Models

All models are implemented to match the boundary conditions in Tables 7.1–7.4. No size and weight limitations are given for the "FPSO" case, hence no such restrictions are implemented in the models. It is possible to reduce the weight, by sacrificing steam production and consequently power output and desalination capacity. This needs to be considered for each case.

To summarize the chosen design parameters for the steam cycle:

- Once through heat recovery steam generator.
  - Vertical design to reduce footprint.
  - Exhaust gas pressure drop: 25 mbar.
  - $\Delta T_{pinch} = 33$  K.
  - Incoloy as HRSG tube material to avoid bypass stack and corrosion.
  - Staggered tubes ( $\approx 30^\circ$ ) for compactness.
  - TP409 Stainless steel, serrated fins.
- Back-pressure turbine.
- Sliding pressure regulation in the steam turbine.
- 60 Hz power generation.

CO<sub>2</sub> capture technology:

- MEA based CO<sub>2</sub> capture.
- 65 bar compression, given from Sleipner injection pressure.

Desalination design:

- MED-TVC technology.

The sizing results for all models are collected in Tables C.9, C.10 and C.11, they will not be further discussed in this study.

### 8.2.1 Model 1 – Steam Cycle

The most important results from model 1 is the total weight of 474.5 tons and the steam turbine mass flow of  $37.72 \frac{kg}{s}$ . This cycle delivers  $28.89 \frac{kg}{s}$  of steam to a potential CO<sub>2</sub> plant, from a sub-stream after the back-pressure steam turbine outlet. The steam is saturated with an absolute pressure of 5 bar and the temperature is 152°C, this is according to the CO<sub>2</sub> plant reboiler specifications.

The total steam production is  $38.99 \frac{kg}{s}$ . This mass flow is provided from the feedwater tank at 82°C, see Fig. C.17. At this temperature level, it is necessary with a low temperature economizer in the heat recovery steam generator. The HRSG has an overall heat transfer surface of 27.5 k·m<sup>2</sup>, and the pinch point temperature is 33K, see HRSG TQ diagram in Fig. C.18.

The steam turbine has a gross power output of 14.4 MW. When auxiliary loads are considered, the net power output is 13.9 MW. From Fig. C.19 it is observed that the steam turbine operates with sliding pressure. The Exergy balance for this process model is found in Fig. C.20.

Table 8.7: GT PRO model 1, weight estimates.

Property	Value	Unit
Steam turbine weight	21.95	[ton]
Steam turbine generator weight	43.61	[ton]
HRSG total weight (dry)	409.0	[ton]
Total weight (dry)	474.5	[ton]

Table 8.8: GT PRO model 1, overall plant results.

Property	Value	Unit
Steam turbine gross power	14.4	[MW]
Net power output	13.9	[MW]
Main IP process mass flow	10.10	$[\frac{kg}{s}]$
1st IP substream mass flow	28.89	$[\frac{kg}{s}]$
Steam turbine mass flow	37.72	$[\frac{kg}{s}]$
CHP efficiency	54.7	[%]
HRSG overall heat transfer surface	27.5	k·[m <sup>2</sup> ]

More figures from the simulations are found in Appendix C.3.

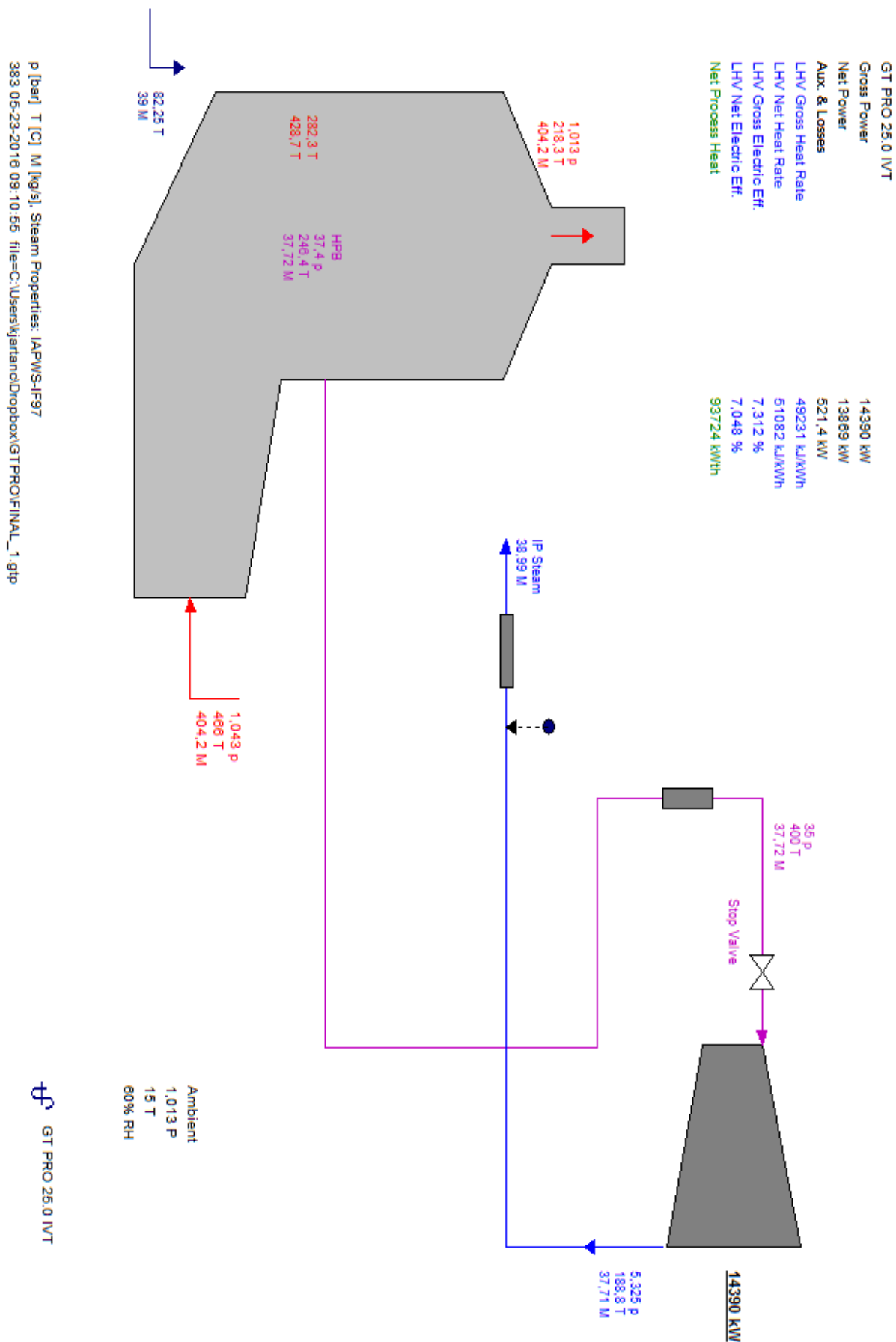


Figure 8.10: GT PRO model 1, combined cycle with back-pressure turbine.

### 8.2.2 Model 2 – CO<sub>2</sub> Capture

The total weight of model 2 is 437.8 tons, and the steam turbine mass flow is  $37.72 \frac{kg}{s}$ . This cycle delivers  $28.89 \frac{kg}{s}$  of saturated steam to the CO<sub>2</sub> plant. The total steam production is  $39.07 \frac{kg}{s}$ . This mass flow is provided from the feedwater tank at 134°C, see Fig. C.23. At this temperature level, a low temperature economizer is superfluous in the heat recovery steam generator. The HRSG has an overall heat transfer surface of 25.3 k·m<sup>2</sup>, and the pinch point temperature is 33K, see HRSG TQ diagram in Fig. C.24.

The steam turbine has a gross power output of 14.4 MW. When auxiliary loads and CO<sub>2</sub> power consumption are considered, the net power output is 5.72 MW. The total electrical power consumption from the CO<sub>2</sub> plant is 8.2 MW, where more than 50% is related to compression, in Fig. C.25 the CO<sub>2</sub> plant is presented. From Fig. C.26 it is observed that the steam turbine operates with sliding pressure. The Exergy balance for this process model is found in Fig. C.27.

Table 8.9: GT PRO model 2, weight estimates.

Property	Value	Unit
Steam turbine weight	21.95	[ton]
Steam turbine generator weight	43.61	[ton]
HRSG total weight (dry)	372.2	[ton]
Total weight (dry)	437.8	[ton]

Table 8.10: GT PRO model 2, overall plant results.

Property	Value	Unit
Steam turbine gross power	14.4	[MW]
Net power output	5.72	[MW]
Main IP process mass flow	10.18	$[\frac{kg}{s}]$
1st IP substream mass flow	28.89	$[\frac{kg}{s}]$
Steam turbine mass flow	37.72	$[\frac{kg}{s}]$
CHP efficiency	15.3	[%]
HRSG overall heat transfer surface	25.3	k·[m <sup>2</sup> ]

Table 8.11: GT PRO model 2, CO<sub>2</sub> plant.

Property	Value	Unit
Heating steam mass flow	28.89	$[\frac{kg}{s}]$
Cooling water mass flow	2803	$[\frac{kg}{s}]$
CO <sub>2</sub> captured per day	1446	$[\frac{ton}{day}]$
Heat input per unit of CO <sub>2</sub>	3639	$[\frac{kJ}{kg}]$
CO <sub>2</sub> compression power consumption	4.7	[MW]
Total electrical power consumption	8.2	[MW]

More figures from the simulations are found in Appendix C.4.

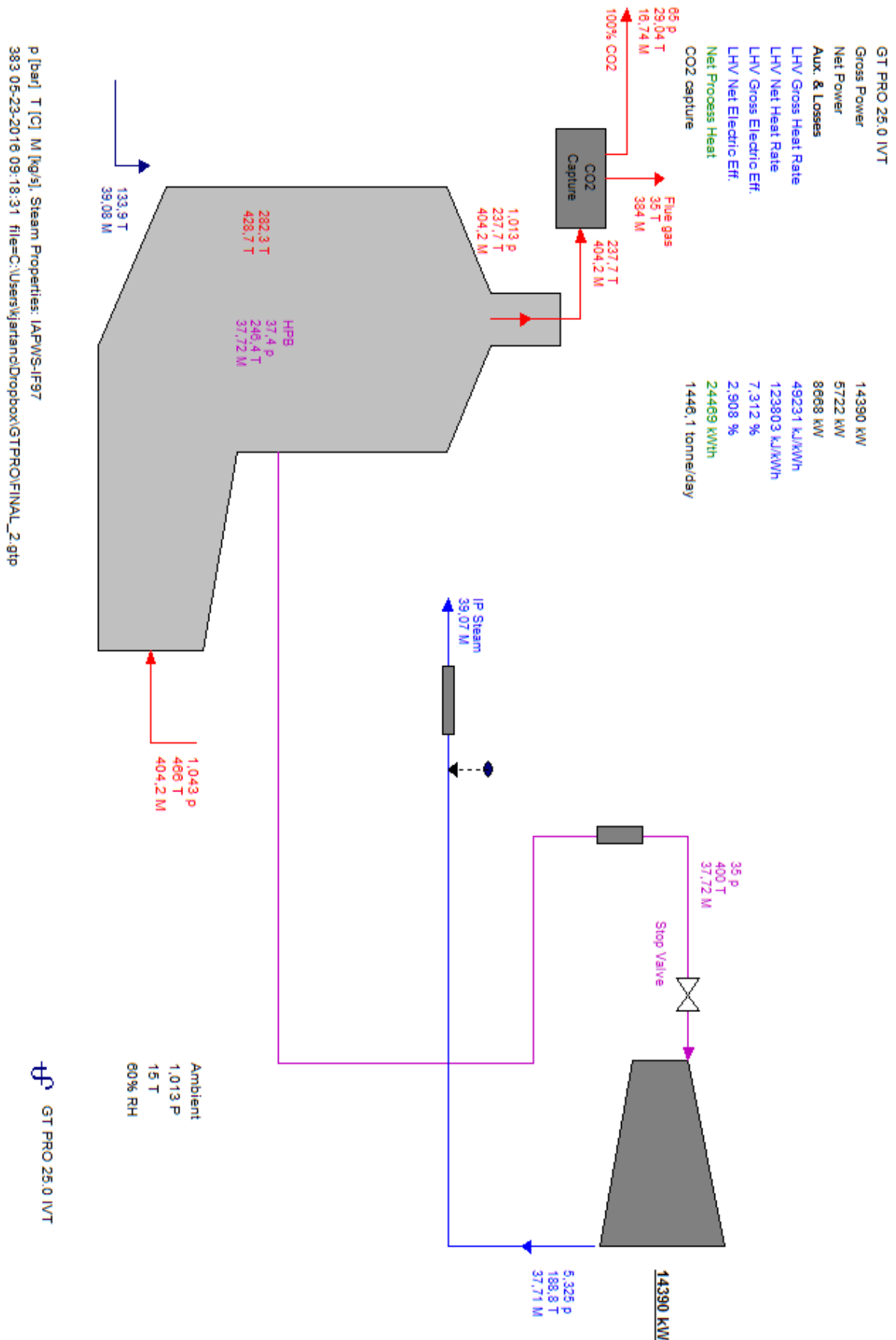


Figure 8.11: GT PRO model 2, combined cycle with back-pressure turbine and CO<sub>2</sub> capture.

### 8.2.3 Model 3 – CO<sub>2</sub> Capture and Desalination

The total weight of model 3 is 455.9 tons, and the steam turbine mass flow is  $37.46 \frac{kg}{s}$ . This cycle delivers  $28.89 \frac{kg}{s}$  of steam to the CO<sub>2</sub> plant, and  $10.04 \frac{kg}{s}$  to the desalination plant. The total steam production is  $39.46 \frac{kg}{s}$ . This mass flow is provided from the feedwater tank at 122°C, see Fig. C.30. At this temperature level, a low temperature economizer is superfluous in the heat recovery steam generator. The HRSG has an overall heat transfer surface of 25.6 k·m<sup>2</sup>, and the pinch point temperature is 33K, see HRSG TQ diagram in Fig. C.31.

The steam turbine has a gross power output of 14.1 MW. When auxiliary loads, CO<sub>2</sub> power consumption and desalination power are considered, the net power output is 5.13 MW. The total electrical power consumption from the CO<sub>2</sub> plant is 8.2 MW, see Fig. C.32, and 0.28 MW for the distillation process. From Fig. C.33 it is observed that the steam turbine operates with sliding pressure. The Exergy balance for this process model is found in Fig. C.34.

In Fig. C.35 the eight effect distillation process is displayed. The total weight is 318 tons, for a desalinated water mass flow of  $72.92 \frac{kg}{s}$ . The multi effect distillation TQ diagram is found in Fig. C.36, the eight pressure levels are observed.

Table 8.12: GT PRO model 3, weight estimates.

Property	Value	Unit
Steam turbine weight	21.73	[ton]
Steam turbine generator weight	39.49	[ton]
HRSG total weight (dry)	394.7	[ton]
Total weight (dry)	455.9	[ton]

Table 8.13: GT PRO model 3, overall plant results.

Property	Value	Unit
Steam turbine gross power	14.1	[MW]
Net power output	5.13	[MW]
Main IP process mass flow	10.04	$[\frac{kg}{s}]$
1st IP substream mass flow	28.89	$[\frac{kg}{s}]$
Steam turbine mass flow	37.46	$[\frac{kg}{s}]$
CHP efficiency	2.6	[%]
HRSG overall heat transfer surface	25.6	k·[m <sup>2</sup> ]

More figures from the simulations are found in Appendix C.5. The most important results for the CO<sub>2</sub> capture plant and desalination plant is found in Tables C.12 and C.13.

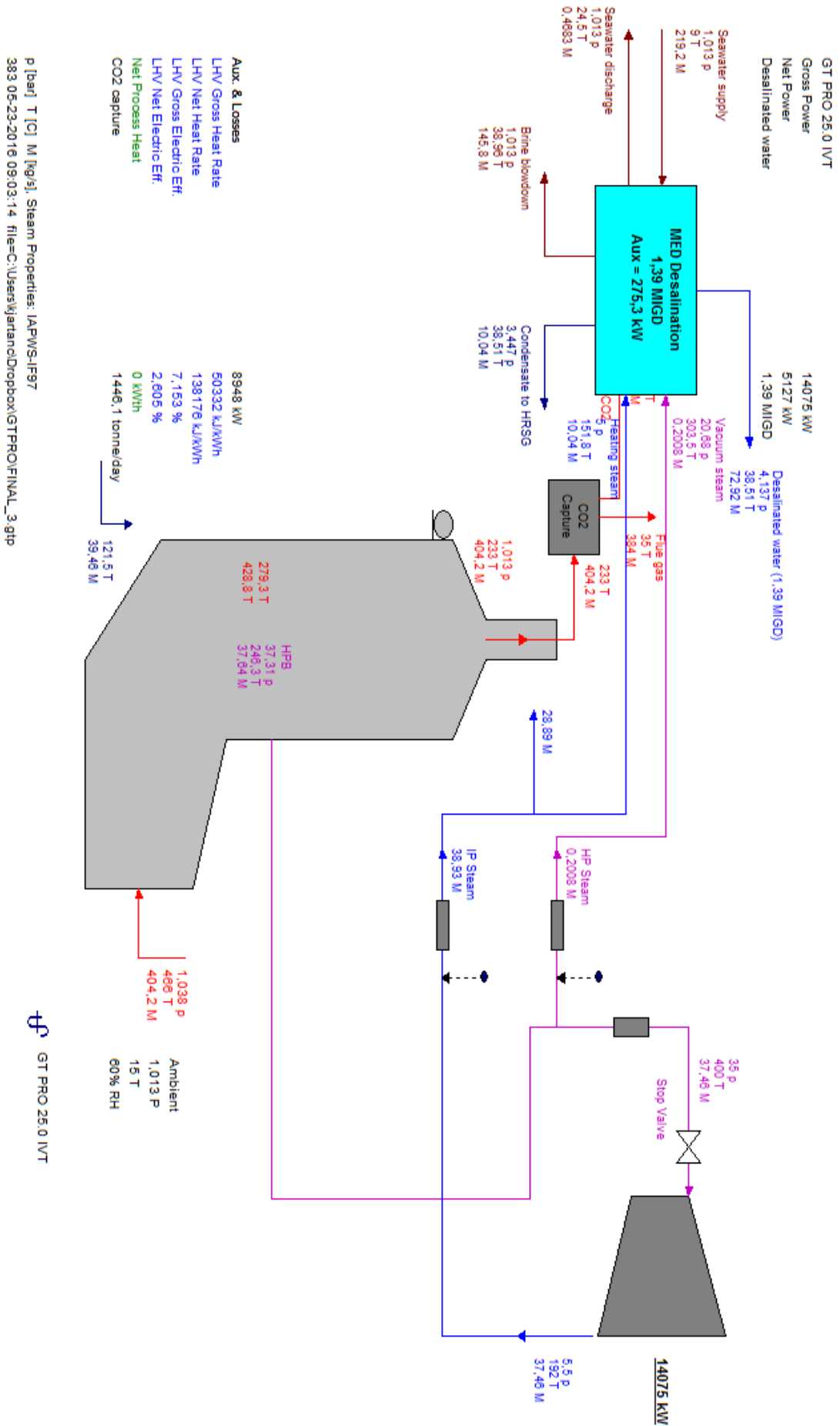


Figure 8.12: GT PRO model 3, combined cycle with back-pressure turbine, CO<sub>2</sub> capture and desalination.

### 8.3 Polynomial Representation

For the polynomial representation, a second order polynomial was chosen, see Eq. 8.1. This polynomial can easily be changed in the MATLAB code, e.g. to higher order polynomials or trigonometric functions. To test the method, described in Section 7.10, a total of three polynomials are calculated and tested. Two polynomials for model 1, and one polynomial for model 2.

$$W = a_1x_1^2 + a_2x_1x_2 + a_3x_1x_3 + a_4x_1 + a_5x_2^2 + a_6x_2x_3 + a_7x_2 + a_8x_3^2 + a_9x_3 + a_{10} \quad (8.1)$$

#### 8.3.1 Model 1 - Polynomial 1

In Table 8.14, the variables and their range are presented. The chosen variables are based on sensitivity analysis and which parameters that most likely will vary when different real life cases are considered. Exhaust mass flow and temperature will vary with the gas turbine, and the amount of steam to the CO<sub>2</sub> plant will vary with e.g. exhaust gas composition, capturing technology and exhaust mass flow. The range for each variable is determined from physical limitations on the model and real gas turbine data.

From the weighted least squares regression process, the polynomial coefficients are given in table 8.16. The coefficient of performance ( $R^2$ ) is 0.9985 for this polynomial. It is observed that terms containing  $a_3$  and  $a_6$  could be neglected without any large effect on the weight estimate.

#### 8.3.2 Model 1 - Polynomial 2

To better understand how the accuracy of the polynomial is affected by number of nodes, 64 additional nodes were implemented in model 1. All these nodes were made with a random number generator. It is normally better to have an organized grid, but this approach was inspired by Monte Carlo simulations. The original nodes are also included in the calculation of this polynomial. From the regression process, the polynomial coefficients are given in table 8.17. The coefficient of performance ( $R^2$ ) is 0.9960 for this polynomial.



### 8.3.3 Model 2 – Polynomial 3

This polynomial was more difficult to implement, because GT PRO and ELINK change the mass flows automatically to match the pinch point temperature and ensure the correct steam mass flow according to the CO<sub>2</sub> plant specifications. Because of this, the  $x_3$  variable was limited to only 16 different values. Because when  $x_1$  and  $x_2$  are kept constant, the CO<sub>2</sub> plant demands the same steam mass flow. This is obviously affecting the accuracy of the polynomial. For this approach, the polynomial showed better accuracy when the total steam flow, rather than CO<sub>2</sub> plant flow was considered. In Table 8.15, the variables and range for the model 2 polynomial are presented. The polynomial coefficients are given in table 8.18. The coefficient of performance ( $R^2$ ) is 1.000 for this polynomial.

Table 8.14: The model 1 polynomial variables and their given range.

Property	Variable	Range	Base case
$\dot{m}_{exh}$	$x_1$	360–450	404.2
$T_{exh}$	$x_2$	445–550	466
$\dot{m}_{steam, CO_2}$	$x_3$	26–30.5	28.89

Table 8.15: The model 2 polynomial variables and their given range.

Property	Variable	Range	Base case
$\dot{m}_{exh}$	$x_1$	360–450	404.2
$T_{exh}$	$x_2$	445–550	466
$\dot{m}_{steam, Tot}$	$x_3$	30–50	39.07

Table 8.16: Coefficients for polynomial 1, 64 nodes.

$a_1$	$a_2$	$a_3$	$a_4$	$a_5$	$a_6$	$a_7$	$a_8$	$a_9$	$a_{10}$
-0.293	2.860	-0.001	46.18	6.344	0.000	-5893	0.248	-13.54	1333168

Table 8.17: Coefficients for polynomial 2, 128 nodes.

$a_1$	$a_2$	$a_3$	$a_4$	$a_5$	$a_6$	$a_7$	$a_8$	$a_9$	$a_{10}$
-1.157	2.660	2.624	766.0	5.617	10.02	-5410	-195.4	4851	1014359

Table 8.18: Coefficients for polynomial 3, 64 nodes.

$a_1$	$a_2$	$a_3$	$a_4$	$a_5$	$a_6$	$a_7$	$a_8$	$a_9$	$a_{10}$
13.11	-949.0	-235.5	259413	50.11	-656.9	-49772	1045	2215182	12053249

Table 8.19: Validation test for all polynomials.

	GT PRO Weight [ton]	Polynomial [ton]	Error [%]	Max error [%]
Polynomial 1	474.5	473.4	0.23	3.48
Polynomial 2	474.5	477.4	0.60	2.44
Polynomial 3	437.8	443.8	1.37	2.19

### 8.3.4 Testing and Validation

To estimate the accuracy for the polynomials, a test sequence was implemented in ELINK and MATLAB. The base case, some extrapolation, the boundaries and random values inside the range were investigated. These polynomial estimates were compared with the GT PRO weight calculations. The full test sequences are found in the Appendix, Tables C.14-C.16, while the most important results are collected in Table 8.19.

#### Polynomial 1

To determine the accuracy, the weight from the polynomial is compared with the GT PRO weight. The largest error made by this polynomial was 3.48%, this occurred when extrapolated values were tested. For the base case, the error was 0.23%.

#### Polynomial 2

To have a comparative basis, the same test sequence as for the first polynomial was used. The largest error made by this polynomial was 2.44%, this occurred in the mid-range for all variables. For the base case, the error was 0.60%. The trend, compared to polynomial 1, is that the biggest mistakes are reduced. This is expected, because the numbers of data points are doubled.

#### Polynomial 3

The same test sequence with modifications for the  $x_3$  value was used. The largest error made by this polynomial was 2.19%, and occurred for random values inside the range. For the base case, the error was 1.37%.

## 8.4 Scaling Laws

Many scenarios were tested in GT PRO, but the most interesting ones are with fixed temperature and pressure out of the steam turbine. It is assumed that CO<sub>2</sub> plants with varying exhaust loads are demanding the same steam temperature and pressure, but different steam mass flow. To be able to compare scaling with the polynomial approach, simulations were made in model 1 and model 2. The steam production is determined from the 33K pinch point temperature in the HRSG. Scaling laws are first analyzed according to the analytical suggestions,  $n = 1.0$  or  $n = 1.5$ . Later is the optimal "n"-value found for the total steam cycle weight. The calculated range for the steam mass flow is 29.9-50.4  $\frac{kg}{s}$ .

### GT PRO Scaling, Model 1

Assumptions: The exhaust gas mass flow is varied, while the exhaust temperature is constant. In this case, a constant mass flow of 28.89  $\frac{kg}{s}$  was maintained for the CO<sub>2</sub> plant, even though the steam demand will vary with exhaust gas mass flow. This approach was necessary to ensure sufficient steam mass flow in GT PRO. All the excess steam can be utilized for other applications, and increases the power output from the steam turbine. For the base case, the mass flow is:  $\dot{m}_{ST,BC} = 37.71 \frac{kg}{s}$ .

More figures from this analysis can be seen in Appendix C.6.1. All the GT PRO simulation data are collected in Table C.17, see Appendix C.8. The first column in this table is the results for the base case, and is for testing purposes not part of the analysis.

$$W_{ST} = 0.470 \cdot \dot{m}_{ST} + 4.150 \quad (8.2)$$

$$W_{Gen} = 0.835 \cdot \dot{m}_{ST} + 12.034 \quad (8.3)$$

$$W_{HRSG} = 10.492 \cdot \dot{m}_{ST} + 11.517 \quad (8.4)$$

$$W_{Tot} = 11.924 \cdot \dot{m}_{ST} + 21.989 \quad (8.5)$$

Table 8.20: Testing base case values for the scaling laws from model 1.

	GT PRO Weight [ton]	Scaling Weight [ton]	Error [%]
$W_{ST}$	21.95	21.87	0.34
$W_{Gen}$	43.61	43.52	0.20
$W_{HRSG}$	409.0	407.17	0.45
$W_{Tot}$	474.5	471.64	<b>0.60</b>

### Testing and Validation

The results from this scaling laws are almost too good to be true. But several recalculations are giving the same results. When the base case value is considered, the error is only 0.6% for the total weight. Outside the calculated range, the biggest error is 3.1%, and occurs when the upper interval is exceeded with 7.4%. The scaling relationships are presented graphically in Fig. 8.13–8.16.

The validation within the range is implicit given by the graphical representation in Fig. 8.16. For randomized test values inside the interval, all estimates were less than 1.0% from the GT PRO value.

### Optimal "n"-Value

The coefficient of performance was optimized from varying the "n"-value in MATLAB, the best fit was found when  $n = 0.77$ , see Fig. 8.21. The validation tests for this value are found in Table 8.22.

$$W_{Tot} = 36.216 \cdot (\dot{m}_{ST})^{0.77} - 119.86 \quad (8.6)$$

It is observed that the accuracy is slightly improved for the optimal "n"-value for the base case, with an error of 0.4%. On the other hand, the biggest error is increased to 3.7%.

Table 8.21: Testing total weight for model 1 scaling law,  $n = 1.0$ .

Exhaust flow [ $\frac{kg}{s}$ ]	Steam flow [ $\frac{kg}{s}$ ]	GT PRO Weight [ton]	Scaling Weight [ton]	Error [%]
300	27.99	352.5	355.7	0.92
470	43.86	545.0	545.0	0.00
580	54.12	688.6	667.3	<b>3.09</b>

Table 8.22: Testing total weight for model 1 scaling law,  $n = 0.77$ .

Exhaust flow [ $\frac{kg}{s}$ ]	Steam flow [ $\frac{kg}{s}$ ]	GT PRO Weight [ton]	Scaling Weight [ton]	Error [%]
404.2	37.71	474.5	472.8	0.37
300	27.99	352.5	351.2	0.36
470	43.86	545.0	545.9	0.16
580	54.12	688.6	662.8	<b>3.74</b>

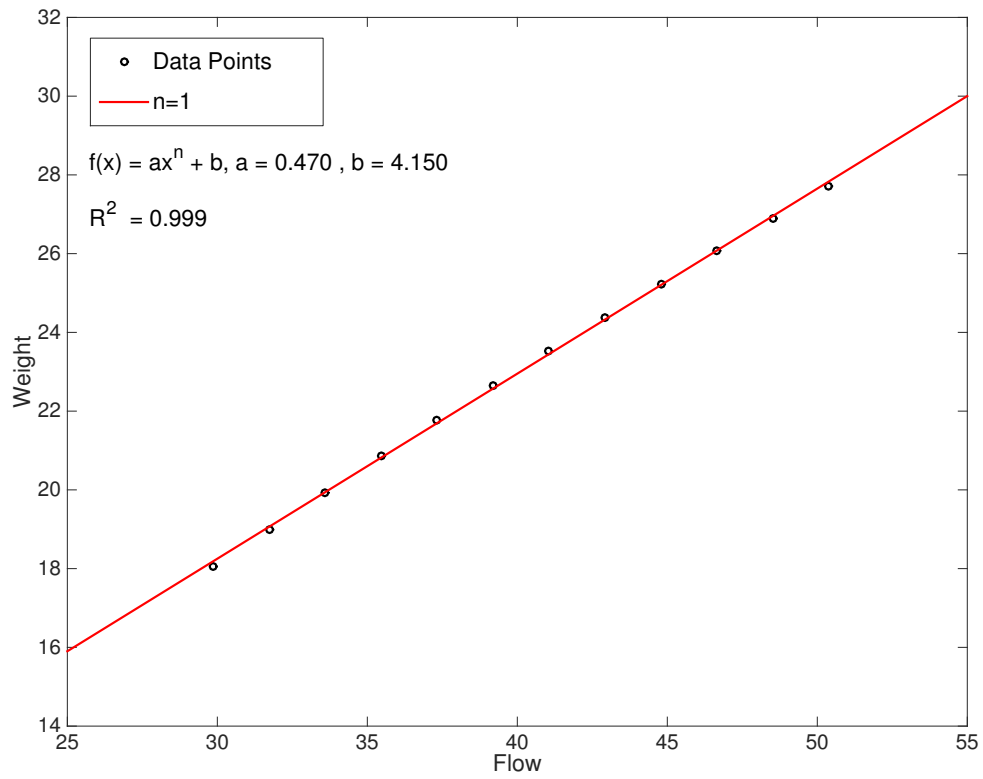


Figure 8.13: Model 1, steam turbine weight as a function of steam mass flow.

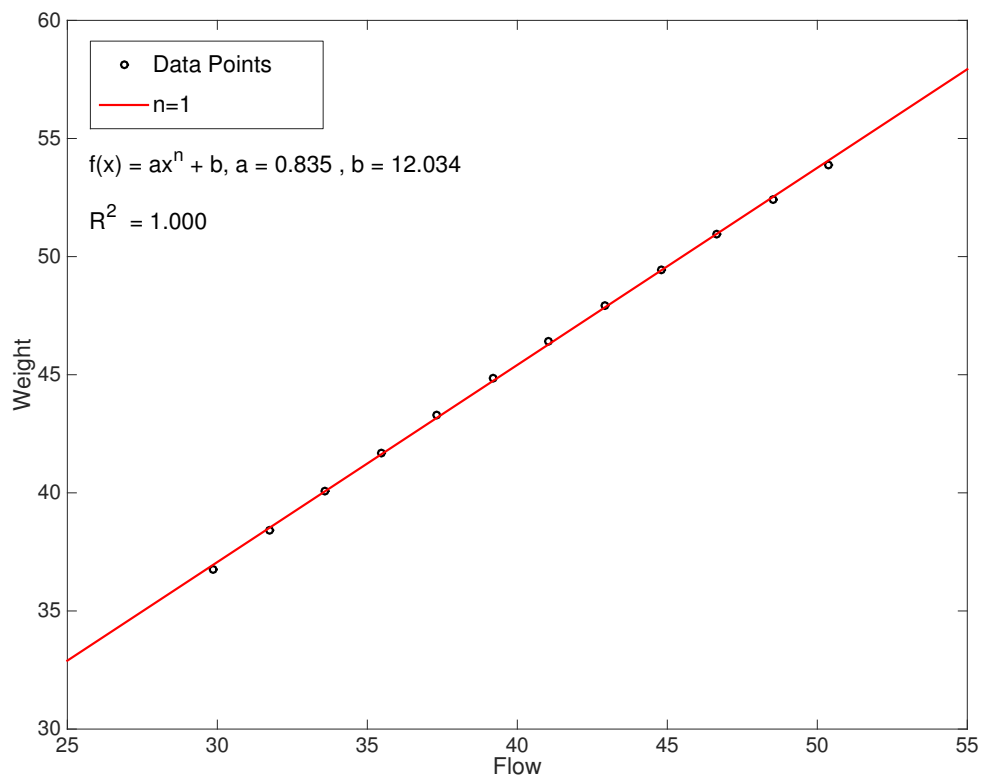


Figure 8.14: Model 1, steam turbine generator weight as a function of steam mass flow.

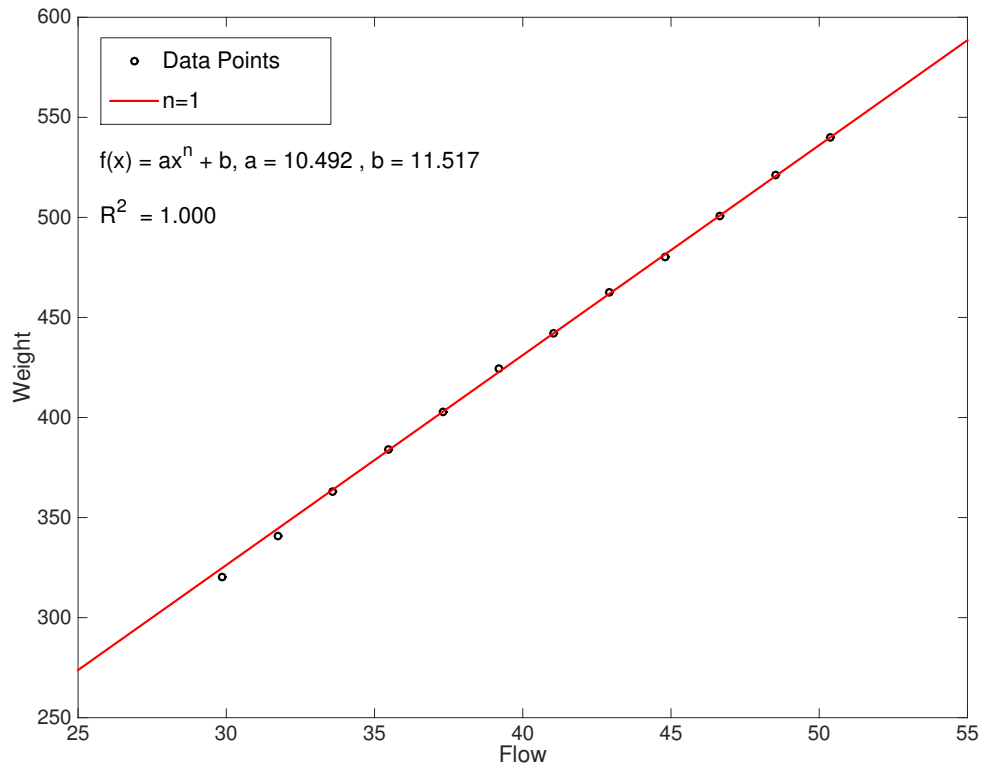


Figure 8.15: Model 1, HRSG (dry) weight as a function of steam mass flow.

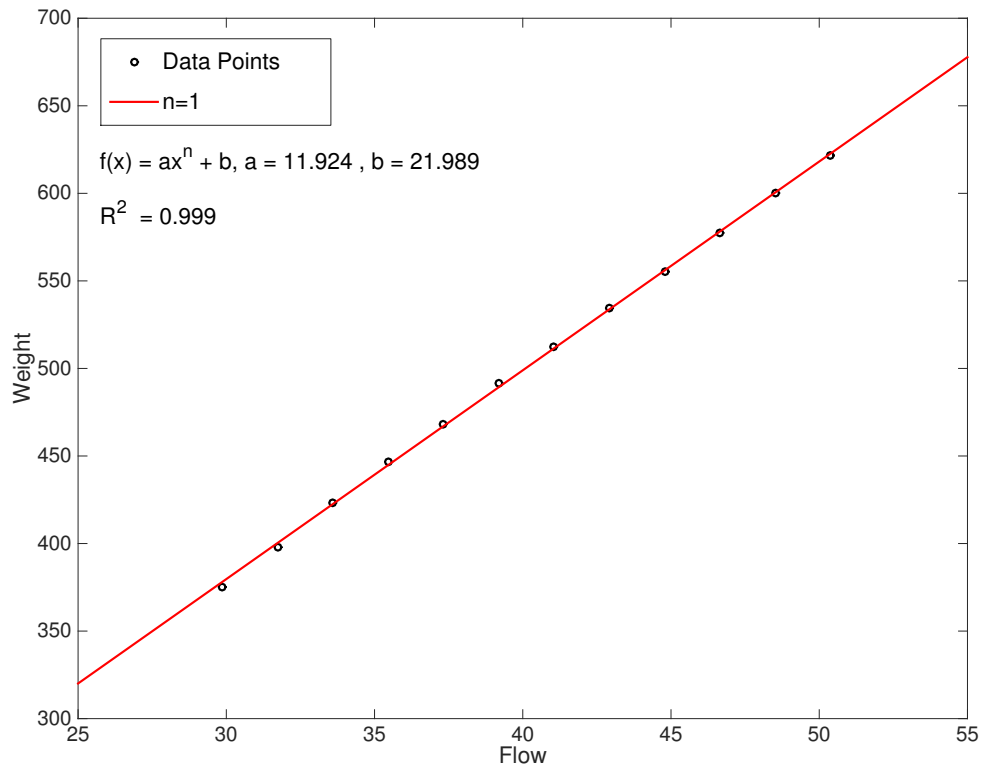


Figure 8.16: Model 1, total weight as a function of steam mass flow power.

### GT PRO Scaling, Model 2

Assumptions: The exhaust gas temperature is kept constant, while the mass flow is changed. In this model, the mass flow to the CO<sub>2</sub> plant is automatically adjusted by GT PRO according to specifications, see Section 7.9. For the base case, the mass flow is:  $\dot{m}_{ST,BC} = 37.72 \frac{kg}{s}$ .

More figures from this analysis can be seen in Appendix C.6.2. All the GT PRO simulation data are collected in Table C.18. The first column in this table is the results for the base case, and is not part of the analysis. Because this model is integrated with the CCS plant, these weight estimates should be the most realistic.

$$W_{ST} = 0.470 \cdot \dot{m}_{ST} + 4.150 \quad (8.7)$$

$$W_{Gen} = 0.835 \cdot \dot{m}_{ST} + 12.034 \quad (8.8)$$

$$W_{HRSG} = 9.892 \cdot \dot{m}_{ST} - 2.766 \quad (8.9)$$

$$W_{Tot} = 11.196 \cdot \dot{m}_{ST} + 13.415 \quad (8.10)$$

Table 8.23: Testing base case values for the scaling laws from model 2.

Name	GT PRO Weight [ton]	Scaling Weight [ton]	Error [%]
$W_{ST}$	21.9	21.9	0.35
$W_{Gen}$	43.6	43.5	0.20
$W_{HRSG}$	372.2	370.3	<b>0.53</b>
$W_{Tot}$	437.8	435.6	0.50

### Testing and Validation

When the base case value is considered, the error is only 0.5% for the total weight. The maximum error is only slightly higher, and is the HRSG weight estimation. Outside the calculated range, the biggest error is 3.1%, and occurs when the upper interval is exceeded with 7.4%. The scaling relationships are presented graphically in Fig. 8.17–8.20.

The validation within the tested interval is implicit given by the graphical representation in Fig. 8.20. For randomized test values inside the interval, all estimates were within 1.0% from the GT PRO value.

### Optimal "n"-Value

From optimization in terms of the  $R^2$ -value in MATLAB, the best fit was found to be  $n = 0.84$ , see Fig. 8.22. The validation tests are found in Table 8.25.

$$W_{Tot} = 24.035 \cdot (\dot{m}_{ST})^{0.84} - 70.625 \quad (8.11)$$

It is observed that the accuracy is slightly improved for the optimal "n"-value for the base case, with an error of 0.3%. On the other hand, the biggest error is increased to 3.6%.

Table 8.24: Testing total weight for model 2 scaling law,  $n = 1.0$ .

Exhaust flow [ $\frac{kg}{s}$ ]	Steam flow [ $\frac{kg}{s}$ ]	GT PRO Weight [ton]	Scaling Weight [ton]	Error [%]
300	27.99	323.0	326.8	1.17
470	43.86	504.4	504.5	0.01
580	54.12	639.3	619.3	<b>3.12</b>

Table 8.25: Testing total weight for model 2 scaling law,  $n = 0.84$ .

Exhaust flow [ $\frac{kg}{s}$ ]	Steam flow [ $\frac{kg}{s}$ ]	GT PRO Weight [ton]	Scaling Weight [ton]	Error [%]
404.2	37.72	437.8	436.6	0.28
300	27.99	323.0	324.1	0.35
470	43.86	504.4	504.4	0.13
580	54.12	639.3	639.3	<b>3.61</b>



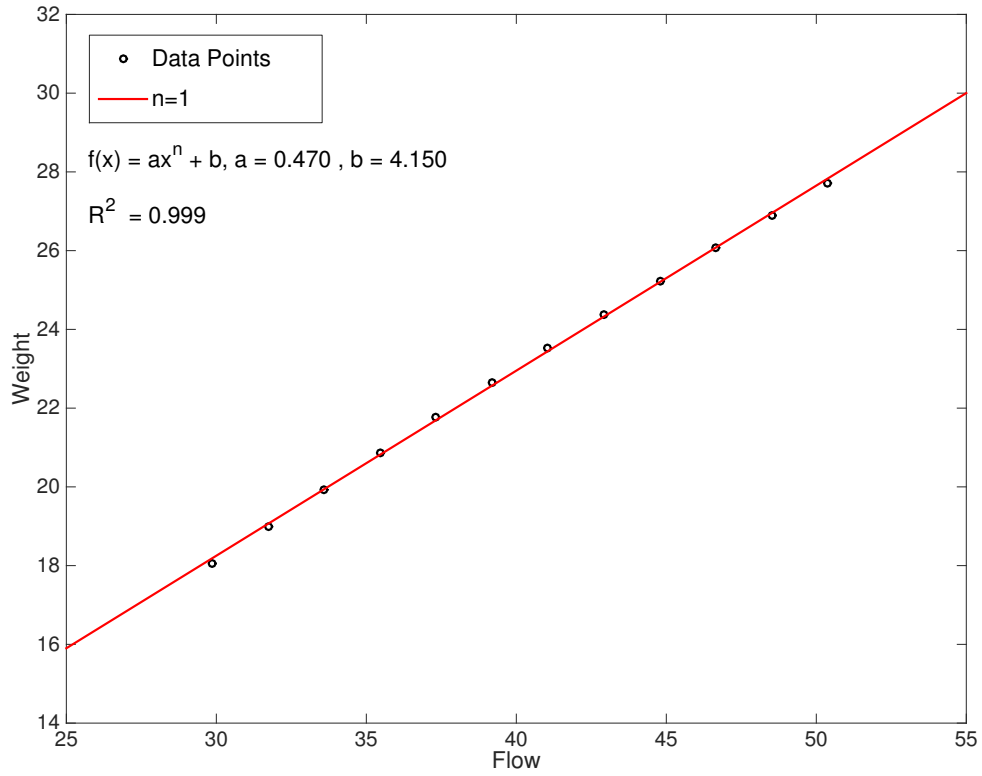


Figure 8.17: Model 2, steam turbine weight as a function of steam mass flow.

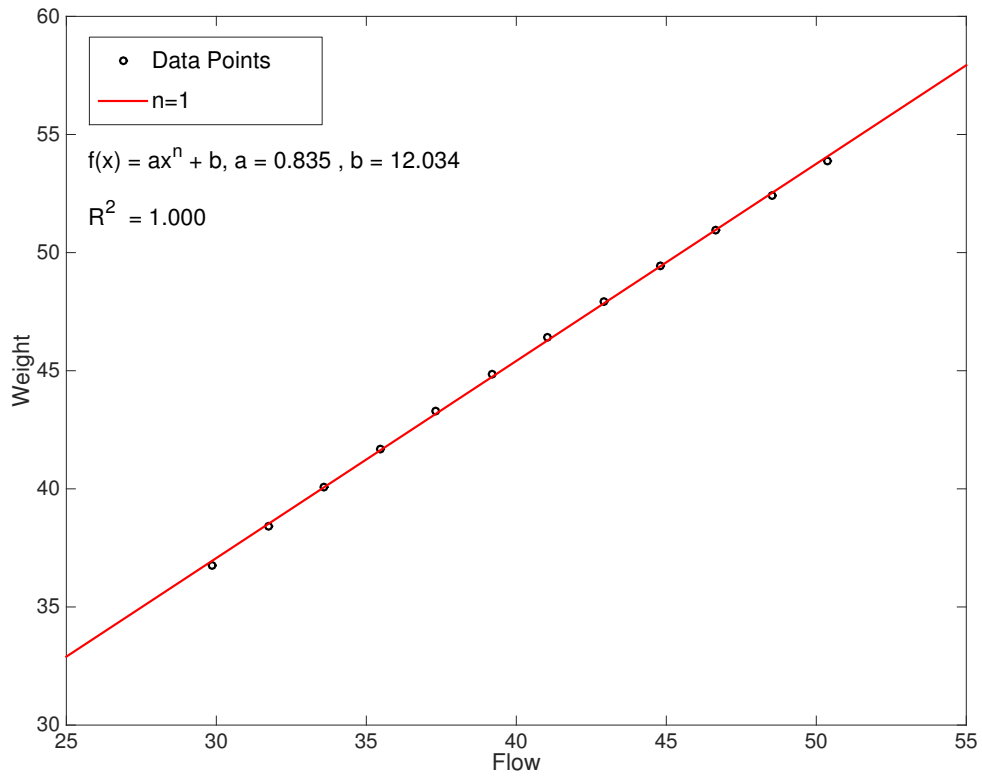


Figure 8.18: Model 2, steam turbine generator weight as a function of steam mass flow.

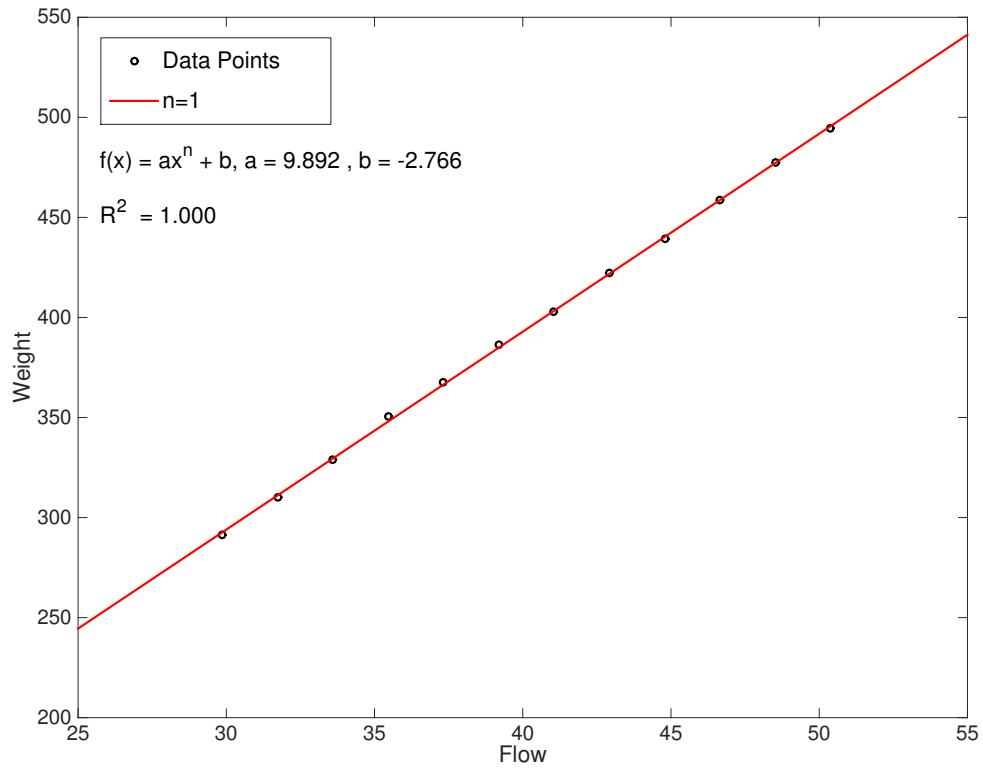


Figure 8.19: Model 2, HRSG (dry) weight as a function of steam mass flow.

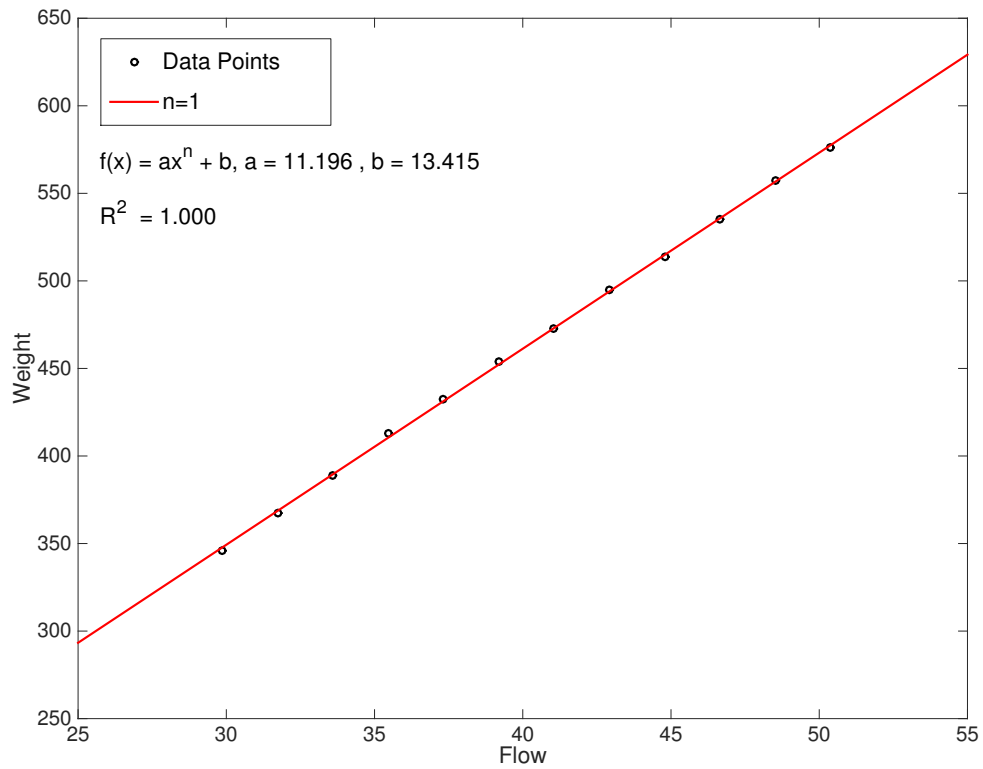
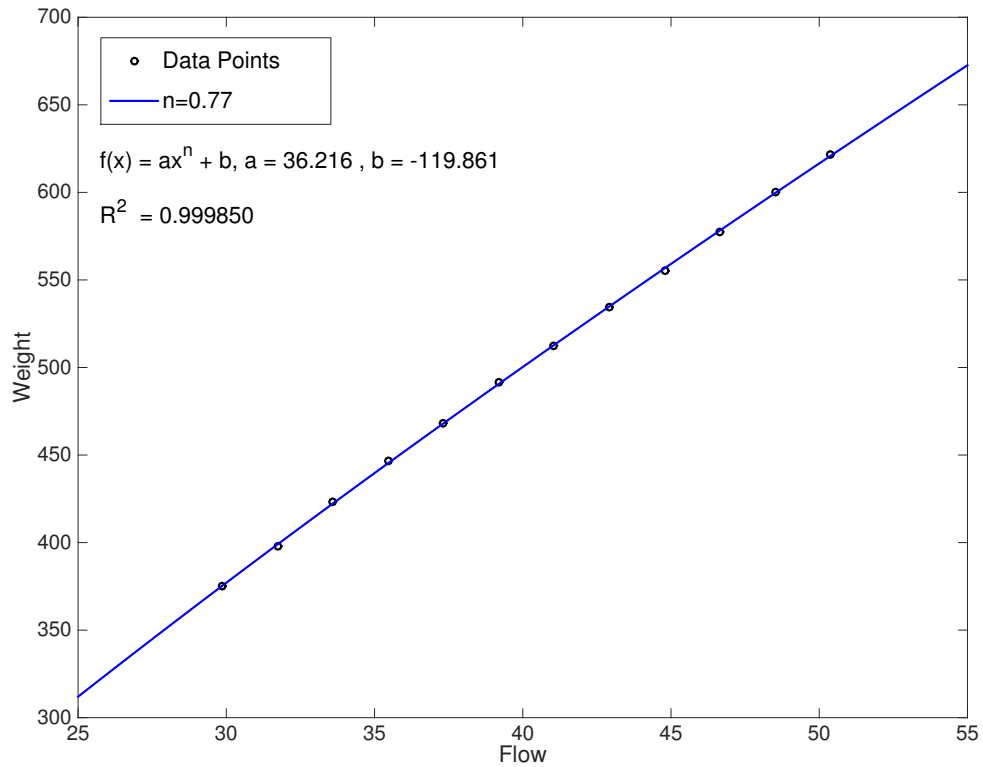
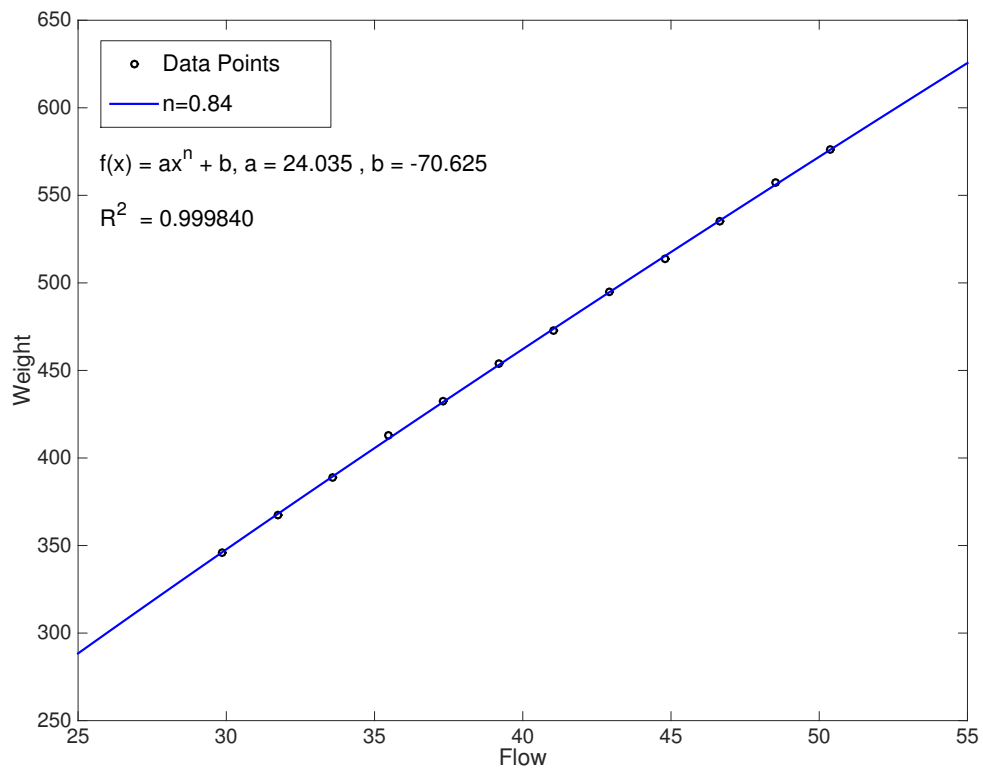


Figure 8.20: Model 2, total weight as a function of steam mass flow power.

Figure 8.21: Model 1, total weight for optimal "n"-value,  $n = 0.77$ .Figure 8.22: Model 2, total weight for optimal "n"-value,  $n = 0.84$ .

## 8.5 Discussion

### Scaling Results from Literature Study

The available turbine data does not give any unambiguous results in terms of scaling relations. The proposed relationship  $W \propto \dot{m}^{\frac{3}{2}}$  seems to be valid when the internal mechanical parts (turbine assembly) are considered. However, this weight is not directly relevant for the applications discussed in this thesis. All other data sets are more supportive to the  $W \propto \dot{m}$  relationship, which is supported by O. E. Balje and his analytic work on similarity relations and design criteria for turbines (Eq. 6.32).

When heat exchangers and heat recovery steam generators are considered, the scaling geometries are more complex. It is therefore difficult to find real weight data for constructions that are guaranteed to be of similar sets. Even emailing with international manufacturers gave no results in this matter, mainly because of sensitive design procedures. The GT PRO simulations gave very consistent results, and supports previous work in terms of the  $W \propto A$  relationship (Eq. 6.41) and the analytic work performed on the heat exchanger model in Excel (Eq. 6.20).

After numerous data sets have been analyzed, the results clearly indicate that weight estimation based on simple scaling laws should be possible. For real turbine data, the relationships are not always as conclusive as desired, but it is not likely that a gas turbine model is an exact scaled version of another. Some modifications always need to be made. This is observed from available manufacturer data, where different models e.g. have the same length even though most other parameters are scaled, see Table C.8. This is most likely due to the fact that reuse of components across different models are cost effective. It should also be mentioned that manufacturer documents appear to have approximate rounded numbers, and that discrepancies across different sources of data are common.

### GT PRO Models

The total weight from GT PRO is higher for model 1 than models 2 and 3. This is mainly because a low temperature economizer (LTE) is integrated in the HRSG section for model 1, see Fig. C.17, and compare with Fig. C.23. When the steam cycle is integrated with a CO<sub>2</sub> plant, the condensed water from the reboiler is automatically returned to the feedwater tank. As this increases the feedwater temperature, the low temperature economizer is superfluous. This was not easily manipulated in GT PRO for model 1, because it was not possible to implement a feedback stream from the steam turbine outlet to the feedwater tank. More advanced Thermoflow software like THERMOFLEX should be able to implement this. The weight estimate for model 2 is therefore the most realistic.

All the designed cycles are able to deliver enough steam at the specified temperature and pressure for the CO<sub>2</sub> plant. The steam turbine creates a positive net power output for all cycles. This is for 65 bar compression, see Fig. 5.8. This pressure level needs to be adjusted for each case, so that the reservoir pressure is matched. Even with a desalination plant installed, the steam turbine is able to deliver a net positive power output of 5 MW. The net power output was positive for all scenarios tested in GT PRO, also extreme values during the polynomial implementation. It should be mentioned that this is for design conditions, and off-design simulations should be performed in future work.

Even though purity issues are a concern for offshore produced fresh water, desalination should be considered if a steam cycle is integrated. Surplus steam is perfect for distillation, and could supply a large mass flow of fresh water for different applications, e.g. drinking water, cleaning, cooling, and makeup water for the steam cycle. In this work, the desalination plant was maximized in terms of available steam. The designed MED-TVC distillation plant is very heavy with 318 tons, and most likely out-sized in terms of production. This part was more of a feasibility study, and should be reduced to reasonable proportions, based on demand. An additional measure that could contribute to a weight reduction in the desalination plant is integration with the CO<sub>2</sub> plant. The exhaust gas cooler (Direct contact cooler), see Figures 5.3 and 7.8, could be integrated with the distillation process. This would reduce the pump work for seawater, because the same water is used for cooling and desalination. The preheated seawater would also require less steam for fresh water production. This is a mutually beneficial situation.

### **Polynomial Representation**

The accuracy from the polynomials is good, even though relatively few simulation points (nodes) are considered. This proposed method for polynomial representation has high flexibility in terms of variables and number of nodes. The underlying mathematical methods are uncomplicated and are easy to implement. If desired, higher order terms can easily be added to the MATLAB function handle. Second order terms were considered to be sufficient for this work, and gave good results. Third order terms were implemented and tested for model 2, but gave no significant improvements. The polynomial accuracy is within acceptable limits, with a maximum error of 3.5% from the validation tests.

GT PRO is not the easiest software to combine with others, e.g. MATLAB, but calculates very fast. Especially the PEACE output is very detailed, and considering the short calculation time, the level of detail is suspicious. Some quite extensive simplifications are most likely implemented in the GT

PRO algorithms. This should not have any considerable effect on the polynomial methodology, but could be very significant for the scaling laws from the similarity approach. The polynomial approach was implemented for several cases during the development of the methodology. When the range for each variable was small and divided into 64 nodes, the accuracy was very good ( $<1\%$  for all tested values inside the range).

### Scaling Laws

The consistency in the simulation results for the scaling laws is exceptionally good. For verification, the same approach should be tested in a different simulation tool. The fit is almost too good to be true, and is most likely related to software limitations. This kind of scaling law accuracy will never be observed for real equipment. This is shown from the scaling relationships from the literature study. For the purpose of this work, the linear relationship with  $n = 1$  should be sufficient. This allows a generalization for all the models. The accuracy is still good, and only slightly reduced compared to the optimal "n"-values.

This weight estimating method has its obvious limitations, because only one variable is considered. Nevertheless, for similar cases as the considered "FPSO" case, the correct exhaust temperature can be given to the GT PRO model. Consequently, only two simulations on the boundaries are sufficient to find the linear relationship. That is an extremely efficient method for steam cycle weight estimation. The maximum error of 3.1% is within acceptable limits, especially since it occurred outside the calculated range. The most important positive and negative factors for both the polynomial and scaling law approach are listed in Table 8.26.

Table 8.26: Positive and negative factors for weight estimating methods.

Polynomial	Scaling Law
+	+
<ul style="list-style-type: none"> <li>• Multivariate analysis.</li> <li>• Flexibility in terms of variables.</li> <li>• All kinds of mathematical relations can be implemented.</li> <li>• Only one session with simulations are necessary if the design is kept constant, and is consequently generalizable.</li> </ul>	<ul style="list-style-type: none"> <li>• Short calculation time.</li> <li>• Simple and elegant solution.</li> <li>• High accuracy within calculated range.</li> </ul>
-	-
<ul style="list-style-type: none"> <li>• Takes long time to build.</li> <li>• The methodology can not handle dependent variables directly.</li> <li>• The calculated polynomial could form a long and complex solution.</li> </ul>	<ul style="list-style-type: none"> <li>• Limited to one variable.</li> <li>• Only suited for cases with fixed boundary conditions.</li> </ul>

### Sources of Error

The most important sources of error for the results are listed here:

- Available weight data from manufacturers has discrepancies, even between internal documents. The given weights are also very rounded and are not well defined in terms of which components are included in the given weight.
- Only General Electric has stated that their designs are based on scaling. Similarity had to be assumed for other manufacturers, often based on a visual approach, see Fig. 8.1. The design procedures are normally confidential information.
- Only steady state operations at design conditions are considered. The best steam cycle design should ideally be assessed on its overall performance. This includes transient and off-design testing.
- There are software limitations in GT PRO, and simplifications in their weight calculations. The scaling laws are very sensitive to this. This kind of compliance will never be observed for real equipment; this is confirmed from the real data analyzed.
- The implemented CO<sub>2</sub> plant in GT PRO is manually adjusted to match the specifications from SINTEF documents that describe the "FPSO" case. Therefore, all results from the CO<sub>2</sub> plant need to be examined with some uncertainty, particularly the power consumption is relevant. The SINTEF documents are not based on simulations in GT PRO.
- Weighted least squares method has no mathematical procedure to directly account for thermo-dynamic dependent variables.





# Chapter 9

## Conclusions and Further Work

### Contents

9.1	Conclusion . . . . .	129
9.2	Further Work . . . . .	131

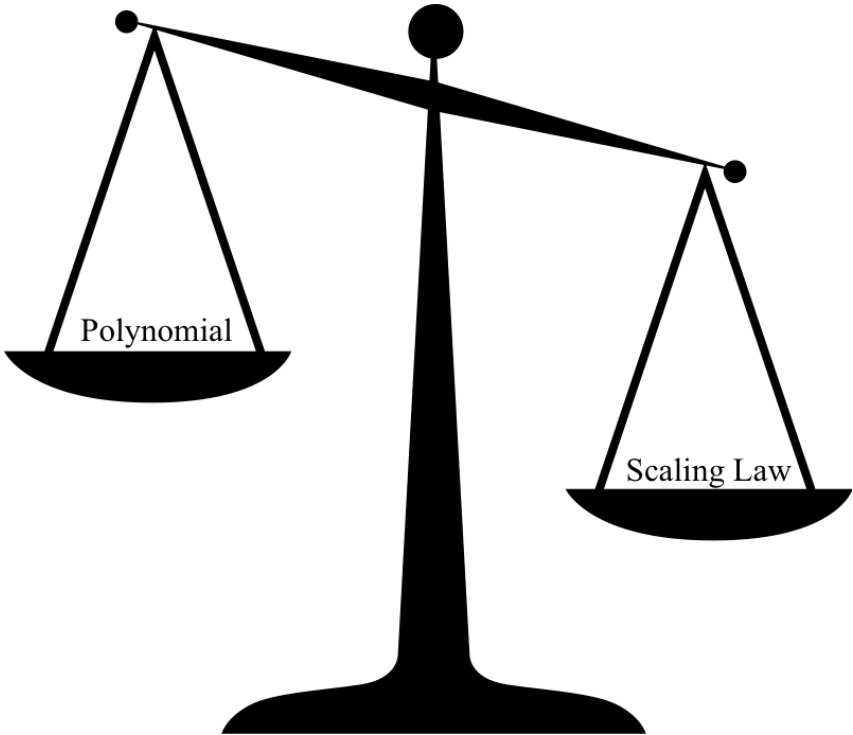


Figure 9.1: What is the preferred method for weight estimation?

To wrap up the work done in this study, this last chapter contains two major parts, the conclusion and suggestions on further work. The first part will conclude the research question and the other key subjects that are discussed in order to answer the given objectives. Further work is important to address; many interesting issues have appeared during the work with this thesis. It was not possible to investigate all these aspects within the scope and allocated time, and they should therefore be considered for future analysis. As mentioned in the beginning of this thesis, the research question was defined as: "What is the preferred weight estimating method for steam bottoming cycles on offshore oil and gas installations, polynomial representation or scaling laws?".

## 9.1 Conclusion

CO<sub>2</sub> capture could potentially contribute to large reductions in the emissions from the oil and gas industry on the Norwegian continental shelf. With carefully considered design, and weight reducing measures, it should be possible to implement a steam cycle in combination with CO<sub>2</sub> capture. The GT PRO simulation results are promising for the proposed design; the back-pressure steam turbine provides the necessary power to operate the CO<sub>2</sub> plant, and has a net positive power output for all the considered cases. Just as significant is the steam mass flow that is feeding the reboiler at the thermodynamic specifications. The steam production is about  $10 \frac{kg}{s}$  larger than the CO<sub>2</sub> plant demand. This should be a sufficient buffer for unexpected circumstances, and offers the opportunity for desalination. Model 2 has the most realistic weight estimate, which is found to be 437.8 tons for the steam cycle.

A promising solution for the exhaust gas cooler in the CO<sub>2</sub> plant is an integration with desalination. Preheating of seawater reduces the necessary heat transfer surface area, and consequently the desalination plant weight. This will also reduce the necessary amount of seawater that is pumped to the installation. If desalination is excluded, the cooler should be integrated with the feedwater tank. This could potentially reduce the weight of the HRSG by excluding the low temperature economizer. After developing this steam cycle through the specialization project and master's thesis, it appears to be a good alternative for offshore implementation.

If GT PRO results are considered correct, the total weight of the steam cycle is accurately estimated from both the polynomial and scaling law approach. The weighted least squares regression based polynomial approach stands out if e.g. a new offshore combined cycle is planned, where flexibility in the input parameters are relevant. If multiple variables have to be considered, this is the only method that allows such analysis. If the proposed steam cycle design is maintained, it should be

possible to apply a precalculated polynomial with high accuracy (many nodes) for all relevant cases within the defined range of each variable. The polynomial approach will then give an instantaneous weight estimate, with no need for additional simulations. Within its respective range, all considered polynomials made very good weight estimates. The biggest error found was 3.15% for polynomial 1. This is acceptable for three variables and 64 nodes.

Scaling laws are limited in terms of flexibility, but is exceptionally fast to calculate and very accurate within its one-variable limitation. For integration with existing plants, this should be the preferred method. The only necessary variable is the steam mass flow from the HRSG. As mentioned in previous discussions, the scaling relationships from the simulation results are almost too consistent to be trustworthy. In this work, the GT PRO weight estimates are the only alternative for similar steam turbine, generator and heat recovery steam generator weight data. The implied scaling laws are extremely precise, especially compared to real weight data for similar gas turbines with generators. Gas turbine design is normally much more standardized than for steam turbines, and should in that sense demonstrate a better match for similarity. On the other hand, it is likely that all steam turbines in GT PRO are designed with the same algorithms. Scaling laws creates a very elegant method for weight estimation based on similarity approach, because linear equations are almost as simple as it gets. The analytical results support the linear scaling relationship between weight and steam mass flow.

For a similar case study as in this master's thesis, the answer to the research question is scaling laws. If more advanced weight analysis is needed, a precalculated polynomial for the chosen design will give immediate results. This require a considerable amount of preparation time, and is the reason why scaling laws should be preferred if they satisfy the necessary level of detail and flexibility.

### **Limitations**

When the weight estimating methods are considered, good results can only be expected inside the chosen range for each variable. If the polynomial or scaling law calculations are well planned, and based on physical limitations and realistic values, it should be no reason to extrapolate results. Nevertheless, it is extremely important to remember that both GT PRO simulations and, consequently, the weight estimates are approximations. It is not likely that real equipment is as compatible as the simulation data. This is clearly shown by the difference in the weight plots from existing turbines, and the turbine data from GT PRO, e.g. Fig. 8.6 vs. Fig. C.38. All results are limited to steady state operations at the design conditions. This should not affect the weight estimating methodology.

## 9.2 Further Work

This last section contains some of the ideas and challenges that emerged during this study. Hopefully some of these aspects can be investigated further.

- Off-design and transient simulations on the considered steam cycles. This is important to ensure sufficient steam production, predict the power supply, adjust the system according to the CO<sub>2</sub> plant steam demand and investigate fluctuations in the fresh water production.
- Implement control systems to handle changes in the operating conditions. If both CO<sub>2</sub> capture and desalination are implemented, this will form a complex system that need robust regulation.
- A back-up system for the steam supply should be considered. This could be as easy as a steam turbine bypass system for unexpected downtime or if steam turbine maintenance is necessary. Parallel system for e.g. the steam turbine are not considered, but could be an alternative to this backup system. A duct burner in the HRSG is also possible.
- More realistic cases like the "FPSO" case should be tested to validate the chosen steam cycle design. The weight estimating approaches should be independent of this.
- The polynomial is most likely possible to improve further. Additional parameters and higher order terms is easy to implement, and can potentially improve the accuracy. Other mathematical methods like approximating Splines and Principal Component Analysis were investigated, but not continued. A polynomial based on a very narrow grid (many nodes) is a natural next step, and should achieve high accuracy when the final design is carved in stone.
- Aspects like maintenance and easy replacements for all designed systems should be investigated.
- Investigate if parallel systems like on Eldfisk could improve the overall design. In that specific case, three gas turbines are feeding two once through heat recovery steam generators, here six gas turbines are feeding one. This is therefore very relevant, even though any size or weight reductions are unlikely from the finding in this work.
- For onshore combined cycles, it is common with a combined generator for the gas and steam turbine, this could potentially save weight for the offshore cycle.
- GT PRO is not able to estimate the weight of the CO<sub>2</sub> capture plant. If such software is available, it would enable a more complete analysis.
- It should be possible to design the distillation plant in a more compact matter. The eight pressure levels in the MED-TVC process could most likely be reduced to save weight. This type of design consideration is not possible to analyze in GT PRO.

# Bibliography

- [1] P. Mores, E. Godoy, S. Mussati, and N. Scenna, "A NGCC Power Plant with a CO<sub>2</sub> Post-Combustion Capture Option. Optimal Economics for Different Generation/Capture Goals," *Chemical Engineering Research and Design*, vol. 92, no. 7, pp. 1329–1353, 2014.
- [2] Y. Tormodsgard, "Facts 2014. The Norwegian Petroleum Sector," *Norwegian Ministry of Petroleum and Energy and Norwegian Petroleum Directorate*, 2014.
- [3] "Emissions of Greenhouse Gases, 2014, Preliminary Numbers.  
<https://www.ssb.no/natur-og-miljo/statistikker/klimagassn/aar-forelopige/2015-05-07?fane=tabellsort=nummertabell=225400> (10.10.15)."
- [4] D. Best and E. Levina, "Facing China's Coal Future," 2012.
- [5] H. d. Coninck, M. Loos, B. Metz, O. Davidson, and L. Meyer, "IPCC Special Report on Carbon Dioxide Capture and Storage," *Intergovernmental Panel on Climate Change*, 2005.
- [6] OECD. Publishing and International Energy Agency, *Energy Technology Perspectives 2010: Scenarios and Strategies to 2050*. Organisation for Economic Co-operation and Development, 2010.
- [7] Global, CCS, "Institute. The global Status of CCS: 2013," *Canberra, Australien*, 2013.
- [8] "Adoption of the Paris Agreement, Proposal by the President, Draft decision –/CP.21  
<http://unfccc.int/resource/docs/2015/cop21/eng/l09.pdf> (14.12.15)."
- [9] A. Baklid, R. Korbol, G. Owren, *et al.*, "Sleipner Vest CO<sub>2</sub> Disposal, CO<sub>2</sub> Injection Into a Shallow Underground Aquifer," in *SPE Annual Technical Conference and Exhibition*, Society of Petroleum Engineers, 1996.
- [10] Norwegian Ministry of Finance, "Norwegian State Budget 2013," p. 24, 2013.
- [11] "Government Revenues from Petroleum Activities  
<https://www.regjeringen.no/no/tema/energi/olje-og-gass/statens-inntekter-fra-petroleumsverksemda/id2076770/> (10.10.15)."
- [12] "SINTEF, The EFFORT Project  
<https://www.sintef.no/projectweb/effort/goals-and-objectives/> (26.09.15)."
- [13] L. O. Nord, E. Martelli, and O. Bolland, "Weight and Power Optimization of Steam Bottoming Cycle for Offshore Oil and Gas Installations," *Energy*, vol. 76, pp. 891–898, 2014.
- [14] L. O. Nord and O. Bolland, "Design and Off-Design Simulations of Combined Cycles for Offshore Oil and Gas Installations," *Applied Thermal Engineering*, vol. 54, no. 1, pp. 85–91, 2013.
- [15] L. O. Nord and O. Bolland, "Steam Bottoming Cycles Offshore – Challenges and Possibilities," *Journal of Power Technologies*, vol. 92, no. 3, pp. 201–207, 2012.

- [16] K. C. Haug, "CCS on Offshore Oil and Gas Installation," 2015.
- [17] "MATLAB R2014b  
<http://se.mathworks.com/products/matlab/>."
- [18] "Excel version 15.16  
<https://products.office.com/en-us/excel>."
- [19] "ThermoFlow Inc  
<http://www.thermoflow.com/>."
- [20] "Gas Turbine Animation  
<http://cset.mnsu.edu/engagethermo/images/gasturbineanimation.png> (22.09.15)."
- [21] S. Lundberg and K. E. Kaski, "Onshore Power to Oil and Gas Platforms," 2011.
- [22] M. J. Mazzetti, P. Nekså, H. T. Walnum, A. K. T. Hemmingsen, *et al.*, "Energy-Efficiency Technologies for Reduction of Offshore CO<sub>2</sub> Emissions," *Oil and Gas Facilities*, vol. 3, no. 01, pp. 89–96, 2014.
- [23] Norwegian Petroleum Directorate, "Power From Shore to the Norwegian Continental Shelf," 2008.
- [24] "Hydro Power Information  
<http://www.nve.no/no/energi1/fornybar-energi/vannkraft/> (12.10.15)."
- [25] "Wind Power Information  
<http://www.nve.no/no/konsesjoner/vindkraft-2/vindkraft/> (12.10.15)."
- [26] "Typical Data for Natural Gas  
<http://gasnor.no/naturgass/typiske-data-naturgass/> (12.10.15)."
- [27] H. Alkabie, R. McMillan, R. Noden, and C. Morris, "Dual Fuel Dry Low Emissions (DLE) Combustion System for the ABB Alstom Power 13, 4 MW Cyclone Gas Turbine," in *ASME Turbo Expo 2000: Power for Land, Sea, and Air*, pp. V002T02A031–V002T02A031, American Society of Mechanical Engineers, 2000.
- [28] O. Bolland, "Thermal Power Generation," 2014.
- [29] "Gas Turbine Pressure, Temperature and Velocity  
<http://i.stack.imgur.com/elcxa.jpg> (22.09.15)."
- [30] "General Electric LM2500 Gas Turbine  
<http://www.centerfieldinc.com/images/lm2500ge.jpg> (22.09.15)."
- [31] E. R. Følgesvold, "Combined Heat and Power Plant on Offshore Oil and Gas Installations," *NTNU*, 2015.
- [32] IPCC, "IPCC Fourth Assessment Report: Climate Change 2007," 2007.
- [33] Norwegian Petroleum Directorate, "Feasibility study  
Environmental impact of power pooling in the Tampen area," 2009.
- [34] "StatoilHydro Awards 58 MUSD Oseberg EPCI contract to Aibel  
<http://aibel.com/en/news-and-media/press-releases/statoilhydro-awards-58-musd-oseberg-epci-contract-to-aibel>  
(12.11.15)."
- [35] "Examining Applications of Offshore Technology to Onshore Gas Compressor Stations for the Profitable Generation of CO<sub>2</sub>-Free Power (12.11.15)."
- [36] P. Kloster *et al.*, "Energy Optimization on Offshore Installations with Emphasis on Offshore Combined Cycle Plants," in *Offshore Europe Oil and Gas Exhibition and Conference*, Society of Petroleum Engineers, 1999.

- [37] "Back Pressure Turbine  
<http://www.greensolpower.com/images/steam-turbine-htcprod4.gif> (22.09.15)."
- [38] M. Boyce, *Handbook for Cogeneration and Combined Cycle Power Plants*. ASME Press, 2002.
- [39] R. Kehlhofer, B. Rukes, F. Hannemann, and F. Stirnimann, *Combined-cycle Gas and Steam Turbine Power Plants*. Pennwell Books, 2009.
- [40] "Horizontal HRSG with Duct Burner and Steam Drum  
<http://www.gasturb.de/gallery/gtheatrecoverysteamgenerator.jpg> (08.06.16)."
- [41] "Solid and Serrated fins  
<http://www.hydrocarbonprocessing.com/article/2598468/understand-the-difference-between-solid-and-serrated-fins.html> (18.11.15)."
- [42] F. Starr, "Background to the Design of HRSG Systems and Implications for CCGT Plant Cycling," *European Technology Development OMMI*, vol. 2, no. 1, 2003.
- [43] "ASTM A335 Chrome Moly Pipe  
<http://www.fedsteel.com/products/alloy-pipe-and-tube/astm-a335-chrome-moly-pipe.html> (15.11.15)."
- [44] "Specification for Seamless Ferritic Alloy Steel Pipe for High Temperatures  
<http://www.fedsteel.com/products/alloy-pipe-and-tube/astm-a335-chrome-moly-pipe.html> (15.11.15)."
- [45] "Special Metals  
<http://www.fedsteel.com/products/alloy-pipe-and-tube/astm-a335-chrome-moly-pipe.html> (15.11.15)."
- [46] L. Pierobon, R. Kandepu, and F. Haglind, "Waste Heat Recovery for Offshore Applications," in *ASME 2012 International Mechanical Engineering Congress and Exposition*, pp. 503–512, American Society of Mechanical Engineers, 2012.
- [47] "Electric Generator  
<https://s-media-cache-ak0.pinimg.com/736x/2c/63/fd/2c63fdef57811e14971a972ad71350eb.jpg> (28.05.16)."
- [48] Thermoflow, "GT PRO Help Files,," 2016.
- [49] "Multi Stage Flash  
<http://www.ee.co.za/wp-content/uploads/2014/12/09-mr-water-desalination-final-fig.021.jpg> (26.05.16)."
- [50] "Multi Effect Distillation  
<http://en.sh-ihw.com/imagerepository/9f595f91-a130-4c42-8362-9352e9878808.jpg> (26.05.16)."
- [51] "Steam Jet Ejector  
<http://www.transvac.co.uk/images/ejector-principle.jpg> (26.05.16)."
- [52] "Condensate Polisher  
<http://dardel.info/ix/processes/columns.html> (17.11.15)."
- [53] M. J. Moran, H. N. Shapiro, D. D. Boettner, and M. B. Bailey, *Fundamentals of Engineering Thermodynamics*. John Wiley & Sons, 2006.
- [54] M. Nakhmkin, "Retrofit of Simple Cycle Gas Turbines for Compressed Air Energy Storage Application," Oct. 10 1989. US Patent 4,872,307.
- [55] "TS Diagram for Combined Cycle  
<http://direns.mines-paristech.fr/sites/thopt/en/res/cc-tschart.jpg> (22.09.15)."

- [56] "Offshore Transport and Storage  
<https://www.globalccsinstitute.com/sites/www.globalccsinstitute.com/files/pages/92241/10-co2-transport-offshore.jpg>  
(03.03.16)."
- [57] United Nations, "The Kyoto Protocol," 1998.
- [58] United Nations, "Doha Amendment to the Kyoto Protocol," 2012.
- [59] R. Zhai and Y. Yang, *MEA-Based CO<sub>2</sub> Capture Technology and Its Application in Power Plants*. INTECH Open Access Publisher, 2010.
- [60] "Large Scale CCS Projects  
[https://www.globalccsinstitute.com/projects/large-scale-ccs-projects\(10.10.15\)](https://www.globalccsinstitute.com/projects/large-scale-ccs-projects(10.10.15))."
- [61] "EPA, Global Greenhouse Gas Emissions Data  
<http://www3.epa.gov/climatechange/ghgemissions/html> (10.10.15)."
- [62] "IUPAC, Loading Capacity  
<http://goldbook.iupac.org/l03599.html> (10.10.15)."
- [63] J. Davis and G. Rochelle, "Thermal Degradation of Monoethanolamine at Stripper Conditions," *Energy Procedia*, vol. 1, no. 1, pp. 327–333, 2009.
- [64] B. R. Strazisar, R. R. Anderson, and C. M. White, "Degradation of Monoethanolamine used in Carbon Dioxide Capture from Flue Gas of a Coal-fired Electric Power Generating Station," *Journal of Energy & Environmental Research*, vol. 1, no. 1, pp. 32–39, 2001.
- [65] M. S. Jassim and G. T. Rochelle, "Innovative Absorber/Stripper Configurations for CO<sub>2</sub> Capture by Aqueous Monoethanolamine," *Industrial and Engineering Chemistry Research*, vol. 45, no. 8, pp. 2465–2472, 2006.
- [66] K. S. Fisher, C. Beitler, C. Rueter, K. Searcy, G. Rochelle, M. Jassim, and J. D. Figueroa, "Integrating MEA regeneration with CO<sub>2</sub> Compression to reduce CO<sub>2</sub> Capture Costs," in *Fourth annual conference on carbon capture and sequestration DOE/NETL*, 2005.
- [67] G. T. Rochelle, "Innovative Stripper Configurations to Reduce the Energy Cost of CO<sub>2</sub> Capture," in *Second Annual Carbon Sequestration Conference, Alexandria, VA*, pp. 5–8, 2003.
- [68] H. Chang and C.-M. Shih, "Simulation and Optimization for Power Plant Flue Gas CO<sub>2</sub> Absorption-Stripping Systems," *Separation science and technology*, vol. 40, no. 4, pp. 877–909, 2005.
- [69] M. R. M. A. Zahra, "Carbon Dioxide Capture from Flue Gas, Development and Evaluation of Existing and Novel Process Concepts," 2009.
- [70] M. R. Abu-Zahra, L. H. Schneiders, J. P. Niederer, P. H. Feron, and G. F. Versteeg, "CO<sub>2</sub> Capture from Power Plants: Part I. A Parametric Study of the Technical Performance Based on Monoethanolamine," *International Journal of Greenhouse Gas Control*, vol. 1, no. 1, pp. 37–46, 2007.
- [71] National Energy Technology Laboratory, "Carbon Capture Approaches for Natural Gas Combined Cycle Systems," vol. Revision 2, no. DOE/NETL-2011/1470, 2010.
- [72] "Amine Gas Treating  
[https://en.wikipedia.org/wiki/amine-gas-treating\(09.10.15\)](https://en.wikipedia.org/wiki/amine-gas-treating(09.10.15))."
- [73] L. Duan, M. Zhao, and Y. Yang, "Integration and Optimization Study on the Coal-fired Power plant with CO<sub>2</sub> Capture Using MEA," *Energy*, vol. 45, no. 1, pp. 107–116, 2012.



- [74] "Carbon Capture and Storage Association, CCS: Transport  
<http://www.ccsassociation.org/faqs/ccs-transport/> (12.12.15)."
- [75] P. W. Parfomak and P. Folger, "Carbon dioxide (CO<sub>2</sub>) Pipelines for Carbon Sequestration: Emerging Policy Issues,"
- [76] "Carbon Capture and Storage Association, CCS: Storage  
<http://www.ccsassociation.org/faqs/ccs-storage/> (12.12.15)."
- [77] "Deep Saline Aquifers  
<http://www.co2club.ro/img/primapagina-img.jpg> (12.12.15)."
- [78] "Caprock Animation  
<http://www.arb.ca.gov/cc/sequestration/caprock.jpg> (12.12.15)."
- [79] A. de Haan, H. Kooijman, and A. Gorak, "Carbon Capture and Storage Experience from the Sleipner Field,"
- [80] "7th IEA International CCS Regulatory Network Meeting 22 – 23 April 2015, IEA Paris  
<https://www.iea.org/media/workshops/2015/sally/neilspeterchristensen.pdf> (03.12.15)."
- [81] "StatoilHydro, Henrik Solgaard Andersen, Carbon Dioxide Capture, Transport and Storage (CCS)  
<http://www04.abb.com/global/seitp/seitp202.nsf/c71c66c1f02e6575c125711f004660e6/9ebcbfaedaedfa36c12576f1004a49de/file/statoilhy>  
(12.12.15)."
- [82] R. Arts, A. Chadwick, O. Eiken, S. Thibeau, and S. Nooner, "Ten Years Experience of Monitoring CO<sub>2</sub> Injection in the Utsira Sand at Sleipner, Offshore Norway," *First break*, vol. 26, no. 1, 2008.
- [83] Wikipedia, "Interpolation Wikipedia The Free Encyclopedia," 2016. [Online; accessed 4-June-2016].
- [84] "Chapter 3 – Interpolation. Mathworks  
<https://www.mathworks.com/moler/interp.pdf> (03.03.16)."
- [85] C. B. Moler, *Numerical Computing with MATLAB: Revised Reprint*. Siam, 2008.
- [86] C. De Boor, *A Practical Guide to Splines*, vol. 27. Springer-Verlag New York, 1978.
- [87] "Splines  
<https://www.physics.utah.edu/~detar/phys6720/handouts/cubic-spline/cubic-spline/node1.html> (03.03.16)."
- [88] Wikipedia, "Regression Analysis Wikipedia The Free Encyclopedia," 2016. [Online; accessed 4-June-2016].
- [89] Wikipedia, "Scaling (geometry) — Wikipedia The Free Encyclopedia," 2016. Online; accessed 14-May-2016.
- [90] A. Seppo, "Principles of Turbomachinery," 2011.
- [91] O. Balje, "A Study on Design Criteria and Matching of Turbomachines: Part A—Similarity Relations and Design Criteria of Turbines," *Journal of Engineering for Power*, vol. 84, no. 1, pp. 83–102, 1962.
- [92] F. Whittle, *Gas Turbine Aero-Thermodynamics: with Special Reference to Aircraft Propulsion*. Elsevier, 2013.
- [93] D. Brandt and R. Wesorick, "GE Gas Turbine Design Philosophy," *GER-3434, General Electric*, 1994.
- [94] A. Rivera-Alvarez, M. J. Coleman, and J. C. Ordonez, "Ship Weight Reduction and Efficiency Enhancement Through Combined Power Cycles," *Energy*, vol. 93, pp. 521–533, 2015.
- [95] "Shell and Tube Heat Exchanger with Fixed Tubesheet  
<http://www.slideshare.net/rehanrex/maintenance-procedurefix-tubesheet-exchanger> (08.06.16)."
- [96] SINTEF, "D1.5.1307 Simulation and Cost Estimation of the Reference Process with a New Solvent," 2013.
- [97] SINTEF, "Characteristics of CO<sub>2</sub> Point Sources – Emphasis on Selected Cases," 2010.
- [98] SINTEF, "D1.5.1205 Reference Cases Simulation and Cost Estimation," 2012.

- [99] W. Wagner and A. Prussb, "The IAPWS Formulation 1995 for the Thermodynamic Properties of Ordinary Water Substance for General and Scientific Use," *J. Phys. Chem. Ref. Data*, vol. 31, no. 2, p. 387, 2002.
- [100] IAPWS, "IAPWS Technical Guidance Document: Volatile Treatments for the Steam-water Circuits of Fossil and Combined Cycle/HRSG Power Plants (July 2015)," 2015.
- [101] W. Wagner, J. Cooper, A. Dittmann, J. Kijima, H.-J. Kretzschmar, A. Kruse, R. Mares, K. Oguchi, H. Sato, I. Stocker, *et al.*, "The IAPWS Industrial Formulation 1997 for the Thermodynamic Properties of Water and Steam," *Journal of Engineering for Gas Turbines and Power*, vol. 122, no. 1, pp. 150–184, 2000.
- [102] M. P. Polsky, "Sliding Pressure Operation in Combined Cycles," *ASME*, 1982.
- [103] "SIEMENS, Operating Mode of Power Plants  
[http://www.energy.siemens.com/mx/pool/hq/power-generation/power-plants/steam-power-plant-solutions/benson\(30.11.15\).](http://www.energy.siemens.com/mx/pool/hq/power-generation/power-plants/steam-power-plant-solutions/benson(30.11.15).)"
- [104] "GT PRO - Thermoflow  
<http://www.thermoflow.com/combinedcycle-gtp.html> (20.11.15)."
- [105] "Processmodeling.org (21.04.16)."
- [106] R. L. Eberlein, "Simplification and Understanding of Models," *System Dynamics Review*, vol. 5, no. 1, pp. 51–68, 1989.
- [107] A. K. Saysel and Y. Barlas, "Model Simplification and Validation with Indirect Structure Validity Tests," *System Dynamics Review*, vol. 22, no. 3, pp. 241–262, 2006.
- [108] Y. Barlas, "President's Address. In 16th International System Dynamics Conference, Quebec City, Canada, July.  
<http://www.albany.edu/cpr/sds/president-newsletter1.htm> [18 september 2006].," 1998.
- [109] "Centaur 40, Centaur 50 and Taurus 60 Gas Turbine - Compressor Sets (12.02.16)."
- [110] "Taurus 70 CS/MD Turbomachinery Package Specification  
<http://s7d2.scene7.com/is/content/caterpillar/c10660338> (20.05.16)."
- [111] "Power Generation - Product Selection Guide - Solar Turbines  
<http://s7d2.scene7.com/is/content/caterpillar/c10550166> (12.02.16)."
- [112] "Saturn 20 CS/MD Turbomachinery Package Specification  
<http://pdf.directindustry.com/pdf/solar-turbines/saturn-20-cs-md-turbomachinery-package-specification/22650-199745.html> (20.05.16)."
- [113] "Centaur 40 CS/MD Turbomachinery Package Specification  
<http://pdf.directindustry.com/pdf/solar-turbines/centaur-40-cs-md-turbomachinery-package-specification/22650-199747.html> (20.05.16)."
- [114] "Taurus 60 CS/MD Turbomachinery Package Specification  
<http://pdf.directindustry.com/pdf/solar-turbines/taurus-60-cs-md-turbomachinery-package-specification/22650-199753.html> (20.05.16)."
- [115] "Mars 90 and Mars 100 CS/MD Turbomachinery Package Specification  
<http://pdf.directindustry.com/pdf/solar-turbines/mars-90-mars-100-cs-md-turbomachinery-package-specification/22650-199755.html> (20.05.16)."
- [116] Elliot Ebara Group, "YR Turbine Products, Flexibility to Meet All Your Needs," 2002.

- [117] M. J. Coleman, "Ship Weight Reduction and Efficiency Enhancement Through Combined Power Cycles," 2013.
- [118] M. O. Willumsen, "Facts 2011. Energy and Water Resources in Norway," 2011.
- [119] H. M. Noorland, "The Effect on Total CO<sub>2</sub> Emissions from the Electricity Sector in Northern Europe with New Power Cables Between Norway and the Continent," 2007.
- [120] L. K. Panton, "Exergy Analysis of Conventional and Electrified Oil and Gas Platforms," 2014.
- [121] Norwegian Petroleum Directorate, "Environmental Technology," 2011.
- [122] "ENI Norway, Goliat – The First Oil Field in the Barents Sea  
[http://www.petroarctic.no/library/files/oil-and-gas/company/eni-norge/goliat\(12.10.15\).](http://www.petroarctic.no/library/files/oil-and-gas/company/eni-norge/goliat(12.10.15).)"
- [123] Statnett, "Grid Development, National Plan for Next Generation Power Grid," 2013.
- [124] Ministry of Petroleum and Energy, "Proposed Electrification of Utsira High," 2014.
- [125] Statoil, "Johan Sverdrup, Impact Assessment," 2014.
- [126] SAFETECH, "Petroleum Safety Authority Norway, Knowledge, Electrical Power from Shore, Reserve Power, and Emergency Power," 2015.
- [127] "Offshore Wind Farm  
<http://corporate.vattenfall.com/about-energy/renewable-energy-sources/wind-power/how-it-works/> (23.09.15)."
- [128] "Offshore Electrification on the Utsira High  
<http://www.tu.no/petroleum/2014/01/22/-elektrifisering-offshore-har-ingenting-for-seg> (12.10.15)."
- [129] R. L. Martin Wall and S. Frost, "Offshore Gas Turbines (and Major Driven Equipment) Integrity and Inspection Guidance Notes," *ESR Technology Ltd*, 2006.
- [130] "Direct Water Cooling Condenser  
<https://en.wikipedia.org/wiki/thermal-power-station/media/file:surface-condenser.png> (16.11.15)."
- [131] "Centrifugal Pump  
<http://www.flowserve.com/files/files/images/products/pumps/low/023-i-nm-cut-large.jpg> (17.11.15)."
- [132] "Powerhouse Deaerator  
<http://www.powerhouse.com/wp-content/uploads/2012/04/hurst-boiler-oxy-miser-deaerator-2.jpg> (24.09.15)."
- [133] E. S. Roderick E. Athey, Brian J. Martin, "Condensate Oxygen Control In A Combined Cycle System Without A Conventional Deaerator – Test Results," *Presented At Electric Power Research Institute Condenser Technology Conference*, pp. 1–8, 1990.
- [134] H. T. Walnum, P. Nekså, L. O. Nord, and T. Andresen, "Modelling and Simulation of CO<sub>2</sub> (Carbon Dioxide) Bottoming Cycles for Offshore Oil and Gas Installations at Design and Off-design Conditions," *Energy*, vol. 59, pp. 513–520, 2013.
- [135] G. Ingram, *Basic Concepts in Turbomachinery*. Bookboon, 2009.
- [136] S. Dixon, "Fluid Mechanics, Thermodynamics of Turbomachinery. Fourth Edition in SI/Metric Units," 1998.
- [137] E. Naess and A. Austegard, "Varmevekslere – NTNU."
- [138] D. Y. Goswami, *The CRC Handbook of Mechanical Engineering*. CRC press, 2004.
- [139] "Common Tube Layouts  
<http://www.industrialseparation.com/wp-content/uploads/2009/09/common-tube.jpg> (21.02.16)."
- [140] "Gas Turbine Generator Systems – Solar Turbines

- <http://me.queensu.ca/courses/mech430/solarturbines2.pdf> (12.02.16)."
- [141] G. . S. T. Directory, "Gas Turbine Technical Data," 2012.
- [142] E. Greitzer and H. Slater, "Volume 2: Appendices-Design Methodologies for Aerodynamics, Structures, Weight, and Thermodynamic Cycles," *Final Report to NASA Glenn Research Center, Massachusetts Institute of Technology, Cambridge, Massachusetts*, 2010.
- [143] "International Aero Engines - V2530-A5  
<http://911research.wtc7.net/essays/reynolds/docs/cfmi-cfm56-5.jpg> (16.02.16)."
- [144] "Pratt & Whitney - PW4090  
<http://www.pw.utc.com/content/v2500-engine/img/b-1-2-v2500-cutaway-high.jpg> (16.02.16)."
- [145] "General Electric - GE90-85B  
<http://www.c-fan.com/images/ge90-reverse-small.jpg> (16.02.16)."
- [146] "CFM International - CFM56-7B27  
<http://www.pw.utc.com/content/pw4000112-engine/img/b-1-4-3-pw4000112-cutaway-high.jpg> (16.02.16)."

# Appendix A

## Supporting Literature

### Contents

A.1	Offshore Heat and Power Generation . . . . .	141
A.1.1	Onshore Power Supply . . . . .	141
A.2	Combined Cycle Technology . . . . .	143
A.2.1	Gas Turbine . . . . .	143
A.2.2	Condenser . . . . .	145
A.2.3	Pumps . . . . .	146
A.2.4	Deaeration . . . . .	147
A.2.5	Onshore Combined Cycle . . . . .	148
A.3	Power Cycles . . . . .	150
A.3.1	Alternative Bottoming Cycles . . . . .	150
A.4	CO <sub>2</sub> Capture, Transport and Storage . . . . .	151
A.4.1	Shore Based Simulations . . . . .	151
A.5	Mathematical Representation . . . . .	153
A.5.1	Scaling and Similitude . . . . .	153
A.5.2	Performance Parameters . . . . .	155

## A.1 Offshore Heat and Power Generation

### A.1.1 Onshore Power Supply

In Norway, it has been an ongoing discussion in both academic and political forums about electrification on some of the installations on the Norwegian continental shelf. Most of the national power production is renewable hydropower [118], which can be transported to offshore facilities by electric cables. Since Norway is electrically interconnected with the European continent, together with high investment costs, the main argument against electrification is that this clean electricity could replace highly polluting power production like coal on the continent instead [119]. Simulations on electricity produced in a typical gas fired combined cycle plant in Germany and transferred to Norwegian offshore facilities gave some interesting results. The total CO<sub>2</sub> emissions would increase for oil installations and be reduced for gas installations [120]. In worst case, imported coal based electricity is sent offshore, this will certainly not give an overall CO<sub>2</sub> reduction.

Regardless of these arguments and very high development costs [23], the Norwegian government is very eager to implement this solution on multiple fields on the NCS. If renewable electricity is used, it obviously contributes to a positive effect on Norway's total CO<sub>2</sub> emissions. Additionally, reduced maintenance and potentially less unwanted shutdowns are good arguments for onshore power supply [121]. The continuously combustion in a gas turbine is a highly relevant source for potential hydrocarbon ignition on oil and gas facilities. This risk is also reduced if onshore power is introduced.

As mentioned in Section 1.1, it is required for all new offshore projects to look at the possibility for connecting to the onshore power grid. This process has already started, Gjøa, Valhall, Ormen Lange, and Troll A [21] are already connected to the grid. The ongoing Goliat project will be partly supplied with onshore power in addition to one installed GT [122][23]. Goliat will in normal operations receive 20–40 MW from the cable, which is limited by a weak power grid in the northern Norway. This could potentially also be a problem in other parts of Norway. Therefore, it is crucial that Statnett expand and reinforce the main power grid to the relevant onshore–offshore power hubs [123]. This is essential if a large scale development should be possible, mainly because a secure and stable power supply is essential for offshore operations. A large scale shutdown on multiple installations would be highly expensive. The Norwegian government has also decided that the large project Johan Sverdrup on the Utsira High should be implemented with onshore power [124]. The surrounding fields: Edvard Grieg, Ivar Aasen, and Gina Krogh are also to be connected with this cable by 2022 [125], see Figure A.2.

The operating companies on the NCS are in general quite positive to the development of more onshore power supply [126]. One of the biggest challenges with removing the gas turbines are easy access to process heat. This will be discussed in Section 2.2. Most likely it will be necessary with either natural gas boilers or electrical heaters, where the last alternative is the most environmental friendly if renewable energy is used according to the Norwegian petroleum directorate [121]. From an exergy perspective, it is very inefficient to use electricity for heat production. Therefore is it necessary to do more research to find the best solution for offshore process heat, when onshore power supply is implemented. It is hard to draw a distinct line between the facilities where onshore power is suitable and not. The most obvious decision parameters are the distances to shore and other facilities that can be interconnected. There is also possible to envisage the opportunity to make centralized power hubs that are fed both from onshore power and e.g. offshore wind farms, see Figure A.1. It should also be possible to install large combined cycles on these hubs, this requires that multiple facilities are gathered in a fair distance from each other.

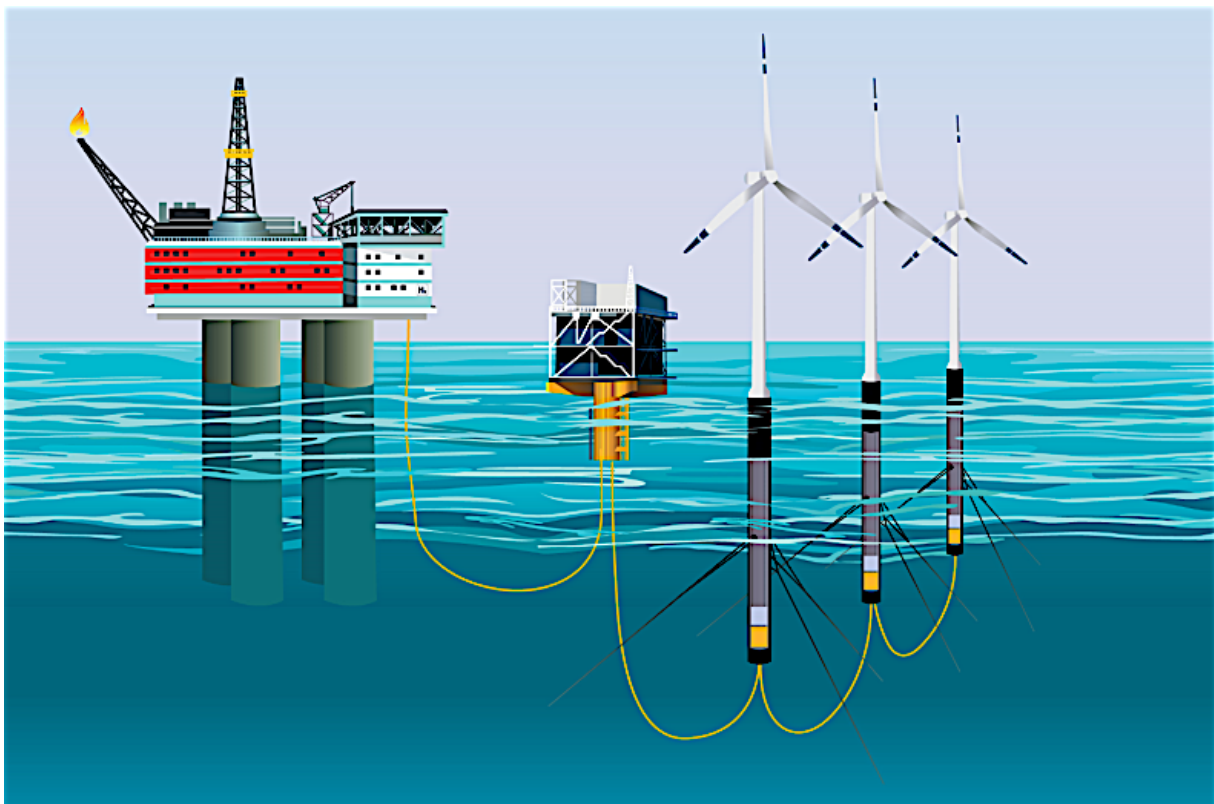


Figure A.1: Offshore installation can be connected to both offshore wind farms and onshore power grid [127].

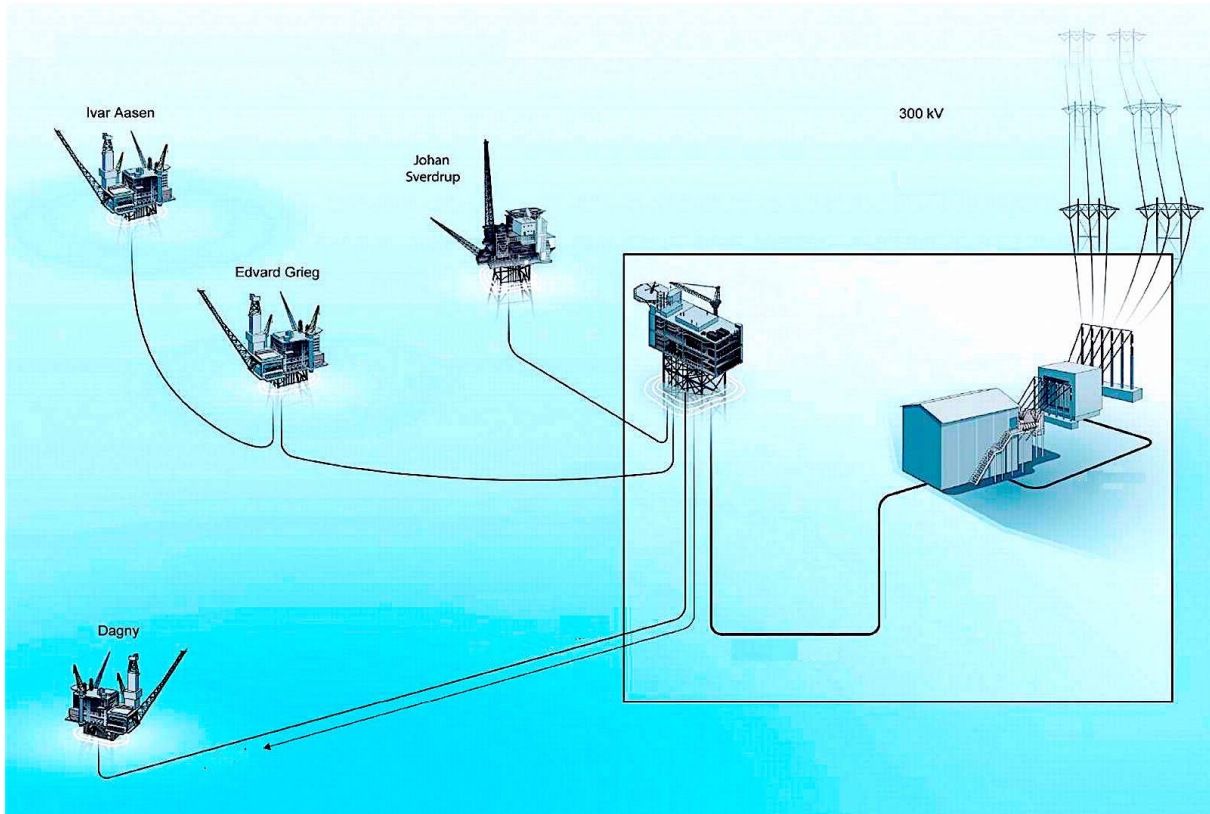


Figure A.2: Possible electrification of the Utsira High on the Norwegian continental shelf [128]

## A.2 Combined Cycle Technology

### A.2.1 Gas Turbine

The GE LM2500 is the most used offshore gas turbine (GT) on the NCS. This turbine and most of the other types installed offshore are based on airplane jet engines. These designs are because of their airborne application based on low weight-to-power ratio. This is also very desired offshore, so it is a very good match. Because of the origin, these gas turbines are called aeroderivative. In the front, the fan is replaced by air intake, and in the back the nozzle has changed place with a turbine that is designed to match the compressor and combustion chamber. These designs are also very robust and have a huge number of operating hours. Downtime is a big concern offshore, so simple repairs and maintenance should be possible and easy to carry out.

Table A.1: Important gas turbine aspects for onshore and offshore operations.

Onshore (Industrial type)	Offshore (Aeroderivative)
High efficiency	Low weight-to-power ratio
Operating costs	Robust equipment
Maintenance costs	Minimal downtime
Maintenance requirements	Simple repairs and maintenance
Marked power demand	Flexible operations (Off-design)



The alternative to aeroderivative gas turbines are industrial types. These types of turbines are mainly bulkier and designed for maximal efficiency, because weight and size are not big concerns onshore. The main task for onshore GTs is to maximize profit on power production. Offshore the most important aspect is reliable delivery of necessary power for varying oil and gas operations. Some lightweight industrial types are actually available [129], but aeroderivative turbines are still the preferred alternative for most installations on the NCS. This is partly due to the normal procedure of replacing the whole GT section if more extensive maintenance is required offshore. Therefore, most of the offshore equipment is mounted on a metal frame. This module is then called a skid and simplifies installations, logistics and replacements on the facilities. The concept can be compared to large scale LEGO-bricks. Aspects that are important for decisions regarding the choice of gas turbines onshore and offshore are found in Table A.1.

### **Offshore Gas Turbine Skid**

A typical GT package/skid that is installed either onshore or offshore contains with some modifications these parts [129]:

- Gas turbine.
- Startup system.
  - Pneumatic.
  - Hydraulic.
  - or Variable speed AC motor.
- Lubrication system.
  - Pumps, filters and tanks.
- Fuel system.
  - Natural gas (NG).
  - or liquid fuel.
- Driven equipment.
- Seal gas system.
  - Compressors.
- Generator.

The following list is not necessarily part of the skid, but is closely integrated with the GT package/skid.

Fire protection is one aspects that is extremely important offshore:

- Enclosures and exhaust stack.
- Fire protections.
- Acoustic housing.
- Inlet system with air filters.
- Lubrication cooler.
- Motor control center and switchgear.

### A.2.2 Condenser

The main task for a condenser is to condense the steam/two-phase exhaust from the ST. This is normally done by removing heat from the exhaust stream using heat exchange with a fluid. Various condenser designs mainly differ in how they perform cooling. The most common designs are listed below.

- Direct contact cooling condenser.
- Air cooled condenser.
- Dry cooling tower.
- Wet cooling tower.

The last two alternatives are because of size foreclosed for offshore operations. Direct contact cooling condensers, see Figure A.3, are generally more compact than air cooled models. Easy access to seawater with relatively low temperatures is beneficial. This is the case for most offshore installations on the NCS, therefore direct water cooling condensers are the chosen alternative. The seawater is flowing in closed tubes normal to the flow direction of the exhaust. Condensation is then occurring on or close to the tube walls before the condensate by gravity collects and exits at the bottom.

It is the temperature of the cooling water (seawater) that determines the minimum pressure in the condenser. Lower temperatures allow condensation at lower pressures which is favorable for power production in the steam turbine. This pressure also determines how low the pressure out of the turbine can be. For maximal power production, this pressure should be minimized because of increased enthalpy change through the turbine. For offshore installations it is not obvious that very low pressure in the condenser is favorable. Sub-atmospheric pressures are common, which imply huge steam expansions in the last part of the steam turbine. Among other things, this leads to increased size and weight on the turbine and condenser design. Therefore, it is not unlikely that a higher condenser pressure offshore is a good solution. Nevertheless, this needs to be examined further, because it is the total weight and size of the system that counts. Condenser pressure will also affect the HRSG design [13].

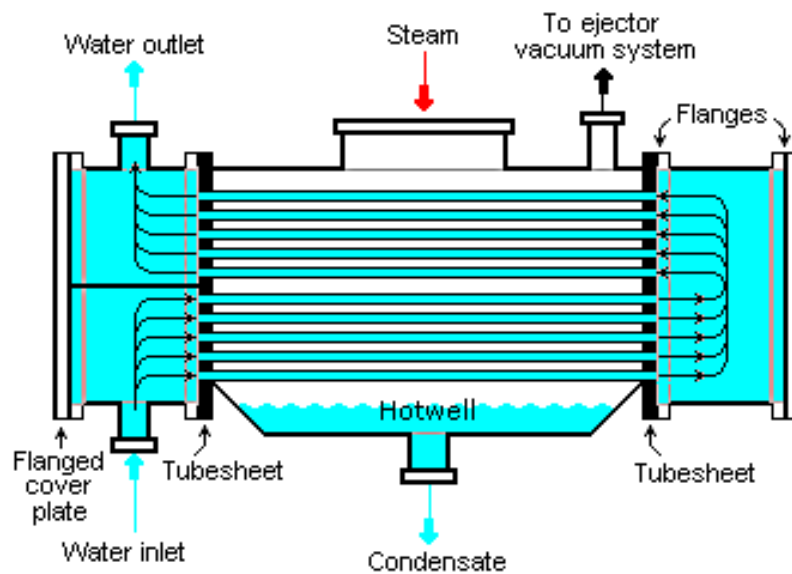


Figure A.3: Direct water cooling condenser [130]

### A.2.3 Pumps

There exists a lot of different pump designs that normally are divided into the two main categories positive displacement and centrifugal. Because pump design is not a huge part of this thesis, only the most relevant pumps will be introduced. On offshore installations the full range between small pumps circulating lubricants to big seawater lifting pumps are installed. The feedwater pump increasing the pressure in front of the HRSG is also one of the major pumps for cogeneration plants. This pump is normally an electric driven multistage centrifugal pump [38], see Figure A.4. Due to high increase in pressure, this pump will run under high temperatures. Therefore, cavitation and corrosion problems need to be examined. It is normal to have a backup pump installed for the most critical operations.

As mentioned earlier, varying power demand is expected offshore. It is therefore necessary to implement control systems for the pumps that are affected by these changes. The most common way to regulate a centrifugal pump is by a change in speed for the running motor. This will directly change the rotational speed of the shaft, which determines velocity/flow rate, pressure or elevation for the flow.

Under normal conditions, flow through the seawater pump is relatively constant and therefore easier to operate. Compared to the other pumps, the seawater lifting pump has a very high volumetric flow due to various cooling applications on the facility.

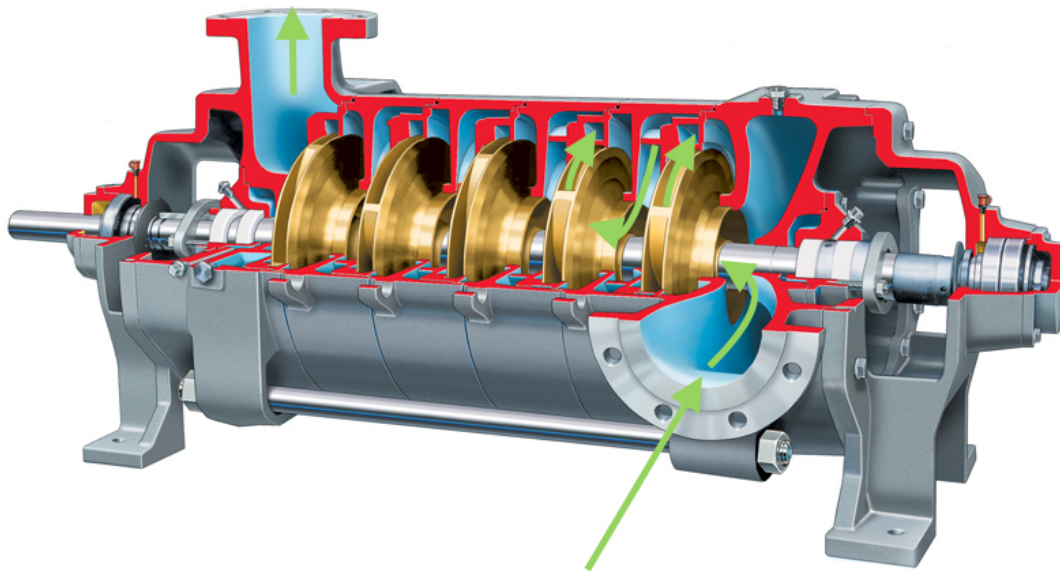


Figure A.4: Multistage centrifugal pump, where the flow pattern is indicated [131].

#### A.2.4 Deaeration

Deaerators perform the essential task of removing dissolved gases from the feedwater. Sources for dissolved gases are normally leakages into the system, very relevant for sub-atmospheric pressures, and raw makeup water. Oxygen is removed because of corrosion in the boiler tubes and dissolved  $\text{CO}_2$  lowers the pH level. Corrosive carbonic acid will also form in contact with water. Low pH levels are also a severe source of corrosion in the system, so gas removal is completely necessary for a lasting and healthy steam system. Dissolved gases is possible to remove chemically, but mechanical separation is more economical [28]. The most used process is called deaeration, and the major parts can be seen in Figure A.5. One last important reason for deaeration, is increased heat transfer in the HRSG. Dissolved gases would increase the thermal resistance by forming a film on the tube walls. This will make the HRSG less efficient because of reduced thermal efficiency (Heat transfer coefficient).

Two thermodynamic principles are built into the deaerator design, and helps to remove all non-condensable gases [28]:

- The solubility for a dissolved gas in a liquid decreases as its partial pressure above the liquid increases (Henry's Law).
- The solubility for a dissolved gas in a liquid decreases as the temperature is increased and approaches saturation temperature.

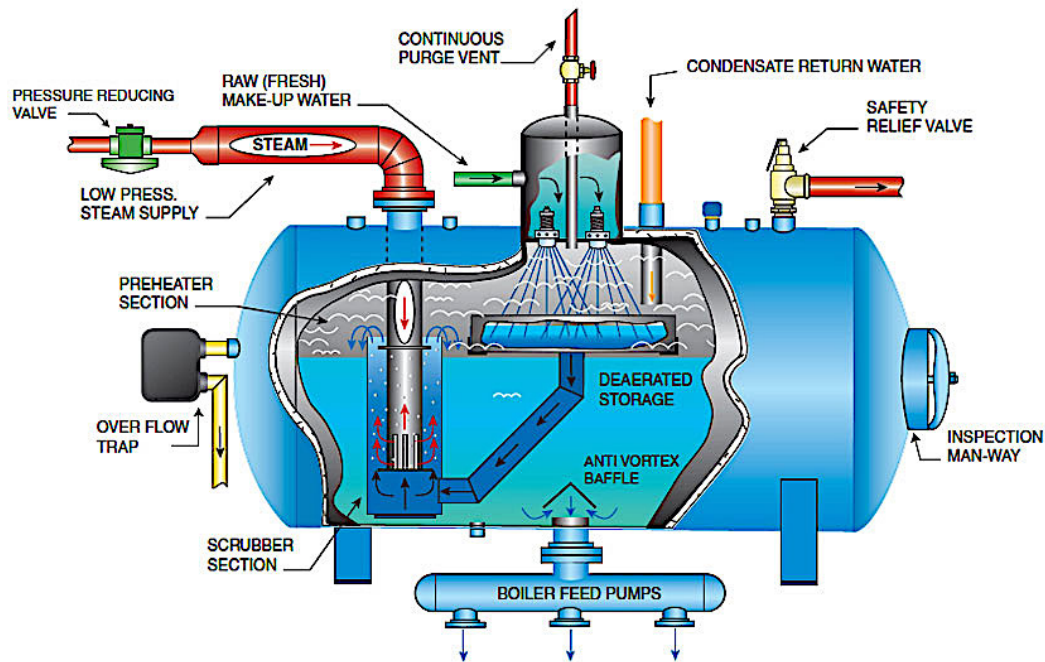


Figure A.5: Deaerator for removal of dissolved gases in the feedwater [132].

The physical processes start when feedwater/condensate is sprayed in thin films into vapor in the preheater section. Here the water is quickly heated to saturation for increased gas removal. Released gases can then flow freely through the purge vent, which is located at the top. The deaerator pressure is typically in the range between 0.2–1.2 bar [28]. Steam is injected into the deaerated water that is stored in the bottom to prevent re-absorption of gases.

For offshore facilities, deaeration is necessary for the same reasons as mentioned in this section. It is considered possible to build a deaerator inside the condenser, but the degree of total weight and size reduction are uncertain [133].

### A.2.5 Onshore Combined Cycle

The modern onshore combined cycle design can be seen in Fig. A.6. All the equipment mentioned in Chapter 3 and this Appendix can be seen here. This plant is a typical high efficiency plant for onshore operations. Therefore, is the offshore relevance limited, because weight and size is way too high. Regardless of this, the basic thermodynamic understanding is highly relevant. The TQ diagram for the HRSG can be seen in Fig. A.7.

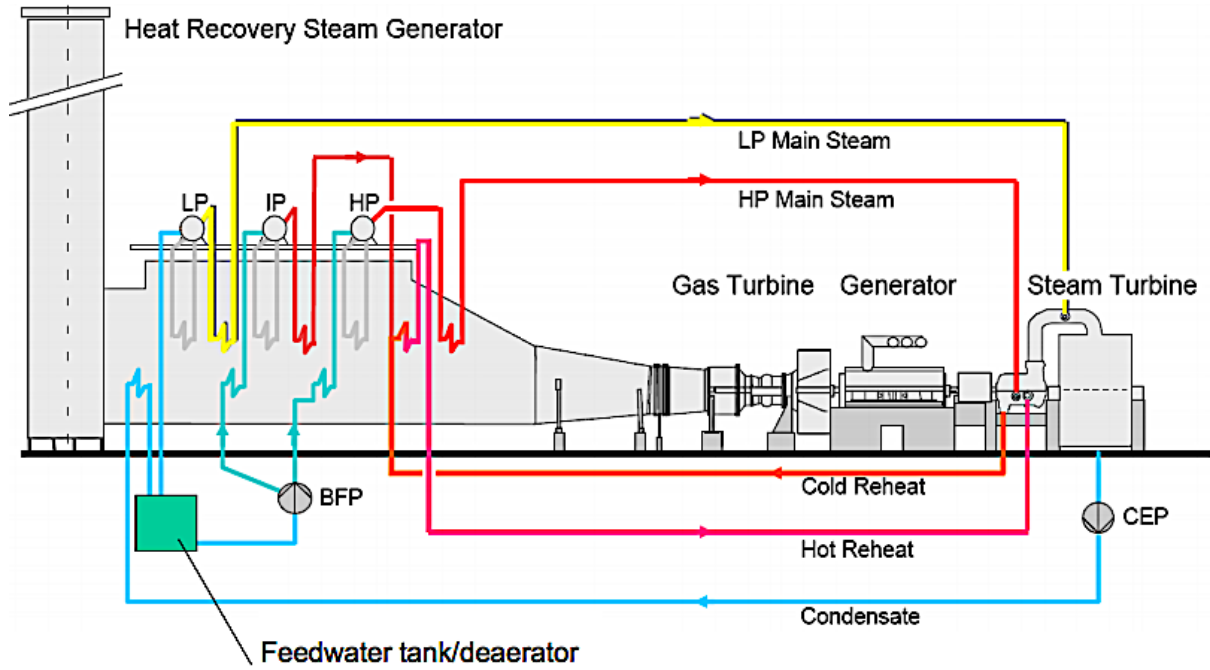


Figure A.6: Combined cycle with three pressure levels and reheat [28].

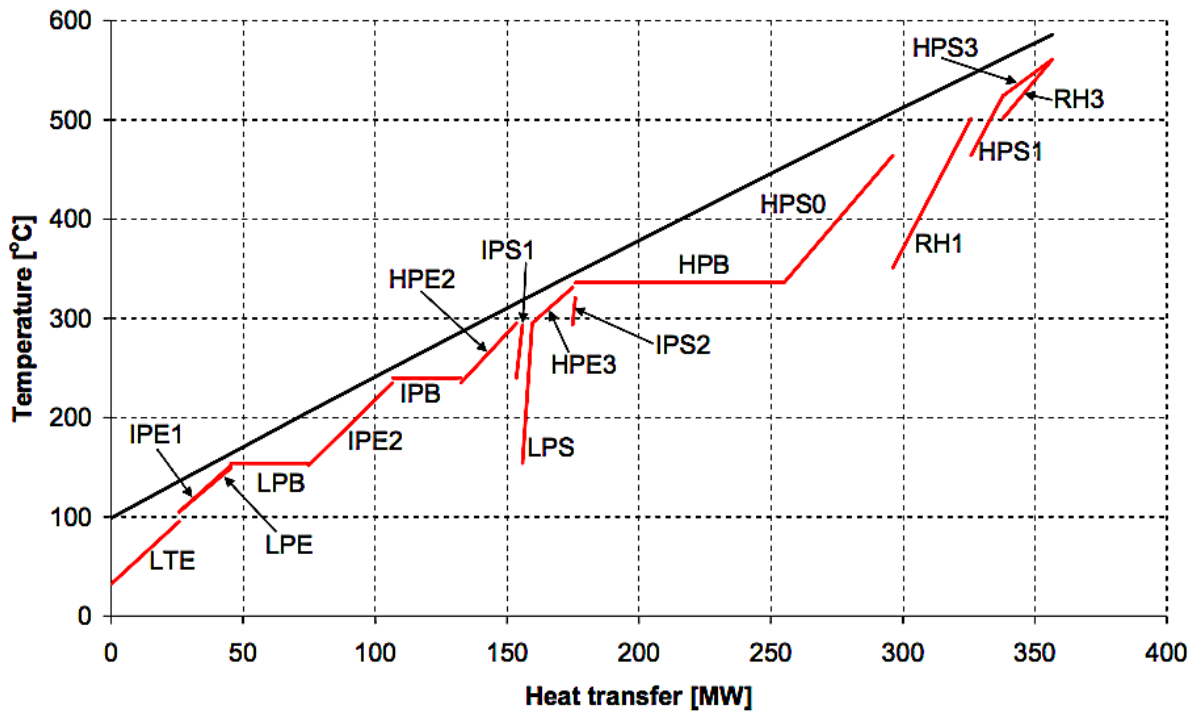


Figure A.7: TQ diagram for a HRSG with three pressure levels and reheat [28].

## A.3 Power Cycles

### A.3.1 Alternative Bottoming Cycles

Some alternative bottoming cycles have been investigated, here is a short introduction to some of them. The main motivation for alternatives to vapor as working medium is high heat of evaporation, which implies high exergy losses in the HRSG. This can be seen in Figure B.1 represented by the mismatch between exhaust gas and evaporator/superheater temperature lines. Another disadvantage with steam as the working medium is low saturation pressure out of the turbine (low temperatures) [28].

The disadvantages with steam cycles have in large extend been solved by introducing multiple pressure levels. This leads to a better match in the heat transfer between the steam and the gas turbine exhaust. This is observed from a better match in TQ diagram lines, see Figure A.7. This is also represented in the last plot in Figure 4.4. Other working mediums could still be very interesting with some technical development. Some alternative bottoming cycles [28] are listed below.

- Ammonia and water mixture.
  - For temperatures up to that of gas turbine exhaust.
- Halogenated hydrocarbons.
  - For low temperatures.
  - Disadvantages: Toxicity and ozone depletion.
- Alkanes.
  - For low temperatures like geothermal energy.
- Combined helium and CO<sub>2</sub>.
  - For high temperatures like gas turbine exhaust and nuclear reactors.
  - Closed Brayton cycles.
- CO<sub>2</sub> [134].
  - For low temperatures.
  - Rankine cycles.
- Air.
  - Open Brayton cycles with compressor intercooling.

## A.4 CO<sub>2</sub> Capture, Transport and Storage

### A.4.1 Shore Based Simulations

The National Energy Technology Laboratory in the US did some simulations on CO<sub>2</sub> capture in Aspen Plus and ThermoFlow's [19] GT PRO software [71]. Their combined cycle reference case (Case1) without CO<sub>2</sub> capture and is shown in Figure A.8. This plant is land based and get its cooling duty from a cooling tower. So these results and findings are not directly comparable with the offshore plant to be designed, however some good indicators can be found. The basic concepts are the same, and give a good foundation for understanding the challenges with a CO<sub>2</sub> capturing system. Figure A.9 shows the other case (Case2) with the capture system integrated.

In Table A.2 the biggest auxiliary loads are listed. It is the CO<sub>2</sub> compression and the amine (MEA) auxiliary system that contributes to the highest power consumptions for the CO<sub>2</sub> system. For the amine auxiliary system, it is the fan for controlling the back-pressure (BP) of the gas turbine that consumes more than 75% of the power. This fan can be seen as "Blower" in Figure 5.3.

In Table A.3 power outputs and requirements can be seen for the two cases with the same flow rate of natural gas. The auxiliary power requirement increased by about 460% with CO<sub>2</sub> capture, and is about 9.5% of the net power output.

Table A.2: Most significant auxiliary loads for both cases

Auxiliary		Case1	Case2
Boiler feedwater pumps	[MW]	2.72	2.71
Amine system auxiliaries	[MW]	-	16.4
CO <sub>2</sub> compression	[MW]	-	15.2
Circulating water pump	[MW]	2.30	4.36

Table A.3: Performance summary for both cases

Performance Summary		Case1	Case2
Gross power output	[MW]	564.7	511.0
Auxiliary power requirement	[MW]	9.620	44.21
Net power output	[MW]	555.1	466.8
Natural gas flow rate	$\left[\frac{kg}{s}\right]$	21.08	21.08
CO <sub>2</sub> capture	[%]	-	90.70



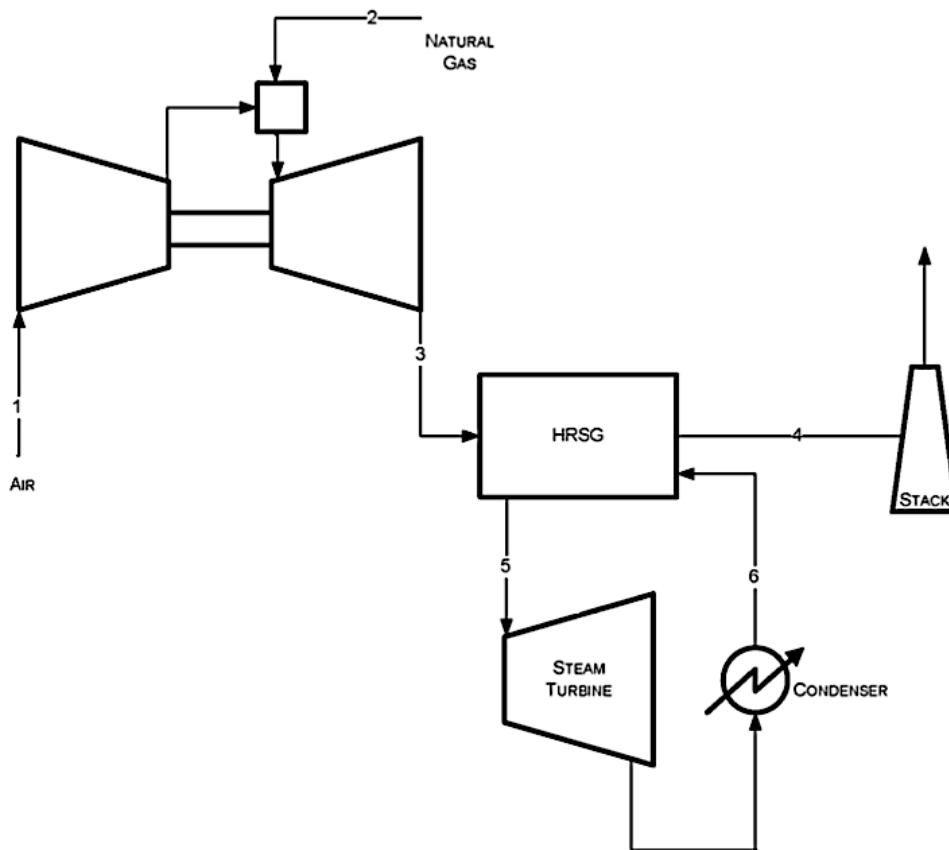


Figure A.8: Combined cycle without CO<sub>2</sub> capture [71]

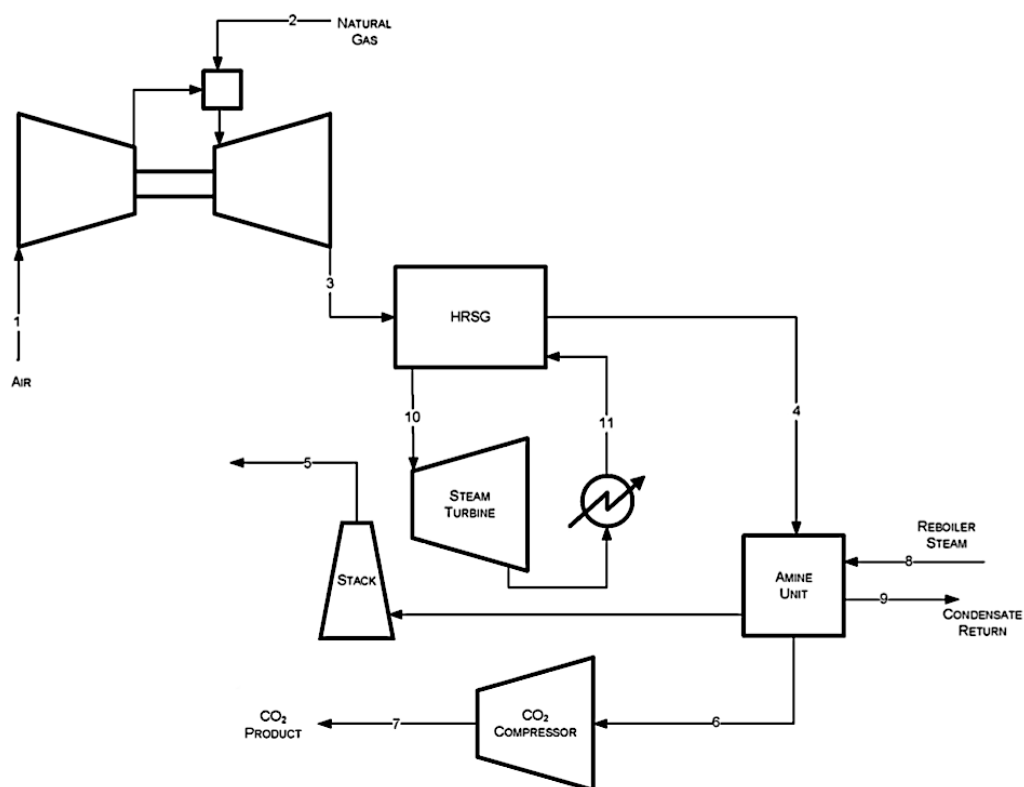


Figure A.9: Combined cycle with MEA based CO<sub>2</sub> capture [71]

## A.5 Mathematical Representation

### A.5.1 Scaling and Similitude

#### Coefficients for Axial Machines

For axial flow turbines, there are some dimensionless coefficients of great importance [135]. The first one is the flow coefficient,  $\phi$ , which is the absolute velocity divided by the mean peripheral speed of the blade.

$$\phi = \frac{c}{u} \quad (\text{A.1})$$

This coefficient gives an indication on the flow through the turbine. The second dimensionless coefficient is the stage loading coefficient or work coefficient,  $\Psi$ , which is the work,  $\omega$ , divided by the square of the peripheral speed.

$$\Psi = \frac{\omega}{u^2} \quad (\text{A.2})$$

The work coefficient is a measurement of the work done in a stage.

#### Incompressible Flow

When incompressible flows are considered, the flow coefficient can be expressed in terms of volumetric flow ( $Q$ ), rotational speed ( $N$ ), and rotor diameter ( $D$ ). It is used that  $c \propto \frac{Q}{D^2}$  and  $u \propto ND$ .

$$\phi_d = \frac{Q}{ND^3} \quad (\text{A.3})$$

The work coefficient can be expressed as the isentropic work divided by the square of rotational speed and diameter.

$$\psi_d = \frac{\omega}{N^2 D^2} \quad (\text{A.4})$$

The Reynolds number can be expressed as the product of rotational speed and diameter squared, divided by kinematic viscosity.

$$Re = \frac{\rho c D}{\mu} = \frac{\rho N D^2}{\mu} = \frac{N D^2}{\nu} \quad (\text{A.5})$$

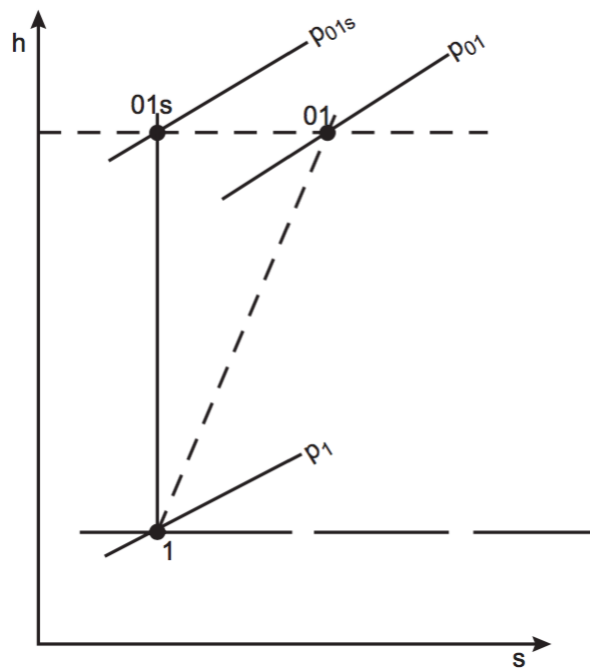


Figure A.10: h-s diagram for the stagnation states [136]

## Compressible Flow

### Stagnation Properties

If the fluid is compressible, large changes in flow velocity will occur. The fluid velocity represents an energy that is convenient to combine with the fluid enthalpy [136]. Together they are called the stagnation enthalpy.

$$h_0 = h + \frac{c^2}{2} \quad (\text{A.6})$$

Stagnation conditions is also represented for other properties like the pressure. In Fig. A.10, point 1 represent the actual or static state of a fluid, point 01 is the stagnation state, and 01<sub>s</sub> is the isentropic stagnation point.

$$p_0 = p + \frac{\rho V^2}{2} \quad (\text{A.7})$$

If perfect gas is assumed,

$$h = C_p T \quad (\text{A.8})$$

where,

$$C_p = \frac{\gamma R}{\gamma - 1} \quad (\text{A.9})$$

the stagnation temperature can be expressed as,

$$T_0 = T + \frac{1}{2} \frac{c^2}{C_p} \quad (\text{A.10})$$

or rewritten as

$$\frac{T_0}{T} = 1 + \frac{1}{2}(\gamma - 1) \frac{c^2}{\gamma RT} \quad (\text{A.11})$$

For compressible fluids, the Mach number plays an important role.

$$M = \frac{c}{a} = \frac{c}{\sqrt{\gamma RT}} \quad (\text{A.12})$$

Based on the definition of the Mach number and previous equations, stagnation temperature can be expressed as,

$$\frac{T_0}{T} = 1 + \frac{M^2}{2}(\gamma - 1) \quad (\text{A.13})$$

stagnation pressure,

$$\frac{P_0}{P} = \left( \frac{T_0}{T} \right)^{\frac{\gamma}{\gamma-1}} = \left( 1 + \frac{M^2}{2}(\gamma - 1) \right)^{\frac{\gamma}{\gamma-1}} \quad (\text{A.14})$$

and stagnation density.

$$\frac{\rho_0}{\rho} = \left( \frac{T_0}{T} \right)^{\frac{1}{\gamma-1}} = \left( 1 + \frac{M^2}{2}(\gamma - 1) \right)^{\frac{1}{\gamma-1}} \quad (\text{A.15})$$

In Fig. A.11, the ideal adiabatic change in stagnations conditions can be seen for a turbine.

$$\frac{T_{02s}}{T_{01}} = \left( \frac{P_{02}}{P_{01}} \right)^{\frac{\gamma}{\gamma-1}} \quad (\text{A.16})$$

The isentropic stagnation enthalpy can also be rewritten.

$$\Delta h_{0s} = C_p T_{01} \left[ \left( \frac{P_0}{P} \right)^{\frac{\gamma}{\gamma-1}} - 1 \right] \quad (\text{A.17})$$

## A.5.2 Performance Parameters

The performance parameters,  $\Delta h_{0s}$ ,  $\eta$  and  $P$ , for a compressible flow, are expressed as: [136]

$$\Delta h_{0s}, \eta, P = f(\mu, N, D, \dot{m}, \rho_{01}, a_{01}, \gamma) \quad (\text{A.18})$$

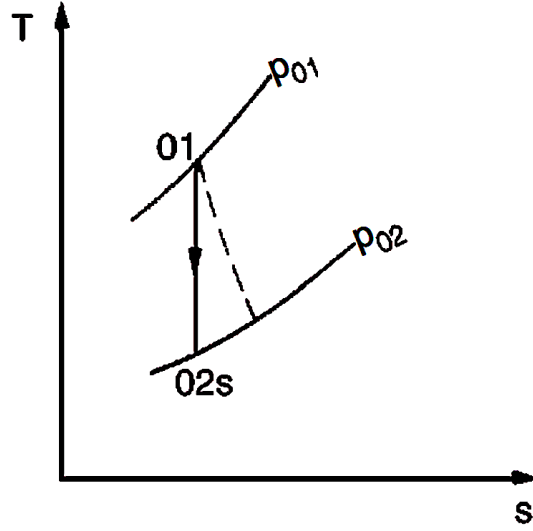


Figure A.11: Change in stagnation conditions across a turbine [136]

$\rho_0$  and  $a_0$  change through the turbomachine, therefore the inlet conditions denoted by subscript 1 is used. By choosing  $\rho_{01}$ ,  $N$  and  $D$  as the common factors, five dimensionless groups can be formed:

$$\frac{\Delta h_{0s}}{N^2 D^2}, \eta, \frac{P}{\rho_{01} N^3 D^5} = f \left( \frac{\dot{m}}{\rho_{01} N D^3}, \frac{\rho_{01} N D^2}{\mu}, \frac{N D}{a_{01}}, \gamma \right) \quad (\text{A.19})$$

Alternatively, the flow coefficient can be expressed as:

$$\phi = \frac{\dot{m}}{\rho_{01} N D^3} = \frac{\dot{m}}{\rho_{01} a_{01} D^2} \quad (\text{A.20})$$

Because  $u \propto ND$  and  $\frac{ND}{a_{01}}$  is regarded as a blade Mach number. The flow coefficient can be even more conveniently expressed as

$$\phi = \frac{\dot{m}}{\rho_{01} a_{01} D^2} = \frac{\dot{m} R T_{01}}{\rho_{01} \sqrt{\gamma R T_{01}} D^2} = \frac{\dot{m} \sqrt{R T_{01}}}{\rho_{01} \sqrt{\gamma} D^2} \quad (\text{A.21})$$

As:

$$\dot{m} \equiv \rho_{01} D^2 (ND) = \rho_{01} N D^3 \quad (\text{A.22})$$

The power produced from the turbine is given by

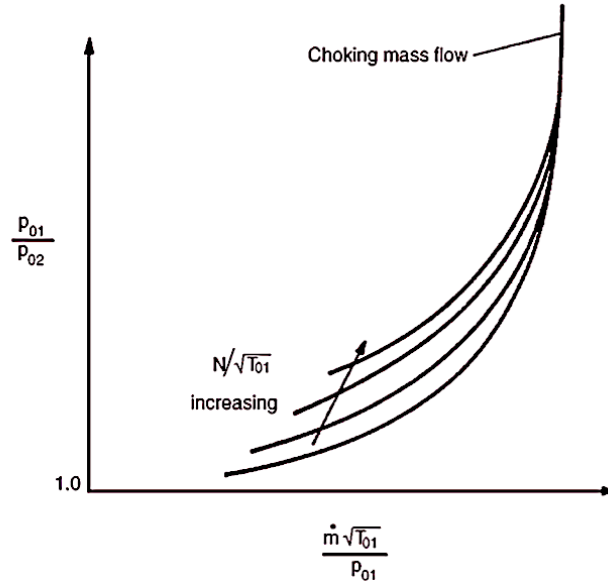


Figure A.12: Overall characteristic for turbines [136]

$$P = \dot{m} C_p \Delta T_0 \quad (\text{A.23})$$

The dimensionless power coefficient can then be expressed as:

$$\hat{P} = \frac{P}{\rho_{01} N^3 D^5} = \frac{\dot{m} C_p \Delta T_0}{[\rho_{01} D^2 (ND)] (ND)^2} = \frac{C_p \Delta T_0}{(ND)^2} \equiv \frac{\Delta T_0}{T_{01}} \quad (\text{A.24})$$

The non-dimensional groups, given by Eq. A.19, can then be expressed in the following way

$$\frac{p_{02}}{p_{01}}, \eta, \frac{\Delta T_0}{T_{01}} = f \left( \frac{\dot{m} \sqrt{RT_{01}}}{D^2 \rho_{01}}, \frac{ND}{RT_{01}}, Re, \gamma \right) \quad (\text{A.25})$$

if the turbine operates at high Reynolds numbers over a small speed range, further simplifications can be made. The overall characteristic of a operating turbine can be seen in Fig. A.12.

$$\frac{p_{02}}{p_{01}}, \eta, \frac{\Delta T_0}{T_{01}} = f \left( \frac{\dot{m} \sqrt{T_{01}}}{\rho_{01}}, \frac{N}{T_{01}} \right) \quad (\text{A.26})$$

# Appendix B

## Analytical Calculations

### Contents

B.1	Simplified Calculations for HRSG . . . . .	159
B.2	Heat Exchanger Design, Basis for Scaling . . . . .	162
B.2.1	Thermal Design of Shell and Tube Heat Exchanger . . . . .	163

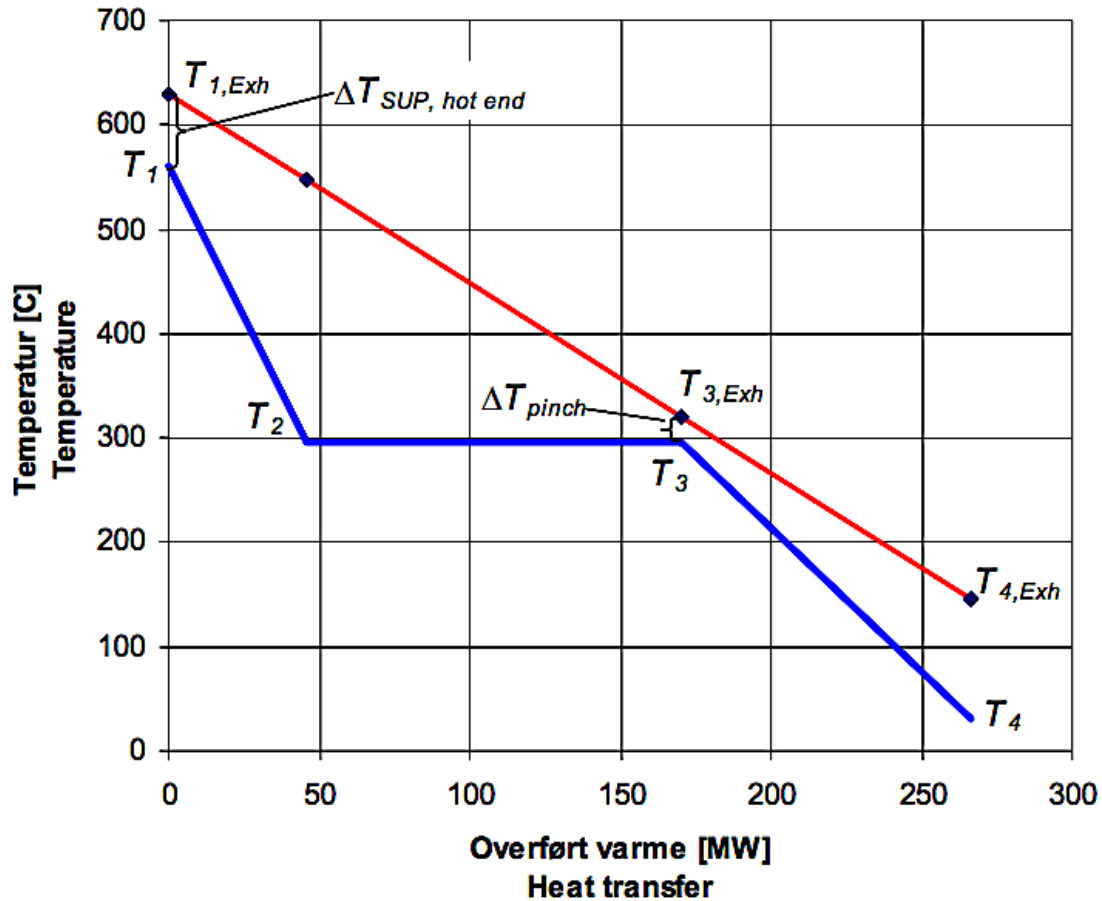


Figure B.1: TQ-diagram for HRSG [28]

## B.1 Simplified Calculations for HRSG

Steam is produced in the heat recovery steam generator, for better understanding of the different stages, see Figure B.1. The following equations gives thermodynamic restrictions on temperature differences, exhaust outlet temperature and steam production in a HRSG.

The smallest temperature difference in the HRSG is called  $\Delta T_{pinch}$ . For combined cycles with gas turbines as topping cycle, this is normally found in the evaporator (EVA) inlet, see Figure B.1. The procedure for calculations on a HRSG with one pressure level can take this form:

- Choose the wanted steam pressure out of the superheater (SUP),  $P_{steam}$ . This is the steam going to your process, and has to be chosen according to the application. Assume same pressure in evaporator (EVA),  $P_{EVA}$ .

$$P_{EVA} = P_1 = P_2 = P_3$$

- A steam table can be used to find the saturation temperature,  $T_{sat}$ , in the EVA. This temperature is determined from the pressure, some saturation temperatures are collected in Table C.5.

$$T_{sat} = T(P_{sat}) = T(P_{EVA}) = T_2 = T_3 = T_{EVA}$$



- Choose  $\Delta T_{pinch}$ . Normally in the range 8–20K, higher for offshore applications.

- Calculate the exhaust temperature between the EVA and the economizer (ECO).

$$T_{3,Exh} = T_3 + \Delta T_{pinch}.$$

- Choose the temperature difference on the hot end of the HRSG,  $\Delta T_{SUP,hot}$ , to find  $T_1$ . Normally in the range 20–40K.

$$\Delta T_{SUP,hot} = T_{1,Exh} - T_1$$

$$\implies T_1 = T_{1,Exh} - \Delta T_{SUP,hot}.$$

- If the calculated  $T_1$  is higher than the allowed steam temperature for the chosen application, change  $T_1$  to the maximum allowed steam temperature.

- Find the steam enthalpy for this temperature,  $h_1 = h(T_1, P_1)$ . This is the enthalpy for the steam leaving the SUP.

- Find the saturated water enthalpy for the EVA, this is the enthalpy for the water entering the EVA.

$$h_3 = h(P_{EVA}) = h(P_3).$$

- This is not very accurate, because  $T_3$  normally is 2–10K below  $T_{sat}$ . A better approximation is to use the enthalpy for the ECO outlet, which is subcooled water.

- Calculate the steam flow rate,  $\dot{m}_{steam}$ , by using Eqs. 7.2 and 7.10 between the steam outlet/exhaust inlet and the location of the pinch point, this is from stage 1 to 3.

$$\frac{dE_{CV}}{dt} = \dot{Q}_{CV} - \dot{W}_{CV} + \sum_i \dot{m}_i \left( h + \frac{1}{2}v^2 + gz \right)_i - \sum_e \dot{m}_e \left( h + \frac{1}{2}v^2 + gz \right)_e$$

$$0 = 0 - 0 + \sum_i \dot{m}_i(h)_i - \sum_e \dot{m}_e(h)_e$$

$$\sum_i \dot{m}_i(h)_i = \sum_e \dot{m}_e(h)_e$$

$$\dot{m}_{steam}h_3 + \dot{m}_{Exh}h_{1,Exh} = \dot{m}_{steam}h_1 + \dot{m}_{steam}h_{3,Exh}$$

$$\dot{m}_{steam}(h_1 - h_3) = \dot{m}_{Exh}(h_{1,Exh} - h_{3,Exh})$$

Assume constant  $c_p$  for the exhaust.

$$\Delta h_{Exh} = c_{p,Exh} \Delta T_{Exh}$$

$$\dot{m}_{steam}(h_1 - h_3) = \dot{m}_{Exh}(h_{1,Exh} - h_{3,Exh})$$

$$\dot{m}_{steam}(h_1 - h_3) = \dot{m}_{Exh}c_{p,Exh}\Delta T_{Exh}$$

$$\dot{m}_{steam} = \frac{\dot{m}_{Exh}c_{p,Exh}\Delta T_{Exh}}{(h_1 - h_3)}$$

This is the maximum steam production for the chosen values in the HRSG.

- Find the enthalpy for water entering the ECO, this is stage 4.

$$h_4 = h_4 = h(T_4, P_{ECO}) = h(T_4, P_4)$$

- Calculate the exit temperature of the exhaust gas,  $T_{4,Exh}$ , by using Eqs. 7.2 and 7.10 between the steam outlet/exhaust inlet and the steam inlet/exhaust outlet, this is from stage 1 to 4.

$$\dot{m}_{steam}h_4 + \dot{m}_{Exh}h_{1,Exh} = \dot{m}_{steam}h_1 + \dot{m}_{steam}h_{4,Exh}$$

$$\dot{m}_{steam}(h_1 - h_4) = \dot{m}_{Exh}(h_{1,Exh} - h_{4,Exh})$$

$$\dot{m}_{steam}(h_1 - h_4) = \dot{m}_{Exh}c_{p,Exh}\Delta T_{Exh} = \dot{m}_{Exh}c_{p,Exh}(T_{1,Exh} - T_{4,Exh})$$

$$T_{4,Exh} = T_{1,Exh} - \frac{\dot{m}_{steam}(h_1 - h_4)}{\dot{m}_{Exh}c_{p,Exh}}$$

In the case considered in this thesis we start with this value, but the same principles apply. The calculations can be reversed and e.g. steam production can be calculated based on this value and the other choices made in the above calculations.

## B.2 Heat Exchanger Design, Basis for Scaling

Some major aspects are important when designing a heat exchanger [137]:

- Minimize heat transfer area, number of heat exchangers, and footprint/size.
  - Reduce capital cost and weight.
- Simple tube arrangement and control systems.
  - Reduce pressure loss for less pump work. High velocities gives more turbulence, which leads to higher heat transfer and larger pressure drops.
  - Easy to operate.
- Maximize energy recovery.
  - Higher heat recovery demands small temperature differences, which implies large heat transfer area.

These aspects counteract each other, therefore is optimization necessary to find the best design in each case. Some aspects that are important to increase efficiency:

- Do not mix streams with large temperature differences.
- Reduce heat transfer to surroundings.

In terms of heat exchange, the value of each stream is given by the exergy ( $E$ ), see Eq. 7.4, and is given by:

$$E = h - T_0s \quad (\text{B.1})$$

$h$  is the enthalpy,  $T_0$  is the surrounding temperature and  $s$  is the entropy. Exergy is the maximum energy that can be transferred to mechanical energy. It is reduced due to heat transportation between different temperatures and friction in e.g. tubes, turbines etc. The loss between temperatures  $T_1$  and  $T_2$  is:

$$\Delta E = Q \frac{T_1 - T_2}{T_1 T_2} T_0 \quad (\text{B.2})$$

For each case, there are some important factors that needs to be considered in terms of geometry and materials:

- Fouling.
- Corrosion.
- Temperature range.
- Pressure.
- Importance of compactness/Size.
- Price.

### B.2.1 Thermal Design of Shell and Tube Heat Exchanger

Shell and tube heat exchangers are the most used type on the Norwegian continental shelf. In this section some basic design calculations will be made for a specific case:

Material and Type:

- Titanium. Fixed tubesheet, see Figure 7.1.

Fluids, given values:

- Shell: Gas,  $c_{p,s} = 2290 \frac{J}{kgK}$ .  $P_{s,in} = 7$  bar.  $T_{s,in} = 111^\circ C$ .  $T_{s,out} = 30^\circ C$ .  $\dot{m}_s = 24.6 \frac{kg}{s}$ .  
Maximum pressure drop:  $\Delta P_s = 1$  bar.
- Tube: Water,  $c_{p,t} = 4200 \frac{J}{kgK}$ .  $T_{t,in} = 10^\circ C$ .  $\dot{m}_t = 50 \frac{kg}{s}$ .

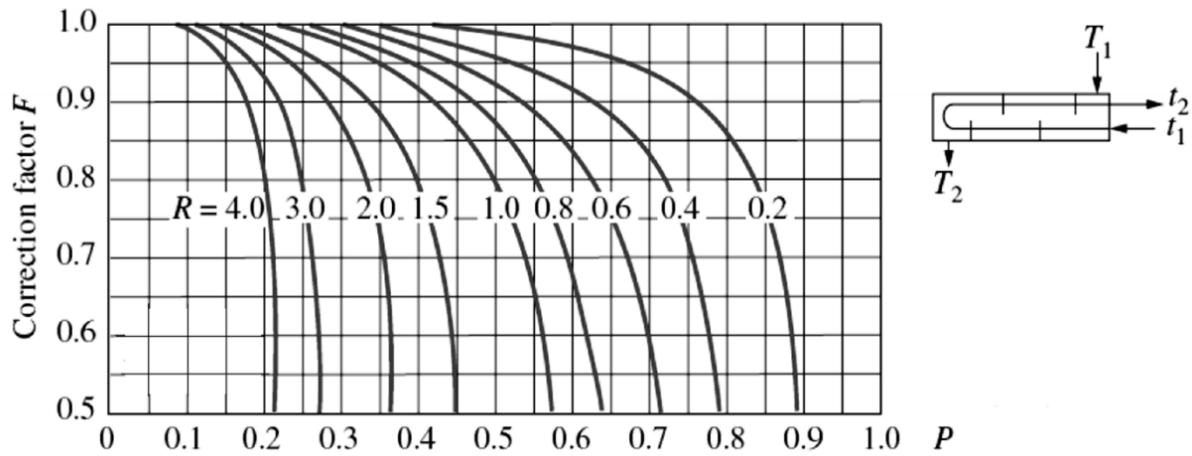
First is the transferred heat (Q) determined:

$$Q = \dot{m}_s c_{p,s} (T_{s,in} - T_{s,out}) = \dot{m}_t c_{p,t} (T_{t,out} - T_{t,in}) = 4.536 \text{ MW}$$

This can be used to find the outlet temperature for the water:

$$T_{t,out} = 31.8^\circ C$$

Then it is possible to use what is known as the LMTD method:

Figure B.2: Correction factor,  $F=F(P,R)$  [138].

$$LMTD = \frac{\Delta T_A - \Delta T_B}{\ln\left(\frac{\Delta T_A}{\Delta T_B}\right)} = 43.0\text{K}$$

Correction factor  $F$ :

$$P = \frac{T_{t,out} - T_{t,in}}{T_{s,in} - T_{t,in}} = 0.22$$

$$R = \frac{\dot{m}_t c_{p,t}}{\dot{m}_s c_{p,s}} = 3.37$$

From Figure B.2:

$$F = F(P, R) = F(0.22, 3.37) = 0.8$$

$$Q = UA \cdot F \cdot LMTD$$

$$U_0 A_0 = \frac{Q}{F \cdot LMTD} = 132.6 \frac{\text{kW}}{\text{K}}$$

Further calculations can be made with simulation tools like NTUEx [137]. Some provisional values can be made without simulations:

Selecting four tube passes with 19 mm tube diameter. Few passes give low velocities, pressure drop and heat transfer. All these parameters will be relatively high for many passes. Tiny diameters give compact heat exchangers, but they are sensitive to vibrations. 19 mm is the smallest diameter that can be mechanically cleaned, and is because of safety requirements the minimum diameter used on the Norwegian continental shelf [137].

Tube thickness is determined by standards, pressure and corrosion. For carbon steel:

- $D_o \in [8,12.1]$  mm  $\rightarrow \tau_w = 1.5$  mm
- $D_o \in [14,20]$  mm  $\rightarrow \tau_w = 2.0$  mm
- $D_o \geq 22$  mm  $\rightarrow \tau_w = 2.5$  mm

If stainless steel or copper are used, the thickness is reduced by 0.5 mm. If the environment is very corrosive or the pressure is high, the diameter is increased.

In this case with titanium,  $\tau_w = 1.5$  mm, is chosen.

To estimate the heat transferring area, it is necessary to find U. From data or experience data:

Wall:  $k_w$  Inner tube:  $h_i$  and coating if necessary,  $R_i$ . Outer tube:  $h_o$  and coating if necessary,  $R_o$ .

$$U = \left[ \frac{1}{h_o} + R_o + \frac{D_o}{2k_w} \ln \left( \frac{D_o}{D_i} \right) + \frac{D_o}{D_i} \left( \frac{1}{h_i} + R_i \right) \right]^{-1}$$

Titanium walls:  $k_w = 18 \frac{W}{mK}$

From experience table:

Gas:  $P = 7$  bar  $\rightarrow h_o = 250-400 \frac{W}{m^2K}$

Water:  $h_i = 5000 \frac{W}{m^2K}$

Almost all of the resistance is on the gas side, for this first estimate:

$$\frac{1}{h_o} \gg R_o, \frac{D_o}{2k_w} \ln \left( \frac{D_o}{D_i} \right), \frac{D_o}{D_i} \left( \frac{1}{h_i} + R_i \right)$$

$$U_0 \approx h_o \approx 300 \frac{W}{m^2K}$$

$$A_0 = \frac{A_0 U_0}{U_0} = 442 \text{ m}^2$$

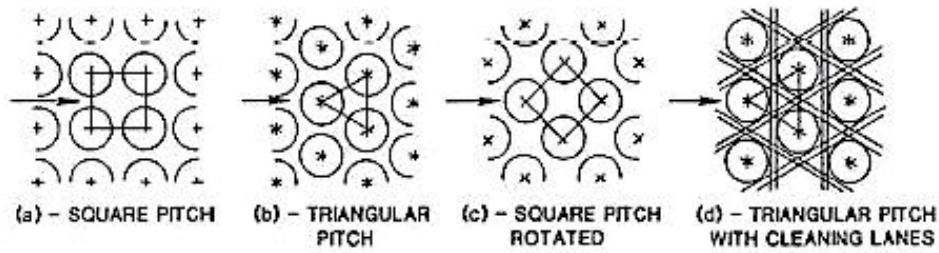


Figure B.3: Common tube layouts for shell and tube heat exchangers [139]

At this stage we can choose the dimension parameter:  $\frac{L_{shell}}{D_{shell}} = \frac{L}{D_s}$

The cost/price is reduced if this parameter is increased with the same heat transferring area.

$$\frac{L}{D_s} \in [3, 15]$$

Tube layout is the next step to consider, see Figure B.3. Layout (b) has the highest  $h$  and  $\Delta P$  and is not possible to clean mechanically. Compactness is the great advantage compared to design (a), which has lower  $h$  and  $\Delta P$ . This design can together with (c) and (d) be mechanically cleaned. Layout (c) has lower  $h$  and  $\Delta P$  compared to (a), and is less compact than (b).

Pitch ratio =  $\frac{\text{Tubedistance}}{\text{Tubediameter}}$ . This ratio is normally in the range: [1.25,1.5]. Low values indicate large  $\Delta P$  and  $h$ , less heat exchanger volume and difficulties with mechanical cleaning.

For the remaining calculations the following values are chosen:  $\frac{L}{D_s} = 6$ , tube layout: triangular pitch (30°), pitch ratio = 1.25

Then it is possible to use this relation:

$$A_{0,fig} = A_0 \cdot F_1 \cdot F_2 \cdot F_3$$

$F_1 = 1.0$ ,  $D = 19$  mm, pitch = 1.25,  $D \cdot \text{pitch} = 23.8$  mm. See Figure B.6.

$F_2 = 1.08$ , tube passes = 4,  $D_{shell} = 0.89\text{--}1.14$  m. See Figure B.7.

$F_3 = 1.0$ , fixed tubesheet. See Figure B.8.

$$A_{0,fig} = 477 \text{ m}^2$$

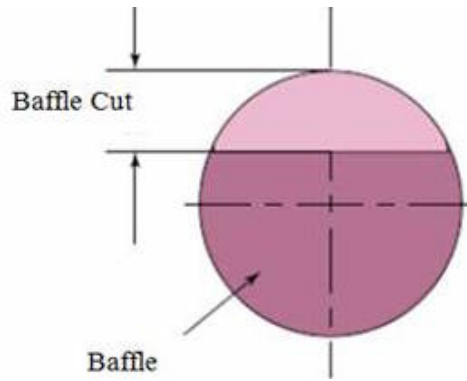


Figure B.4: Baffle cut.

From Figure B.5  $\frac{L}{D_s} = 6 \rightarrow L = 6 \text{ m}, D_s = 1 \text{ m}$

Then it is time to choose the distance between baffles, the baffle cut (Fig. B.4), and if sealing strips are necessary. Sealing strips prevent leakage flows between the tube bank and the shell, baffles etc. This will increase the weight and cost of the heat exchanger.

Here the chosen baffle distance is 0.6 m (Maximum distance is  $D_s$ ), baffle cut is 28% and no sealing strips are used. Putting these values into a program like NTUEx:

$$\Delta P = 1.89 \text{ bar}, U_1 = 663 \frac{\text{W}}{\text{m}^2\text{K}}, h_o = 898 \frac{\text{W}}{\text{m}^2\text{K}}, h_i = 3896 \frac{\text{W}}{\text{m}^2\text{K}}$$

$$\text{Area: } A_1 = 451.2 \text{ m}^2. \text{ Temperature: } T_{s,out} = 22.3^\circ\text{C}. U_1 A_1 = 299.1 \frac{\text{kW}}{\text{m}^2\text{K}}$$

$$\text{Volume: } V_1 = \frac{\pi}{4} \cdot D_s^2 \cdot L = 4.71 \text{ m}^3$$

This first design does not meet the specifications:  $\Delta P > 1 \text{ bar}$ . From LMTD:  $U_0 A_0 = 132.6 \frac{\text{kW}}{\text{m}^2\text{K}}$ .  $\Delta P$  needs to be reduced with about 48%, and UA with 56%. Assume that U is constant, which implies a reduction in area.

Reduction in  $\Delta P$ :

- Shorter heat exchanger.
- Larger shell diameter.
- Longer distance between baffles.
- Allow small shell leakages / No sealing strips.



Reduction in A:

- Shorter heat exchanger.
- Smaller shell diameter.
- Allow small shell leakages / No sealing strips.

Choosing a new values:  $L = 4.0$  m,  $D_s = 0.82$  m

Volume:  $V_2 = 2.11$  m<sup>3</sup>

Baffle distance: 0.8 m, baffle cut: 36%.

New calculations with NTU<sub>EX</sub> [137]:

- $\Delta P = 0.9$  bar
- $U = 642 \frac{W}{m^2K}$
- $A = 184.6$  m<sup>2</sup>
- $T_{s,out} = 31.6$  °C
- $UA = 118.0 \frac{kW}{m^2K}$

$T_{s,out} > 30^\circ\text{C}$ . This can be corrected with sealing strips. New NTU<sub>EX</sub> calculations:

- $\Delta P = 1.0$  bar
- $U = 738 \frac{W}{m^2K}$
- $A = 184.6$  m<sup>2</sup>
- $T_{s,out} = 29.0$  °C
- $UA = 136.2 \frac{kW}{m^2K}$

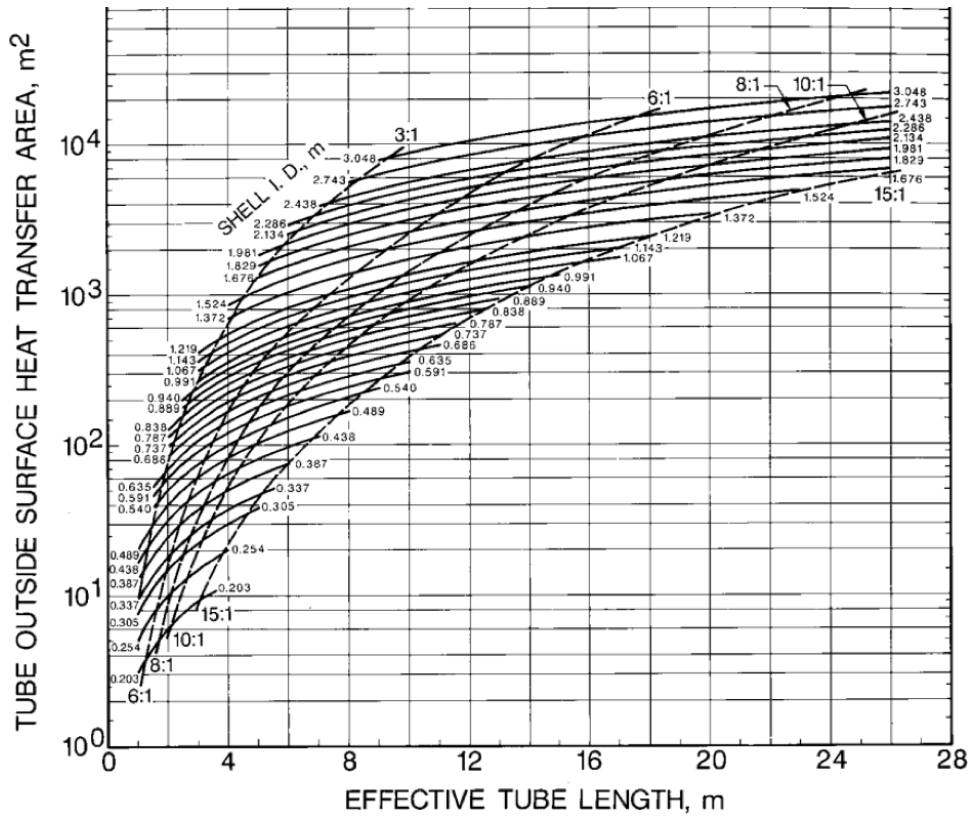


Figure B.5: Effective tube length from heat transfer area [138].

Tube Outside Diameter, in. (mm)	Tube Pitch, in. (mm)	Layout	F <sub>1</sub>
5/8 (15.88)	13/16 (20.6)	→ ◁	0.90
5/8 (15.88)	13/16 (20.6)	→ ◊ ◻	1.04
3/4 (19.05)	15/16 (23.8)	→ ◁	1.00
3/4 (19.05)	15/16 (23.8)	→ ◊ ◻	1.16
3/4 (19.05)	1 (25.4)	→ ◁	1.14
3/4 (19.05)	1 (25.4)	→ ◊ ◻	1.31
1 (25.4)	1 1/4 (31.8)	→ ◁	1.34
1 (25.4)	1 1/4 (31.8)	→ ◊ ◻	1.54

Figure B.6: Values of F<sub>1</sub> [138]

Inside Shell Diameter, in. (mm)	F <sub>2</sub> Number of Tube-Side Passes			
	2	4	6	8
Up to 12 (305)	1.20	1.40	1.80	—
13 1/4 to 17 1/4 (337 to 438)	1.06	1.18	1.25	1.50
19 1/4 to 23 1/4 (489 to 591)	1.04	1.14	1.19	1.35
25 to 33 (635 to 838)	1.03	1.12	1.16	1.20
35 to 45 (889 to 1143)	1.02	1.08	1.12	1.16
48 to 60 (1219 to 1524)	1.02	1.05	1.08	1.12
Above 60 (above 1524)	1.01	1.03	1.04	1.06

<sup>a</sup> Since U-tube bundles must always have at least two passes, use of this table is essential for U-tube bundle estimation. Most floating head bundles also require an even number of passes.

Source: Schlünder, E.U., Ed., *Heat Exchanger Design Handbook*, Begell House, New York, 1985. With permission.

Figure B.7: Values of F<sub>2</sub> [138]

TABLE 4.5.12 F<sub>3</sub> for Various Tube Bundle Constructions

Type of Tube Bundle Construction	F <sub>3</sub> Inside Shell Diameter, in. (mm)				
	Up to 12 (305)	13–22 (330–559)	23–36 (584–914)	37–48 (940–1219)	Above 48 (1219)
Split backing ring (TEMA S)	1.30	1.15	1.09	1.06	1.04
Outside packed floating heat (TEMA P)	1.30	1.15	1.09	1.06	1.04
U-Tube* (TEMA U)	1.12	1.08	1.03	1.01	1.01
Pull-through floating head (TEMA T)	—	1.40	1.25	1.18	1.15

<sup>a</sup> Since U-tube bundles must always have at least two tube-side passes, it is essential to use Table 4.5.11 also for this configuration.

Source: Schlünder, E.U., Ed., *Heat Exchanger Design Handbook*, Begell House, New York, 1983. With permission.

Figure B.8: Values of F<sub>3</sub> [138]

# Appendix C

## Additional Analysis, Figures and Tables

### Contents

C.1	Real Gas Turbine Weight Data – Scaling . . . . .	171
C.2	Airplane Engines Weight . . . . .	175
C.3	GT PRO – Model 1 . . . . .	179
C.4	GT PRO – Model 2 . . . . .	183
C.5	GT PRO – Model 3 . . . . .	188
C.6	GT PRO – Additional Figures for Scaling Laws . . . . .	195
C.6.1	Model 1 . . . . .	195
C.6.2	Model 2 . . . . .	196
C.7	Multivariate Polynomial Approach – Project Work Weight Estimation . . . . .	197
C.8	Large Tables . . . . .	204

## C.1 Real Gas Turbine Weight Data - Scaling

### Solar - Skid Weight

These weights are defined, and include among other components: Gas turbine, gearbox, generator and systems for startup, control and lubrication [140]. The Solar skid weight is suggesting a linear relationship, see Fig. C.1.

Table C.1: Solar skid weight for generator set.

Turbine	Weight [ton]	Flow [ $\frac{kg}{s}$ ]	Power [MW]
Saturn 20	9.98	6.5	1.2
Centaur 40	32.6	18.6	3.5
Centaur 50	32.7	19.1	4.6
Taurus 60	32.8	21.9	5.5
Taurus 70	45.7	26.9	7.5
Mars 90	64.7	40.2	9.5
Titan 130	74.4	49.7	14.0

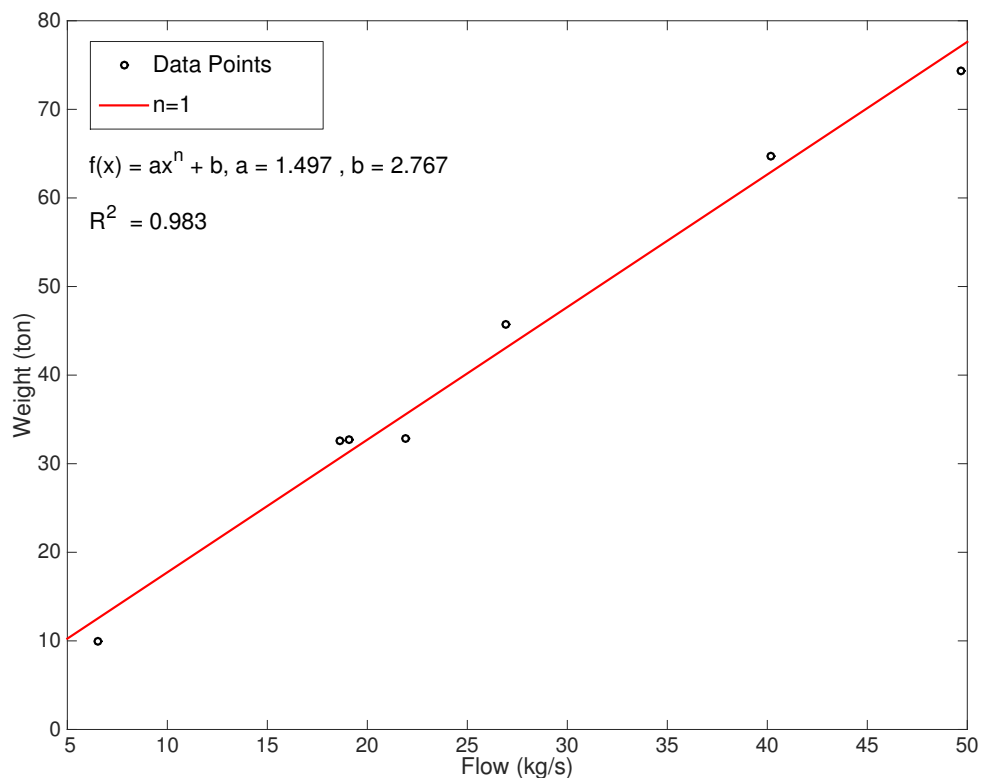


Figure C.1: Skid weight, Solar turbines.

### Power Engineering International

A large gas turbine overview is made by Power Engineering International (PEi) [141]. The weights are not clearly defined in terms of which components that are considered. When the weight data is compared with other sources, it is most likely skid weights, including the generator. Mass flow is not given for all the turbines listed. Therefore, is most of this analysis based on scaling in terms of power. According to the "GE Gas Turbine Design Philosophy" [93] and Table 6.2, the scaling relationship should be the same for power and mass flow. This is tested for some of the manufacturers.

The Solar turbines fit the  $W \propto P^{\frac{3}{2}}$  relationship with high accuracy, see Fig. C.2. For the heavy duty gas turbines from Mitsubishi, a almost perfect linear relationship between weight and power is obtained, see Fig. C.3.

From Fig. C.4, it is observed that the General Electric turbines fit the relationship  $W \propto P^{\frac{3}{2}}$  almost perfectly. This correspond accurately to the GE paper [93] predictions. Surprisingly, this is not the case when mass flow is considered. In this case, see Fig. C.5, the analysis suggest that a linear relationship is the best fit. This is strongly supporting the relationship,  $W \propto \dot{m}$ , when realistic, ready to install, turbines are considered. The isolated turbine assembly weight is of limited relevance for the final steam bottoming cycle.

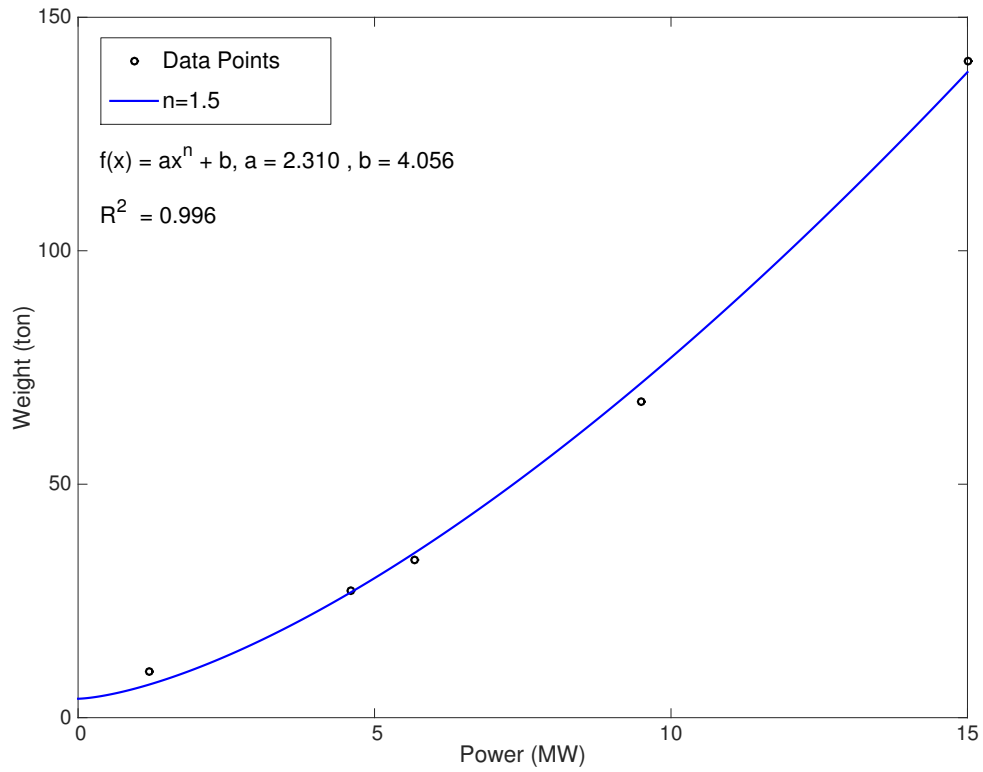


Figure C.2: Solar turbines: Saturn 20, Centaur 50, Taurus 60 and Titan 130 varying with power.

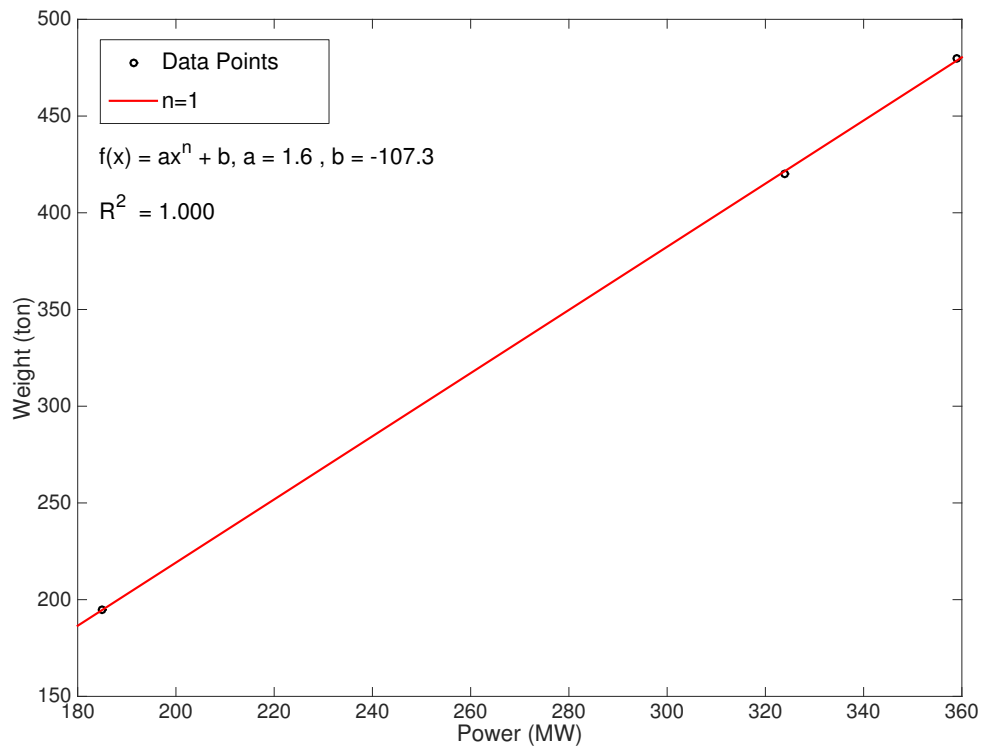


Figure C.3: Mitsubishi heavy duty turbines: M501F3 - M701F4 - M701F5 varying with power.

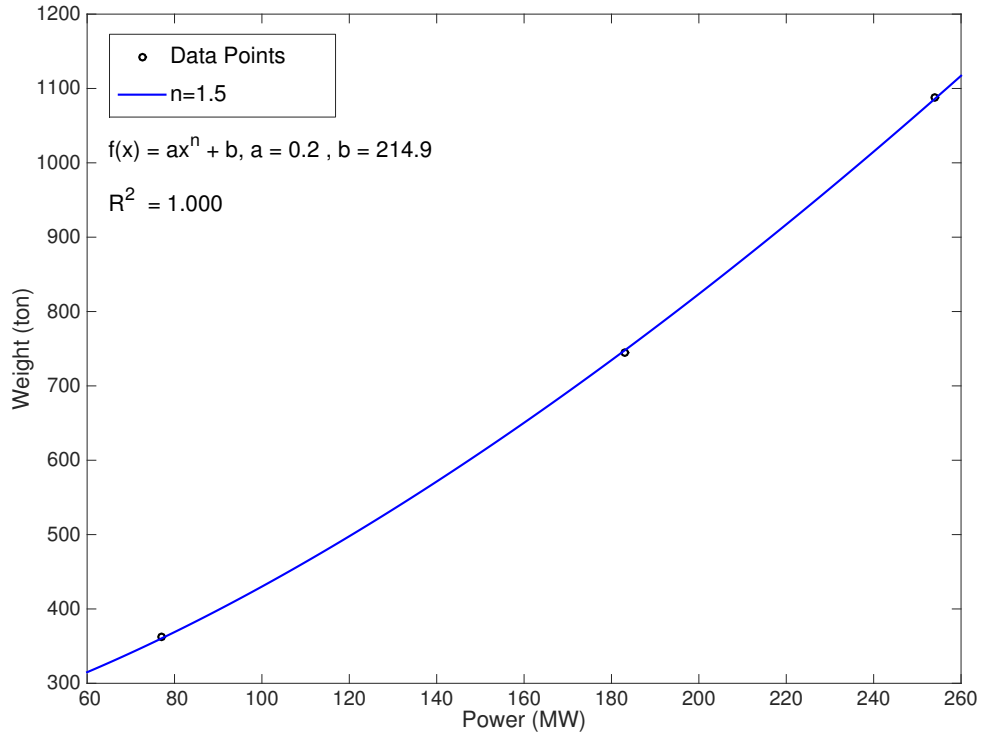


Figure C.4: GE turbines: 106FA - 107FA - 109FA varying with power.

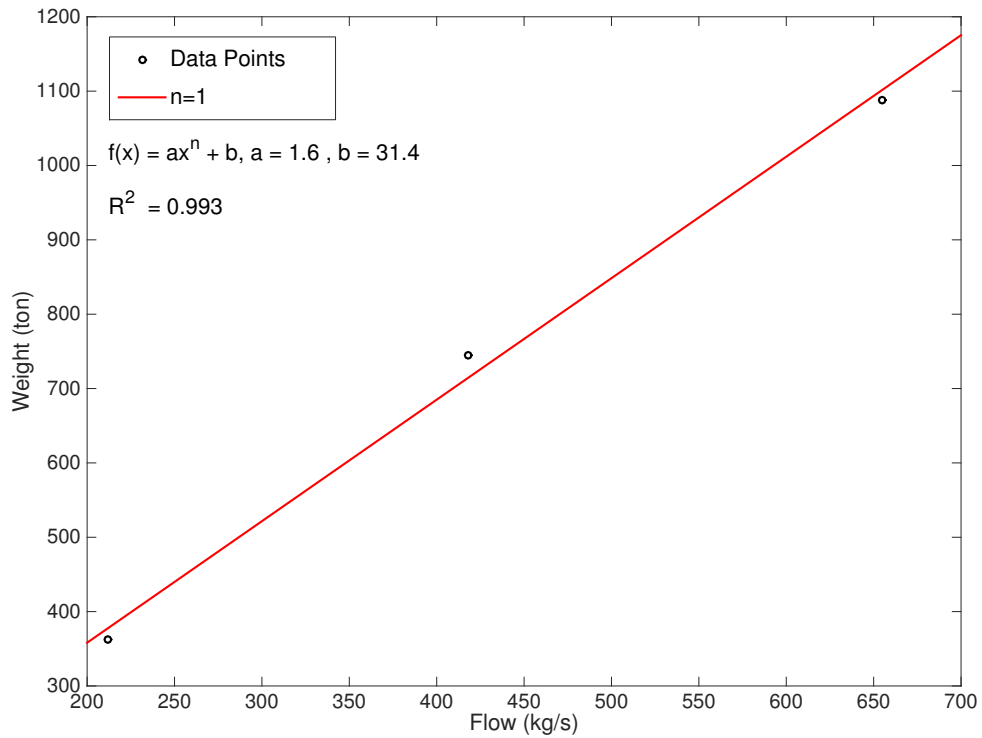


Figure C.5: GE turbines: 106FA - 107FA - 109FA varying with mass flow.

## C.2 Airplane Engines Weight

Aeroderivative gas turbines are highly relevant for offshore implementation. Some engine weight data is available from E. M. Greitzer's work on aerodynamics, see Table C.2 [142]. These engines are not scaled versions of each other, still they are following a very clear trend in terms of weight. This is most likely due to the fact that every airplane engine of this type is designed for minimum weight. From Fig. C.6 – C.9 it is observed that the design is quite similar across different manufactures and models.

From F. Whittle's statement and Fig. C.10, it is observed that,  $W \propto D^2$ , is a good fit for this weight data. When mass flow through the engine fan is considered (not through the turbine), a linear relationship is suggested, see Fig. C.11. Figures C.12 – C.14 includes the weight of the high pressure turbine, low pressure turbine and burner section as a function of mass flow, see Table C.3. It is observed that the low pressure turbine fit the relationship,  $W \propto \dot{m}^{\frac{3}{2}}$ , very good.

Table C.2: Airplane gas turbine engine weight, fan mass flow and diameter.

Turbine	Turbine weight [kg]	Fan Mass flow [ $\frac{kg}{s}$ ]	Diameter [m]
CFM56-7B27	2400	351	1.55
V2530-A5	2363	389	1.63
PW2037	3311	547	2.01
PW4462	4233	851	2.39
PW4168	5171	912	2.54
PW4090	7069	1241	2.84
GE90-85B	7824	1406	3.12

Table C.3: Weight of high pressure turbine, low pressure turbine and burner section in airplane engines.

Turbine	HPT weight [kg]	LPT weight [kg]	Burner weight [kg]
CFM56-7B27	231	440	107
V2530-A5	281	489	128
PW2037	389	728	152
PW4462	604	986	244
PW4168	590	1106	236
PW4090	589	1789	244
GE90-85B	735	2132	327



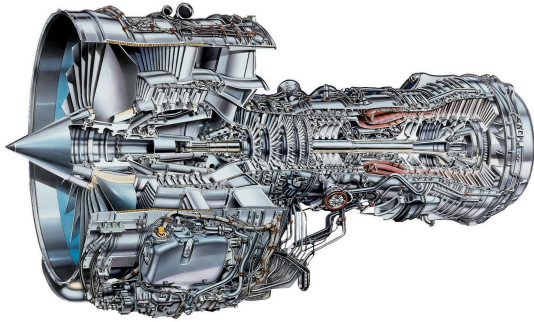


Figure C.6: International Aero Engines - V2530-A5 [143].

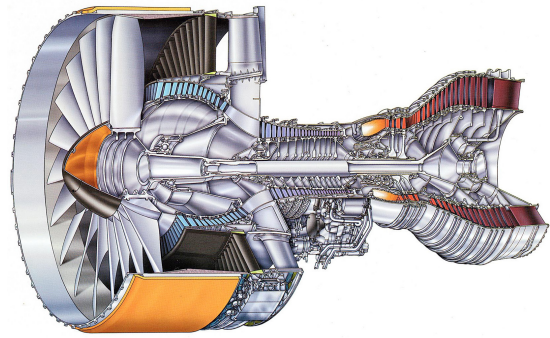


Figure C.7: Pratt & Whitney - PW4090 [144].



Figure C.8: General Electric - GE90-85B [145].

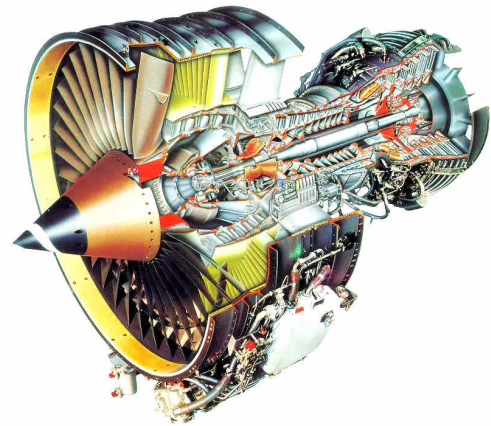


Figure C.9: CFM International - CFM56-7B27 [146].

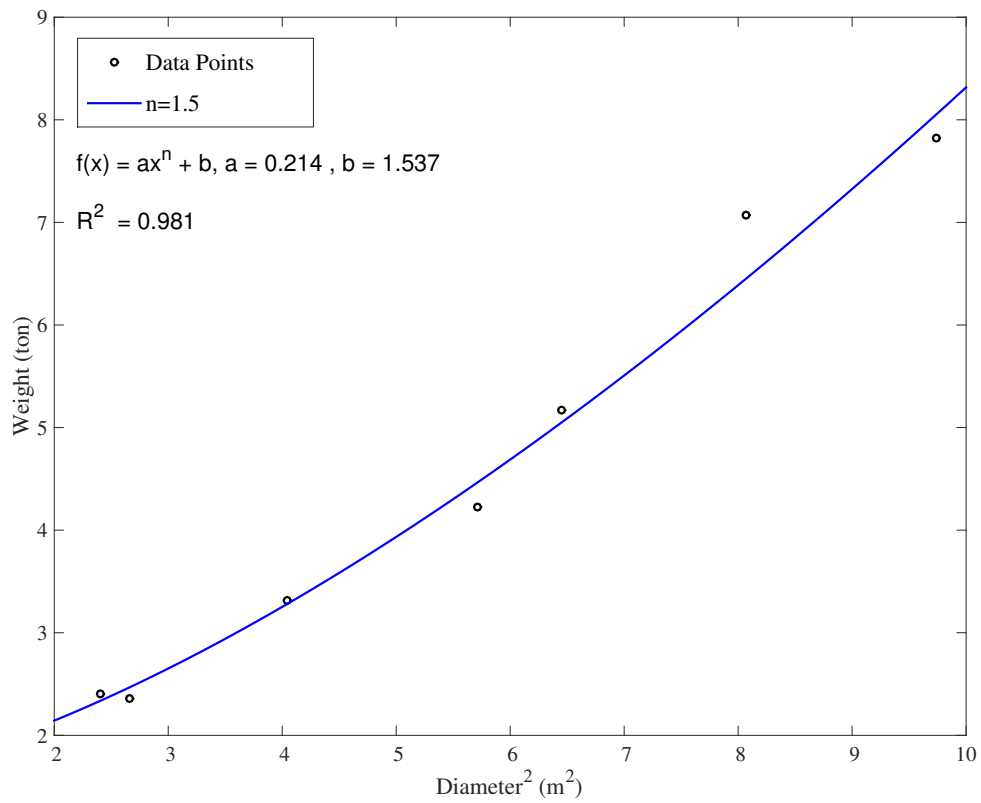


Figure C.10: Airplane gas turbine engine weight, varying with  $D^2$ .

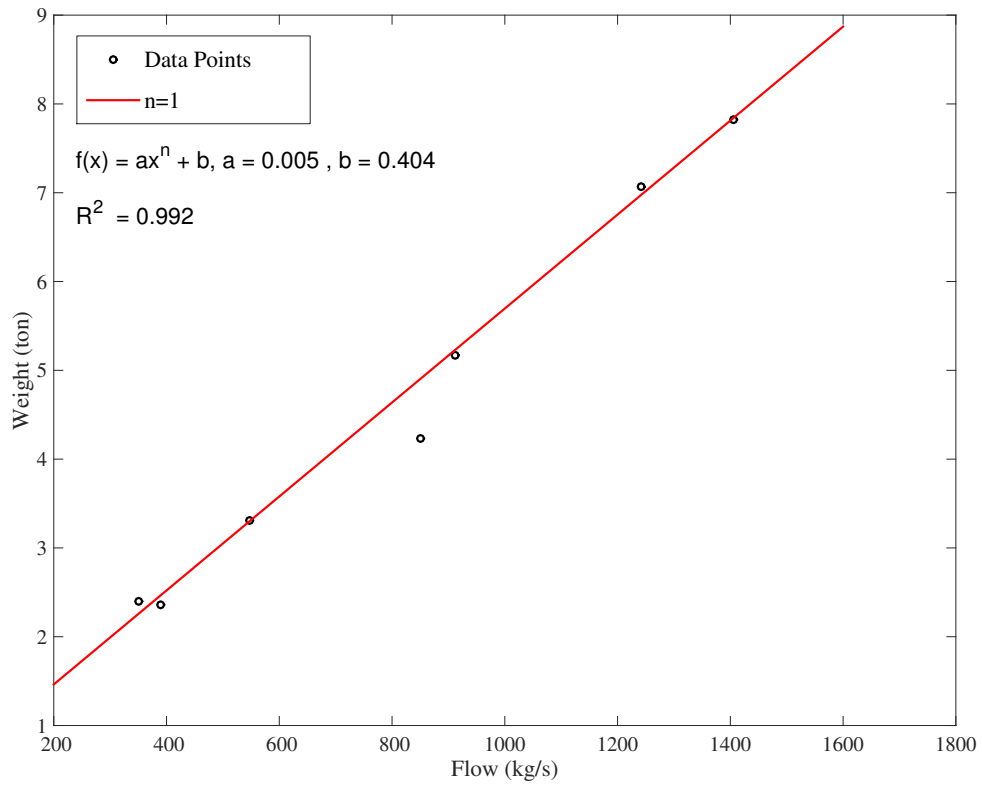


Figure C.11: Airplane gas turbine engine weight, varying with mass flow.

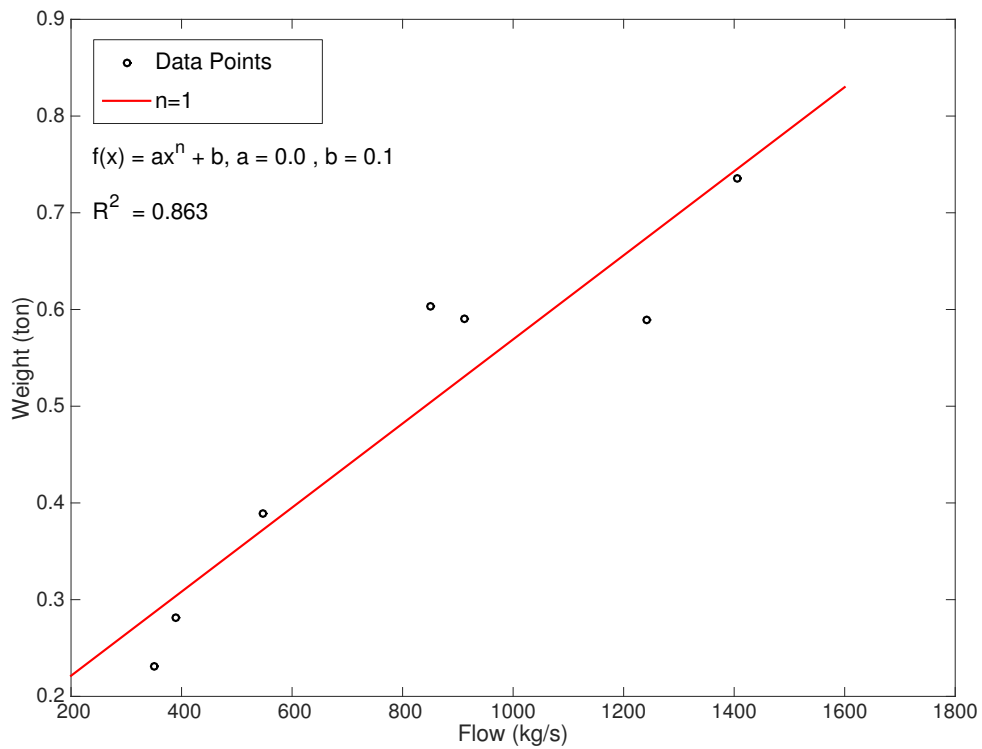


Figure C.12: Airplane engine, high pressure turbine (HPT) weight.

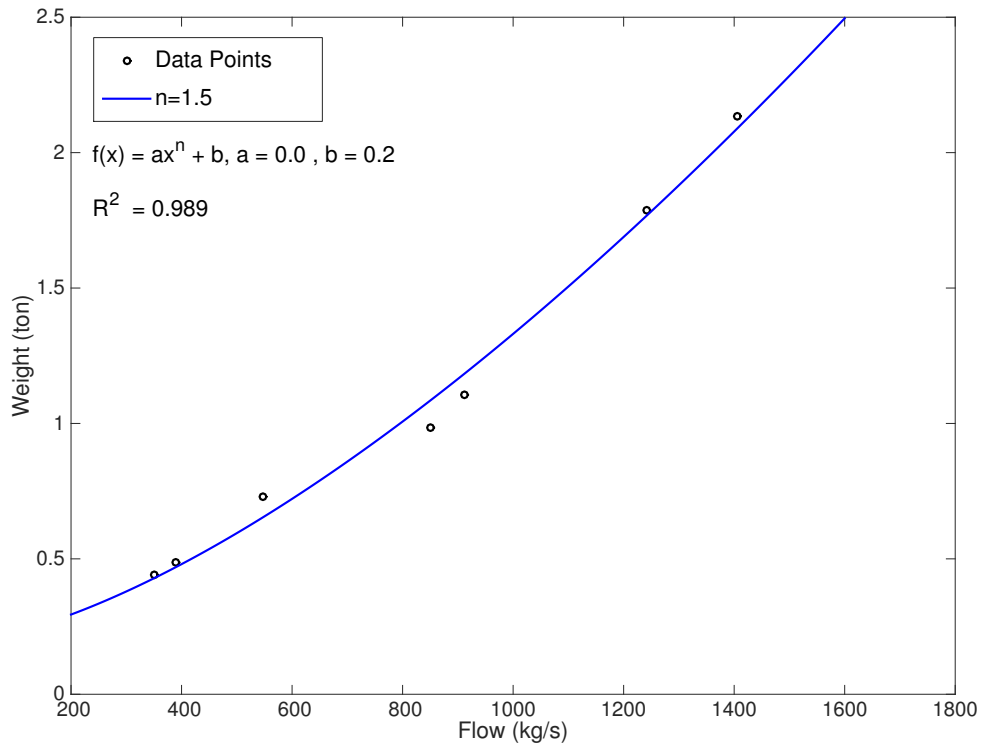


Figure C.13: Airplane engine, low pressure turbine (LPT) weight.

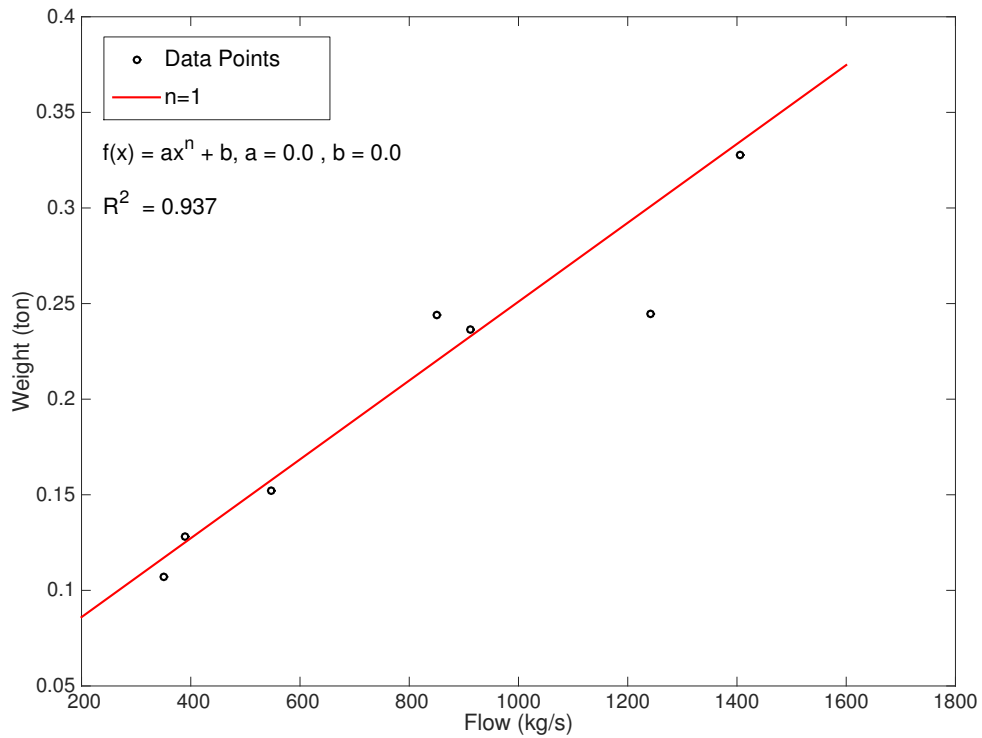


Figure C.14: Airplane engine, burner section weight.

### C.3 GT PRO - Model 1

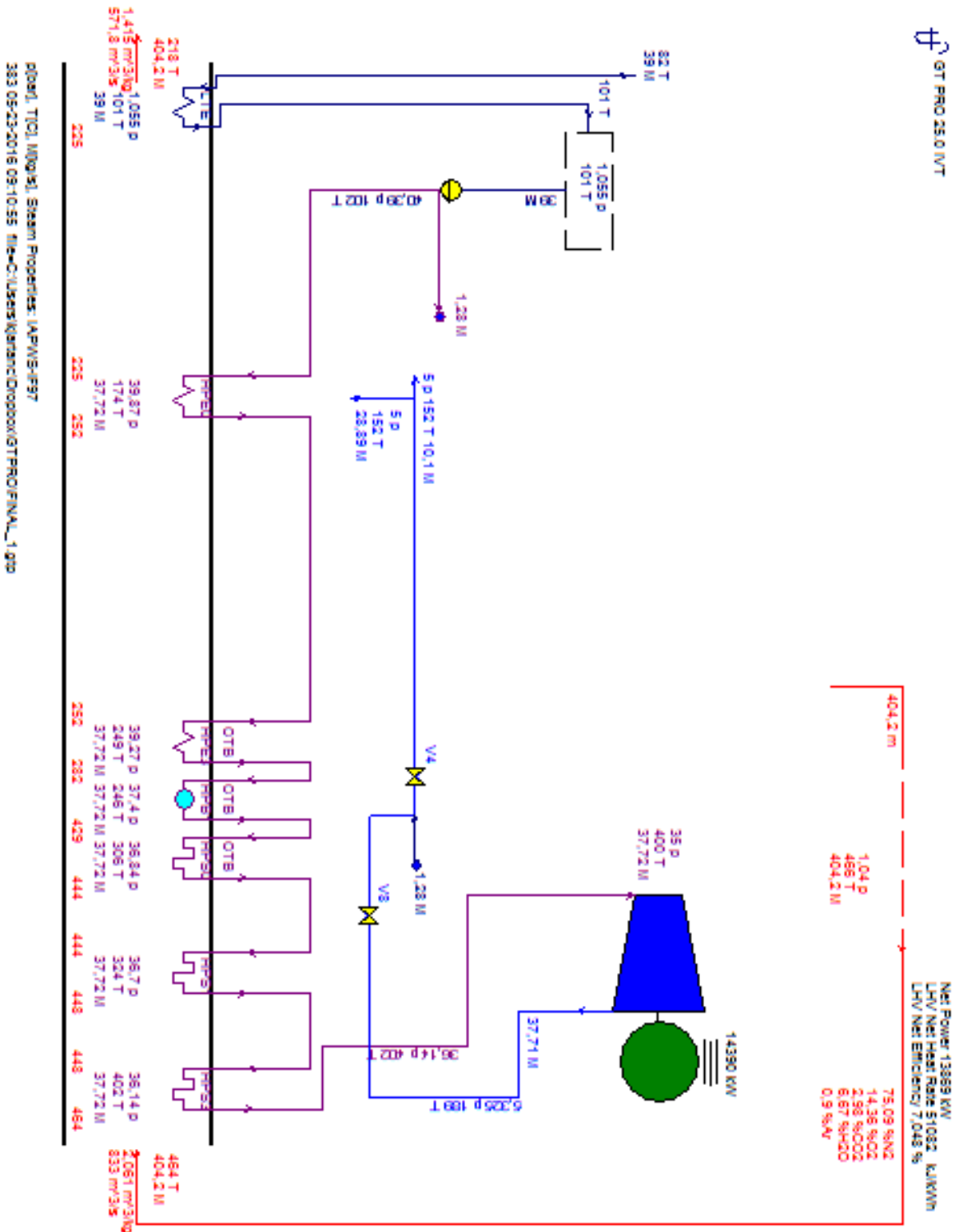


Figure C.15: GT PRO model 1, cycle flow schematic.

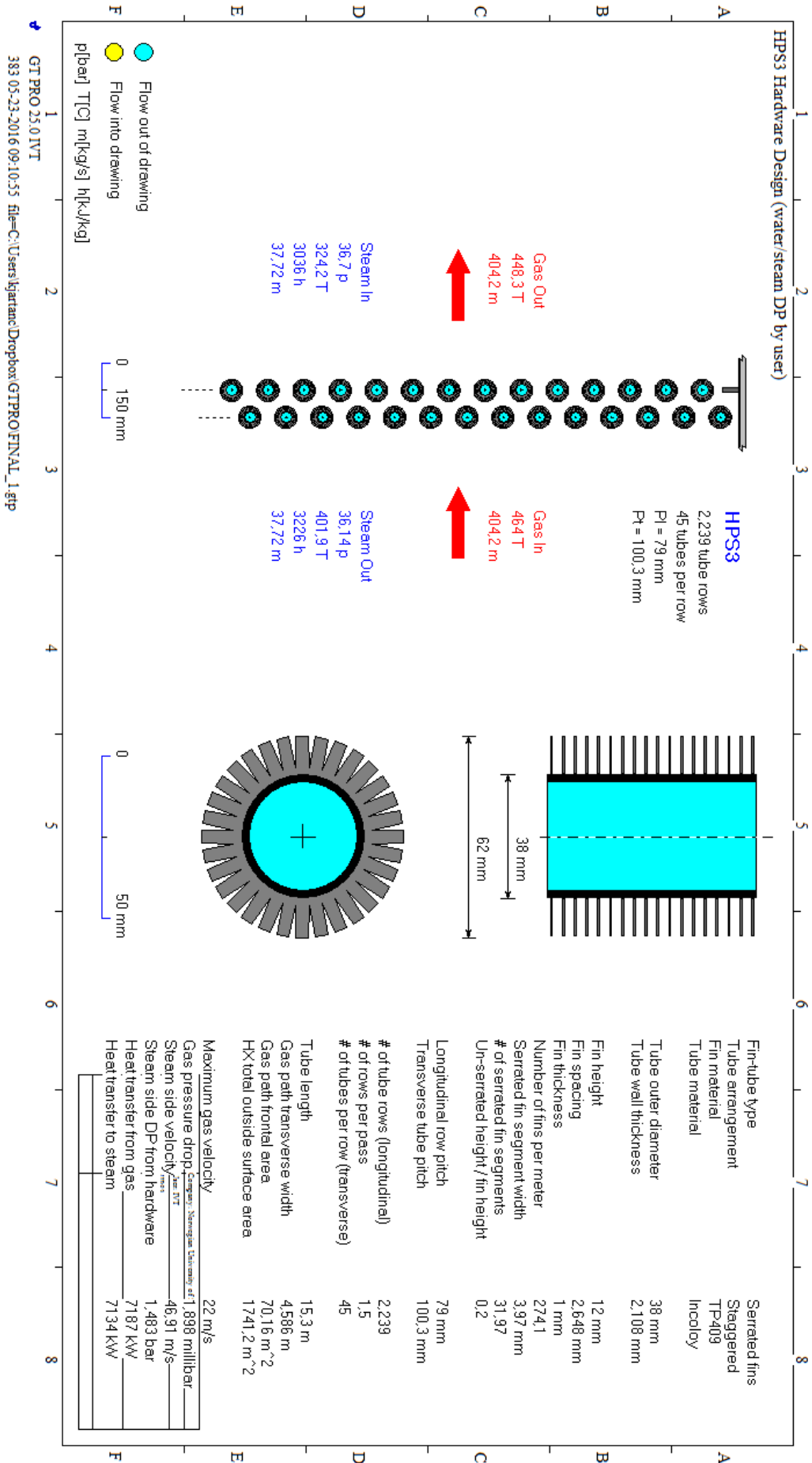


Figure C.16: GT PRO model 1, HRSG layout with Incoloy tubes.

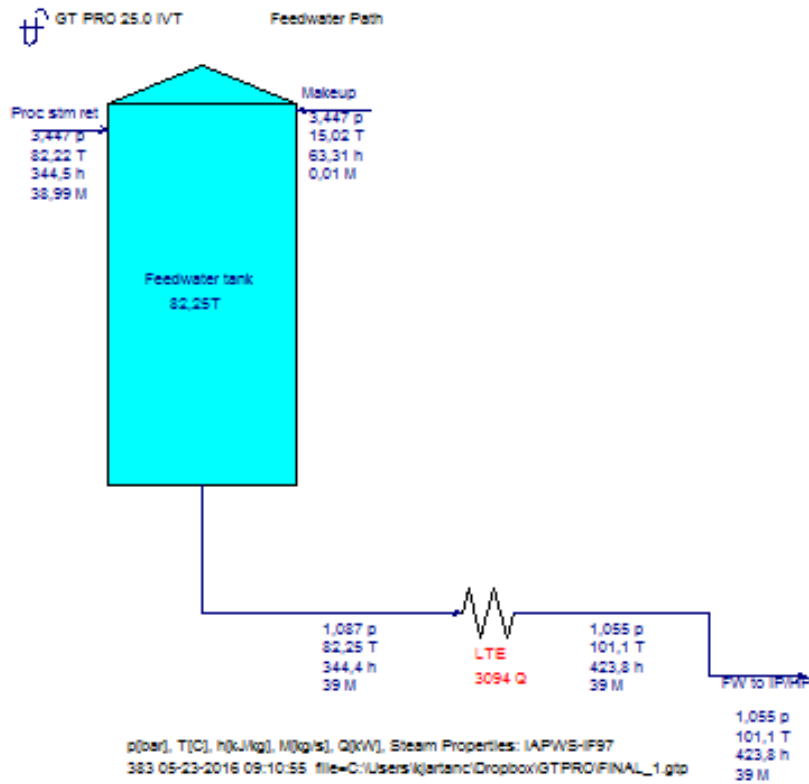


Figure C.17: GT PRO model 1, feedwater tank and low temperature economizer (LTE).

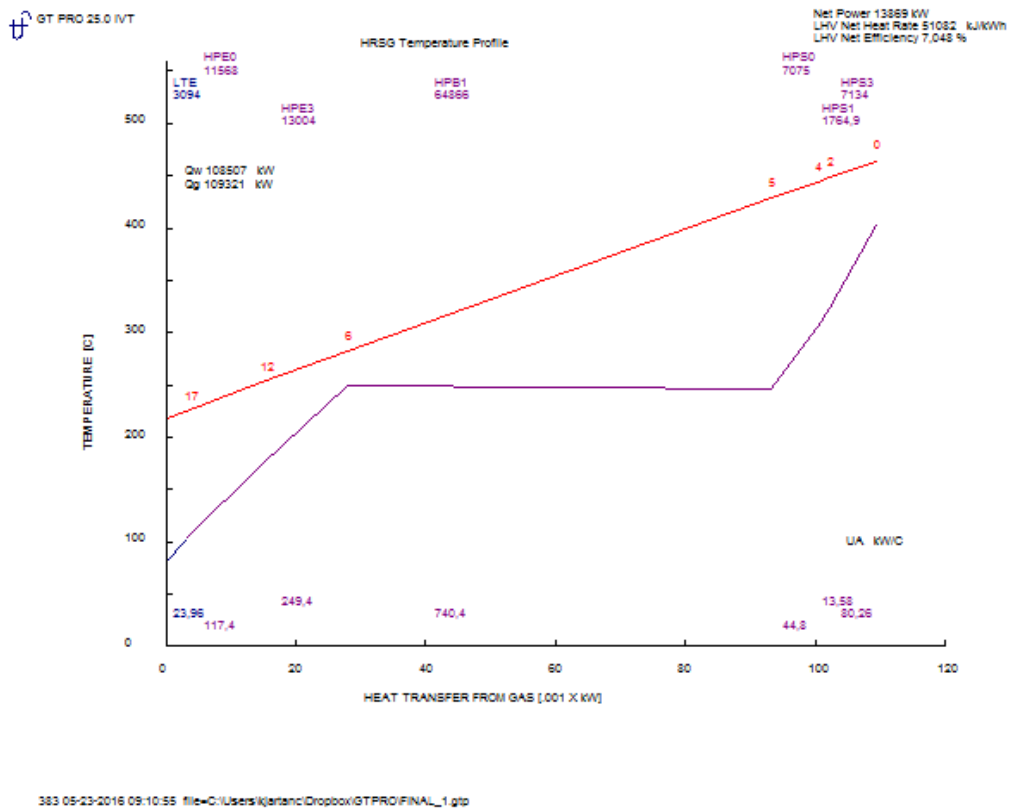


Figure C.18: GT PRO model 1, HRSG TQ diagram.

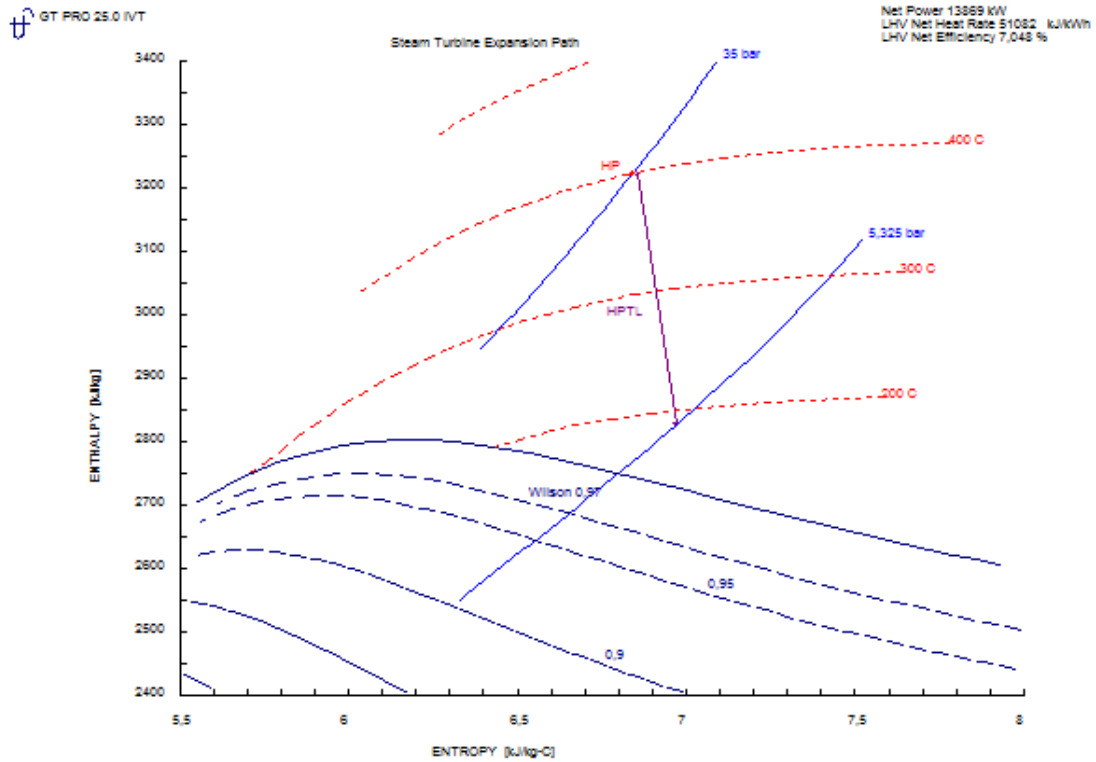
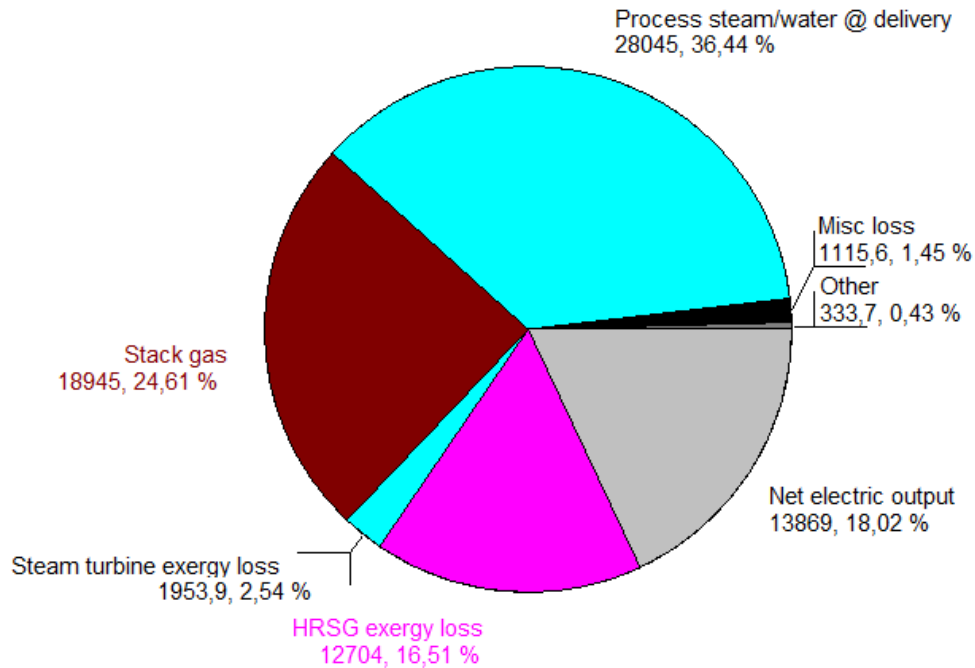


Figure C.19: GT PRO model 1, steam turbine expansion path.

**Plant Exergy Analysis [kW]**

GT PRO 25.0 IVT

Plant exergy input = 76965 kW  
 Plant fuel chemical LHV input = 196786 kW, HHV = 196786 kW



Reference: 1.013 bar, 25 C, water as vapor.

Figure C.20: GT PRO model 1, plant exergy chart.

C.4 GT PRO - Model 2

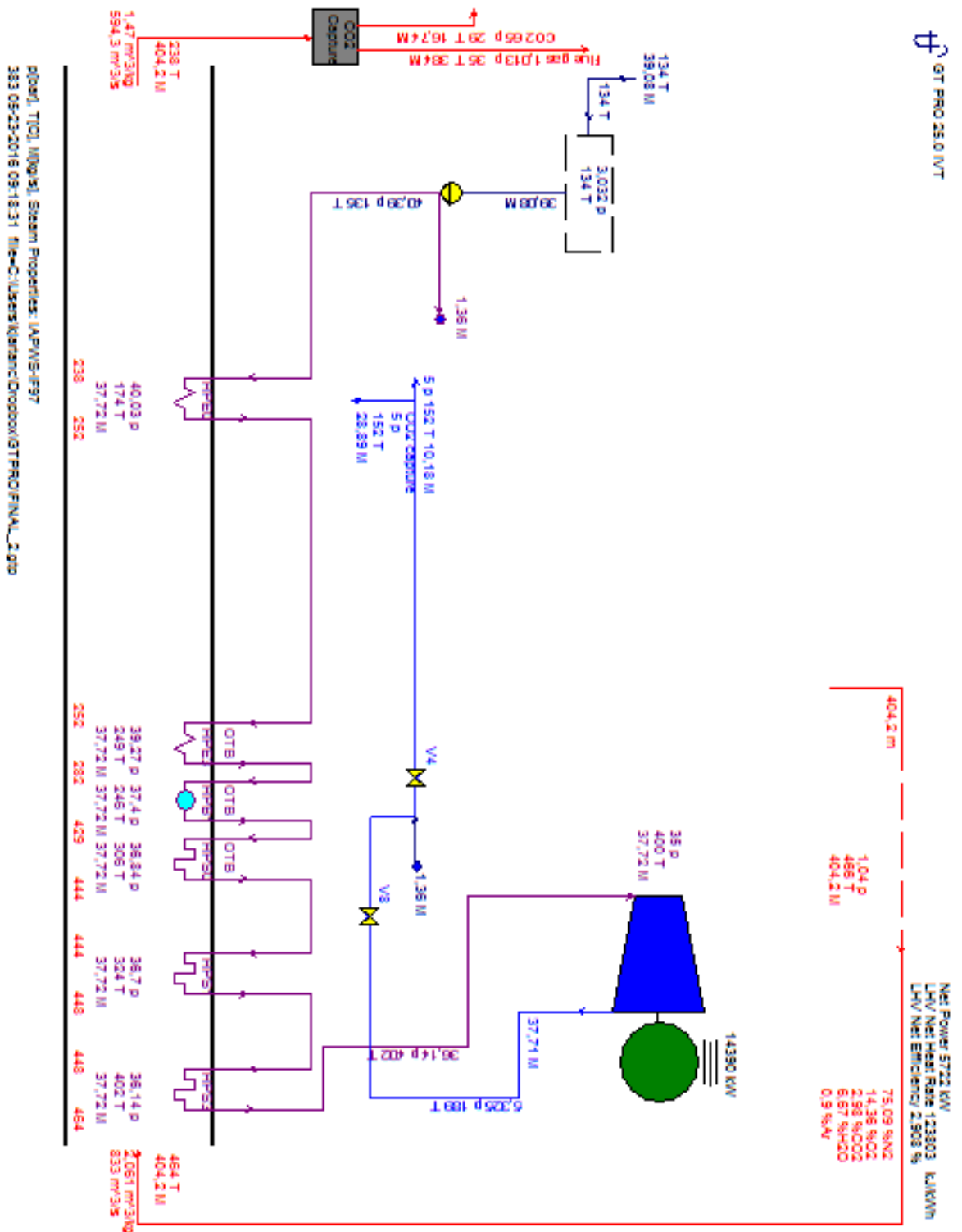


Figure C.21: GT PRO model 2, cycle flow schematic.



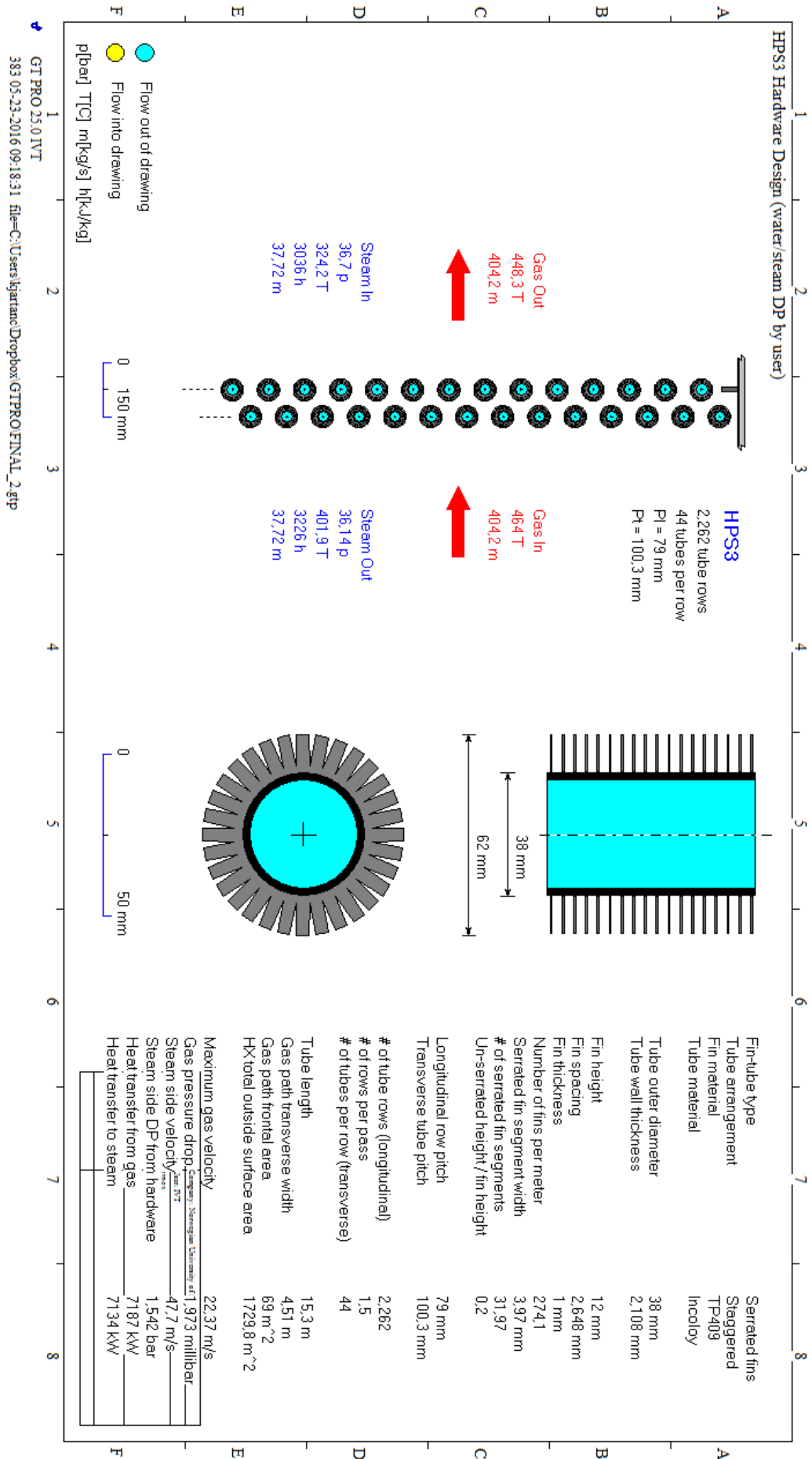


Figure C.22: GT PRO model 2, HRSG layout with Incoloy tubes.

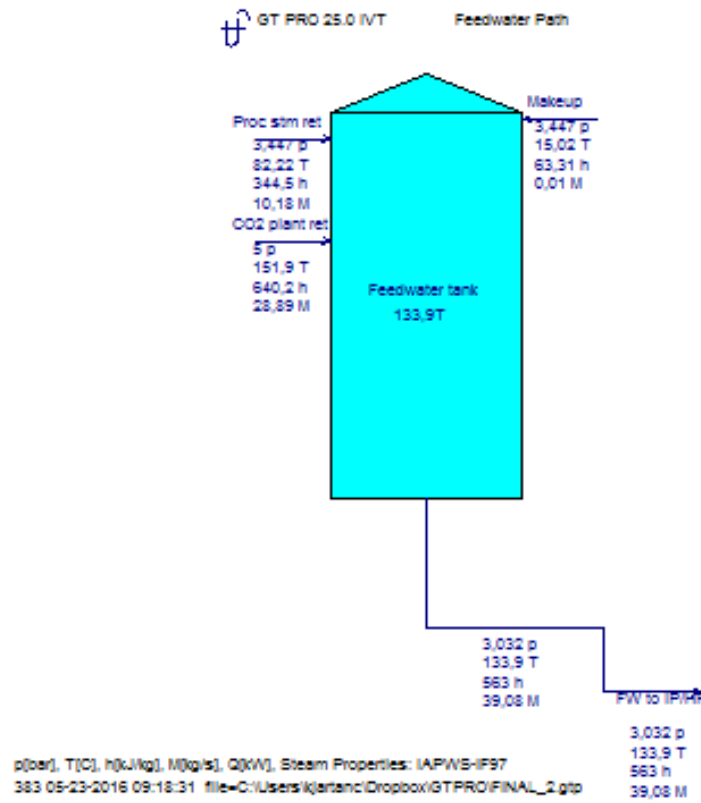


Figure C.23: GT PRO model 2, feedwater tank.

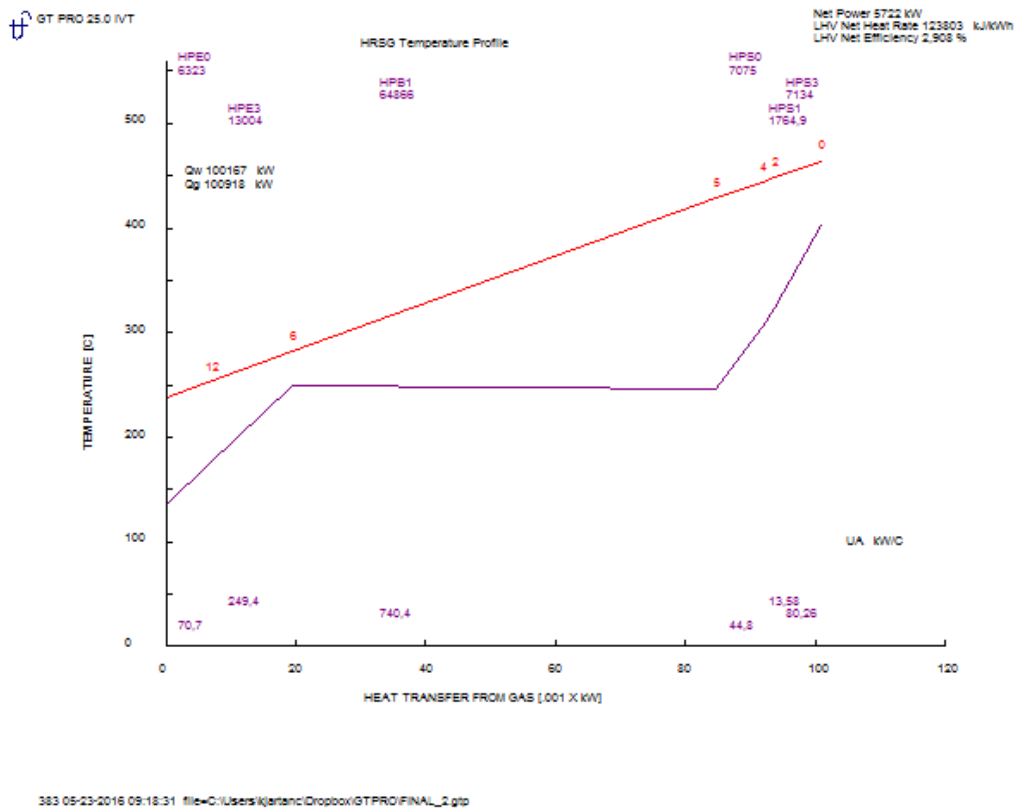


Figure C.24: GT PRO model 2, HRSG TQ diagram.

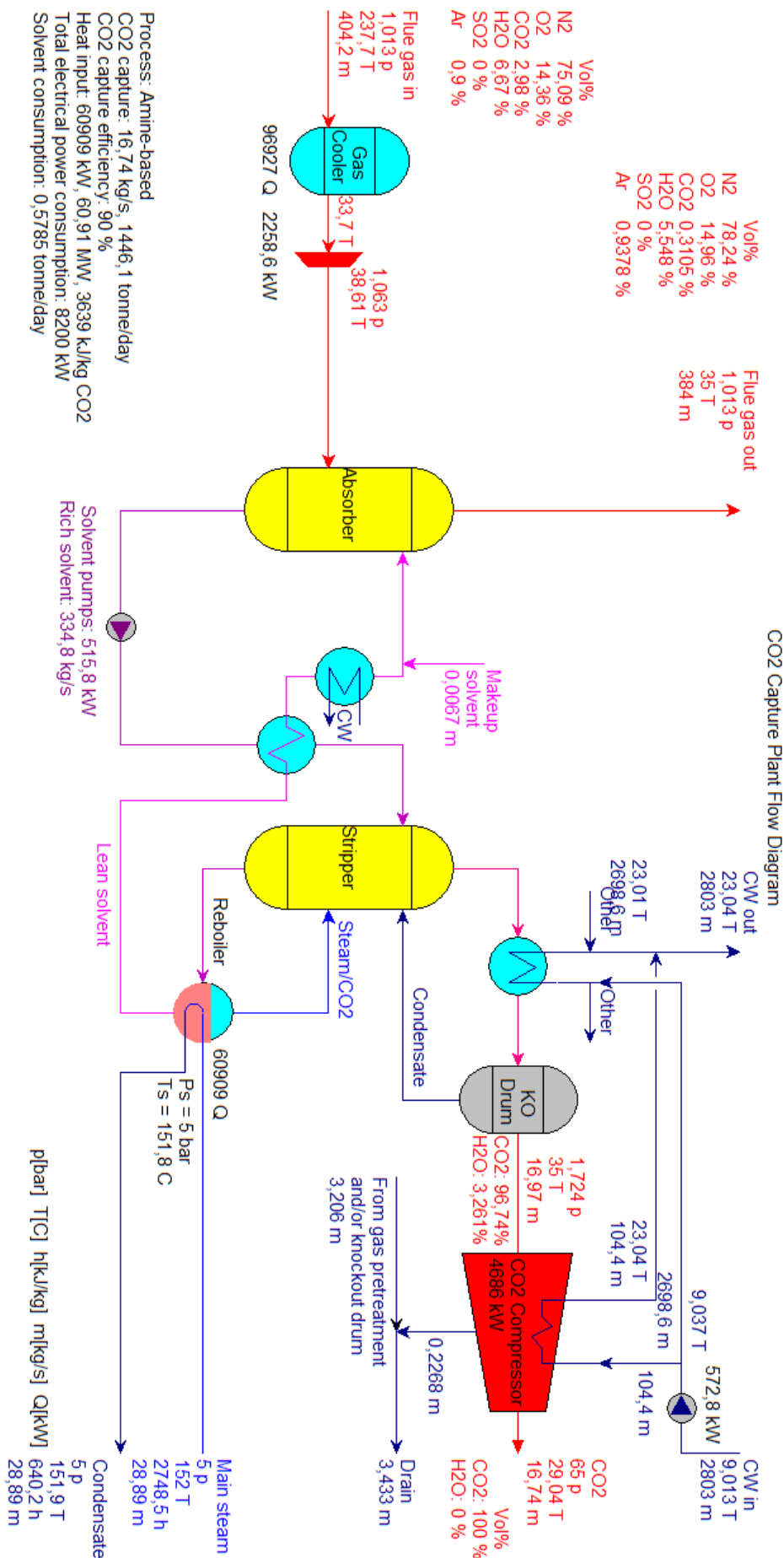
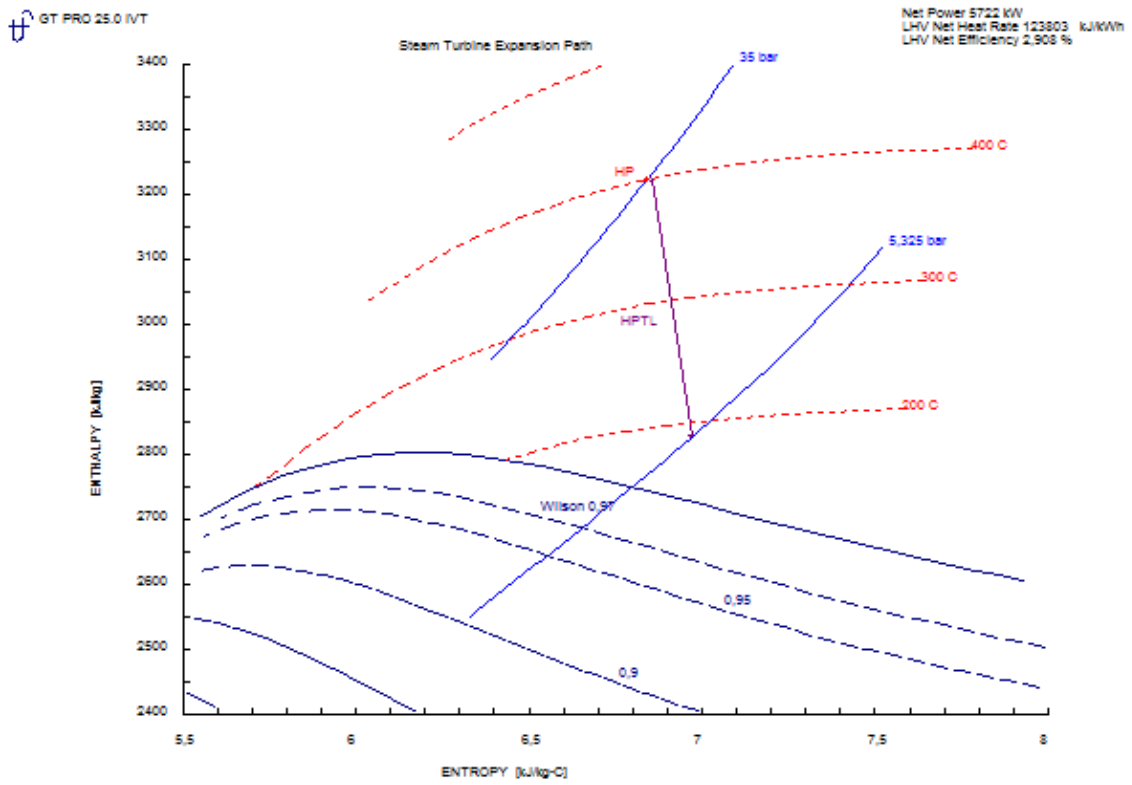


Figure C.25: GT PRO model 2, CO<sub>2</sub> capture plant.

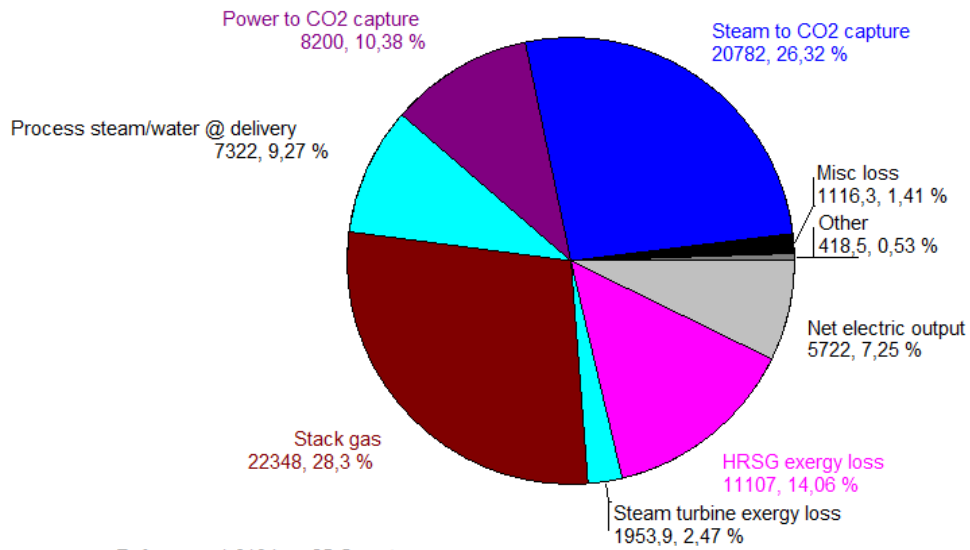


383 05-23-2016 09:18:31 file=C:\Users\k\artanc\Dropbox\GTPRO\FINAL\_2.gtp

Figure C.26: GT PRO model 2, steam turbine expansion path.

**Plant Exergy Analysis [kW]**

Plant exergy input = 78969 kW  
 Plant fuel chemical LHV input = 196786 kW, HHV = 196786 kW



Reference: 1.013 bar, 25 C, water as vapor.

GT PRO 25.0 IVT  
 383 05-23-2016 09:18:31 file=C:\Users\k\artanc\Dropbox\GTPRO\FINAL\_2.gtp

Figure C.27: GT PRO model 2, plant exergy chart.

C.5 GT PRO - Model 3

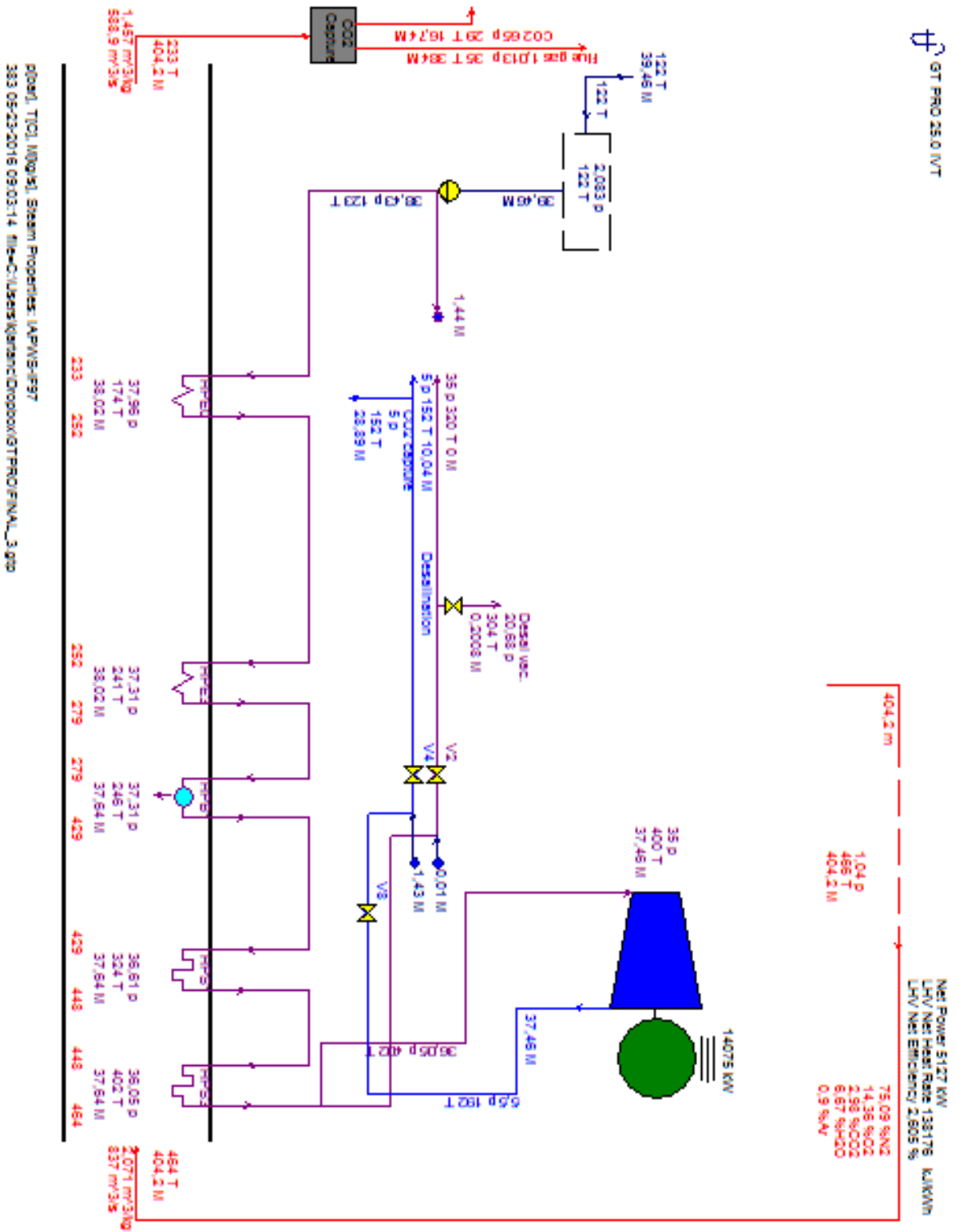


Figure C.28: GT PRO model 3, cycle flow schematic.

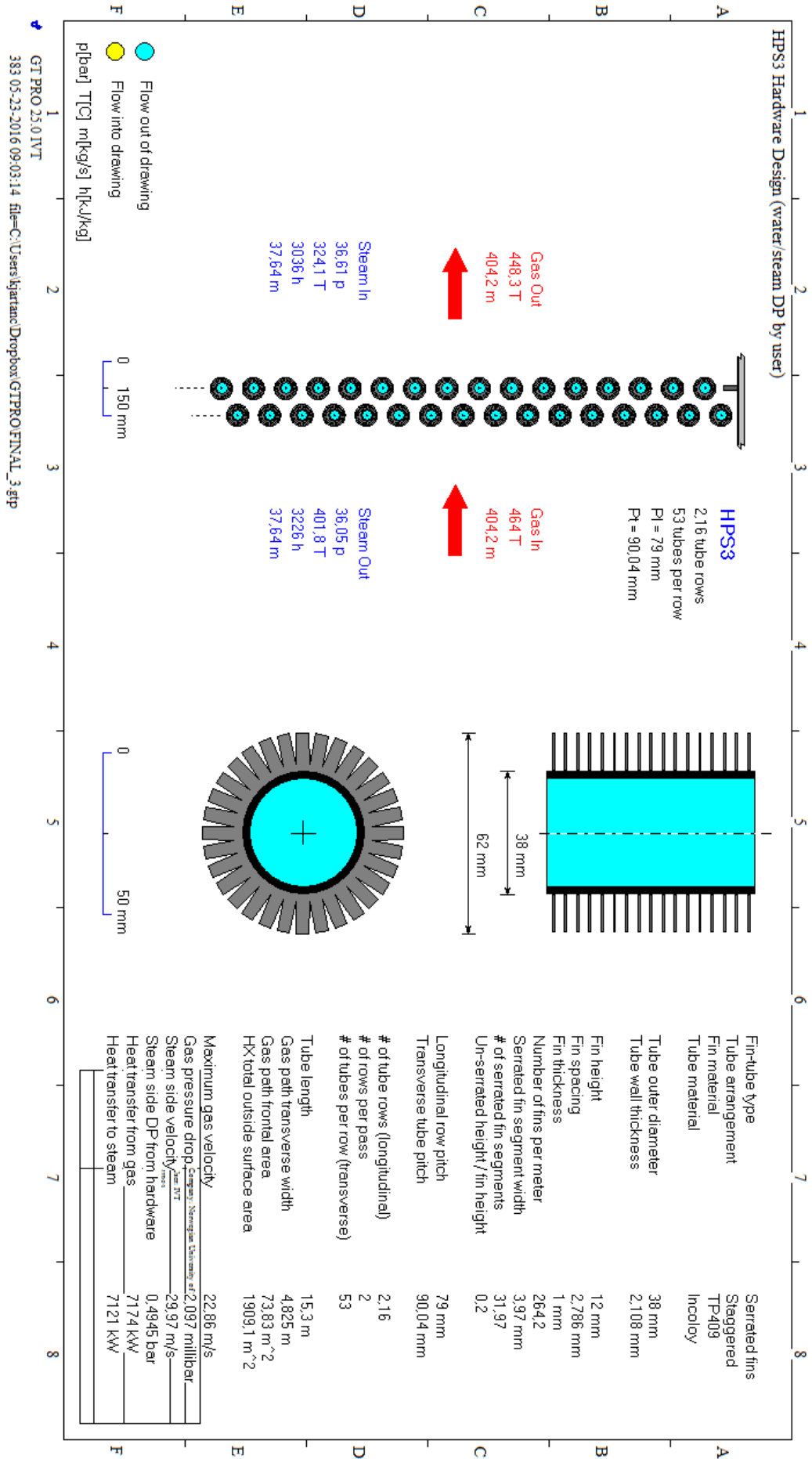


Figure C.29: GT PRO model 3, HRSG layout with Incoloy tubes.

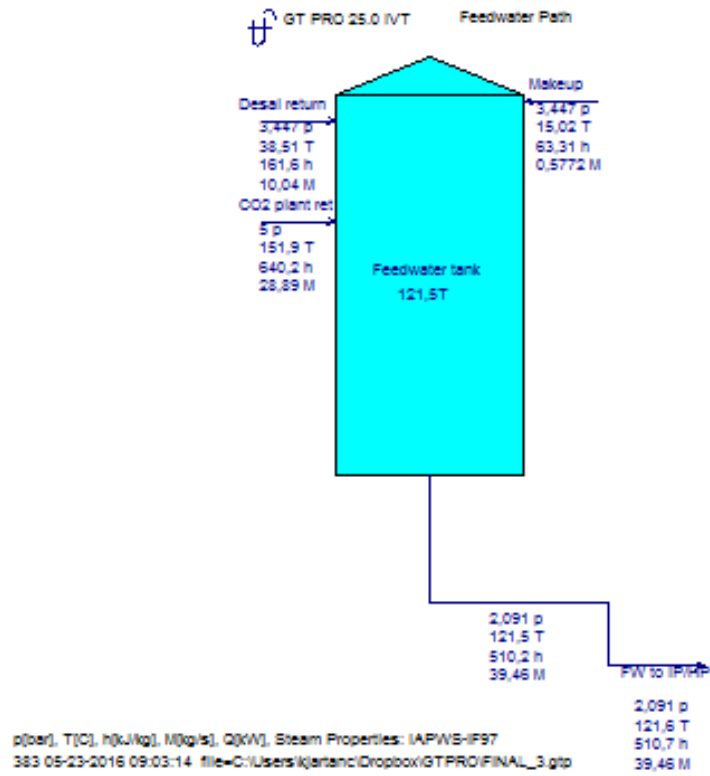


Figure C.30: GT PRO model 3, feedwater tank.

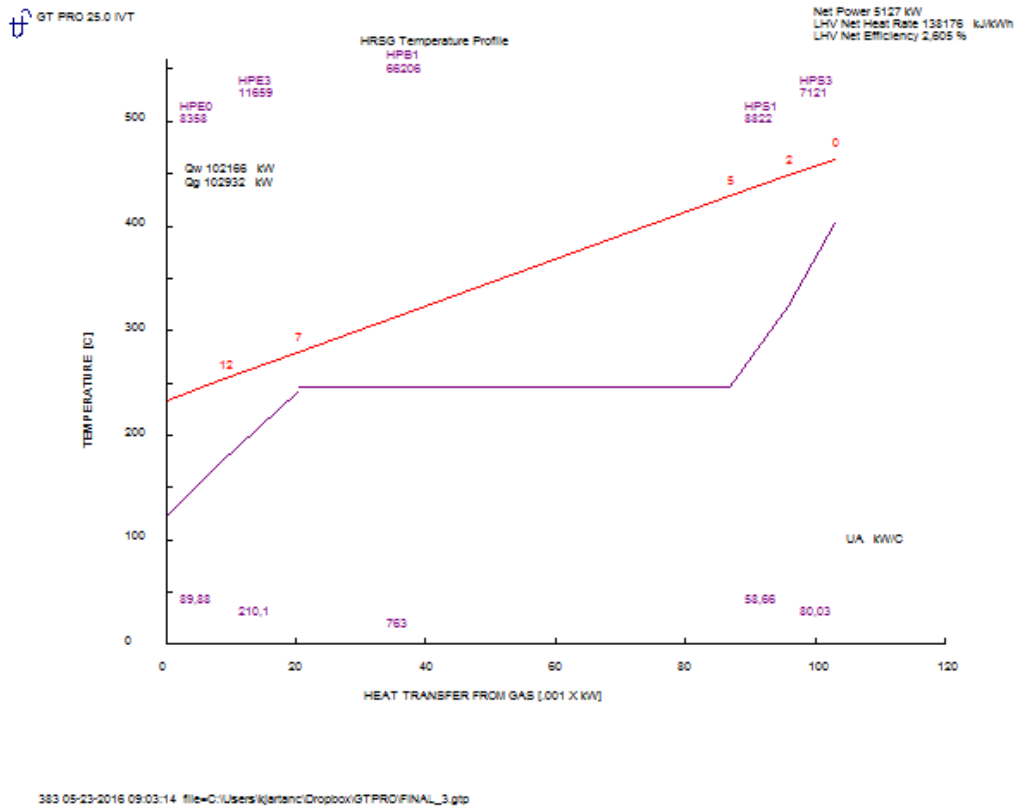


Figure C.31: GT PRO model 3, HRSG TQ diagram.

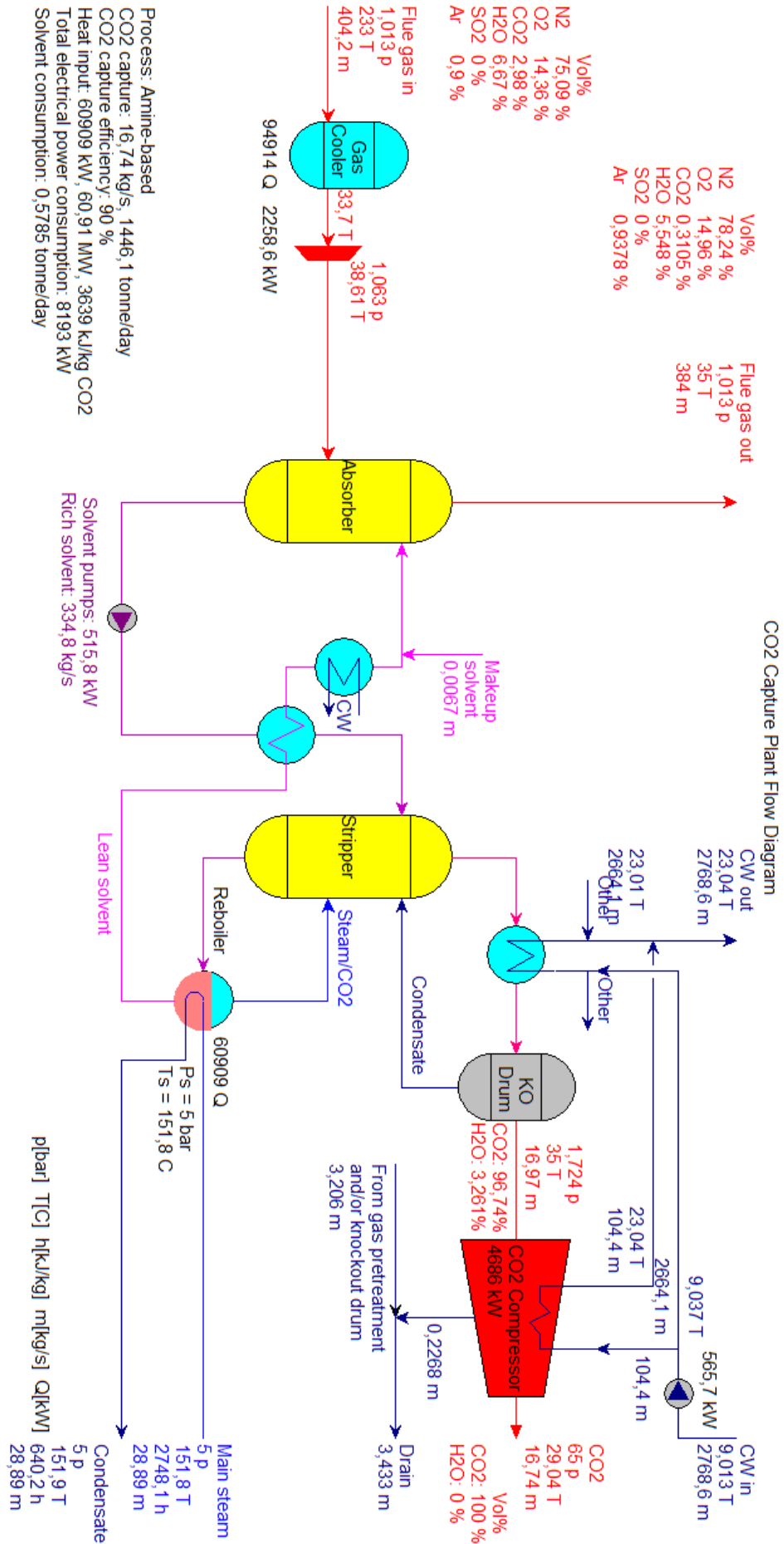
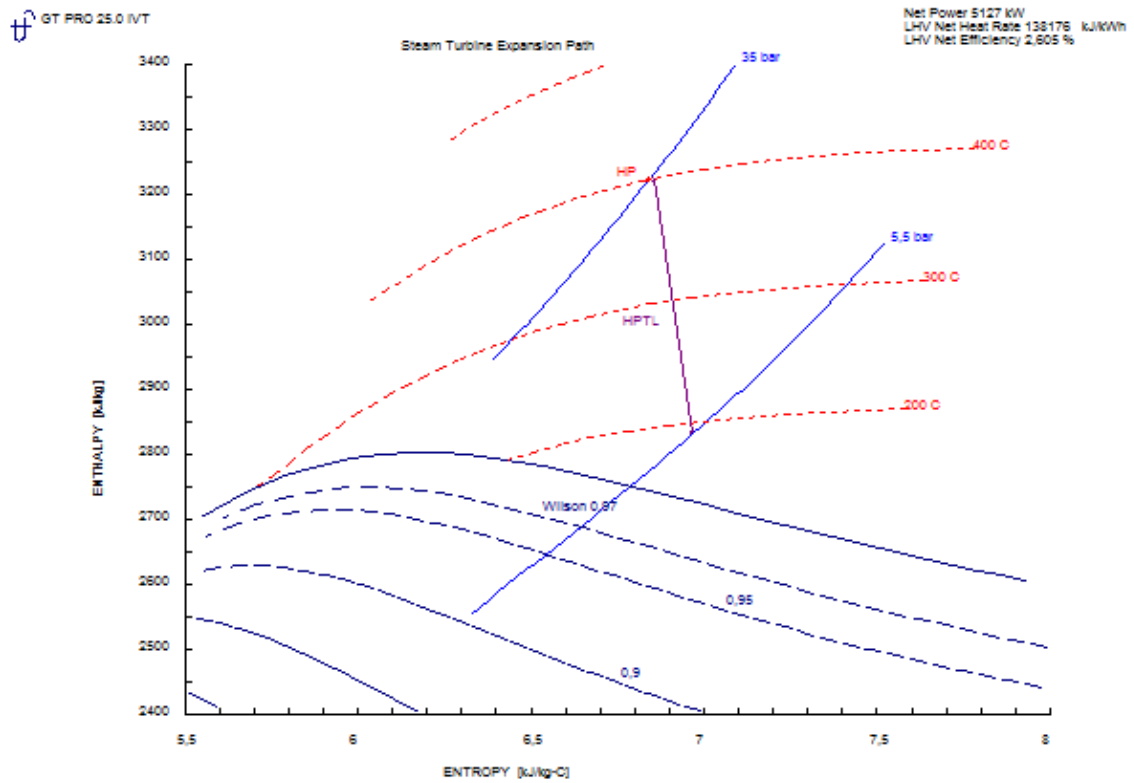


Figure C.32: GT PRO model 3, CO<sub>2</sub> capture plant.

GT PRO 25.01.VT  
 383 05-23-2016 09:03:14 file=C:\Users\kgartana\Dropbox\GTPRO\FINAL\_3.gfp





383 05-23-2016 09:03:14 file=C:\Users\kartanc\Dropbox\GTPRO\FINAL\_3.gtp

Figure C.33: GT PRO model 3, steam turbine expansion path.

**Plant Exergy Analysis [kW]**

GT PRO 25.0 IVT

Plant exergy input = 78605 kW  
 Plant fuel chemical LHV input = 196786 kW, HHV = 196786 kW

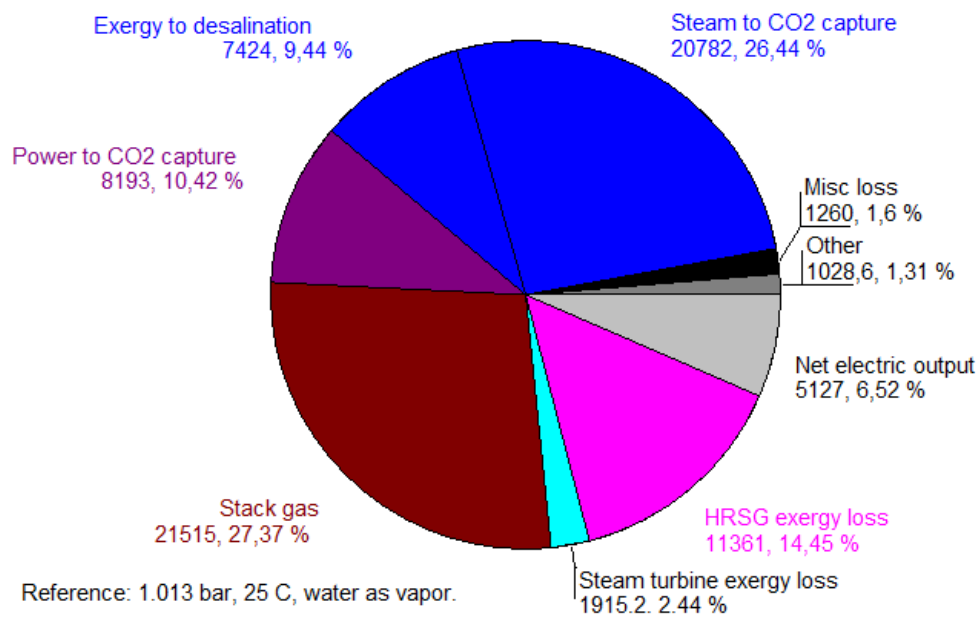


Figure C.34: GT PRO model 3, plant exergy chart.

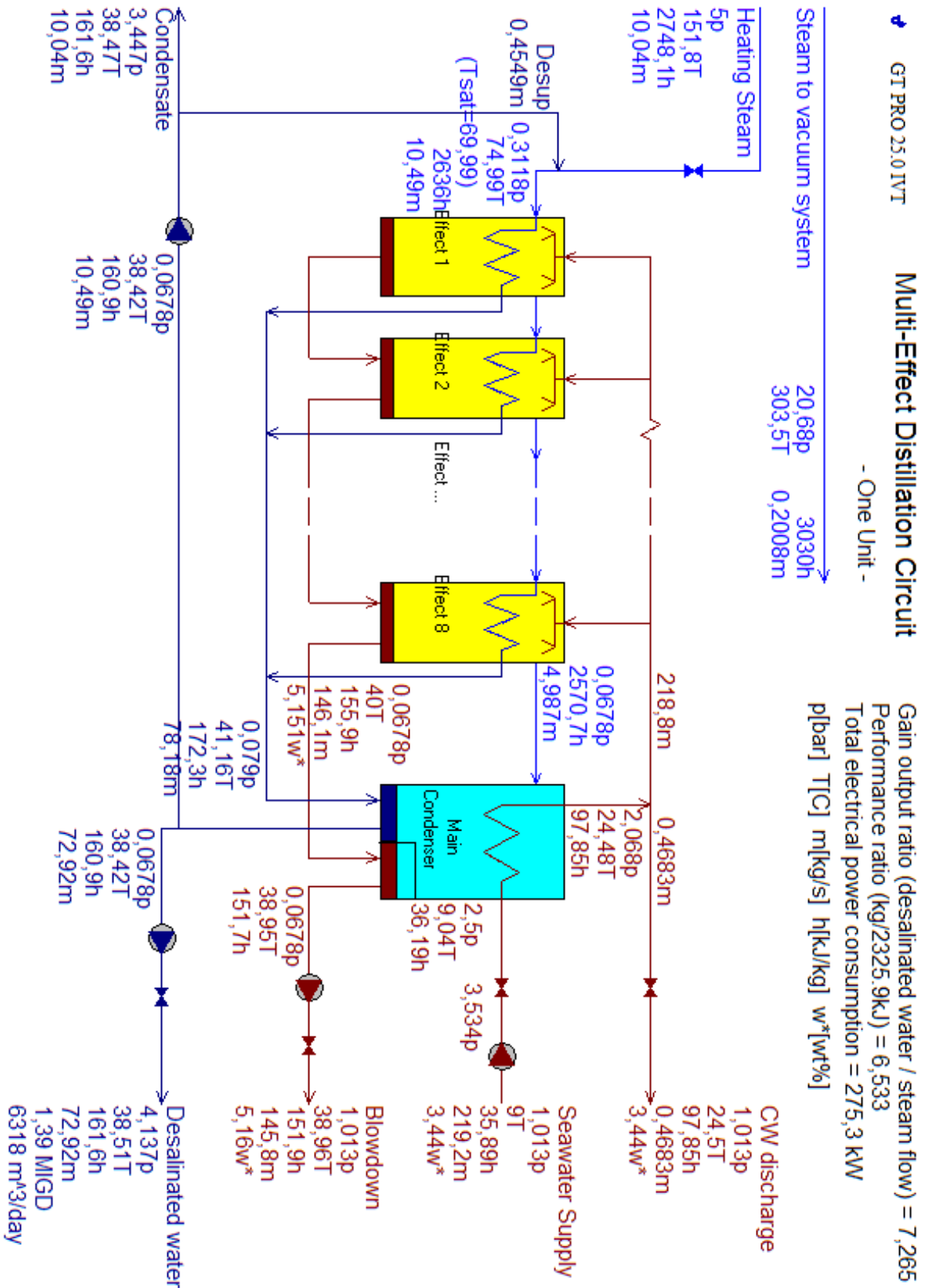


Figure C.35: GT PRO model 3, desalination plant. Multi-Effect Distillation (MED) circuit.

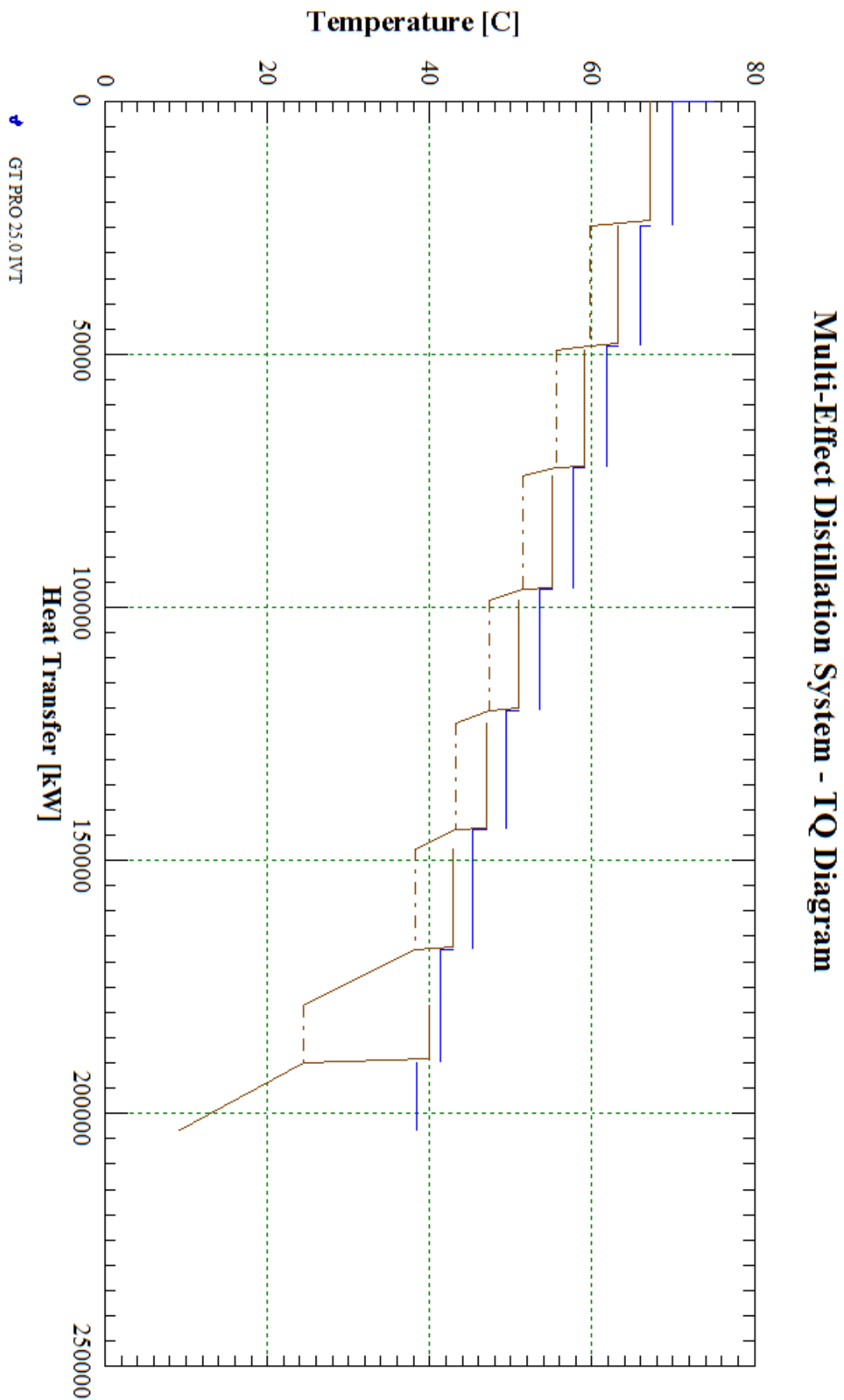


Figure C.36: GT PRO model 3, MED circuit TQ diagram.

## C.6 GT PRO - Additional Figures for Scaling Laws

### C.6.1 Model 1

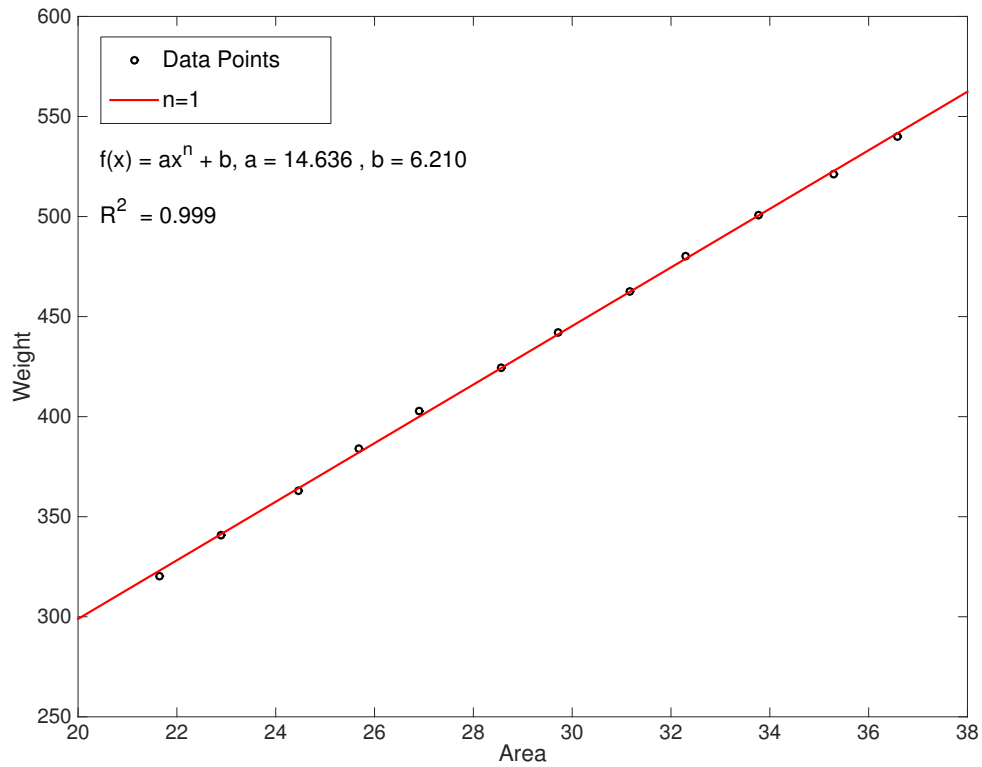


Figure C.37: Model 1, HRSG (dry) weight as a function of heat surface area.

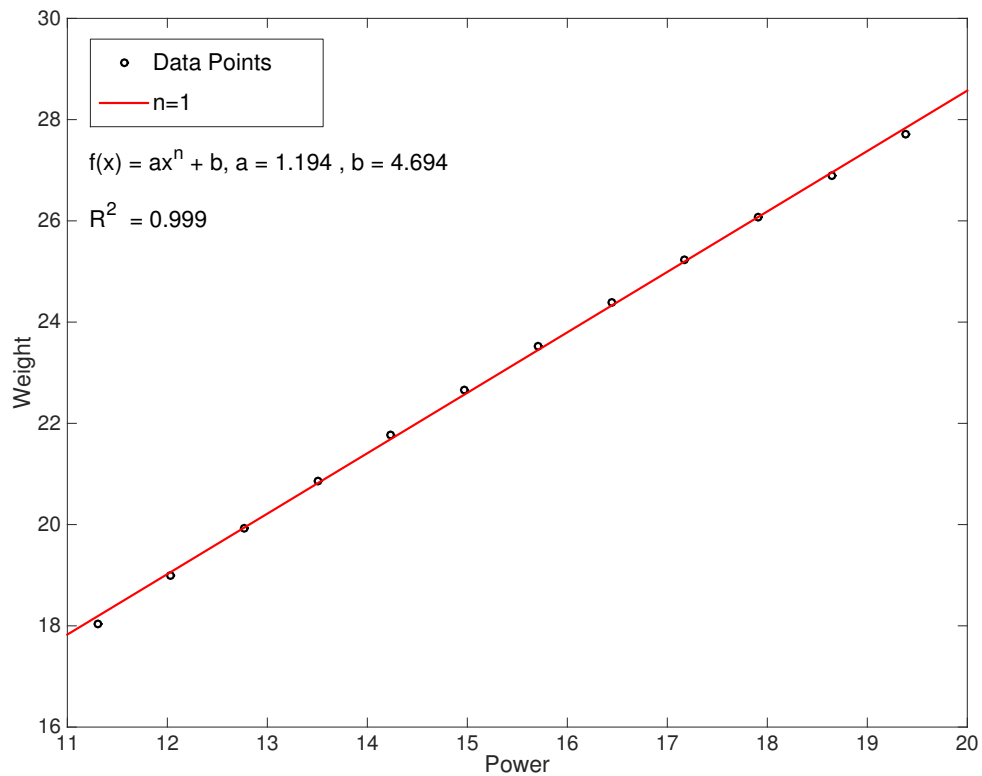


Figure C.38: Model 1, steam turbine weight as a function of steam turbine power.

C.6.2 Model 2

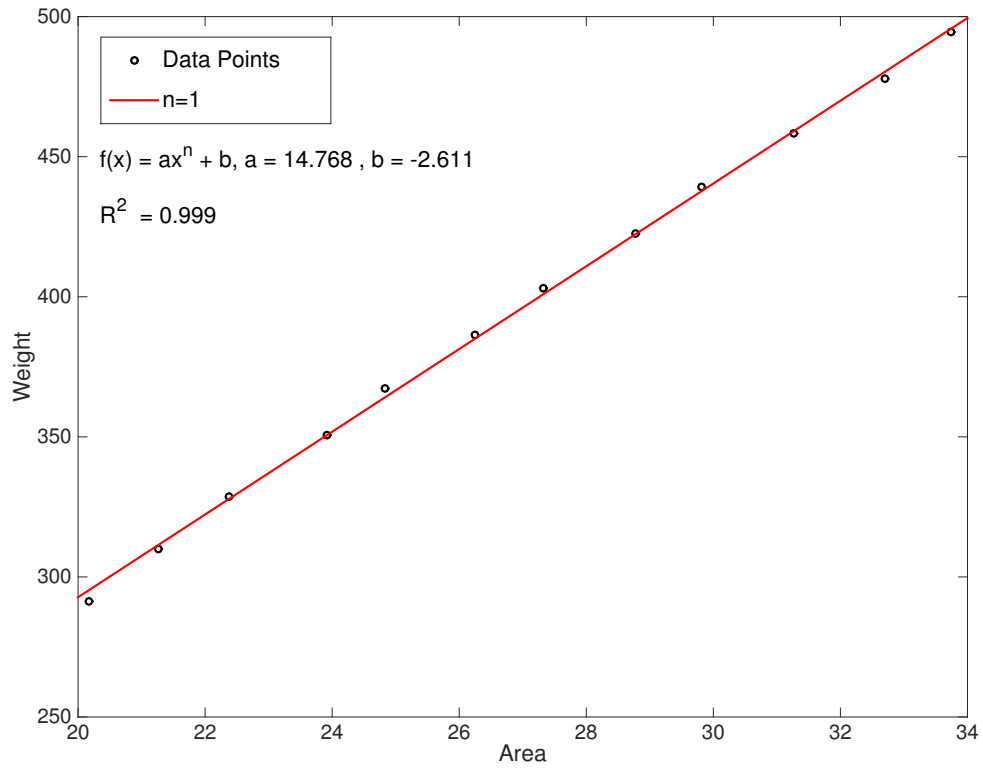


Figure C.39: Model 2, HRSG (dry) weight as a function of heat surface area.

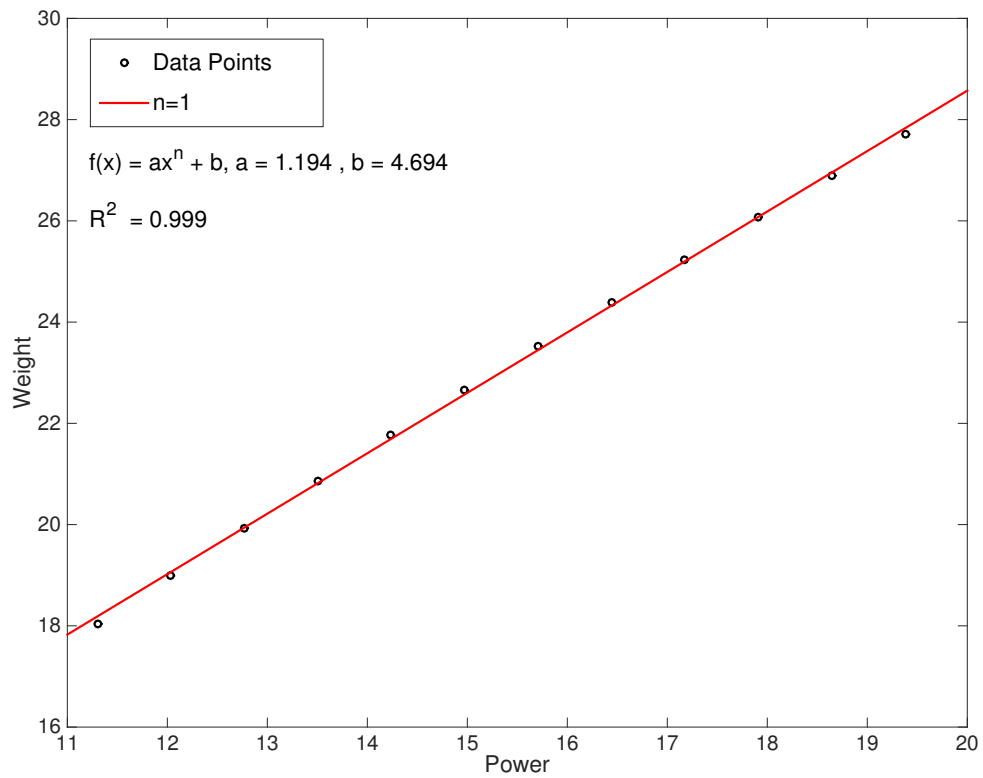


Figure C.40: Model 2, steam turbine weight as a function of steam turbine power.

## C.7 Multivariate Polynomial Approach – Project Work Weight Estimation

### Nomenclature

$\Lambda$	Steam Cycle Weight	[kg]
$\psi$	Reduction factor	[-]
$\Gamma$	Correction term	[-]
$\gamma$	Correction term	[-]

### Approach

One of the major tasks for this thesis was to develop a polynomial for weight estimation. Lot of simulations were done in GT PRO, with the Excel add in, ELINK. To decide which parameters that affected the weight most, sensitivity analysis was performed on all relevant parameters. Based on this work, five parameters were chosen for the weight estimating polynomial.

Table C.4: Variables in weight estimating polynomial

Parameter	Property
$x_1$	$\dot{m}_{exh}$
$x_2$	$T_{exh}$
$x_3$	$T_{steam}$
$x_4$	$P_{steam}$
$x_5$	$\Delta T_{pinch}$

The polynomial was developed by a type of parametric run. It is most likely more mathematical efficient methods for this type of work, but the partly self-developed procedure worked quite well. It was important for the author to show some independent work, because much of this thesis is based on literature study. The following steps were performed:

- First, the examined parameter varied in a 20 stage interval in GT PRO. All results were then saved in Excel for further processing. The chosen values were both bigger and smaller than the base case value for the actual parameter.

It is further assumed that steam leaving the turbine is at saturated and therefore is connected to the steam pressure. Some plausible conditions are collected in Table C.5 and the parameter  $x_{34}$  is defined as:  $x_{34} = \frac{x_3}{x_4} = \frac{T_{steam}}{P_{steam}}$ .

Table C.5: Saturation temperatures

$P_{sat}$ [bar]	$T_{sat}$ [°C]
1.0	99.6
1.5	111.4
2.0	120.2
2.5	127.4
3.0	133.5
3.5	138.9
4.0	143.6
4.5	147.9
5.0	151.8
5.5	155.5
6.0	158.8
6.5	162.0
7.0	165.0
7.5	167.8
8.0	170.4
8.5	172.9
9.0	175.4
9.5	177.7
10.0	179.9

- Data was then put into MATLAB for plotting and curve fitting. For consistency, second order curve fitting was used, see Figures C.41, C.42, C.43, and C.44. The polyfit function in MATLAB gave the second order polynomial that was fitted to the parametric run for each parameter. All other parameters were kept constant at base case conditions. From here it was easy to see which parameters that affected the weight most, and based on these results an appropriate range for each parameter was chosen.

Because the  $x_{34}$  parameter affects the change in weight significantly less than the other parameters (less sensitive), it was chosen as a scaling term for simplified calculation. The next steps are therefore performed on the three other parameters. Second order weight polynomials for the other parameters were found, and named  $\Lambda_1$ ,  $\Lambda_2$ , and  $\Lambda_5$ .

- The first attempt on a weight polynomial was to multiply  $\frac{1}{3}$  with the added polynomials  $\Lambda_1$ ,  $\Lambda_2$ , and  $\Lambda_5$ . This polynomial was tested with different values, and the results compared with GT PRO results for the same values. As expected, the accuracy was poor for values far away from the base case.

The weight polynomial took the form:

$$\Lambda(x_1, x_2, x_5) = \frac{1}{3}[\Lambda_1 + \Lambda_2 + \Lambda_5] \quad (\text{C.1})$$

- To make the accuracy better, the idea was to introduce linear correction terms. The polynomials for each parameter were built into Excel. Starting with parameter  $x_1$ , its value was minimized

and maximized within the chosen range. By simulating this values in GT PRO, it was possible to see the error made by each polynomial.

The average slope for a linear line found by minimizing and maximizing  $x_1$  was used to estimate a correction term for both  $\Lambda_2$  and  $\Lambda_5$  polynomials. When this were done, all polynomials had two correction terms, one for each of the other parameters. An example of this method is (without taking the average, just using the minimized value to show the approach):

$$\text{Base case } x_1 = 404.2 \frac{\text{kg}}{\text{s}}. \text{ Range considered} = [340-440].$$

$$\text{Minimize } x_1 = 340 \frac{\text{kg}}{\text{s}}.$$

$$\text{Correct weight from GT PRO} = 346469 \text{ kg}$$

Weight calculated with the polynomial for  $x_2 = 407551 \text{ kg}$  (to high, should be reduced)

$$\text{Ratio} = \frac{346469}{407551} = 0.85 = 85\%$$

$$\text{Reduce by: } 1 - 0.85 = 0.15 = 15\%$$

$$\text{Reduction factor} = \psi_{2-1} = \frac{404.2-340}{0.15} = 427$$

$$\text{Correction term} = \gamma_{2-1} = 1 - \frac{404.2-x_1}{427}$$

General correction term for  $W_2$  for parameter  $x_1$

$$\gamma_{2-1}(x_1) = 1 - \frac{x_{1,BC} - x_1}{\psi_{2-1}}$$

The new weight estimating polynomial took the form:

$$\Lambda(x_1, x_2, x_5) = \frac{1}{3}[\gamma_{1-2}\gamma_{1-5}\Lambda_1 + \gamma_{2-1}\gamma_{2-5}\Lambda_2 + \gamma_{5-1}\gamma_{5-2}\Lambda_5] \quad (\text{C.2})$$

Where  $\gamma_{1-2}$  is the correction term for the weight given by  $\Lambda_1$  when  $x_2$  changes, etc.

- When all the correction terms were finished, a relation between  $x_{34}$  and  $\Lambda(x_1, x_2, x_5)$  was developed. With the other parameters both minimized and maximized,  $x_3$  and  $x_4$  were changed and calculated in GT PRO. The linear scaling term was found with the same procedure as for the correction terms and is named  $\Gamma(x_3, x_4)$ .

$$\Gamma(x_3, x_4) = 1 - \frac{\frac{x_{3,BC}}{x_{4,BC}} - \frac{x_3}{x_4}}{\psi_{34}} \quad (\text{C.3})$$

The final weight polynomial takes the form:

$$\Lambda = \Lambda(x_1, x_2, x_3, x_4, x_5) = \frac{\Gamma(x_3, x_4)}{3}[\gamma_{1-2}\gamma_{1-5}\Lambda_1 + \gamma_{2-1}\gamma_{2-5}\Lambda_2 + \gamma_{5-1}\gamma_{5-2}\Lambda_5] \quad (\text{C.4})$$



For easy and fast calculations, this polynomial is implemented in an Excel spreadsheet. NB: The steam flow rate for the chosen parameter values needs to be calculated separately, see Section B.1.

## Results

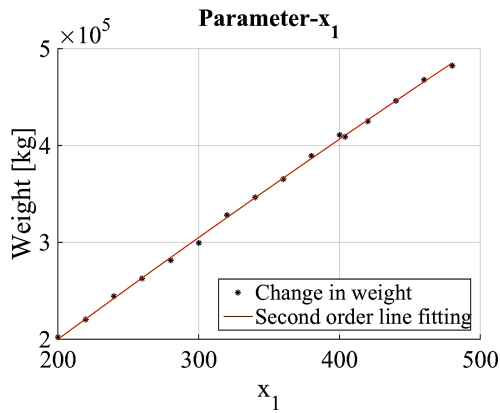


Figure C.41: Second order curve fitting from varying parameter  $x_1$

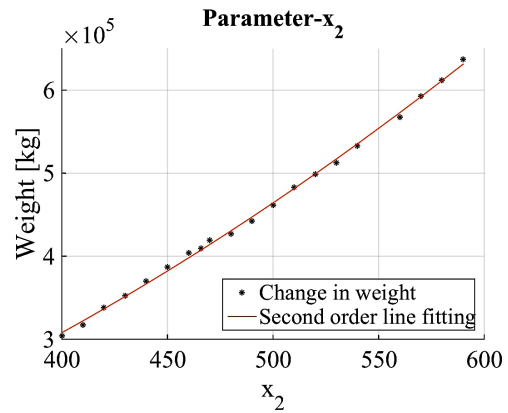


Figure C.42: Second order curve fitting from varying parameter  $x_2$

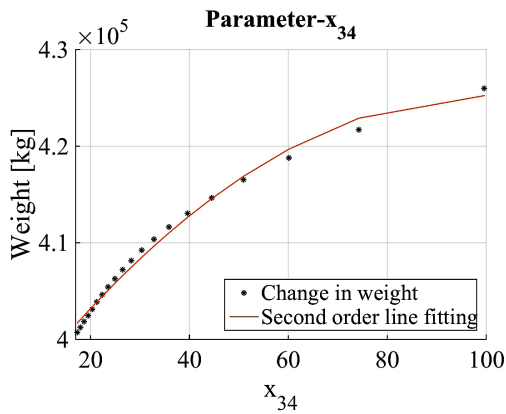


Figure C.43: Second order curve fitting from varying parameter  $x_{34}$

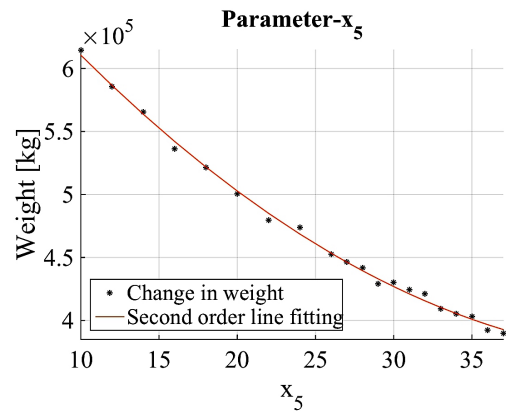


Figure C.44: Second order curve fitting from varying parameter  $x_5$

## Weight Estimating Polynomial

The polynomial for estimating weight of back-pressure steam turbine, OTSG, and generator is a function of the variables collected in Table C.6.

## Sensitivity Analysis

From varying one parameter at the time in ELINK, the polynomial parameters were chosen based on how large the impact was on the total weight.  $\Delta T_{pinch}$  and exhaust gas flow rate ( $\dot{m}_{exh}$ ) and temperature ( $T_{exh}$ ) were the most important ones. Those are also significant variables for the boundary conditions and the HRSG design. Related to the plots for each parameter, they are recognized as polynomials with the steepest slope.

**Range**

The range for each parameter is not considered analytically, but based on visual considerations in the plots for each parameter.

**Calculations**

Calculations from the procedure in Section C.7. The polynomials are found in MATLAB [17], see Figures C.41, C.42, C.43, and C.44:

$$\Lambda_1 = -0.00654964x_1^2 + 1025.03x_1 - 3066.41 \quad (\text{C.5})$$

$$\Lambda_2 = 1.54710x_2^2 + 170.995x_2 - 8094.44 \quad (\text{C.6})$$

$$\Lambda_5 = 159.664x_5^2 - 15568.5x_5 + 750263 \quad (\text{C.7})$$

The correction terms:

$$\gamma_{1-2} = 1 - \frac{466 - x_2}{280.1} \quad (\text{C.8})$$

$$\gamma_{1-5} = 1 + \frac{33 - x_5}{74.2} \quad (\text{C.9})$$

$$\gamma_{2-1} = 1 - \frac{404.2 - x_1}{403.6} \quad (\text{C.10})$$

$$\gamma_{2-5} = 1 + \frac{33 - x_5}{77.3} \quad (\text{C.11})$$

$$\gamma_{5-1} = 1 - \frac{404.2 - x_1}{412.0} \quad (\text{C.12})$$

$$\gamma_{5-2} = 1 - \frac{466 - x_2}{280.7} \quad (\text{C.13})$$

The final polynomial is calculated to be:

$$\Lambda = \frac{1 - \frac{\frac{152 - x_3}{5} - x_4}{1676}}{3} \cdot \left[ \left(1 - \frac{466 - x_2}{280}\right) \cdot \left(1 + \frac{33 - x_5}{74}\right) \cdot \left(-0.00655x_1^2 + 1025x_1 - 3066\right) \right. \\ \left. + \left(1 - \frac{404.2 - x_1}{404}\right) \cdot \left(1 + \frac{33 - x_5}{77}\right) \cdot \left(1.55x_2^2 + 171x_2 - 8094\right) \right. \\ \left. + \left(1 - \frac{404.2 - x_1}{412}\right) \cdot \left(1 - \frac{466 - x_2}{281}\right) \cdot \left(160x_5^2 - 15569x_5 + 750263\right) \right] \quad (C.14)$$

This polynomial is also implemented in Excel [18], see Figure C.45.

Table C.6: Parameters used in weight estimating polynomial

Variable	Property	Unit	$x_{n,BC}$	Range
$x_1$	$\dot{m}_{exh}$	$\left[\frac{kg}{s}\right]$	404.2	340-440
$x_2$	$T_{exh}$	$[^{\circ}C]$	466	430-490
$x_3$	$T_{steam}$	$[^{\circ}C]$	152	99.6-182
$x_4$	$P_{steam}$	$[bar]$	5	1.0-10.5
$x_5$	$\Delta T_{pinch}$	$[^{\circ}C]$	33	27-37

To test the accuracy, weight calculations from the polynomial were compared with GT PRO results, see Table C.7. For the base case, the error is only 0.04%. The polynomial is tested both inside and outside the given range. Except for the BC, only the extreme cases are collected in the table. More moderate and realistic cases gave better and more accurate results.

Table C.7: Compared weight from polynomial calculations and GT PRO simulations.

Base case and maximum/minimum values							
$x_1$	$x_2$	$x_3$	$x_4$	$x_5$	Weight (Polynomial)	Weight (GT PRO)	Error [%]
404.2	466	152	5	33	409368	409224	0.04
340	430	99.6	1	27	337250	329137	2.5
440	490	182	10.5	37	457696	455391	0.5
440	490	99.6	1	27	546792	542656	0.8
340	430	182	10.5	37	282296	259531	8.8
200	400	99.6	1	10	220337	233295	-5.6
560	590	182	10.5	37	789391	828606	-4.7

Polynomial Implemented in Excel

				x1c	x2c	x5c	x1c	x2c	x5c	2	1	0	a	b	c		Weight Poly	x34c	x34c	Weight Poly	Error %	
	404.2	p1	0.333333		280.0851	-74.1862	1	1	1	16337.6	404.2	1	-0.00655	1025.03	-3066.41	410180.7	409368.06	30.4	1676	1	409368.1	0.04%
	466	p2	0.333333	403.6137		-77.3183	1	1	1	2171.66	466	1	1.5471	170.995	-8094.44	407551.3						
	33	p5	0.333333	411.9647	280.7013		1	1	1	1089	33	1	159.66	-15568.5	750263	410372.2						
Correct:	409224																					
INPUTS	x1	404.2	404.2				Weight	409368.1	kg													
	x2	466	466																			
	x3	152	152						0.04%													
	x4	5	5																			
	x5	33	33																			
Correct:	409224		409224																			

Figure C.45: Weight estimating polynomial implemented in Excel

## C.8 Large Tables

Table C.8: Sizing data for Solar skids with generator set [140]

Turbine	Length [m]	Width [m]	Height [m]	Volume [m <sup>3</sup> ]	Average Density [ $\frac{kg}{m^3}$ ]
Saturn 20	5.8	1.7	2	19.7	506
Centaur 40	9.8	2.5	2.9	71.1	459
Centaur 50	9.8	2.5	2.9	71.1	460
Taurus 60	9.8	2.5	2.9	71.1	462
Taurus 70	10.4	2.8	3.3	96.1	475
Mars 90	14.5	2.8	3.6	146	443
Mars 100	14.5	2.8	3.6	146	500
Titan 130	14	3.3	3.3	153	488

Table C.9: GT PRO model 1, size estimates.

Property	Value	Unit
Steam turbine length	4.1	[m]
Steam turbine width	1.4	[m]
Steam turbine generator length	6.4	[m]
Steam turbine generator width	2.6	[m]
HRSG overall length	25.8	[m]
HRSG overall width	5.0	[m]

Table C.10: GT PRO model 2, size estimates.

Property	Value	Unit
Steam turbine length	4.1	[m]
Steam turbine width	1.4	[m]
Steam turbine generator length	6.4	[m]
Steam turbine generator width	2.6	[m]
HRSG overall length	25.7	[m]
HRSG overall width	4.9	[m]

Table C.11: GT PRO model 3, size estimates.

Property	Value	Unit
Steam turbine length	4.1	[m]
Steam turbine width	1.4	[m]
Steam turbine generator length	6.2	[m]
Steam turbine generator width	2.5	[m]
HRSG overall length	25.9	[m]
HRSG overall width	5.2	[m]

Table C.12: GT PRO model 3, CO<sub>2</sub> plant.

Property	Value	Unit
Heating steam mass flow	28.89	$[\frac{kg}{s}]$
Cooling water mass flow	2769	$[\frac{kg}{s}]$
CO <sub>2</sub> captured per day	1446	$[\frac{ton}{day}]$
Heat input per unit of CO <sub>2</sub>	3639	$[\frac{kJ}{kg}]$
CO <sub>2</sub> compression power consumption	4.7	[MW]
Total electrical power consumption	8.2	[MW]

Table C.13: GT PRO model 3, desalination plant.

Property	Value	Unit
Unit dry weight	318	[ton]
Unit length	118	[m]
Unit width	12.2	[m]
Unit height	6.9	[m]
Total power consumption	0.275	[MW]
Total desalinated water flow	72.92	$[\frac{kg}{s}]$
Total heating steam flow	10.04	$[\frac{kg}{s}]$
Total seawater supply flow	219.2	$[\frac{kg}{s}]$

Table C.14: Validation of polynomial 1, 64 nodes.

x <sub>1</sub>	x <sub>2</sub>	x <sub>3</sub>	Weight [ton]	Polynomial [ton]	Error [%]
404.2	466	28.89	474.5	473.4	0.23
320	420	23	334.2	345.8	<b>3.48</b>
360	445	26	403.5	403.3	0.05
405	497	28.5	533.8	517.0	3.15
450	550	30.5	679.5	679.5	0.01
480	600	32	853.2	858.6	0.63
360	550	26	554.9	555.4	0.09
450	445	30.5	501.6	500.4	0.25
436	520	26	606.1	596.3	1.62
364	491	30	468.8	457.6	2.38
392	546	27	584.7	591.3	1.13
385	486	29	490.5	476.4	2.87
378	480	28	456.6	460.0	0.75
360	458	28	421.8	414.5	1.72
422	483	29	522.1	516.3	1.11

Table C.15: Validation of polynomial 2, 128 nodes.

$x_1$	$x_2$	$x_3$	Weight [ton]	Polynomial [ton]	Error [%]
404.2	466	28.89	474.5	477.4	0.60
320	420	23	334.2	341.6	2.21
360	445	26	403.5	405.8	0.57
405	497	28.5	533.8	520.8	<b>2.44</b>
450	550	30.5	679.5	677.1	0.35
480	600	32	853.2	845.6	0.90
360	550	26	554.9	552.5	0.43
450	445	30.5	501.6	500.6	0.22
436	520	26	606.1	596.4	1.60
364	491	30	468.8	459.2	2.05
392	546	27	584.7	590.9	1.06
385	486	29	490.5	479.9	2.16
378	480	28	456.6	463.7	1.57
360	458	28	421.8	416.9	1.15
422	483	29	522.1	520.0	0.41

Table C.16: Validation of polynomial 3, 64 nodes.

$x_1$	$x_2$	$x_3$	Weight [ton]	Polynomial [ton]	Error [%]
404.2	466	39.07	437.8	443.8	1.37
360	445	30.74	381.3	381.3	0.00
405	497	45.94	487.9	479.8	1.66
450	550	64.07	617.1	617.1	0.00
480	600	81.59	768.0	772.8	0.61
360	550	51.29	500.3	500.3	0.00
450	445	38.39	473.8	473.8	0.01
436	520	54.91	551.9	547.9	0.72
364	491	40.12	435.4	425.9	<b>2.19</b>
392	546	54.97	537.5	534.8	0.51
385	486	41.38	450.7	444.1	1.46
378	480	39.40	430.2	429.8	0.09
360	458	33.26	389.8	390.1	0.07
422	483	44.66	489.9	481.3	1.75

Table C.17: GT PRO simulation on model 1 for scaling analysis.

Steam turbine weight	[ton]	21.9	18	19	19.9	20.9	21.8	22.7	23.5	24.4	25.2	26.1	26.9	27.7
Generator weight	[ton]	43.6	36.7	38.4	40.1	41.7	43.3	44.9	46.4	47.9	49.5	51	52.4	53.9
HRSG weight dry	[ton]	409	320.1	340.6	363.2	383.9	402.9	424.1	442.2	462.3	480.3	500.5	521	540.2
Total weight	[ton]	474.5	374.9	398	423.2	446.4	468	491.7	512.1	534.6	555	577.5	600.3	621.8
Steam turbine flow	$[\frac{kg}{s}]$	37.7	29.9	31.7	33.6	35.5	37.3	39.2	41.1	42.9	44.8	46.7	48.5	50.4
Steam flow to CO <sub>2</sub> plant	$[\frac{kg}{s}]$	28.89	28.89	28.89	28.89	28.89	28.89	28.89	28.89	28.89	28.89	28.89	28.89	28.89
Total steam mass flow	$[\frac{kg}{s}]$	39	30.9	32.8	34.7	36.7	38.6	40.5	42.4	44.3	46.3	48.2	50.1	52
Surface area HRSG	$k \cdot [m^2]$	27.5	21.6	22.9	24.5	25.7	26.9	28.6	29.7	31.2	32.3	33.8	35.3	36.6
Steam turbine power	[MW]	14.4	11.3	12	12.8	13.5	14.2	15	15.7	16.4	17.2	17.9	18.6	19.4
Exhaust mass flow	[°C]	404	320	340	360	380	400	420	440	460	480	500	520	540



Table C.18: GT PRO simulation on model 2 for scaling analysis.

Steam turbine weight	[ton]	21.9	18	19	19.9	20.9	21.8	22.7	23.5	24.4	25.2	26.1	26.9	27.7
Generator weight	[ton]	43.6	36.7	38.4	40.1	41.7	43.3	44.9	46.4	47.9	49.5	51	52.4	53.9
HRSG weight dry	[ton]	372.2	291.4	310	328.8	350.4	367.4	386.3	403.1	422.4	439.2	458.5	477.7	494.5
Total weight	[ton]	437.8	346.2	367.4	388.8	413	432.5	453.8	473.1	494.7	513.9	535.5	557	576.1
Steam turbine flow	$[\frac{kg}{s}]$	37.7	29.9	31.7	33.6	35.5	37.3	39.2	41.1	42.9	44.8	46.7	48.5	50.4
Steam flow to CO <sub>2</sub> plant	$[\frac{kg}{s}]$	28.9	22.9	24.3	25.7	27.2	28.6	30	31.4	32.9	34.3	35.7	37.2	38.6
Total steam mass flow	$[\frac{kg}{s}]$	39.1	37	37.5	38	38.5	39	39.5	40	40.5	40.9	41.4	41.9	42.4
Surface area HRSG	$k \cdot [m^2]$	25.3	20.2	21.3	22.4	23.9	24.8	26.2	27.3	28.8	29.8	31.3	32.7	33.7
Steam turbine power	[MW]	14.4	11.3	12	12.8	13.5	14.2	15	15.7	16.4	17.2	17.9	18.6	19.4
Exhaust mass flow	[°C]	404	320	340	360	380	400	420	440	460	480	500	520	540
CO <sub>2</sub> captured per day	$[\frac{ton}{day}]$	1446.1	1144.9	1216.4	1288	1359.6	1431.1	1502.7	1574.2	1645.8	1717.3	1788.9	1860.4	1932
Heat input	[MW]	60.9	48.2	51.2	54.2	57.3	60.3	63.3	66.3	69.3	72.3	75.3	78.4	81.4
Heat input per unit of CO <sub>2</sub>	$[\frac{kWh}{kg}]$	3639	3639	3639	3639	3639	3639	3639	3639	3639	3639	3639	3639	3639
Total electrical power consumption	[MW]	8.2	6.5	6.9	7.3	7.7	8.1	8.5	8.9	9.3	9.7	10.1	10.5	11



# Appendix D

## Computer Code

### Contents

D.1	Excel Code . . . . .	211
D.1.1	Heat Exchanger Scaling Model . . . . .	211
D.2	MATLAB Code . . . . .	214
D.2.1	km32.m . . . . .	214
D.2.2	combo_3_4.m . . . . .	216
D.2.3	poly_3_4.m . . . . .	217
D.2.4	poly_eval.m . . . . .	218

## D.1 Excel Code

### D.1.1 Heat Exchanger Scaling Model

Part	Numbers	Surface Area	Face Area (1)	Volume	Volume Shell %	Volume %	Weight
Disk	2		4,908738521	0,093511469	5,90 %		748,09
Casing	1		4,908738521	0,558931141	35,29 %		4471,45
Support	8		0,813399053	0,061981008	3,91 %		495,85
Shell				0,714424	45,11 %	45,11 %	22861,56
Tubes	2588	1259,73	0,000506707	0,86940757209	54,89 %	54,89 %	6937,87
Dry Volume				1,58	100,00 %	100,00 %	29799,43
# Pases	2						
Pi	3,141593					Corr. Terms	
Support Cover	70,00 %					Shell Weight	4,0
						# tubes	1,2
						Tube length	0,8
						Shell length	0,8
Scaling							
N	1,3						
					Orginal	Shell	Tube
	Shell	Tube					
Do	2,5	0,02540			Do	1,9	0,0254
Di	2,48095	0,02398			Di	1,88095	0,0239800
Length	7,5	6,10			Length	7,6	5,8
Thickness	0,009525	0,0007112			Thickness	0,009525	0,0007112
Density	8000	7980			Density	8000	7980

Figure D.1: Heat exchanger model built in Excel.

Part	Numbers	Surface Area	Face Area [1]	Volume	Volume Shell %	Volume %	Weight
Disk	2		=W20/4*W31*W31	=W20/4*W31*W34*W7	=Z7/SZ516		=Z7*SW536
Casing	1		=W20/4*W31*W31	=W20/4*(W31*W31*W32*W32)*W8*W33	=Z8/SZ516		=Z8*SW536
Support	8		=(Y7*W22.W1.4*W19*(14)	=Y9*W34*W9	=Z9/SZ516		=Z9*SW536
Shell				=SUMMER(Z7Z9)	=Z11/SZ516		=Z11*SW536*AC21
Tubes	=AVRUND(1691 *SW526* AC22,0)	=W20*X31*X33*W14	=W20/4*X31*X31	=W20/4*(X31*X31*X32*X32)*W14*X33	=Z14/SZ516		=Z14*SW536
Dry Volume				=Z11+Z14	=Z16/SZ516		=AC11+AC14
# Pases	2						
PI	=PI()						
Support Cover	0,7						
Scaling							
N	1,3						
Shell		Tube			Original		Tube
Do	=AVRUND(A831*SW526;1)	=AC31					=25.4*10^-3
Di	=W31.2*W34	=AC32					=23.98*10^-3
Length	=AVRUND(A833*SW526*AC24;1)	=AC34					5.8
Thickness	=AB34						0,0007112
Density	=AB36	=AC36					7980
Corr. Terms							
Shell Weight	4						
# tubes							=0.590895*SW526+0.409105
Tube length							=0.626995*SW526+1.62699
Shell length							=0.807524*SW526+1.80752
Original							
Do							
Di							
Length							
Thickness							
Density							

Figure D.2: Heat exchanger model built in Excel, formulas.

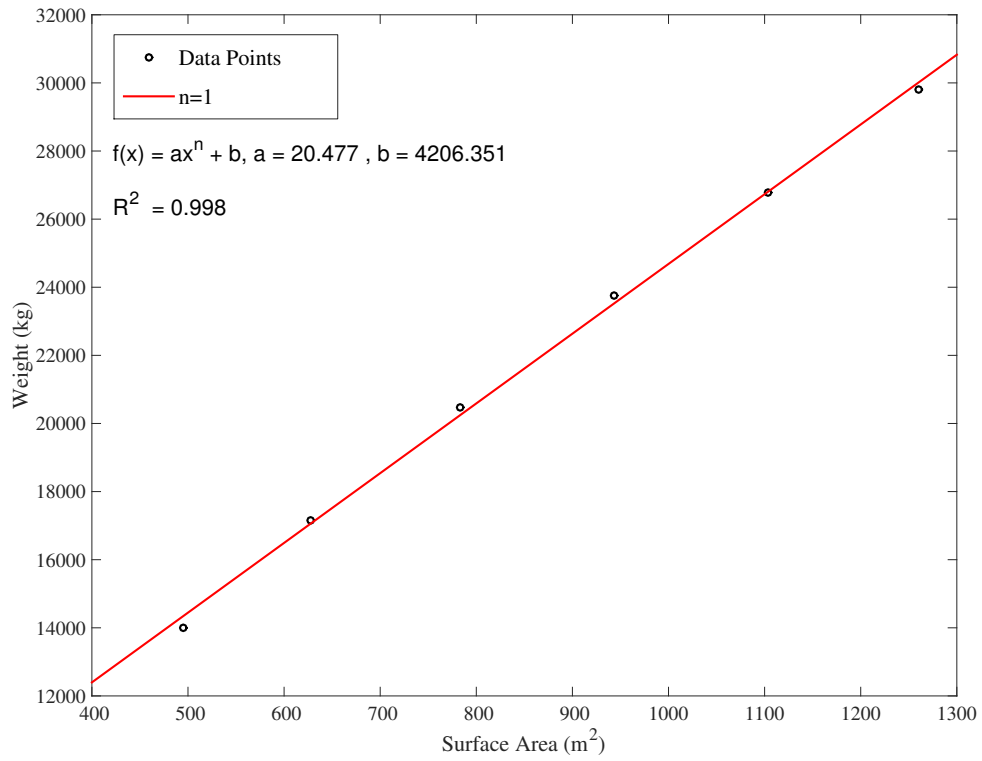


Figure D.3: Heat exchanger scaling model in Excel, weight varying with heat transfer surface area.

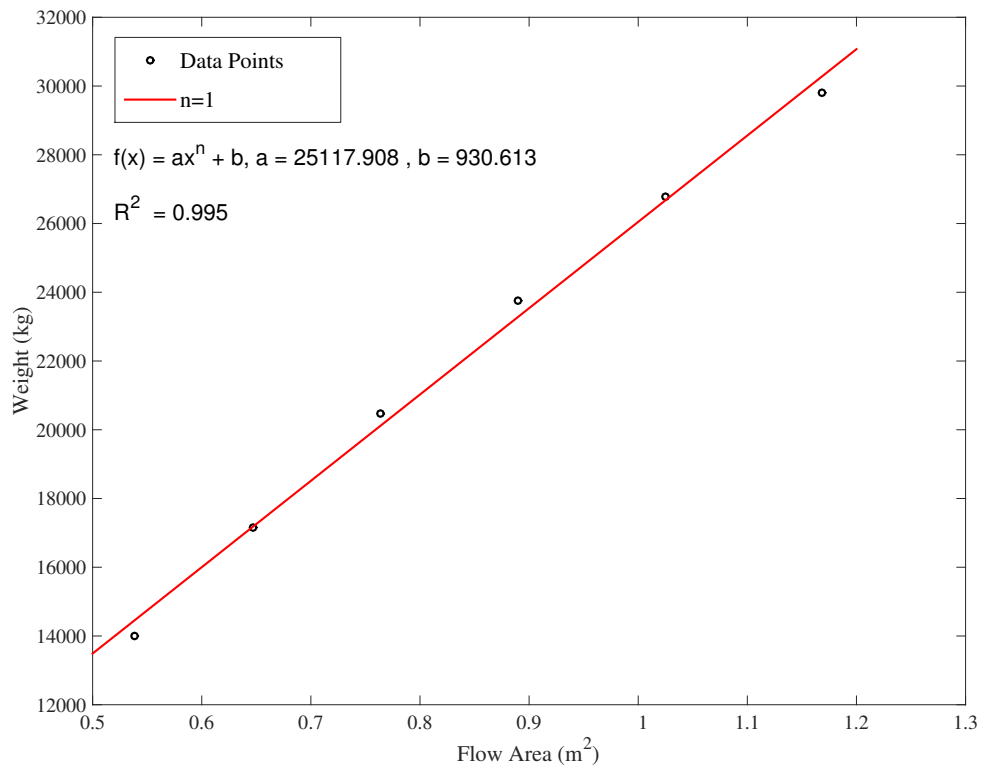


Figure D.4: Heat exchanger scaling model in Excel, weight varying with total steam flow area.

## D.2 MATLAB Code

### D.2.1 km32.m

```

1  function y = km32(x1,x2,nr,name,xlab      30
    ,ylab,n1,n2,gri,titl)                  31  r3 = gof3.rsquare;
2                                          32
3  % Font settings                          33  coeffvals = coeffvalues(curve3);
4  font_title = 26;                        34  a3 = coeffvals(1);
5  font_legend = 20;                       35  b3 = coeffvals(2);
6  font_axes = 20;                         36
7  font_markers = 6;                       37  l1 = [ n= num2str(n1) ];
8  font_linewidth = 1.9;                  38  l2 = [ n= num2str(n2) ];
9                                          39
10 figure_name = sprintf(name);            40  plot(x1,x2,ko)
11                                          41  hold on;
12 % Plot settings                          42
13 h(nr) = figure( units , normalized ,    43  if r2 >= r3
    ,outerposition ,[0 0 0.7 0.92]);      44  R2 = r2;
14 set(h(nr), DefaultAxesFontSize ,      45  plot(curve2, r )
    font_axes);                            46  str = sprintf( f(x) = ax^n + b, a =
15 set(h(nr), DefaultLineMarkerSize ,    %3.3f , b = %3.3f , a2, b2);
    font_markers);                          47  l = l1;
16 set(h(nr), defaultlinelinewidth ,    48
    font_linewidth)                        49  else
17                                          50
18 fo = fitoptions( Method ,              51  R2 = r3;
    NonLinearLeastSquares , Robust ,      52  plot(curve3, b )
    on , StartPoint ,[0 0]);              53  str = sprintf( f(x) = ax^n + b, a =
19 ft = fittype( a*(x)^(n)+b , problem    %3.3f , b = %3.3f , a3, b3);
    , n , options ,fo);                    54  l = l2;
20                                          55  end
21 [curve2,gof2] = fit(x1 ,x2 ,ft ,      56
    problem ,n1);                          57  if gri == 1
22                                          58  grid on;
23 r2 = gof2.rsquare;                       59  end
24                                          60
25 coeffvals = coeffvalues(curve2);        61  ylabel(ylab, FontSize , font_axes)
26 a2 = coeffvals(1);                       62  set(gca, YTickLabel ,num2str(get(gca
27 b2 = coeffvals(2);                       , YTick ) ) )
28                                          63
29 [curve3,gof3] = fit(x1 ,x2 ,ft ,      64  xlabel(xlab, FontSize , font_axes)
    problem ,n2);                          65  set(gca, XTickLabel ,num2str(get(gca

```

```

        , XTick ) ))
66
67 set(gca, fontsize ,font_axes - 2)
68 if titl == 1
69 t = title (figure_name);
70 set(t, FontSize , font_title);
71 end
72
73 aaa = legend( Data Points ,num2str(l
        ));
74
75 set(aaa, FontSize ,font_legend ,
        position ,[0.15 0.8 0.2 0.1]);
76 % Location , northwest
77
78 set(gcf, color , white )
79
80 text(0.025,0.8, str , Units ,
        normalized , FontSize ,
        font_legend);
81
82 text(0.025,0.72, sprintf( R^2 =
        %3.3f ,R2) , Units , normalized
        , FontSize ,font_legend);
83
84 pdfname = [figure_name .pdf ];
85
86 export_fig (pdfname)
87
88 y = ok ;
89
90 end

```



## D.2.2 combo\_3\_4.m

```

1  close all;
2  clear all;
3  clc;
4
5  variables = 3;
6  interval = 4;
7
8  comb = interval^variables;
9
10 x1 = linspace(360,450,interval);
11 x2 = linspace(445,550,interval);
12 x3 = linspace(30,50,interval);
13
14 A = zeros(comb,variables);
15
16 t1 = 1;
17 t2 = 1;
18 t3 = 1;
19
20 for i=1:comb
21 A(i,variables) = x3(t3);
22 t3 = t3 + 1;
23 if t3 > length(x3)
24 t3 = 1;
25 end
26 end
27 b2 = length(x2);
28
29 for i=1:b2:comb
30 A(i:1:i+b2-1,variables-1) = x2(t2);
31 t2 = t2 + 1;
32 if t2 > length(x2)
33 t2 = 1;
34 end
35 end
36
37 %%
38
39 b1 = length(x1)^2;
40
41 for i=1:b1:comb
42 A(i:1:i+b1-1,variables-2) = x1(t1);
43 t1 = t1 + 1;
44 if t1 > length(x1)
45 t1 = 1;
46 end
47 end
48
49 T = [A(1:16,:)
50 A(17:32,:)
51 A(33:48,:)
52 A(49:64,:) ];
53
54 filename = 'simdata';
55 xlswrite(filename,T)

```

## D.2.3 poly\_3\_4.m

```

1 clear all;
2 close all;
3 clc;
4
5 %%
6
7 filename = POLY_3_4.xlsx ;
8 A = xlsread(filename);
9
10 xx1 = A(1,:) ; % Variable x1
11 xx2 = A(2,:) ; % Variable x2
12 xx3 = A(3,:) ; % Variable x3
13
14 zz = A(4,:) ; % Weight
15
16 % To get the same magnitude
17
18 m1 = max(xx1);
19 m2 = max(xx2);
20 m3 = max(xx3);
21 m4 = max(zz);
22
23 x1 = 1/m1*xx1;
24 x2 = 1/m2*xx2;
25 x3 = 1/m3*xx3;
26 x = [x1 x2 x3];
27
28 z = 1/m4*zz;
29
30 % Correction vector
31
32 mag = [m4/(m1*m1) m4/(m1*m2) m4/(m1*
          m3) m4/m1 m4/(m2*m2) m4/(m2*m3)
          m4/m2 m4/(m3*m3) m4/m3 m4];
33
34 %%
35
36 % Making table with simulation
          results
37 tbl = table(x1,x2,x3,z);
38
39 % Second order model
40 modelfun = @(a,x)a(1).*x(:,1).*x
          (:,1) + a(2).*x(:,1).*x(:,2) + a
          (3).*x(:,1).*x(:,3) + a(4).*x
          (:,1) + a(5).*x(:,2).*x(:,2) + a
          (6).*x(:,2).*x(:,3) + a(7).*x
          (:,2) + a(8).*x(:,3).*x(:,3) + a
          (9).*x(:,3) + a(10);
41
42 % Start point for simulations
43 beta0 = ones(1,10);
44
45 % Robust settings
46 opts = statset( nlinfit );
47 opts.RobustWgtFun = bisquare ;
48
49 % Regression model
50 mdl2 = fitnlm(tbl,modelfun,beta0,
          Options ,opts);
51
52 % Regression results
53 R2 = mdl2.Rsquared.Ordinary;
54 mdl2.CoefficientNames;
55 coff2 = mdl2.Coefficients(:,1);
56
57 % Adjusting results with magnitude
          vector
58 C2 = table2array(coff2) .* mag;
59
60 % Printing results
61 fprintf( \n\nW(x1,x2,x3) = a1*x1^2 +
          a2*x1*x2 + a3*x1*x3 + a4*x1 +
          a5*x2^2 + a6*x2*x3 + a7*x2 + a8*
          x3^2 + a9*x3 + a10 \n\n )
62
63 for i = 1:10
64
65 str = [ a num2str(i) = ];
66
67 fprintf(str);
68 fprintf( %3.4f \n ,C2(i));

```

```

69
70 end
71
72 %%
73
74 %Testing polynomial accuracy with
    all nodes.
75 Test = zeros(1,64);
76 poly_weights = Test;
77
78 for i = 1:64
79
80 x1 = A(1,i);
81 x2 = A(2,i);
82 x3 = A(3,i);
83 w = A(4,i);
84
85 poly_weights(i) = poly_eval(C2,x1,x2
    ,x3);
86
87 Test(i) = (poly_eval(C2,x1,x2,x3)/w)
    *100;
88
89 end
90
91 % Largest polynomial over estimate
92 maxtest = max(Test)
93 % Smallest polynomial under estimate
94 mintest = min(Test)
95
96 % Calculating estimate for base case
97 Basecase = poly_eval(C2,x1_bc,x2_bc,
    x3_bc)
98 % Percent deviation
99 BC_test = abs(1-Basecase/W_bc)*100
100
101 % R-squared from polynomial
102 Rsquared = R2

```

#### D.2.4 poly\_eval.m

```

1 function y = poly_eval(a,x1,x2,x3)
2
3
4 x = a(1).*x1.*x1 + a(2).*x1.*x2 + a
    (3).*x1.*x3 + a(4).*x1+ a(5).*x2
    .*x2 + a(6).*x2.*x3 + a(7).*x2 +
    a(8).*x3.*x3 + a(9).*x3 + a(10)
    ;
5 y = sprintf( %3.0f\n\n ,x);
6
7 y = str2num(y);
8
9 end

```